

1972

Geology Of Chromitite Occurrences And Ultramafic Rocks Of The Thetford Mines--disraeli Area, Quebec

Niyazi Kacira

Follow this and additional works at: <https://ir.lib.uwo.ca/digitizedtheses>

Recommended Citation

Kacira, Niyazi, "Geology Of Chromitite Occurrences And Ultramafic Rocks Of The Thetford Mines--disraeli Area, Quebec" (1972). *Digitized Theses*. 583.
<https://ir.lib.uwo.ca/digitizedtheses/583>

This Dissertation is brought to you for free and open access by the Digitized Special Collections at Scholarship@Western. It has been accepted for inclusion in Digitized Theses by an authorized administrator of Scholarship@Western. For more information, please contact tadam@uwo.ca, wlsadmin@uwo.ca.

The author of this thesis has granted The University of Western Ontario a non-exclusive license to reproduce and distribute copies of this thesis to users of Western Libraries. Copyright remains with the author.

Electronic theses and dissertations available in The University of Western Ontario's institutional repository (Scholarship@Western) are solely for the purpose of private study and research. They may not be copied or reproduced, except as permitted by copyright laws, without written authority of the copyright owner. Any commercial use or publication is strictly prohibited.

The original copyright license attesting to these terms and signed by the author of this thesis may be found in the original print version of the thesis, held by Western Libraries.

The thesis approval page signed by the examining committee may also be found in the original print version of the thesis held in Western Libraries.

Please contact Western Libraries for further information:

E-mail: libadmin@uwo.ca

Telephone: (519) 661-2111 Ext. 84796

Web site: <http://www.lib.uwo.ca/>

GEOLOGY OF CHROMITITE OCCURRENCES
AND ULTRAMAFIC ROCKS
OF THE THETFORD MINES - DISRAELI AREA, QUEBEC

by

Niyazi Kaçira

Department of Geology

Submitted in partial fulfillment of the
requirements for the degree of
Doctor of Philosophy

Faculty of Graduate Studies
The University of Western Ontario
London, Canada
December 1971

© Niyazi Kacira 1971

ABSTRACT

Numerous intrusive bodies, felsic to ultramafic in composition, constitute the Appalachian Serpentine Belt of southeastern Canada and northeastern United States. The belt is approximately 4,600 km long and is parallel to the regional, northeasterly fold trend. In southern Quebec this Serpentine Belt is located near the boundary between the Acadian geosyncline and the St. Lawrence platform. The ultramafic rocks of the Appalachian Serpentine Belt reach their maximum development near Thetford Mines, in Megantic and Wolfe counties, in Quebec, where they form a horsehoe-shaped, northeast-southwest oriented body and contain numerous small chromitite occurrences. The present study attempts to contribute to the understanding of the genesis and distribution of these occurrences.

The non-intrusive rocks of the map-area consist of mafic to felsic metavolcanic and metasedimentary rocks, Cambrian? (or Precambrian?) to Ordovician in age. Igneous rocks are represented by gabbro and ultramafic rocks, including pyroxenite, "olivine" pyroxenite, "herzolite", peridotite (harzburgite), olivine orthopyroxenite, dunite, serpentinite and chromitite.

The ultramafic rocks are comparable texturally, structurally, chemically and in mode of occurrence with alpine-type peridotites as described from other parts of the world. Layering in the ultramafic rocks is vertical or steeply dipping, it is discordant to the schis-

tosity and bedding of the country rock and, locally, also discordant to the boundaries between major ultramafic rock groups. The olivine and pyroxene have high Mg/Fe ratios, are unzoned and exhibit no significant compositional variation within a rock type. All the ultramafic rocks, except pyroxenite, contain accessory chromite, which is usually anhedral. The ultramafic rocks are coarsely granular, exhibit cataclastic texture and are serpentinized to varying degrees. Dunite is usually completely serpentinized.

Chromitite occurs only in dunite. From the published descriptions of mine workings and the present study of chromitite occurrences, it appears that the commercially explored chromite deposits occurred as isolated lenses or as a string of lenses confined to well-defined, narrow zones. It is postulated that this distribution has resulted from the deformation and boudinage of original chromitite layers accumulated by crystal settling.

It appears possible that the gabbro and the accompanying ultramafic rocks derived from the same mantle material. The gabbro could represent an early fractional melt while further melting produced an ultrabasic magma from which the ultramafic rocks formed by fractional crystallization and gravity settling. Differentiation of the ultrabasic magma probably occurred at depth, possibly in the upper mantle. After the differentiation the ultramafic material was intruded into the crust likely as a crystal mush and solidified at depth. Subsequently, the ultramafic rocks have been emplaced as large, coherent blocks into their present position.

ACKNOWLEDGMENTS

Supervision of this project was provided by Drs. J. Starkey, N.D. MacRae and W.R. Church, Department of Geology, University of Western Ontario. Their help is gratefully acknowledged. Dr. MacRae also gave instruction in the use of the electron microprobe analyser. His patient assistance is appreciated.

Most of the field work was carried out in the summer of 1967 with financial and technical aid from Union Carbide Exploration Ltd. and was continued in the summer of 1968 with the aid of the Quebec Department of Natural Resources. A grant from Union Carbide Exploration covered the cost of most laboratory research in the academic year 1967-68.

I have accumulated much indebtedness to Dr. R.Y. Lamarche, Quebec Department of Natural Resources, on whose critical judgement I have relied heavily, especially concerning the regional geology and stratigraphy of the area of this study.

During the 1967 field season, Dr. R.W. Wilson, then on the staff of Union Carbide Exploration, advised on the techniques of mapping and studying the ultramafic rocks. His contribution was invaluable.

Most of the drafting was done by Mrs. R. Ringsman, thin sections and polished thin sections were prepared by Mr. J. Forth, both of the Department of Geology, University of Western Ontario. The late

Mr. J. Wanberra made the polished thin sections.

I am indebted to my wife Nilgün Serâ, who patiently and gracefully undertook the not too glamorous chores of typing and editing.

TABLE OF CONTENTS

	page
Certificate of Examination	ii
ABSTRACT	iii
ACKNOWLEDGMENTS	v
TABLE OF CONTENTS	vii
LIST OF TABLES	xii
LIST OF FIGURES	xiv
CHAPTER I - INTRODUCTION	1
History of the chromite industry in the Eastern Townships	2
CHAPTER II - GENERAL GEOLOGY	4
1. PREVIOUS WORK	4
2. REGIONAL GEOLOGY	5
3. GEOPHYSICAL DATA	7
4. LOCAL GEOLOGY	7
5. DISCUSSION AND CONCLUSION	13
CHAPTER III - GENERAL GEOLOGY OF THE INTRUSIVE COMPLEX	17
1. INTRODUCTION	17
2. FORM OF THE INTRUSIVE COMPLEX	17
3. CONTACT RELATIONSHIPS	20
A. Ultramafic rock/country rock contact relationship	20
Amphibolite: Possible contact metamorphism	24
B. Ultramafic rock/non-ultramafic rock contact relationship	26

	page
4. DISTRIBUTION OF ROCKS AND LARGE-SCALE FIELD RELATIONSHIPS	26
A. Distribution	26
Gabbroic Suite	26
Pyroxenite - "olivine" pyroxenite - "lherzolite" assemblage	26
Peridotite	28
Dumite	28
Serpentinite	30
B. Field relationships between major ultramafic rock groups	30
Definitions	30
Northern Assemblage	30
Southern Assemblage	31
Northern Assemblage and Southern Assemblage field relationships	31
5. MEGASCOPIC DEFORMATION OF ULTRAMAFIC ROCKS	33
6. INTERNAL STRUCTURES OF ULTRAMAFIC ROCKS	33
A. Layering and foliation	33
B. Discordant features	36
7. AGE OF INTRUSION	36
A. The time of emplacement of ultramafic rocks	36
B. The time of intrusion of gabbroic rocks	37
8. DISCUSSION AND CONCLUSION	37
CHAPTER IV - GABBROIC SUITE AND ACID ROCKS	38
1. INTRODUCTION	38
2. GABBRO	38
A. Field relationships	40
Gabbro/non-intrusive rock relationship	41
Gabbro/pyroxenite relationship	41
The field relationship between Gabbroic and Ultramafic Suites	42
B. Petrography of the gabbro	43
C. Chemistry of the gabbro	43
3. ACIDIC ROCKS	45
4. CONCLUSION	51
CHAPTER V - ULTRAMAFIC SUITE	52
1. INTRODUCTION	52
2. PYROXENITE	53
A. Field relationships	53

	page
Concordant pyroxenite	53
Discordant pyroxenite	55
B. Petrography	59
C. Chemistry	61
D. Discussion and conclusion	61
3. OLIVINE PYROXENITE	63
A. Field relationships	63
B. Petrography	63
C. Chemistry	66
4. LHERZOLITE	66
5. PERIDOTITE	68
A. Internal structures	68
Foliation in peridotite	68
Layering in peridotite	69
B. Petrography	72
Olivine	75
Orthopyroxene	77
Clinopyroxene	81
Chromite	83
C. Chemistry	83
D. Discussion	92
Aluminum-rich accessory chromite in peridotite	95
6. OLIVINE ORTHOPYROXENITE	98
7. ORTHOPYROXENITE	99
8. DUNITE	102
A. Field relationships	103
Dunite-peridotite interlayering	103
Dunite bodies and discordant dunite dykes in peridotite	103
B. Petrography	106
C. Chemistry	109
D. Discussion	112
9. SERPENTINITE	114
10. DISCUSSION	120
11. CONCLUSION	132
CHAPTER VI - CHROMITITE AND CHROMITE DEPOSITS	133
1. INTRODUCTION	133
2. STRUCTURES OF CHROMITITE	134
Banded chromitite	134

	page
Nodular chromitite	137
Pencil-shaped concentrations, chromitite pods and schlieren	142
Chromitite veins and chromitite with "chain structure"	144
3. CLASSIFICATION AND DISTRIBUTION OF CHROMITE DEPOSITS	147
A. General statement	147
B. Classification of chromite deposits	147
Banded, lenticular deposits	147
Lenticular deposits with schlieren	148
"Podiform" deposits	148
Veined deposit	149
C. Distribution of chromite deposits	149
4. DEFORMATION OF CHROMITITE	150
5. PETROGRAPHY OF CHROMITITE	150
Olivine inclusions in chromite	156
6. CHEMISTRY	161
7. DISCUSSION AND CONCLUSION	164
CHAPTER VII - SERPENTINIZATION	173
1. INTRODUCTION	173
2. PERVASIVE SERPENTINIZATION	173
Mode of serpentization	174
3. LATE SERPENTINIZATION	177
4. THE SERPENTINIZATION PROCESSES	177
5. SERPENTINIZATION OF ULTRAMAFIC ROCKS IN THE MAP-AREA	181
CHAPTER VIII - GENESIS OF ULTRAMAFIC ROCKS AND ASSOCIATED CHROMITITE	185
1. INTRODUCTION	185
2. FORMATION OF ULTRAMAFIC ROCKS	186
A. Differentiation process	186
B. Nature of the original magma and place of differentiation	187
3. FORMATION OF CHROMITITE	192

	page
4. EMPLACEMENT AND RE-EMPLACEMENT OF THE ULTRAMAFIC ROCKS	195
A. First stage: Flow	195
B. Second stage: Re-emplacement	197
5. OPHIOLITE HYPOTHESIS	198
6. GENERAL PROBLEM OF ALPINE-TYPE ULTRAMAFIC ROCKS	203
REFERENCES	208
APPENDIX I	216
Gabbroic Suite	216
Ultramafic Suite	216
APPENDIX II - CHROMITE DEPOSITS	218
The Sterrett Mine	218
American Chrome Company's Deposits	221
APPENDIX III - CHEMICAL ANALYSES	223
A. Whole rock analyses	223
B. Whole rock trace element analyses	223
C. Mineral analyses	225
Analytical procedure	225
Presentation of the data	225
Precision and accuracy	227
VITA	xx
MAPS (in back pocket)	
Map No. 1: Compilation Map. Ultrabasic Rocks of the Thetford - Disraeli Area. Scale: 1:25,000	
Map No. 2: Exposure Map. Distribution of Observed Exposures. Scale: 1:25,000	
Map No. 3: Chromite Workings and Ore Zones of the Northern Dunite Zone. Scale: 1:3,850 1 inch=367 feet	

LIST OF TABLES

TABLE	page	
I	TABLE OF FORMATIONS	11
II	INTRUSIVE ROCKS	18
III	A and B: WHOLE ROCK ANALYSES	47
IV	WHOLE ROCK TRACE AND MINOR ELEMENT ANALYSES	48
V	Microprobe Analyses: Mean composition of minerals in pyroxenite, "olivine" pyroxenite and "herzolite" of the Ultramafic Suite	62
VI	Microprobe Analyses: Mean composition of minerals in peridotite, olivine orthopyroxenite and orthopyroxenite	86
	A) Accessory chromite in peridotite and olivine orthopyroxenite	86
	B) Olivine in peridotite	87
	C) Clinopyroxene in peridotite and orthopyroxenite	87
	D) Orthopyroxene in peridotite, olivine orthopyroxenite and orthopyroxenite	88
VII	Microprobe Analyses: Mean composition of minerals in dunite	111
	A) Olivine in dunite bodies in peridotite	111
	B) Accessory chromite in dunite	111
VIII	Microprobe Analyses: Mean composition of chromite in chromitite	161
	A) Chromitite within dunite bodies in peridotite	161
	B) Chromitite in dunite zones	161
	IN THE APPENDICES	
IX	Molecular Norm Calculations	224
X	Precision and accuracy of mineral analyses	226
XI	MICROPROBE ANALYSES OF MINERALS	228
	A) CHROMITE ANALYSES	228
	Accessory chromite in "olivine" pyroxenite and "herzolite"	228

TABLE

page

Accessory chromite in peridotite and olivine orthopyroxenite	228
Accessory chromite in chromitite-bearing dunite bodies in peridotite	231
Accessory chromite in dunite layer and dunite body in peridotite	231
Accessory chromite in dunite from the Olivine Pyroxenite Zone	232
Accessory and disseminated chromite in dunite from dunite zones	232
Chromitite within dunite bodies in peridotite	234
Chromite in chromitite from dunite zones	235
B) OLIVINE ANALYSES	239
Olivine in peridotite and olivine orthopyroxenite	239
Olivine in dunite	241
C) ORTHOPYROXENE ANALYSES	242
Orthopyroxene in peridotite and olivine orthopyroxenite	242
Orthopyroxene in orthopyroxenite layer and orthopyroxenite vein	243
Orthopyroxene in pyroxenite	244
D) CLINOPYROXENE ANALYSES	245
XII Equilibrium constant $K_T = \frac{(Fe^{++}/Mg)_{ol}}{(Mg/Fe^{++})_{opx}^2}$ for the olivine-orthopyroxene pair in peridotite samples	246
XIII Compositions of clinopyroxenes from "herzolite", "olivine" pyroxenite recalculated according to the convention used by O'Hara (1967b), and parameters α and β .	246

LIST OF FIGURES

FIGURE		page
1A	Bouguer gravity anomaly map of southern Quebec	8
1B	Generalized geological and crustal section and observed Bouguer anomalies	8
2	Map showing major structural elements of southern Quebec and the northern parts of the adjoining states of New York, Vermont, and New Hampshire	9
3	Outcrop distribution of major rock units in the map-area	12
4	Peridotite-metasedimentary rock contact relationship	22
5	Major units of the Intrusive Complex	27
6	Nadeau Hill seen from the east	32
7	Banding in pyroxenite and dunite	35
8	Mafic gabbro patches in gabbro, crosscut by coarse-grained, feldspar-rich gabbro	39
9	A very thin microgabbro vein crosscuts and offsets chromitite bands in dunite	39
10	Serpentinite-gabbro contact	44
11	"Acidic" rock dyke of very irregular shape enclosing a peridotite block	44
12	Plots of the whole rock analyses of phaneritic rocks and aphanitic rocks	49
13	Dunite-pyroxenite interlayering	54
14	Detail of the dunite-pyroxenite interlayering	54
15	A dunite layer in "olivine" pyroxenite has been cut and offset by a pyroxenite dyke	56
16	Brecciated, interlayered dunite-pyroxenite	56

FIGURE		page
17	Dunite blocks in pyroxenite	57
18	Breccia. Blocks of dunite and dunite with pyroxenite layers in a pyroxenite matrix	57
19	Dunite breccia	58
20	Eye-shaped dunite block in coarse pyroxenite	58
21	Photomicrograph: Pyroxenite composed of about 25% orthopyroxene, now mostly serpentized, and clinopyroxene	60
22	Photomicrograph: Pyroxenite, variety websterite	60
23	Layering in "olivine" pyroxenite	64
24	Layering in "olivine" pyroxenite	64
25	Layering in "olivine" pyroxenite	65
26	Internal layering in "olivine" pyroxenite	65
27	Zoning in chromite. Electron microprobe scanning profile showing variation of aluminum, chromium and iron in a chromite grain	67
28	Foliation in peridotite	70
29	Pyroxene-rich layers in peridotite (type 1 layering)	70
30	Olivine orthopyroxenite layers in peridotite (type 1 layering)	71
31	Olivine orthopyroxenite layers interbanded with peridotite (type 1 layering)	71
32	Orthopyroxenite layers in peridotite (type 2 layering)	73
33	Orthopyroxenite layers in peridotite (type 2 layering)	73
34	Thin dunite layers in peridotite (type 3 layering)	74
35	Photomicrograph: Mosaic texture of peridotite	74
36	" : Straight boundaries of olivine crystals in peridotite	76
37	" : Recrystallized(?) olivine	76
38	" : Subhedral chromite grain included in enstatite	78

FIGURE		page
39	Photomicrograph: Regular, continuous exsolution lamellae of clinopyroxene in enstatite	78
40	" : Thick, discontinuous exsolution lamellae of diopside and thin, continuous ones in enstatite	80
41	Photomicrograph: Thick, discontinuous exsolution lamellae of diopside in enstatite	80
42	" : Exsolution lamellae bent by the twinning of enstatite	82
43	" : Bent exsolution lamellae in deformed enstatite	82
44	Trace element variations in peridotite	84
45	Compositional variations in coexisting olivine, orthopyroxene and chromite in peridotite of Caribou Mountain	89
46	Aluminum content of coexisting enstatite and chromite in peridotite and olivine orthopyroxenite	91
47	Compositions of coexisting orthopyroxene and olivine in ultramafic and mafic igneous rocks and in a pyroxene granulite	94
48	Variations of equilibrium constant K_T (ol-opx) versus temperature of equilibration for olivine-orthopyroxene pairs in the peridotite	96
49	Coarse-grained orthopyroxenite veins in peridotite	100
50	The exposed face of a planar orthopyroxenite vein in peridotite	100
51	Orthopyroxenite pod in peridotite	101
52	Photomicrograph: Anhedral enstatite grains in an orthopyroxenite vein in peridotite	101
53	Dunite layer in peridotite	104
54	Dunite layer in peridotite	104
55	A layer and a pod in peridotite	105
56	A dunite layer in peridotite, slightly offset by a fracture	105

FIGURE		page
57	A dunite pod with discordant apophyses in peridotite	107
58	Dunite in peridotite	108
59	Photomicrograph: Magnetite rimming chromite grains	108
60	Magnesium, iron and nickel contents of olivine in peridotite and in dunite bodies within peridotite	110
61	Zoning in chromite. Electron microprobe scanning profile showing variation of chromium and aluminum	113
62	Chromium content of chromite	116
63	Aluminum content of chromite	117
64	Total iron content of chromite	118
65	Magnesium and average titanium content of chromite	119
66	Photomicrograph: Irregularly shaped chromite	121
67	" : Irregularly shaped chromite in peridotite	121
68	" : Chromite grain across the boundary between two olivine grains	122
69	" : Irregularly shaped chromite	122
70	Ranges of Fo and En contents of olivine and coexisting orthopyroxene respectively from ultramafic rocks	125
71	Compositions of clinopyroxenes coexisting with orthopyroxene versus temperature of crystallization	130
72	Variation of compositions of clinopyroxenes from "herzolite" and "olivine" pyroxenite versus temperature and pressure of formation of these rocks	130
73	Coarse, massive chromitite layer	135
74	Chromitite with low chromite content interlayered with dunite	135
75	Detail of chromitite-dunite interlayering	136
76	Chromitite layer with low chromite content	136

FIGURE		page
77	Nodular chromitite, variety "grape ore" in serpentized dunite	138
78	Nodular chromitite, variety "grape ore"	138
79	Ill-defined layering of "grape ore" now largely deformed	139
80	Fine layering of chromite ore with occasional "grapes" of chromitite	139
81	Pencil-shaped concentrations in serpentized dunite	143
82	Chromitite schlieren and lenses in dunite	143
83	Chromitite veins	145
84	Chromitite in veins grading into chromitite with "chain structure"	145
85	A layer(?) of chromitite with "chain structure"	146
86	Chromitite with "chain structure"	146
87	Vertical and plane view of a hypothetical ore zone showing the inferred distribution pattern of chromite deposits	151
88	Folded chromitite layers	152
89	Faulted chromitite layer	152
90	Photomicrograph: Mortar texture of fractured chromite	154
91	" : Irregular fracturing of chromite	154
92	" : Magnetite replacing chromite	157
93	" : Corrosion and replacement of chromite by uvarovite	157
94	" : Olivine inclusions in chromite	158
95	" : Olivine inclusions in chromite	158
96	Composition of chromite in Bélanger pit	163
97	Total iron versus magnesium variation in chromite	165
98	Chromium versus aluminum variation in chromite	166

FIGURE		page
99	Plots of mean composition of chromite in chromitite from the map-area and analyses of chromite in "chromite seams" in four major stratiform complexes, the Bushveld, Great Dyke, Stillwater, and MuskoX intrusions	168
100	Plots of Cr versus Fe_{total} and Cr versus Mg in chromite of chromitite from the map-area, in chromite concentrates and massive chromitites from alpine-type ultramafic rocks elsewhere and from the Vourinos Ophiolitic Complex	169
101	Chromium versus Al in chromite of chromitite from the map-area, in chromite concentrates and massive chromitites from alpine-type ultramafic rocks elsewhere and from the Vourinos Ophiolitic Complex	170
102	Photomicrograph: Detail of serpentinization of olivine	175
103	" : Completely serpentinized olivine	175
104	" : The grid structure of serpentinized dunite	176
105	Radial fracture system in massive chromitite surrounding serpentinized dunite	176
106	Photomicrograph: Radial fractures in chromite around a serpentinized olivine island	182
107	" : Alteration of chromite by serpentinization	182
108	Types of chromitite structures in relation to the inclination of the primary magmatic layering	
IN THE APPENDICES		
109	Geological plan of the area around Sterrett Mine	219
110	Distribution of open pits in Sterrett Mine	220
111	American Chrome Company's Pits: Distribution of Old Workings	222
112	Plots of Mg-Fe distribution coefficients against Y_{Cr}^{sp} for coexisting orthopyroxene and chromite, and olivine and chromite	247

CHAPTER I

INTRODUCTION

The genesis of ultramafic-mafic rock associations in orogenic belts is very controversial. Hypotheses regarding their origin, mode of emplacement, serpentinization and their relationship to the host rocks are numerous and often contradictory. Similar controversy exists regarding the genesis of chromite deposits in the ultramafic rocks of orogenic belts.

The present work attempts to contribute to the understanding of the genesis of the chromite concentrations in ultramafic rocks which occur in the Eastern Townships of Quebec, Canada. It is hoped that the detailed documentation of these rocks will also contribute to the understanding of ultramafic rocks in orogenic belts in general.

The area of investigation is located in Megantic and Wolfe counties, in the Province of Quebec. The map-area lies between Thetford Mines to the north, Disraeli village to the south, Lake Bécancour to the east and includes King Mountains and Belmina Ridge to the west. It appears on the 1:50,000 topographical sheets 21 E/14 (east and west sheets), 21 E/13 (east sheet), 21 L/3 (east and west), and 21 L/2 (west sheet).

This area includes rocks of the Appalachian Serpentine Belt, which is a narrow zone of isolated felsic to ultramafic igneous rocks oriented parallel to the NE-SW trend of regional folding. The Serpentine Belt

can be traced from North Carolina in the southwest to the Gaspé Peninsula and eventually into Newfoundland to the northeast. Although the name "Serpentine Belt" has been given to this zone, volcanic rocks of various compositions constitute the major rock type; the ultramafic rocks occur as discontinuous bodies within this belt.

In Southern Quebec, ultramafic rocks of the Serpentine Belt reach their maximum development in the area of this study. Here, they form a horseshoe-shaped, northeast-southwest oriented body reaching a width of 12 km. The ultramafic rocks represented are dunite, harzburgitic peridotite, "lherzolite", "olivine" pyroxenite and several types of pyroxenite. There is also a large amount of gabbro present. Chromite, talc and important asbestos deposits are associated with the ultramafic rocks.

The ultramafic rocks, gabbro and other phaneritic rocks associated with these rocks are thought to be intrusive and the data pointing to their intrusive origin are presented later.

History of the chromite industry in the Eastern Townships

The first reference to the existence of chrome ore in the Eastern Townships of Quebec is in reports of the Geological Survey of Canada for the year 1846. The first ore shipment from this area was made in 1861 (Denis, 1932, p. 20). However, the first production of importance dates from 1894 in which year nearly one thousand tons of ore were shipped from deposits in Coleraine Township. With further ore discoveries, a small but steady production continued until 1910. Then outside competition, mainly from Rhodesia and New Caledonia, forced the Quebec chromite industry to stop. The total ore production from Coleraine Township up to 1910 was about 60,000 tons with the highest

production in 1906 when over 9,000 tons of ore were produced (Denis, 1932, p. 22).

During World War I the production of chromite resumed in the Eastern Townships area. Intensive prospecting resulted in the discovery of the Reed-Bélanger (Chromeraine) property in Coleraine Township and of the Sterrett Mine in Cleveland Township. Both deposits became major ore producers in the Eastern Townships. Over 114,000 tons of ore were produced from 1915 to 1918 (Denis, 1932, p. 23). At the end of the war, the chromite production from the Eastern Townships declined rapidly and ceased almost completely in 1923. Between the two world wars a yearly production of 100 to 300 tons of ore was shipped from Coleraine Township.

During the second World War operations were resumed with technical and financial help from the Federal Government. Active and quite systematic exploration and drilling, mainly near known deposits, proved new ore reserves, especially in the Reed Bélanger, Caribou and Montreal Pit deposits of Coleraine Township and in the Sterrett Mine, Cleveland Township. Several concentrating mills were built in Coleraine Township during the war period. The recorded shipment during the war totalled 90,619 tons of ore. (Mineral Production of Canada, 1956; Dominion Bureau of Statistics) After the war, production declined rapidly and ceased in 1950.

CHAPTER II

GENERAL GEOLOGY

II.1. PREVIOUS WORK

Sir William Logan's early reports for the Geological Survey of Canada are the first published geological records of the district. His descriptions, supplemented by Sterry Hunt's lithological and chemical analyses, were embodied in "The Geology of Canada" in 1863. Subsequently it became acknowledged that serpentinites generally resulted from the alteration of ultramafic rocks rather than from the alteration of magnesian limestone. In 1883, Adams suggested that the Quebec serpentinites supported this more modern hypothesis.

The first detailed consideration of the ultramafic rocks of this area was by Dresser (1913). He advanced the hypothesis that the granites, gabbros and ultramafic rocks of the region were derived from one magma by fractional crystallization, subsequent to intrusion. This conclusion has been subsequently supported by Knox (1917), Harvie (1923), and partially supported by Cooke (1937) and Riordon (1952). Denis (1932) studied the chromite deposits of the Eastern Townships and concluded that they are products of gravity settling from a magma.

Recently, Lamarche (1971, in press) suggested that ultramafic, mafic, acidic phaneritic rocks and aphanitic rocks in the map-area are in situ differentiation products of a giant submarine flow which, he

thought, was peridotitic in composition.

II.2. REGIONAL GEOLOGY

The Serpentine Belt is located in rocks which were deposited in the Appalachian geosyncline and subsequently involved in the Appalachian orogeny. The Appalachian geosynclinal system persisted from late Proterozoic to Permian time, and during this period there was a complex history of development of subsiding geosynclines and concomitant uplifts to form platforms. At the close of the Precambrian, the Avalon geosyncline, which was situated in the southeastern part of the Canadian Appalachians (in southern New Brunswick - Cape Breton Island), was folded and uplifted to form the Avalon platform. From Cambrian to Devonian time this Avalon platform separated the Acadian geosyncline to the northwest from the Meguma geosyncline to the southeast. The Serpentine Belt is located entirely within rocks deposited in the Acadian geosyncline.

Deposition within the Acadian geosyncline was continuous from late Precambrian to, perhaps, late Ordovician time (Poole, 1967). During this period, feldspathic sandstones, shales, limestones and conglomerates were deposited in the northwestern part of the Acadian geosyncline, in the area closest to the St. Lawrence platform, while volcanic rocks, greywackes and shales were deposited further away from the platform. It is these latter rocks which are host to the rocks of the Serpentine Belt.

According to Poole (1967), in the latest part of early Ordovician time, early phases of the Taconic orogeny caused uplift which interrupted deposition on the Avalon and St. Lawrence platforms. However, in southern Quebec the Acadian geosyncline seems to have undergone

orogenesis, accompanied by igneous activity, in latest Cambrian or in very early Ordovician time (Lamarche, oral comm., 1968).

In the Acadian geosyncline, deposition of a greywacke-volcanic sequence continued until early middle Ordovician time. In mid-middle Ordovician time, the second phase of the Taconic orogeny resulted in uplift and folding of the emerged Avalon platform. Poole (1967) believes that the ultramafic, mafic and minor granitic bodies of the Serpentine Belt were intruded at this time, mostly near the northwestern margin and to a lesser extent near the southeastern margin of the Acadian geosyncline. Henceforth, the designation "Serpentine Belt" will be applied only to the igneous belt near the northwestern margin. The northwestern margin of the Acadian geosyncline was uplifted during the second phase of the Taconic orogeny, contemporaneously with, or soon after, the emplacement of ultramafic bodies. Some formations (e.g. Sutton, Bennett, Shick Shock) within the marginal zone (i.e. west of the Serpentine Belt) were regionally metamorphosed. The late middle Ordovician rocks contain some boulders probably derived from these folded rocks (Enos, 1965).

In the Eastern Townships the late middle Ordovician rocks are dominantly greywacke and shale with few volcanic rocks. They constitute the Beauceville Group. The latest phase of the Taconic orogeny affected certain belts of the Acadian geosyncline toward the close of middle Ordovician time.

Subsequently, in the middle and late Devonian, the Acadian geosyncline was involved in the intense Acadian orogeny. This resulted in folding, faulting, granite intrusion, and uplift. The folds due to this orogeny have steep axial planes and their plunge varies, from

steeply northeast through horizontal to steeply southwest. Faulting is intense. Normal faults are most numerous, although transcurrent faults are also common. Some faults are thrust faults with overthrusting toward the St. Lawrence platform to the north. No ultramafic rocks appear to have been intruded during the Acadian orogeny, although there are numerous granitic intrusions. After the Acadian orogeny "The Appalachian geosyncline was transformed to a stable craton which thereafter was deformed mainly by faults, warps and gentle basinal subsidence." (Poole, 1967).

II.3. GEOFYSICAL DATA

A gravity survey of southern Quebec (Innes and Argun-Weston, 1967) has revealed the presence of a ridge-like positive gravity anomaly in the Eastern Townships (Fig. 1 A). A gravity profile, passing through Asbestos across the anomalous area, and the suggested interpretation (Fitzpatrick, 1953, in Innes and Argun-Weston, 1967) are shown in Fig. 1 B. According to this interpretation ultramafic mantle material forms a wedge, 20 km wide at its base and rises to a height of 25 km (Innes and Argun-Weston, 1967, p. 74). Since the positive gravity anomaly is ridge-like, it is possible that the inferred mantle wedge is also ridge-like and extends from the U.S. - Canada border to north of the Thetford Mines area.

II.4. LOCAL GEOLOGY

The area of this study is situated on the southeastern flank of an anticlinorium which is the northeasterly continuation of the Green Mountain-Sutton Range structure (Fig. 2). Geologically the area is rather

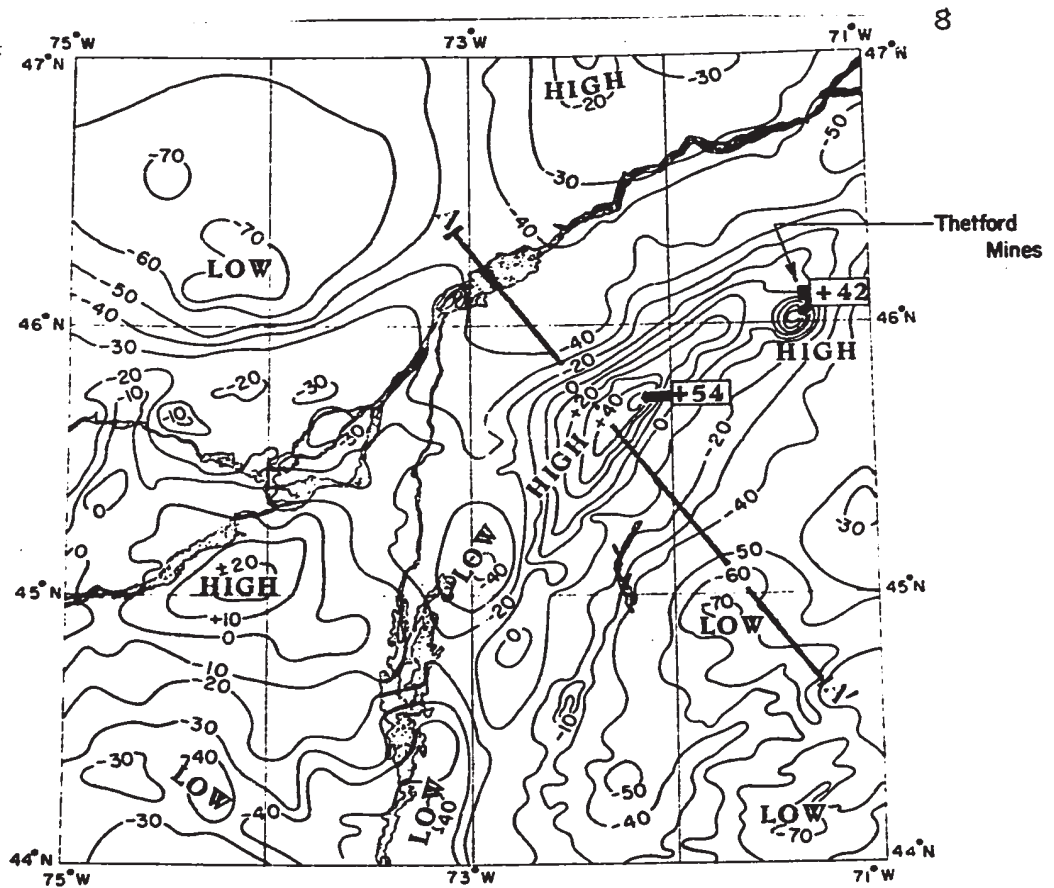


Figure 1 A. Bouguer gravity anomaly of southern Quebec and the northern parts of the adjoining states of New York, Vermont and New Hampshire.
From M.J.S. Innes and A. Argun-Weston (1967)

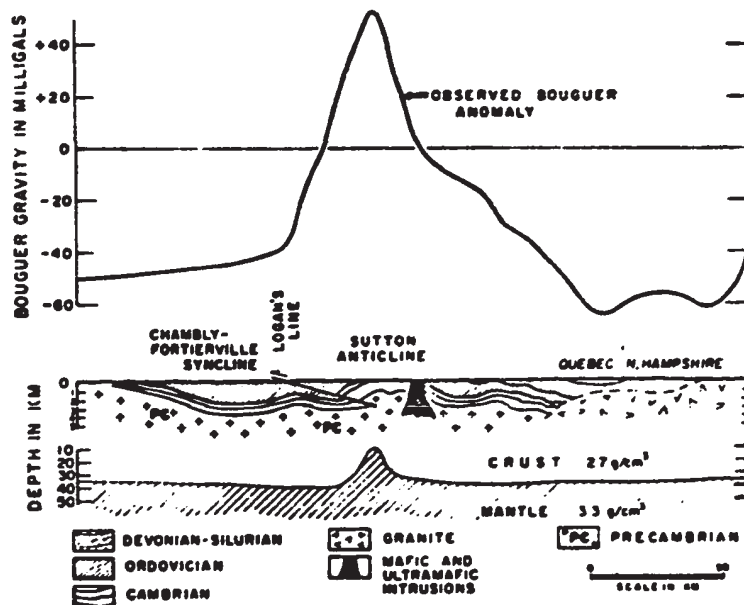


Figure 1 B. Generalized geological and crustal section and observed Bouguer anomalies for profile A-A' (after Fitzpatrick, 1953).
From M.J.S. Innes and A. Argun-Weston (1967)

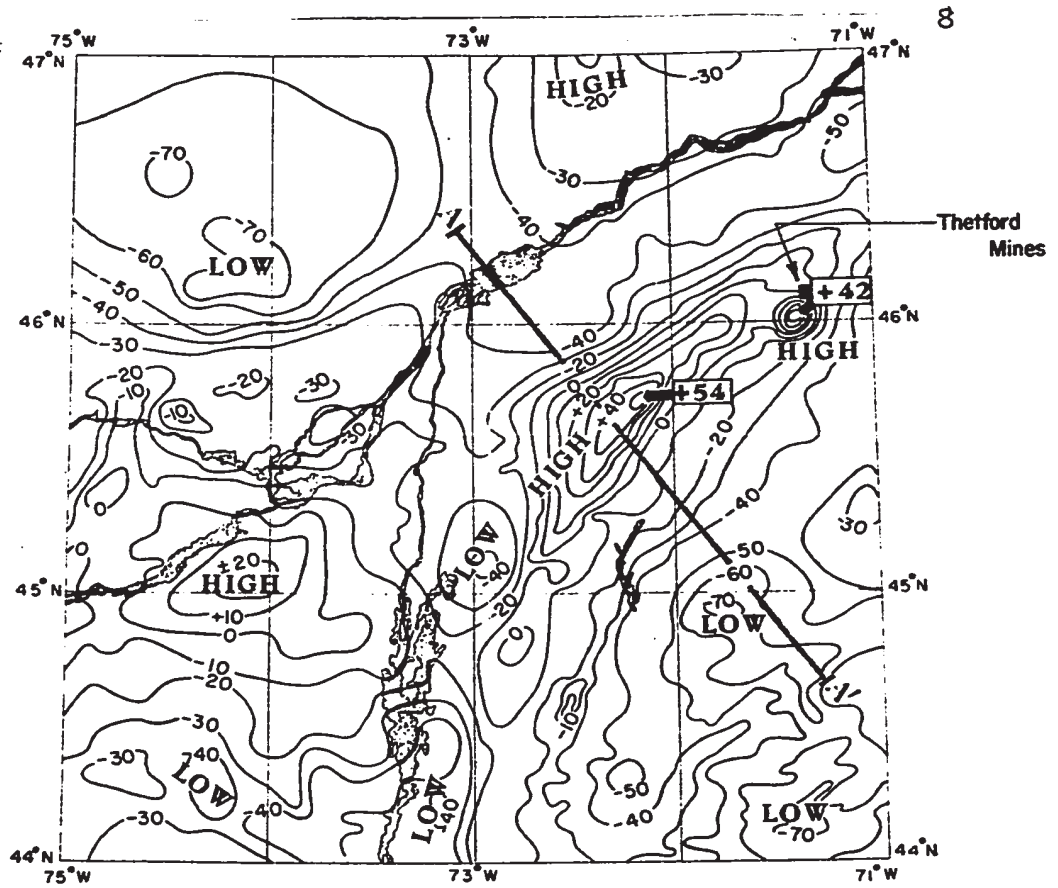


Figure 1 A. Bouguer gravity anomaly of southern Quebec and the northern parts of the adjoining states of New York, Vermont and New Hampshire.
From M.J.S. Innes and A. Argun-Weston (1967)

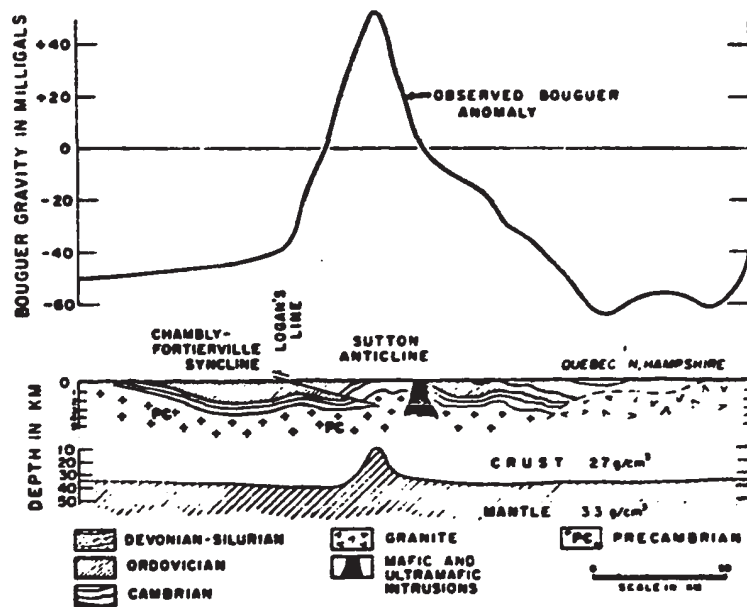


Figure 1 B. Generalized geological and crustal section and observed Bouguer anomalies for profile A-A' (after Fitzpatrick, 1953).
From M.J.S. Innes and A. Argun-Weston (1967)

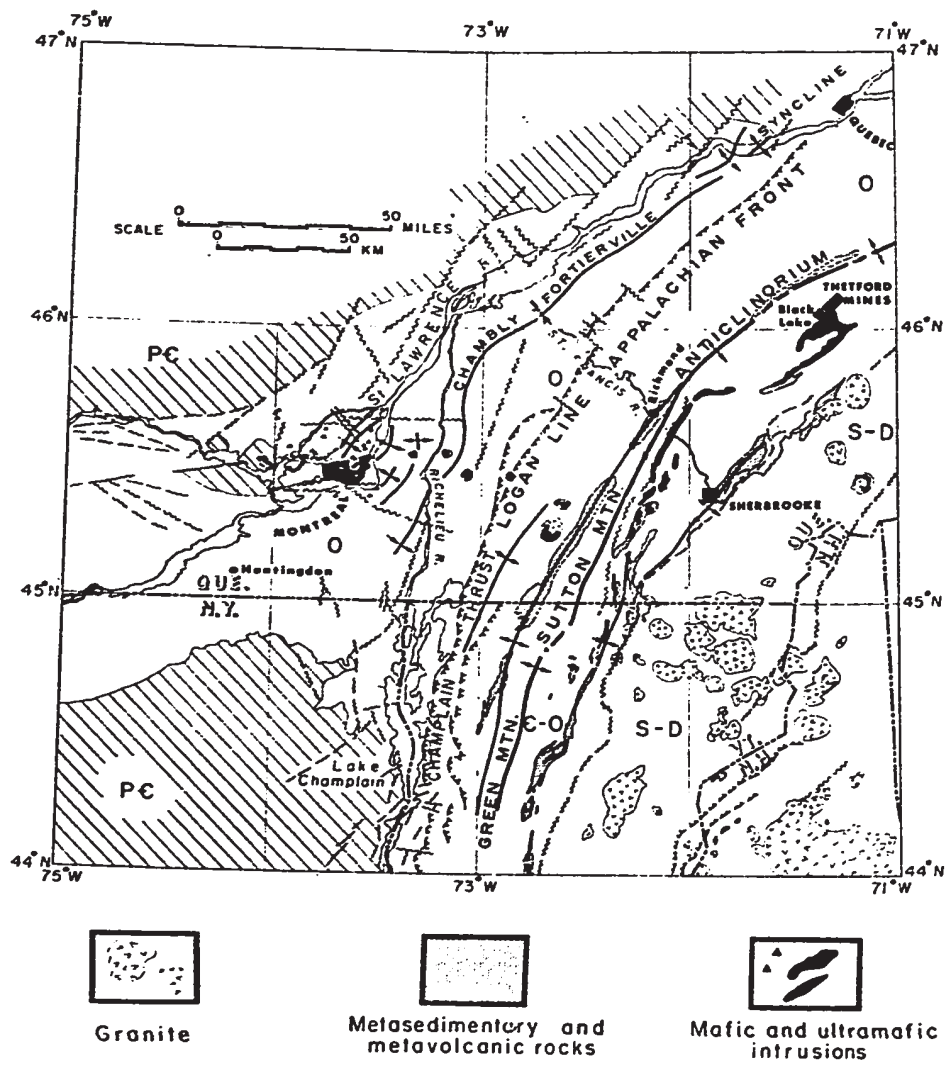


Figure 2. Map showing major structural elements of southern Quebec and the northern parts of the adjoining states of New York, Vermont, and New Hampshire. From M.J.S. Innes and A. Argun-Weston (1967)

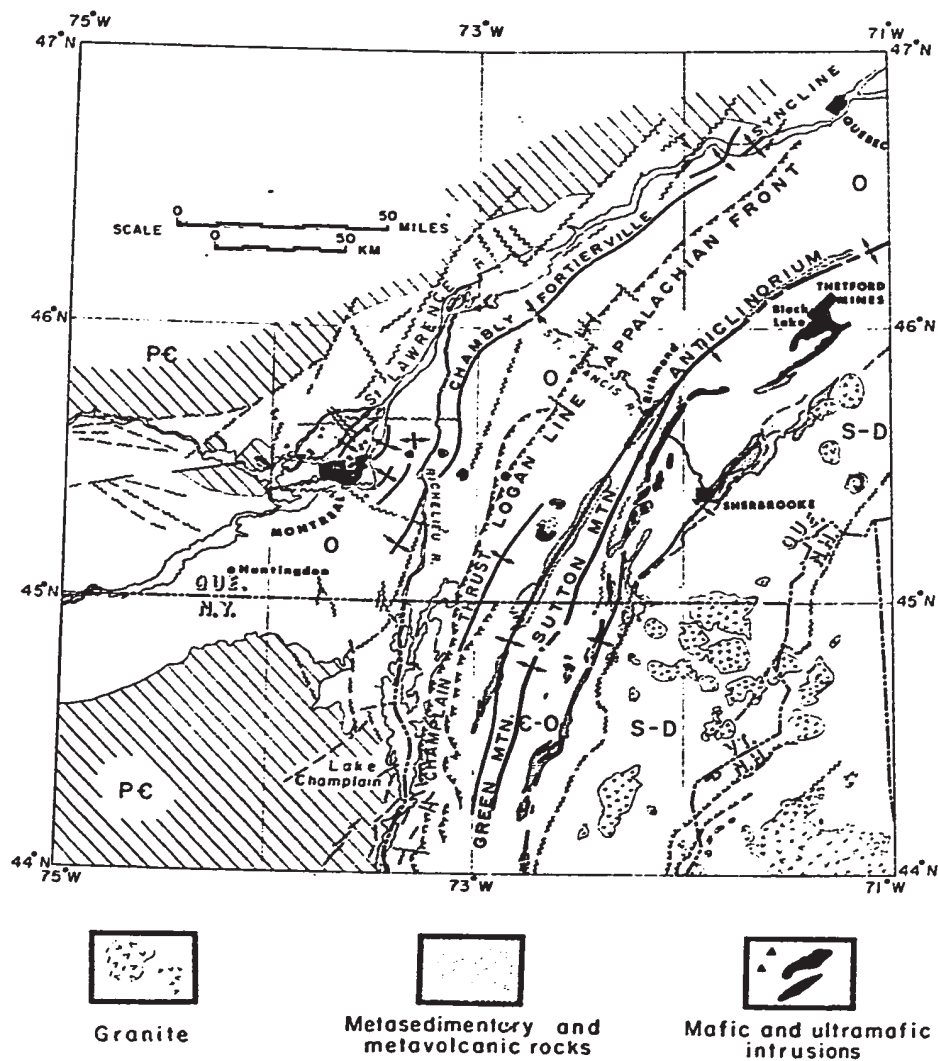


Figure 2. Map showing major structural elements of southern Quebec and the northern parts of the adjoining states of New York, Vermont, and New Hampshire.
From M.J.S. Innes and A. Argun-Weston (1967)

complex and, in spite of considerable work completed in this region since the middle of the nineteenth century, the stratigraphic and tectonic problems are not entirely resolved.

Geological and exposure maps based on the mapping by the present author have been prepared at the scale of 1:25,000 (Maps 1 and 2 respectively, back pocket). The geological succession in the map-area is given in Table I, largely based on unpublished regional mapping by Lamarche. The stratigraphic positions of the ultramafic and gabbroic rocks in Table I are proposed by the present author. The interpreted distribution of igneous and metasedimentary rock formations is shown in Fig. 3. This interpretation is based on maps by Cooke (1937) and Lamarche (1967-1971, unpublished) and on the present mapping (Map 2, back pocket). Where discrepancies existed, Lamarche's data have been taken as final, except for the distribution of ultramafic and mafic phaneritic rock types which have been mapped in greater detail by the present author.

Lamarche (1971, in press) has suggested that all the spatially related phaneritic and aphanitic rocks of the map-area are comagmatic differentiates of an alpine-type ophiolite complex. He believes this complex extruded on a geosynclinal ocean floor, during the lower Ordovician epoch. According to Lamarche the ophiolite complex conformably overlies the grey and green slates (basal St. Daniel) and unconformably overlies the Caldwell Formation. Lamarche (1971, oral comm.) observed basic pillow lavas conformably overlying the grey slates. He also observed unconformable contacts between the Caldwell Formation and overlying volcanic rocks.

TABLE I: TABLE OF FORMATIONS

CENOZOIC

Pleistocene: Glacial till, stream and lake deposits

Great unconformity

PALEOZOICMiddle Ordovician:

Beauceville Group: (not present in the map-area)
slate, tuff, siltstone

Unconformity

Middle and/or Lower Ordovician:

Gabbro and diorite
Ultramafic rocks
Gabbro, associated pyroxenite, diorite

Intrusive contact

St. Daniel Formation

Slate, phyllade, "wildflysch-type" metasedimentary rocks; slates and phyllade containing blocks of siltstone and greywacke

Volcanic rocks: (partly interbedded with metasedimentary rocks above); pillowed andesite, basalt, dacite, "Coleraine Breccia", intrusive? breccia, agglomerates, lapillis tuff. Pyroclastic rocks contain blocks of gabbro, pyroxenite and angular schistose blocks of Caldwell and Bennett metasedimentary rocks and blocks of chert.

Gabbro with some pyroxenite (inferred from gabbro and pyroxenite boulder in pyroclastic rocks; e.g. "Coleraine Breccia")

Grey and green slates








Metamorphism - Great unconformity

Cambrian









Caldwell Formation: metagreywacke, quartz-sericite schist; chlorite schist, minor quartzite, phyllade, basic lavas

Bennett Schists: phyllade, quartzite, graphitic schists, quartz-sericite, sericite, albite-sericite-chlorite schists, basic lavas

INTRUSIVE ROCKS

-  Gabbro, diorite
-  Pyroxenite associated with gabbro
-  "Acidic" rocks
-  "Olivine" pyroxenite, pyroxenite, "herzolite", some dunite
-  Dunite
-  Peridotite, some dunite, orthopyroxenite
-  Serpentinite

METASEDIMENTARY AND METAVOLCANIC ROCKS

-  Slate, phyllade and "argille à blocs" or "wildflysch-type" metasedimentary rocks
-  Mainly agglomerate, volcanic breccia with some basic lava
-  "Coleraine breccia"
-  Mainly basic lava
-  Grey and green slates
- Caldwell Formation
-  Mainly greywacke, some quartzite
-  Amphibolite
- Bennett schists
-  Phyllade, quartzite, schists
- Bedding, igneous layering
- Prevalent schistosity (usually S₁ or S₂).

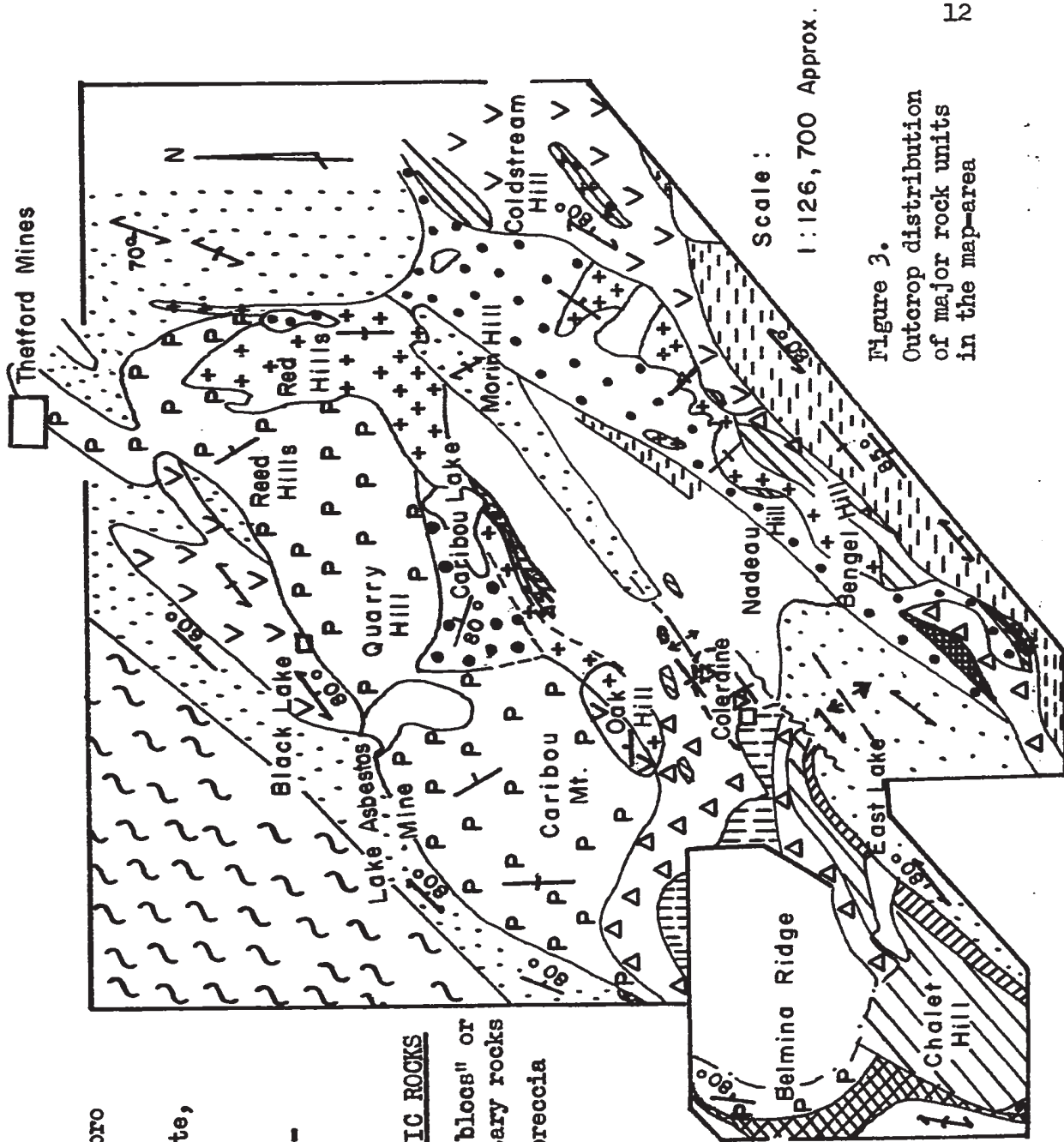

















Figure 3.
Outcrop distribution
of major rock units
in the map-area

INTRUSIVE ROCKS

-  Gabbro, diorite
-  Pyroxenite associated with gabbro
-  "Acidic" rocks
-  "Olivine" pyroxenite, pyroxenite, "Iherzolite", some dunite
-  Dunite
-  Peridotite, some dunite, orthopyroxenite
-  Serpentinite

METASEDIMENTARY AND METAVOLCANIC ROCKS

-  Slate, phyllade and "argile à blocs" or "wildflysch-type" metasedimentary rocks
-  Mainly agglomerate, volcanic breccia with some basic lava
-  "Coleraine breccia"
-  Mainly basic lava
-  Grey and green slates
- Caldwell Formation
-  Mainly greywacke, some quartzite
-  Amphibolite
- Bennett schists
-  Phyllade, quartzite, schists
- Bedding, igneous layering
- Prevalent schistosity (usually S₁ or S₂).

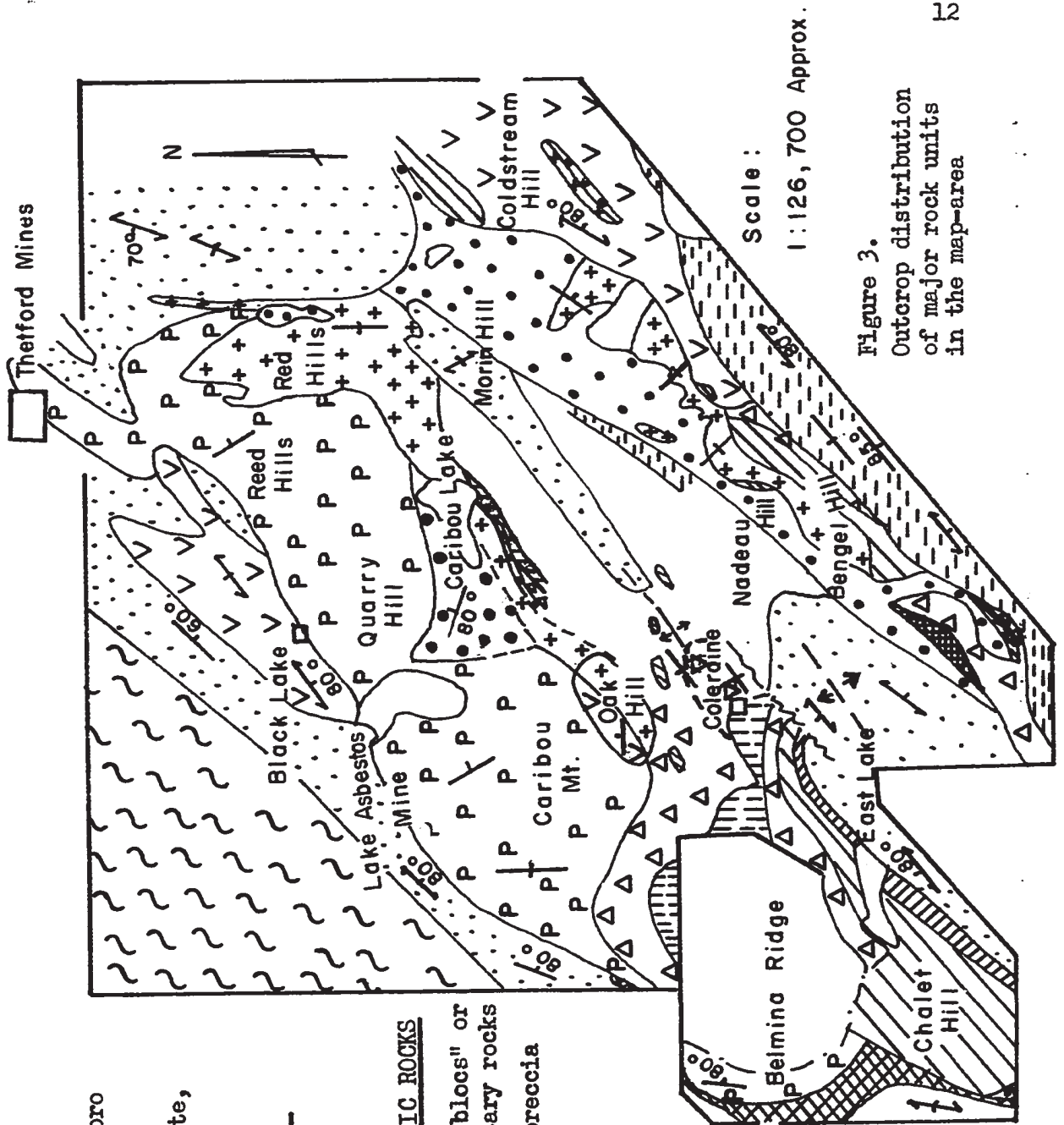


Figure 3.
Outcrop distribution
of major rock units
in the map-area.

Of particular interest to the history of the intrusive rocks is the "Coleraine Breccia" which contains abundant subrounded boulders of gabbro and basic lava. Subrounded and angular blocks of felsic aphanitic rocks and lenses and blocks of chert are also common. A pyroxenite boulder has been identified at the exposure of "Coleraine Breccia" at Coleraine village. Lamarche (1971, oral comm.) reports the presence of pebbles of a silicified talc-carbonate rock containing chromite, which presumably are pieces of olivine-bearing ultramafic rocks. "Coleraine Breccia" also contains large blocks of schist comparable to the Caldwell schist.

Lamarche's detailed regional mapping indicates that there is no large-scale thrusting in the Eastern Townships. Unconformable contacts between volcanic rocks and the Caldwell Formation seem to be depositional (Lamarche, 1971, oral comm.).

II.5. DISCUSSION AND CONCLUSION

The ultramafic and gabbroic rocks of the map-area belong to the Appalachian Serpentine Belt which is a narrow zone in which occur discontinuous intrusive and extrusive rocks. In southern Quebec, the Serpentine Belt is located near the boundary of the Acadian geosyncline with the stable St. Lawrence platform to the north.

The flexure zone between the stable continental platform and the geosynclinal basin was possibly a tension zone and thus the locus of deep and extensive fracturing. Such fractures perhaps served as channels along which ultramafic rocks intruded and other igneous activity took place. The deep fracturing along the continental slope probably developed during downwarping of the geosynclinal basin, hence perhaps very early in the history of the Acadian geosyncline. Thus,

the ultramafic material has been emplaced within a mobile environment which was subsequently affected by orogenic movements.

This postulated geological setting would explain, in part, some of the characteristics of the ultramafic rocks in the Serpentine Belt:

- (1) The association of ultramafic rocks with volcanic and gabbroic rocks
- (2) Their highly deformed nature
- (3) Their occurrence in a long, narrow belt parallel to regional fold trend

The presence of Caldwell schist-like blocks in the "Coleraine Breccia" and the presence of an unconformity between the Caldwell Formation and the overlying rocks suggest that the Caldwell Formation has undergone orogenic movements before the deposition of the "Coleraine Breccia". This is further suggested by the considerably higher metamorphic grade of Caldwell rocks compared with the overlying formations (Table I). This postulated orogeny should have occurred in, or before, Cambrian time, depending on the age of the Caldwell Formation.

No ultramafic and mafic intrusives associated with this orogeny have been described. However, it is at least possible that some of the serpentinite and serpentitized peridotite bodies occurring within the Bennett schists may have been emplaced during this orogeny.

In the map-area the phaneritic rocks are not confined to a precise stratigraphic horizon. Many small sill-like ultramafic bodies occur in the Bennett schists and in the Caldwell Formation. Pennington Dyke (2 km northwest of Thetford Mines, outside the map-area) is one of these sills and exhibits garnet-amphibolite contact metamorphism (Riordon, 1952). The large peridotite mass of Belmina Ridge is intrusive into the Caldwell metagreywackes and caused metamorphism of the country

rock (see Chapter III), while another large peridotite body to the northwest of Sunday Lake (3 km southwest of Chalet Hill, outside the map-area) is intrusive into similar rocks but does not have exposed contact metamorphism (Lamarche, oral comm., 1971). Along its northwest contact the main ultramafic mass in the map-area is in contact with volcanic rocks and metagreywackes belonging to different formations and ages. A similar situation exists along its southeastern contact where it is also in contact with gabbroic rocks (Fig. 3).

Nevertheless, it is perhaps significant that the ultramafic rocks occur at, or near, the contact of the Caldwell Formation with overlying unmetamorphosed rocks. The Caldwell Formation perhaps behaved as a cratonic block with respect to the overlying rocks during post-Cambrian orogenies and hence its upper contact was a favorable surface of intrusion. It is possible that during the late stage of their intrusive history some of the ultramafic rocks under study ascended along this contact.

Gabbroic rocks occur almost everywhere in the map-area. They may be located in volcanic rocks, between volcanic rocks and ultramafic rocks or between these latter and metasedimentary rocks (see Map 1 and Fig. 3). The large gabbro mass of Lemay Hill - Chalet Hill is intrusive into the Caldwell Formation (Fig. 3).

Recent regional mapping indicates that in the general area of the present study the mafic and ultramafic phaneritic rocks and the bulk of the mafic extrusive rocks are restricted to formations older than the Beauceville Group (Lamarche, 1971, in press). Furthermore, the bulk of the basic volcanic rocks occurs stratigraphically above the Caldwell Formation and below the Beauceville Group (Fig. 3 and Table I).

This somewhat stratigraphically restricted occurrence of the mafic and ultramafic igneous rocks is perhaps not coincidental. As suggested earlier, volcanism and intrusion of mafic and ultramafic material are different manifestations in the same period of igneous activity which presumably occurred early in the development of the eugeosyncline. Therefore, a somewhat restricted stratigraphic occurrence of igneous rocks, particularly basic extrusive rocks, is to be expected. Furthermore, since the phaneritic rocks do not intrude the Beauceville Group it is possible that their intrusion predated the deposition of this group.

It is further suggested that thick metavolcanic rocks, especially lavas, acted as a barrier to the intrusion of the mafic and ultramafic rocks. Extrusive and intrusive rock formations, in turn, acted as a barrier to the ascent of the other ultramafic masses. This damming effect, together with the fact that all the igneous rocks appear to have used the same fracture system as channels, are thought to have been the determining factors in the location and spatial association of igneous rocks in the map-area.

CHAPTER III

GENERAL GEOLOGY OF THE INTRUSIVE COMPLEX

III.1. INTRODUCTION

The igneous complex which consists of ultramafic, gabbroic and medium to coarsely granular felsic igneous rocks is henceforth referred to as the Intrusive Complex. As the name implies, it is petrologically and structurally complex and the rocks within it all exhibit the characteristics of plutonic rock with the exception of some diabase dykes.

The Intrusive Complex consists, in the main, of a large body of ultramafic rocks and a much smaller body of gabbroic rocks to the southeast of the ultramafic rocks (Map 1). The rock types present in the Intrusive Complex are defined in Table II. All the rocks are altered to varying degrees, but the name of the original rocks is used wherever this can be inferred, regardless of the degree of alteration. In the forthcoming descriptions, the terms "Ultramafic Suite" and "ultramafic rocks" do not include the pyroxenite of the Gabbroic Suite.

III.2. FORM OF THE INTRUSIVE COMPLEX

The aeromagnetic data (Geol. Survey, Canada, Maps No. 156G, 159G), where not complicated by the presence of basic igneous rocks, suggest

TABLE II
INTRUSIVE ROCKS

GABBROIC SUITE

Gabbro: a pyroxene-plagioclase rock with usually more than 40% pyroxene. Gabbro is medium to coarse grained.

Diorite or Leucogabbro: a plagioclase-pyroxene rock containing more than 60% feldspar. This rock grades into gabbro by an increase in pyroxene content.

Microgabbro, Microdiorite or Microleucogabbro: fine- to medium-grained gabbro and diorite or leucogabbro respectively.

Quartz diorite: a rock consisting of feldspar, ferromagnesian minerals and quartz.

Pyroxenite: a dull grey or brown weathering coarse-grained rock consisting of pyroxene. The pyroxene is mostly clinopyroxene; orthopyroxene is rare. Pyroxenite grades into melanogabbro by the appearance of plagioclase.

DIABASE? a fine- to medium- grained, brown weathering rock, which occurs in narrow dykes, has been mapped as diabase. It mainly consists of amphibole and epidote. Whether or not diabase is related to the Gabbroic Suite could not be established.

"ACIDIC"ROCKS: leucocratic rocks, acid to intermediate in composition. They are essentially feldspar - quartz - micas and/or amphibole rocks.

ULTRAMAFIC SUITE

Pyroxenite: grey or brown weathering, coarse-grained rock composed entirely of varying proportions of clino- and orthopyroxene. Pyroxenite is moderately altered.

Websterite: Pyroxenite consisting of clinopyroxene and 20 to 50% orthopyroxene.

"Olivine" pyroxenite: "Olivine" pyroxenite is identified by its brown weathering surface on which pyroxene grains appear in relief.

"Olivine" pyroxenite consists of orthopyroxene (up to 30% approximately), clinopyroxene (40 to 80% approximately) and accessory chromite. It is believed to have contained olivine. "Olivine" pyroxenite is strongly serpentinized.

"Lherzolite": it consists of serpentine (60 to 80%), clinopyroxene and accessory chromite. It is believed to have contained more than 50% olivine and some orthopyroxene.

Peridotite (Harzburgite): an olivine-orthopyroxene rock with accessory chromite and very rare clinopyroxene. Orthopyroxene constitutes 3 to 35% of the rock. Peridotite is moderately serpentinized.

Pyroxene-rich peridotite: peridotite containing 35 to 50% orthopyroxene.

Olivine orthopyroxenite: an orthopyroxene-olivine rock with accessory chromite and rare clinopyroxene. Orthopyroxene constitutes 50 to 95% of the rock.

Orthopyroxenite: consists almost entirely of orthopyroxene with rare olivine and clinopyroxene.

Dunite: olivine rock with accessory chromite (av. 2.5%). Dunite is commonly entirely serpentinized.

Serpentinite: a rock which consists almost entirely of serpentine, some amphibole and accessory chromite. The characteristics of the original rock have been obliterated by serpentinization.

Chromitite: a rock containing more than 35% chromite.

ULTRABASIC DYKES: very coarse-grained diopside - plagioclase dykes. Ultrabasic dykes are not common and occur only in rocks of the ultramafic suite.

that the boundaries of the exposed ultramafic body of the map-area are steep. Further, a gravity survey (Innes and Argun-Weston, 1967) has revealed the presence of a Bouguer gravity anomaly of + 42 miligals (Fig. 2A) centered on the ultramafic rocks under study. This anomaly has a steep gradient and rises from 0 to + 42 miligals within 8 km. The shape of the anomaly suggests that the exposed ultramafic body is steep-sided and continues to a considerable depth (2 km or more). This anomaly is superimposed on a broader anomaly which could be caused by another ultramafic body at a still greater depth. The available data do not permit one to conclude whether or not the two bodies are connected.

III.3. CONTACT RELATIONSHIPS

A. Ultramafic rock/country rock contact relationship

The contacts of the ultramafic rocks with metasedimentary and meta-volcanic rocks are almost everywhere sheared and appear to be fault-contacts. Furthermore, each contact is commonly parallel to the prevailing schistosity and bedding in the country rock and likewise appears to be steeply dipping. However, discordances and dyke-like offshoots of ultramafic material intruding the country rocks have been observed locally. Some easily accessible places, where the ultramafic rock/country rock contacts have been observed, are described below.

Nine hundred meters east of Granite Hill, on the southwest side of the road, peridotite can be seen intruding quartz-sericite schists of the Caldwell Formation. At the most westerly exposure, a peridotite dyke, 7 m wide, intrudes the schists. The contacts of the peridotite dyke are wavy. The dyke parallels the schistosity of the metasedimentary rocks, and the peridotite is schistose near the contacts. Both ends of

the dyke are drift-covered. Three hundred and fifty meters southeast of this exposure, a larger peridotite exposure forms a small hill. Here, the peridotite has a rounded and, in detail, wavy contact with meta-sedimentary rocks (Fig. 4). In a zone approximately 2 m wide around the contact, the schistosity of the metasedimentary rocks does not follow the general strike but turns around the ultramafic body, being more or less parallel to the rounded contact. The dip of the schistosity is variable but is always toward the ultramafic body. At the contact between schist and ultramafic rock, there is a 3 to 150 cm thick zone of a white chalky rock formed of acicular crystals of amphibole up to 4 cm long, in a talc groundmass. In a zone about 1 m wide around the contact the metasedimentary rocks, which are normally rich in quartz veins, do not contain any quartz veins. Probably quartz has been used up to form the rock of the reaction zone. A similar reaction zone is better displayed on an exposure 35 m to the south. Similar reaction zones and impoverishment of metasedimentary rocks in quartz have been observed around a number of serpentinite lenses in the Caldwell schists, south of Lemay Hill.

Four km. northwest of Black Lake village, near Highway 49, are four small elliptical bodies of serpentinite oriented with their long axes parallel to the schistosity of the enclosing metasedimentary rock. The best exposed of these bodies is on the northeast side of Highway 49, 500 m. from the road. This is a lenticular body 250 m long and 30 m wide at the widest part. A 30 to 60 cm wide drift-covered zone masks the actual contact with metasedimentary rocks. The remarkable thing is that nowhere around this body, nor around most others, does the schistosity of the metasedimentary rocks seem to be disturbed noticeably.

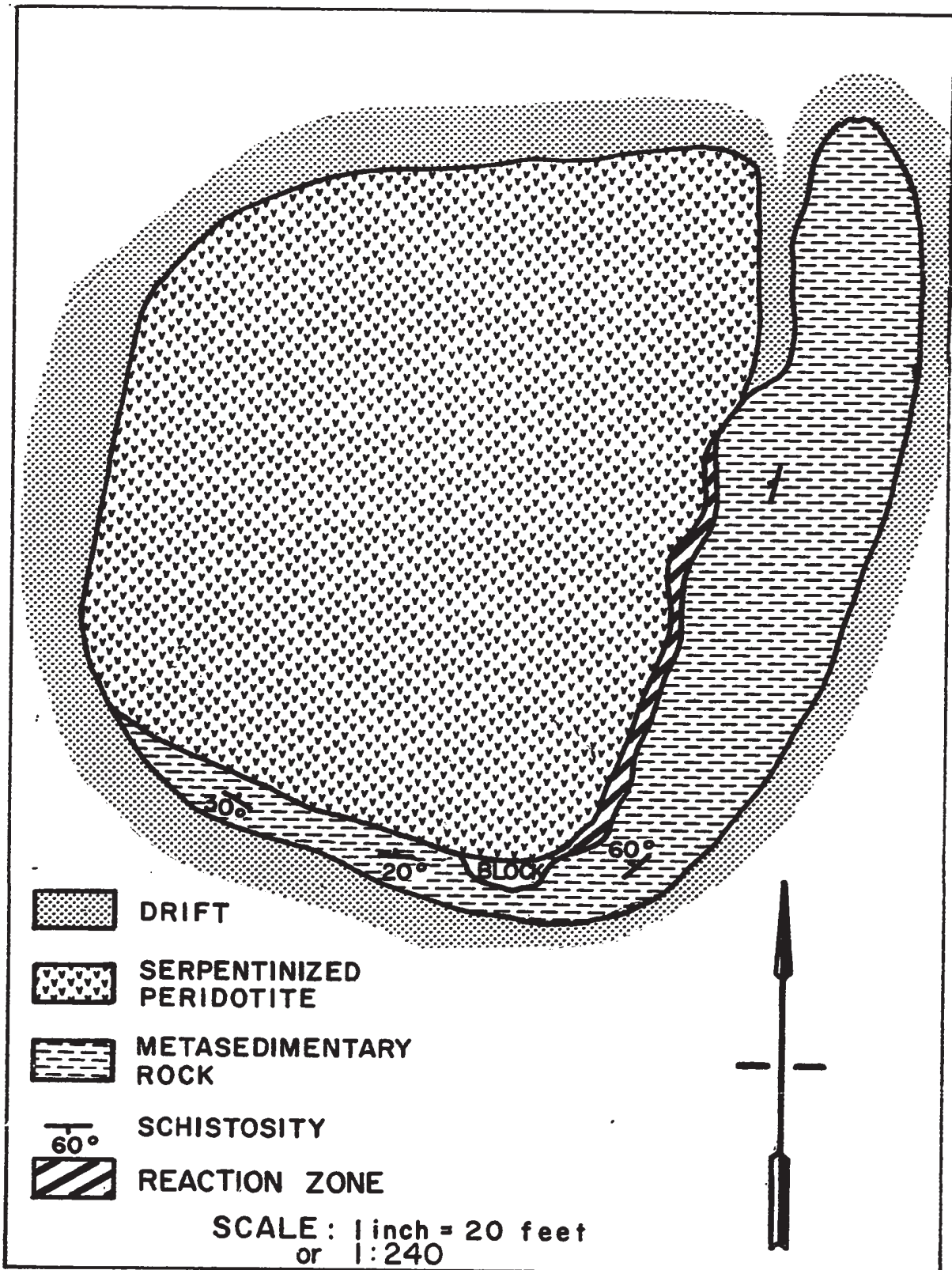


Figure 4. Peridotite-metasedimentary rock contact relationship (1200 meters east of Granite Hill, on the southwest side of the road)

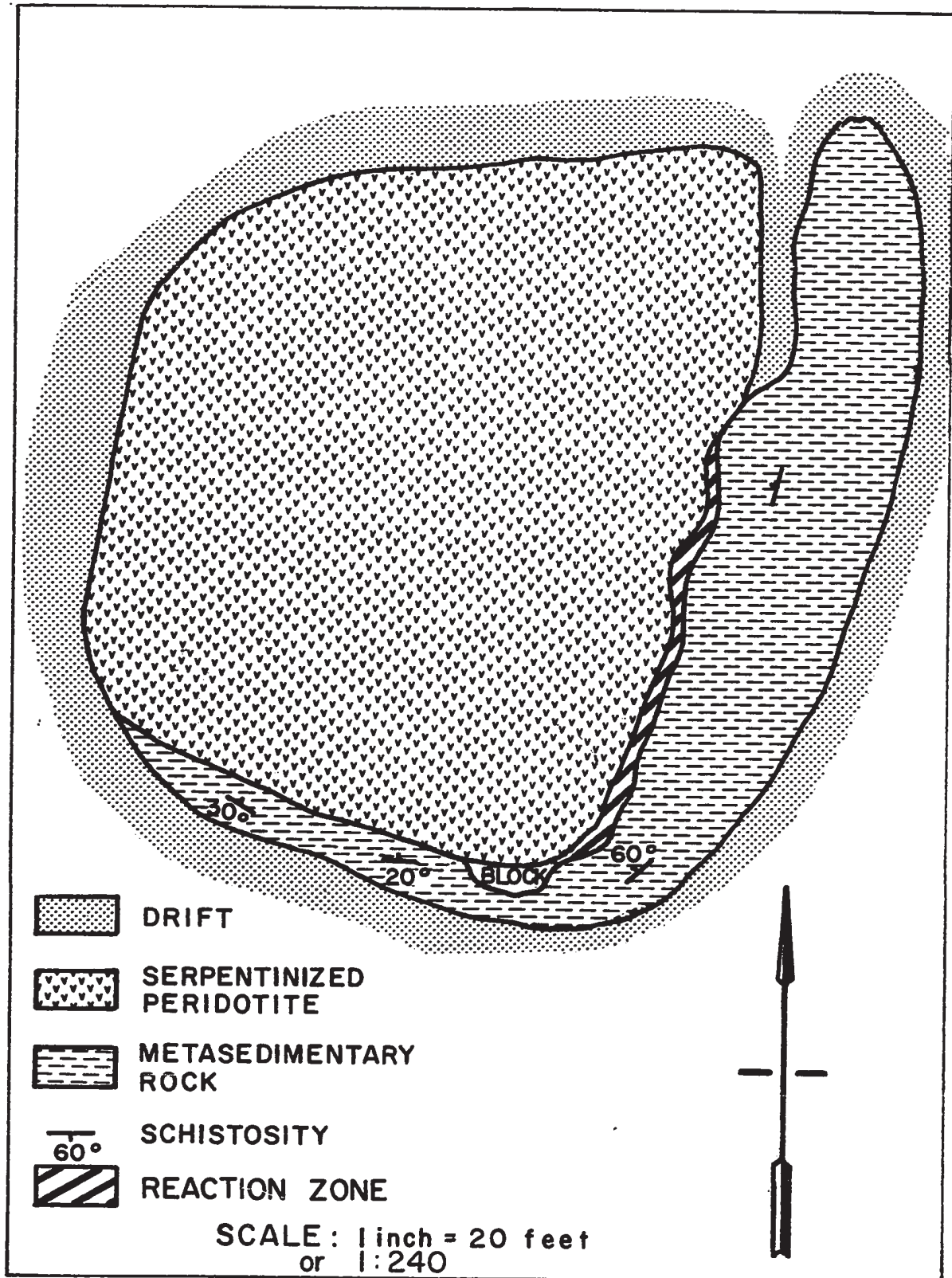


Figure 4. Peridotite-metasedimentary rock contact relationship (1200 meters east of Granite Hill, on the southwest side of the road)

There is no brecciation nor fracturing of the metasedimentary rocks. This observation is thought to indicate that the emplacement of the ultramafic rocks involved predates the development of the latest schistosity, which is apparently related to the Acadian orogeny.

A metasedimentary rock/peridotite contact is well exposed in the Normandie Mine (asbestos) where the north and northwest walls of the open pit consist mostly of metasedimentary rocks of the Caldwell Formation. The mine plan indicates an irregular contact. The metasedimentary rock extends toward the south-southeast into the lower levels of the pit as a tongue-like protrusion. The metasedimentary rock/ultramafic rock contact is commonly schistose and near the contact the metasedimentary rocks exhibit intense folding. "Acidic" rocks are intruded locally along the contact. Some vertical boreholes around the Normandie Mine which began in the metasedimentary rocks passed into peridotite and back into metasedimentary rocks, indicating an interfingering contact between Caldwell rocks and the peridotite. Borehole information also indicates that on a larger scale the northwest contact of the ultramafic rocks dips 65 to 75° toward the northwest which is perpendicular to the bedding in the country rock.

A small amphibolite exposure has been uncovered 500 m southwest of the Normandie Mine and boreholes intersected amphibolite at the contact of the ultramafic rocks and the Caldwell metagreywackes 400 m southwest of the open pit. No other data are available at present about this occurrence. It is probable that this amphibolite occurrence is related to a wedge of the Belmina Ridge peridotite body which has caused contact metamorphism described in the following pages.

Amphibolite: Possible contact metamorphism

To the west of Chalet Hill and Belmina Ridge, there is an extensive area underlain by amphibolite. Amphibolite has also been mapped 2.5 km southwest of King Mountains and it is not known whether or not this outcrop is the continuation to the north of the previous one. West of Chalet Hill, the amphibolite outcrop is about 500 m. wide and becomes more than 1 km. wide along the peridotite mass of Belmina Ridge. The true thickness of the amphibolite zone is not known.

The amphibolite is a dark green or black rock. It usually contains up to 20% feldspar and green hornblende. Sericite, chlorite, epidote and garnet have been observed locally. The grain size varies from very fine to coarse. Banding, due to the alternation of layers of different feldspar content, is very common. Usually, but not always, away from the gabbro and the ultramafic intrusions, the amphibolite exhibits well-developed schistosity but no obvious banding. Approaching the intrusions, the schistosity disappears and the amphibolite becomes darker, coarser grained and banded, feldspar-rich layers alternating with feldspar-poor layers.

The amphibolite/metasedimentary rock contact can be gradational or sharp (see Map 1). Intermediate rocks, such as amphibole-epidote schist and epidote-sericite schist, are found along most of the amphibolite/metasedimentary rock contact. However, in places, coarse black amphibolite is in direct contact with weakly metamorphosed metagreywackes. Locally, within one exposure, discontinuous, massive amphibolite layers can be seen adjacent to epidote and/or sericite-bearing foliated layers. This type of inhomogeneity could perhaps have been inherited from the original rock from which the amphibolite was derived.

The inhomogeneity of the amphibolite, the similarity of the surface appearance to the adjacent Caldwell metagreywacke and the gradational contact with this latter suggest that the amphibolite was derived from the Caldwell metagreywacke.

The mineralogical and textural changes in the amphibolite approaching the contact with peridotite, described earlier (p. 24), suggest that the development of amphibolite is related to its intrusion and is perhaps due to contact metamorphism of the metasedimentary rocks. However, it is striking to find such a wide amphibolite zone here, while nothing of comparable magnitude exists along other parts of the intrusive/country rock contact within the map-area. The fact that similar contact effects are not found associated with larger, but otherwise comparable ultramafic bodies suggests that the postulated metamorphism did not occur at the present place. This is further suggested by the existence of amphibolite where there are virtually no exposed ultramafic rocks (e.g. west of Chalet Hill). Therefore, it is tentatively proposed that amphibolitization occurred at depth and that the amphibolite and part of the Caldwell metagreywacke, into which it grades, have been emplaced by faulting.

The above interpretation, if correct, has important implications. The suggestion here is that the ultramafic rocks have caused considerable metamorphism at depth. Contact metamorphic aureoles resembling the amphibolite zone of the map-area occur around the peridotite intrusions of Lizard (Cornwall, Tinaquillo (Venezuela) and Mt. Albert (Canada), for which Green (1967) suggested temperatures of intrusions in the range 1000° to 3300° C. Therefore, the presence of amphibolite perhaps suggests that some of the ultramafic material in the map-area

was hot when it reached the upper crust.

B. Ultramafic rock/non-ultramafic rock contact relationship

Contacts between the ultramafic rocks and rocks of the Gabbroic Suite are sharp. No gradation and no interlayering have been observed nor has evidence of chilling been found except in one location. The exception is found 1 km southeast of Peach Lake where chilled gabbro is in contact with serpentized, schistose dunite. Some microgabbro is observed to cut dunite and act as cement in dunite breccia.

"Acidic" rocks crosscut the ultramafic rocks and occur almost exclusively in peridotite and dunite.

III.4. DISTRIBUTION OF ROCKS AND LARGE-SCALE FIELD RELATIONSHIPS

A. Distribution

Gabbroic Suite

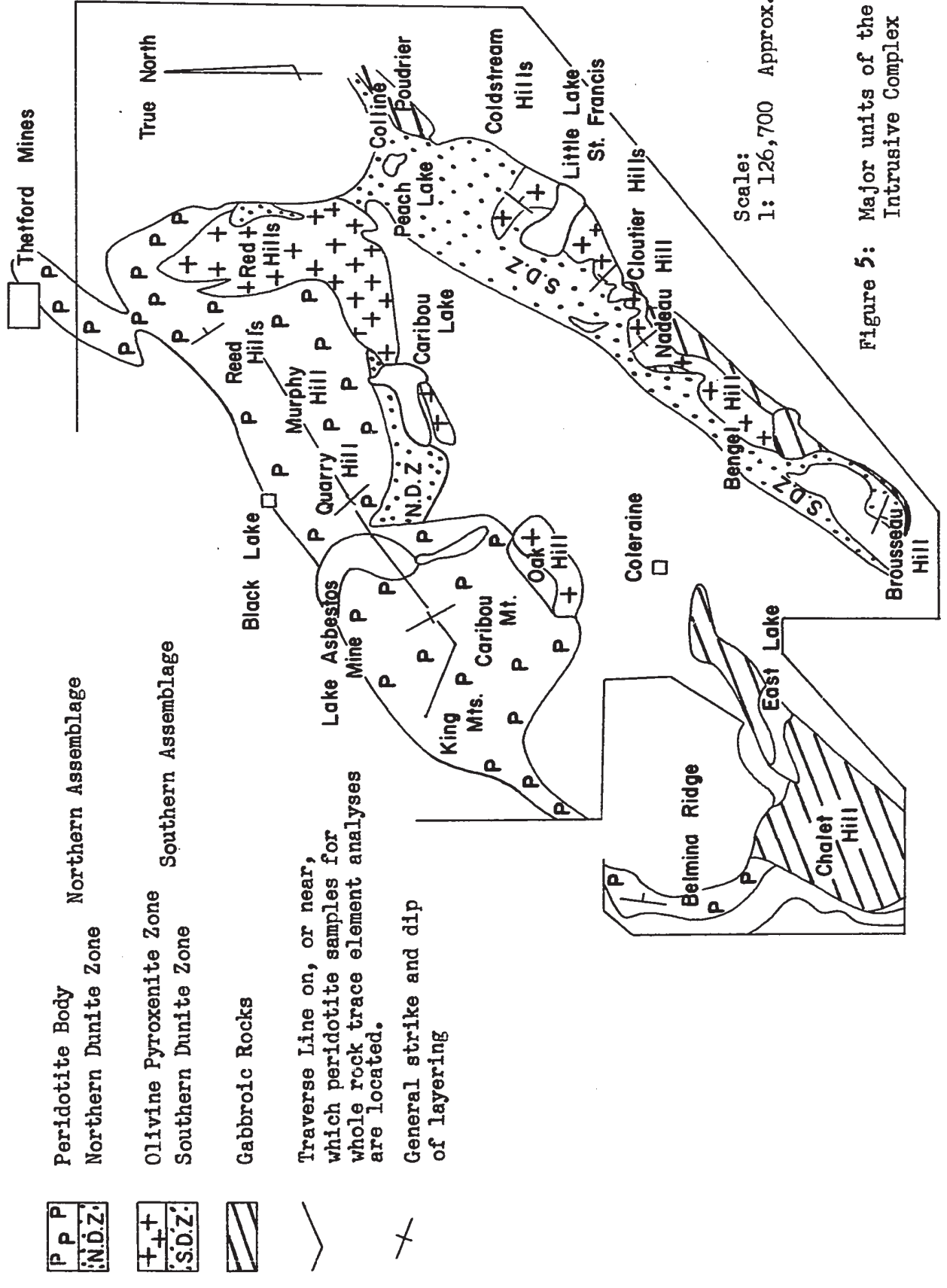
The main gabbro zone extends southwest-northeast from east of Brousseau Hill to west of Little Lake St. Francis, along the eastern margin of the ultramafic outcrops (see Map 1 and Fig. 5). This gabbro is discontinuous, being interrupted by both volcanic and sedimentary rocks.

A second major gabbro body extends east from Peach Lake to Trout Lake (outside the map-area). It forms Adstock Mountain, the highest hill in the region.

A third gabbro body, with some pyroxenite, outcrops to the west of Coleraine and underlies large areas to the southwest of East Lake. Several other smaller gabbro bodies are present.

Pyroxenite - "olivine" pyroxenite - "herzolite" assemblage

Because of their intimate association the distribution of



P	P	P
Northern Dunite Zone		

+	+
S.D.Z.	

Olivine Pyroxenite Zone	
Southern Dunite Zone	

Peridotite Body	
Northern Assemblage	

Olivine Pyroxenite Zone	
Southern Dunite Zone	

Gabbroic Rocks	
----------------	--

Traverse Line on, or near, which peridotite samples for whole rock trace element analyses are located.	
--	--

General strike and dip of layering	
------------------------------------	--

Northern Assemblage	
Southern Assemblage	

Olivine Pyroxenite Zone	
Southern Dunite Zone	

Gabbroic Rocks	
----------------	--

Traverse Line on, or near, which peridotite samples for whole rock trace element analyses are located.	
--	--

General strike and dip of layering	
------------------------------------	--

Scale: 1: 126,700 Approx.

Figure 5: Major units of the Intrusive Complex

"herzolite", "olivine" pyroxenite and pyroxenite is not described separately. This assemblage also contains dunite. Numerous faults cut the areas underlain by rocks of this assemblage which are apparently resistant to weathering, since each block forms a steep-sided hill above the adjacent serpentized dunite.

Two major areas of these rocks were mapped. The first forms a belt extending from east of Little Lake St. Francis to Brousseau Hill, and the second appears as a southwesterly trending ridge from Red Hills to Caribou Lake (see Map 1). Airborne magnetic data suggest continuation of this belt past Caribou Lake to Oak Hill.

Peridotite

Peridotite occurs on the northwestern side of the Intrusive Complex. It forms a continuous body extending to the southwest from Thetford Mines beyond the limits of the map-area. The peridotite of Belmina Ridge in the south-southwest extremity of the map-area is probably in contact with this body. The contact of peridotite with sedimentary and volcanic rocks in the northwest is almost everywhere schistose and faulted and it is along this contact that the asbestos deposits of Thetford - Black Lake are situated. To the south and southwest, the peridotite is in contact with dunite and "olivine" pyroxenite.

Dunite

Dunite occurs throughout the ultramafic portion of the Intrusive Complex as scattered bodies, as layers within the other rock types and also as wide, continuous zones. It generally occupies low-lying, poorly-exposed areas flanking hills formed by pyroxenite and peridotite. There are two major dunite zones in the map-area.

The Northern Dunite Zone extends from northeast of Caribou Lake to northwest of Colline Provencal. The eastern edge of this zone, beyond Caribou Lake, has been located on the basis of topographic relief and aeromagnetic data and is thus only approximate. The western and northwestern extension is inferred from observed exposures and drill core information. This dunite zone contains some of the most important chromite workings of the region, such as Reed-Bélanger, the Caribou, the Greenshields and a dozen or so smaller ones (see Map 3). Between the Northern Dunite Zone and the peridotite of Quarry Hill is a mixed zone of dunite and peridotite.

The Southern Dunite Zone is much more extensive than the Northern Dunite Zone. It extends from north of Adstock Mountain in the northeast to Brousseau Hill to the southwest. The Southern Dunite Zone is poorly exposed and its northwestern boundary is largely hypothetical, especially in the southwestern part of the map-area, however, the zone appears to be continuous. The Southern Dunite Zone is more schistose, faulted and much more serpentized than the Northern Dunite Zone. The weathered surface of the dunite is reddish-brown and rough due to the protrusion of small dunite fragments. This "inhomogeneous" dunite forms extensive exposures in the Southern Dunite Zone. East of Peach Lake, it forms Poudrier Hill with steep cliffs and slopes just like the hills formed by "olivine" pyroxenite. Southwest from Peach Lake to Little Lake St. Francis, "inhomogeneous" dunite forms an area of high relief which is interrupted north of Little Lake St. Francis by the low valley of Asberham River. High relief caused by dunite again occurs at the north of Nadeau Hill where the Beebe Realty Chrome prospects are. To the southwest the exposures are much smaller and discontinuous.

Serpentinite

Small isolated serpentinite lenses occur to the northeast of East Lake and to the west of Chalet Hill, in the northwest of the map-area.

B. Field relationships between major ultramafic rock groups

Definitions

In the forthcoming descriptions, the ultramafic outcrop, which consists mainly of peridotite with small amounts of dunite, olivine orthopyroxenite and orthopyroxenite and which extends from Thetford Mines to Belmina Ridge, is referred to as the Peridotite Body. The Peridotite Body and the Northern Dunite Zone, defined earlier, are grouped under the name of the Northern Assemblage (Fig. 5).

The mixture of "olivine" pyroxenite, "herzolite", pyroxenite and dunite that forms Bisby Ridge, Cloutier Hills and Red Hills is referred to as the Olivine Pyroxenite Zone. The ultramafic rocks of Oak Hill are also included in this zone. The Southern Dunite Zone, defined earlier, and the Olivine Pyroxenite Zone form the Southern Assemblage (Fig. 5).

Northern Assemblage

At Colline Provencal and on the southern slope of Quarry Hill, there is fairly continuous exposure from the Northern Dunite Zone to the Peridotite Body. One passes from dunite with very rare bands of peridotite in the south into peridotite with few dunite bands to the north. Thus the transition occurs by intermixing of the rock types. However, the areas where peridotite and dunite occur intermixed do not form a single, regular zone.

Southern Assemblage

The contact between the Southern Dunite Zone and the Olivine

Pyroxenite Zone is faulted in places but transitional in others. The transition between these two zones results from the intermixing of pyroxene-rich rocks with dunite either as distinct layers or irregular bodies, one in the other, too small to be mapped separately. There is no intermediate rock type between dunite and pyroxene-rich rocks. Along Bisby Ridge, Cloutier Hills and Diamond Hills dunite outcrops in each valley between "olivine" pyroxenite hills, suggesting that dunite underlies the Olivine Pyroxenite Zone which must then be a thin sheet gently dipping to the southeast (Fig. 6). It is likely that almost the entire Southern Dunite Zone was once overlain by the Olivine Pyroxenite Zone. The isolated "olivine" pyroxenite exposure to the north of Nadeau Hill might represent a remnant of this sheet.

Northern Assemblage and Southern Assemblage field relationships

Nowhere is the contact between the Northern and Southern Assemblages exposed. The closest approach is where peridotite of Reed Hills is separated by 160 m from "olivine" pyroxenite of Red Hills. Here, there is no variation in petrography or grain size of the rocks approaching the contact from either side. Therefore, the contact appears to be sharp.

Except for dunite, each of the ultramafic rock types occurs either only in the Northern Assemblage or only in the Southern Assemblage. On the basis of their dissimilar petrography and their sharp contact relationship, it is suggested that the Northern and Southern Assemblages were intruded separately and that they do not represent a continuous differentiation series. The Southern Assemblage is noticeably more altered and schistose than the Northern Assemblage. Furthermore,



Figure 6. Nadeau Hill seen from the east. The Olivine Pyroxenite Zone bordered by the cliffs forms a sheet dipping 15 to 20° to the southeast (i.e. to the left). Dunite occurs just below the cliffs.



Figure 6. Nadeau Hill seen from the east. The Olivine Pyroxenite Zone bordered by the cliffs forms a sheet dipping 15 to 20° to the southeast (i.e. to the left). Dunite occurs just below the cliffs.

layering in the Southern Assemblage is more irregular than in the Northern Assemblage. Perhaps the Southern Assemblage was emplaced first and hence was subjected to deformation for a longer time than the Northern one.

III.5. MEGASCOPIIC DEFORMATION OF ULTRAMAFIC ROCKS

Identifiable folds are rare in the ultramafic rocks. Faults are numerous. Where displacement cannot be seen, the presence of faults can be inferred from more intense serpentinization or carbonitization or from a sharp break in the topography.

In the Southern Assemblage, one set of fractures strikes northeast-southwest and another set is close to north-south. In the Northern Assemblage, the mean strike of fractures is north-south for one set and east-west for the second. Some faulting predates serpentinization, however, some faulting and brecciation post-dates serpentinization as indicated by numerous slickenside surfaces coated with serpentine. Locally, post-serpentinization deformation of chromitite has produced a rock consisting of serpentine-coated chromite fragments.

Except on Reed Hills, the rocks of the Northern Assemblage exhibit more or less well-developed jointing. In contrast, the rocks of the Southern Assemblage do not exhibit marked jointing.

III.6. INTERNAL STRUCTURES OF ULTRAMAFIC ROCKS

A. Layering and foliation

Layering is very common in the ultramafic rocks. The most common type of layering is the interlayering of different rock types, for instance, dunite, olivine orthopyroxenite and orthopyroxenite occur as layers in peridotite, while interlayering of dunite=pyroxenite, dunite-

chromitite, dunite - "herzolite", "herzolite" - "olivine" pyroxenite and "olivine" pyroxenite - pyroxenite is very common. Layering due to varying proportions of constituent minerals within one rock type is also very common. The thickness of layers varies from about 1 mm. to 3 m., although most of them are 1 cm. to 50 cm. thick.

Foliation is common in peridotite. It is brought about by planar arrangement of unoriented pyroxene crystals.

Figure 7 shows pyroxenite + "olivine" pyroxenite and dunite exposures at the southern part of Red Hills in the Southern Assemblage. In spite of the several faults and fractures that have been mapped, it can be seen that the strike of layering is, in the main, northeast-southwest. This suggests that, at the time of emplacement, layering probably had a fairly constant strike throughout large areas, and the presently observed variations are mainly due to subsequent deformation.

Layering and foliation are almost everywhere vertical or steeply dipping, even where the boundaries between the major ultramafic rock units appear to be gently dipping. The strike of layering is locally discordant to the strike of contacts between major ultramafic rock units and is also, in the main, perpendicular to the elongation of the ultramafic bodies, with the exception of Belmina Ridge where they are subparallel to the elongation of the ridge. The strike and dip of layering and foliation are not parallel to the schistosity or bedding of the country rock, in fact, they are commonly mutually perpendicular.

With the exception of Murphy Hill and Reed Hills, the strike and dip of layering are fairly constant in the Peridotite Body. They are variable in the Southern Assemblage, perhaps due to fracturing and faulting.

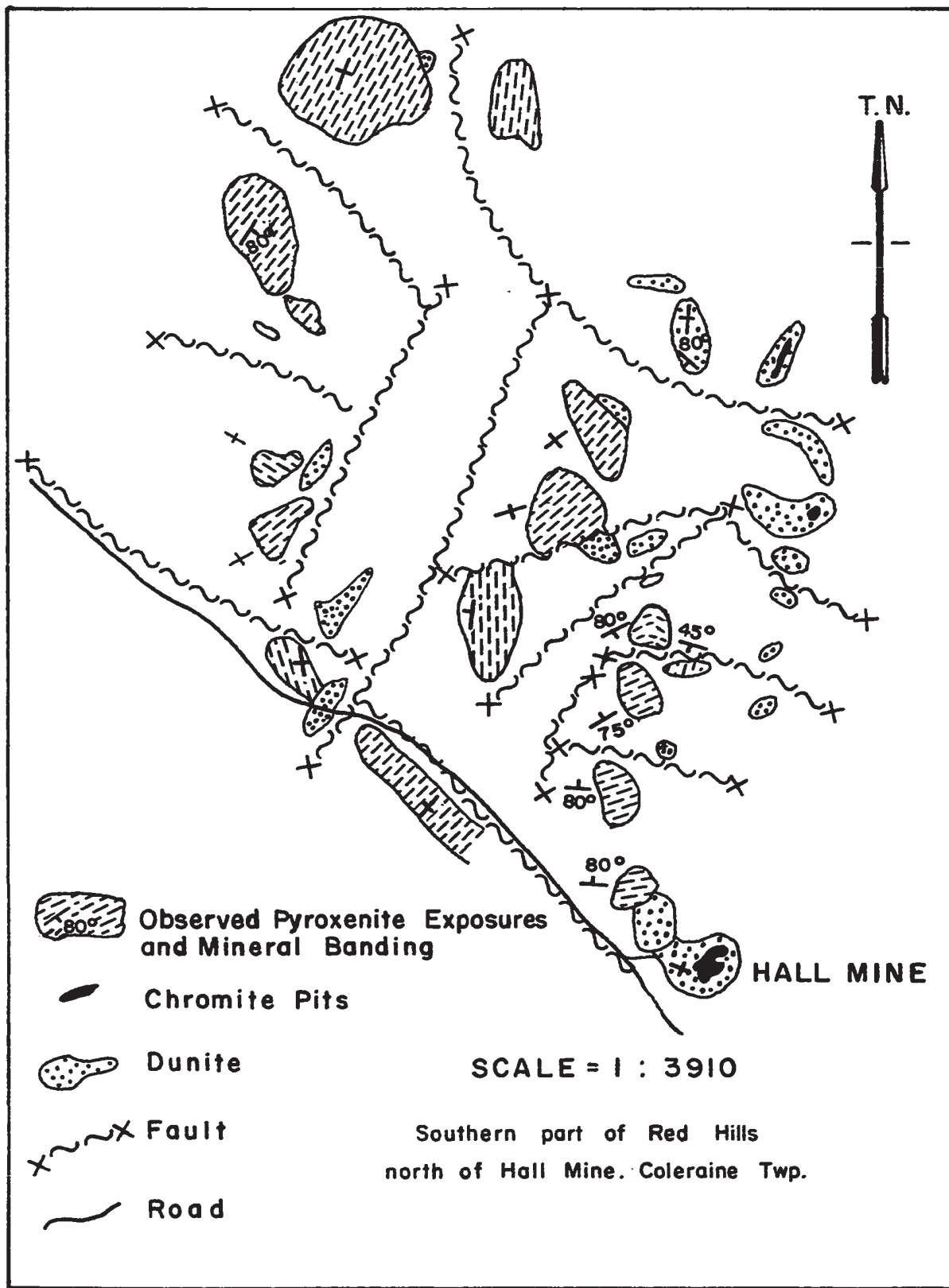


Figure 7. Banding in pyroxenite and dunite.

B. Discordant features

There are masses of ultramafic rocks which crosscut other ultramafic rocks. Dunite occurs commonly in peridotite as lenses subparallel to the layering, irregular bodies and veins. Orthopyroxenite veins occur in peridotite. Dykes and irregular masses of pyroxenite cut the layering in the "lherzolite" - "olivine" pyroxenite - pyroxenite assemblage. Pyroxenite cements brecciated dunite and brecciated, layered dunite - "olivine" pyroxenite masses. Because of their considerable genetic significance, some of the discordant features are discussed in detail in Chapter V.

III.7. AGE OF INTRUSION

A. The time of emplacement of ultramafic rocks

The ultramafic rocks are intruded into the St. Daniel Formation. Although ultramafic rocks intrude rocks believed to be as young as Devonian in Frontenac and Beauce counties in southern Quebec (Marleau, 1968), nowhere in the immediate vicinity of the map-area have they been observed in contact with rocks younger than the St. Daniel Formation. Therefore, the final emplacement of the bulk of the ultramafic rocks probably occurred in uppermost lower Ordovician or middle Ordovician time, during the Taconic orogeny. However, Lamarche (1971, oral comm.) reported occurrence of an ultramafic fragment in "Coleraine Breccia". Hence some ultramafic rocks, within or outside the map-area, intruded earlier than the bulk of the ultramafic masses under study.

In the Thetford Mines district, K-Ar age determinations of "acidic" rocks, which cut the ultramafic rocks, have yielded 471-481 m.y. (Leech et al., 1963), thus indicating a pre-Ordovician age for the ultramafic rocks. These ages do not agree with those deduced from geological

evidence.

This apparent contradiction as to the age of emplacement of the ultramafic rocks might mean that the ultramafic rocks of the Acadian geosyncline were not all emplaced at the same time, and that the ultramafic rocks under study were emplaced long after their formation.

B. The time of intrusion of gabbroic rocks

Some gabbro was present prior to the deposition of the volcanic rocks, as evidenced by the presence of gabbro boulders in the "Coleraine Breccia". Gabbro also intrudes the volcanic rocks. Furthermore, some microgabbro has been observed as dykes cutting the ultramafic rocks as cement in dunite breccia. Therefore, gabbro of different age of emplacement exists in the map-area.

III.8. DISCUSSION AND CONCLUSION

The intrusive rocks are located within weakly metamorphosed sedimentary and volcanic rocks. The ultramafic rocks caused contact metamorphism prior to their final emplacement, if one accepts the author's interpretation of the amphibolite. A narrow, low-temperature reaction zone is developed at most of the observed ultramafic rock/country rock contacts. Autochthonous, high-temperature contact metamorphism is absent. Furthermore, no chilling has been observed at the margin of the ultramafic rocks. These observations are interpreted as indicative of cold intrusion of the ultramafic rocks to their present location.

Absolute age dates (471-481 m.y.) obtained from the "acidic" rocks should be considered as minimum ages of formation of the ultramafic rocks. If the ultramafic rocks have been formed during the early phase in the development of the Acadian geosyncline, as postulated earlier, then they should have been formed in, or before, Cambrian time. However, their emplacement to their present location appears to have been in, or later than, lower Ordovician time.

CHAPTER IV

GABBROIC SUITE AND ACIDIC ROCKS

IV.1. INTRODUCTION

Gabbro is the most abundant rock type of the Gabbroic Suite. Gabbro grades into diorite which in turn grades into quartz diorite and the three rock types form an inhomogeneous assemblage, henceforth referred to only as gabbro. Quartz diorite occurs also as dykes and irregular bodies. Some pyroxenite is intimately associated with the gabbro.

Dykes, lenses and isolated bodies of "acidic" rocks are associated almost exclusively with the dunite and peridotite of the Ultramafic Suite.

IV.2. GABBRO

Gabbro is most commonly medium to coarse grained. The feldspar content varies from 70 to 5% over short distances (Fig. 8) but is usually about 50%. Microgabbro with an average grain size of 1 mm and pegmatitic varieties with an average grain size of up to 3 cm also occur. Interlayering of gabbro of different feldspar content, though uncommon, is locally observed. The gabbro intrusions commonly contain patches of microgabbro near their borders.

A. Field relationships

The relationship of the gabbro to ultramafic rocks is of prime



Figure 8. Mafic gabbro patches (dark) in gabbro, crosscut by coarse-grained, feldspar-rich gabbro (whiter).
(1 km southeast of Chalet Hill, in the river bed)

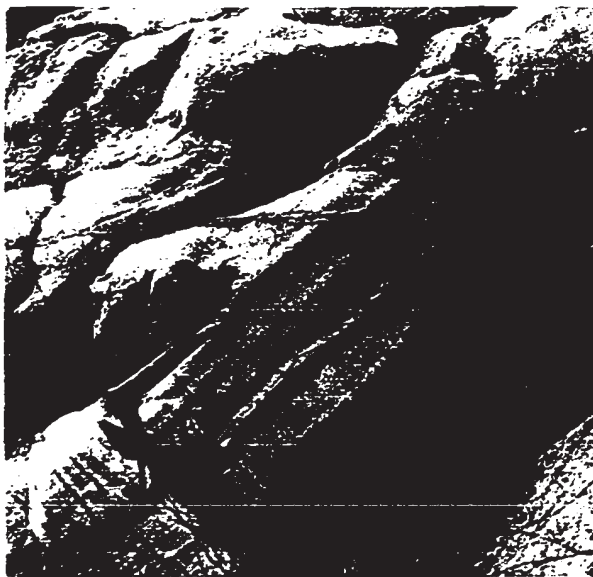


Figure 9. A very thin microgabbro vein crosscuts and offsets chromitite bands (two high-reliefed layers) in dunite.
(West slope of Nadeau Hill)

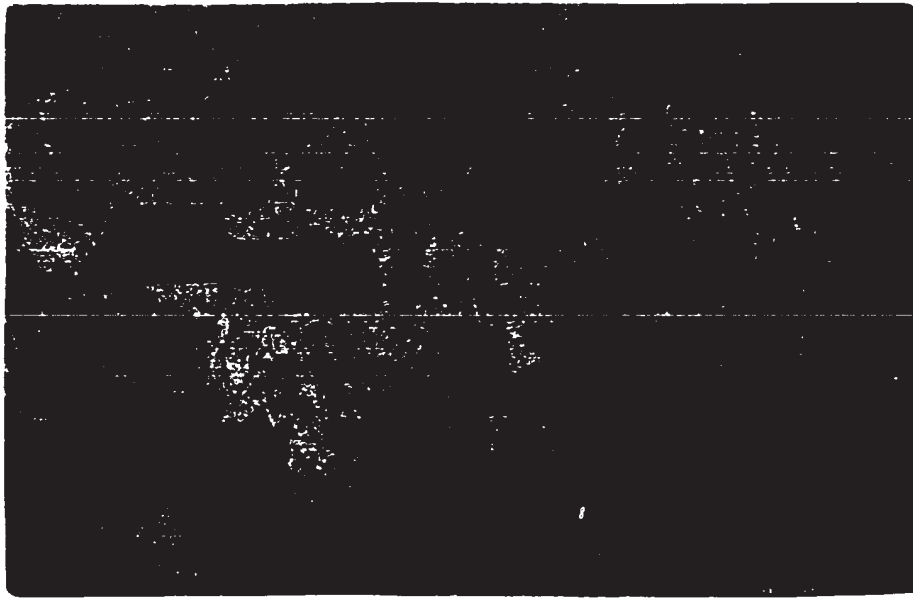


Figure 8. Mafic gabbro patches (dark) in gabbro, crosscut by coarse-grained, feldspar-rich gabbro (whiter).
(1 km southeast of Chalet Hill, in the river bed)



Figure 9. A very thin microgabbro vein crosscuts and offsets chromitite bands (two high-reliefed layers) in dunite.
(West slope of Nadeau Hill)

importance to the problem of the genesis of the ultramafic rocks. In the map-area, the apparent location of gabbro bodies relative to the ultramafic rocks is highly misleading. From northwest to southeast, there appears to be an orderly succession from peridotite - dunite - "herzolite" - "olivine" pyroxenite - pyroxenite to gabbro, suggesting an in situ differentiation series, the top of which is to the southeast. The orderly succession from ultramafic rocks to gabbroic rocks along Nadeau and Bisby Ridge led Riordon (1952, p. 32) to the conclusion that the gabbro here was " ... derived through gravitational differentiation of the magma which gave rise to the ultrabasic rocks."

Gabbro/non-intrusive rock relationship

The gabbro and its related pyroxenite zone extending from southwest of Coleraine village to Chalet Hill form a sill-like igneous body, the top of which is to the northwest as suggested by the basal pyroxenite. In the Chalet Hill area this body is entirely located within the Caldwell Formation, whereas at Lemay Hill it is located along the unconformity between the Caldwell Formation to the south and basic volcanic rocks, mostly pyroclastics, to the north. Therefore, the intrusion of the gabbro appears to post-date the deposition of the volcanic rocks. Furthermore, the gabbro cuts volcanic rocks near the western shore of Disraeli Bay; there is no visible chilling of the gabbro. This contact is weathered brown due to the presence of pyrrhotite in the volcanic rocks near the contact. Similar contact relationships are observed southeast of Bengel Hill, 90 m south of the transmission line - Bisby River intersection, and about 200 m east of Lac Coulombe on the Highway (outside the map-area).

The gabbro body south of Peach Lake has a chilled margin at its contact with pillow lavas. A chilled margin is also observed in the small gabbro body south of Caribou Mountain. The gabbro body to the northwest of Brousseau Hill exhibits chilling approaching its contact with metasedimentary rocks to the east.

Gabbro/pyroxenite relationship

Field observations indicate that some pyroxenite is closely related to gabbro and differentiated from it. This pyroxenite is characterized by its coarseness, dull grey weathering surface, absence of olivine, immediate proximity to and, locally, gradational contact with gabbro.

A pyroxenite outcrop occurs along the southeast side of the gabbro body extending from southwest of Coleraine to Chalet Hill. Eight hundred meters southwest of the top of Bengel Hill, coarse pyroxenite to the west is associated with gabbro to the east. Most of the contact is gradational over 30 to 65 cm, the pyroxenite grades into melanogabbro by the appearance of feldspar. However, locally, the gabbro/pyroxenite contact is sharp. The same contact relationships are seen between gabbro and associated pyroxenite at the top and on the west side of Bengel Hill.

In general, wherever coarse, grey weathering pyroxenite masses have been observed, a gabbro body is always observed nearby. However, many gabbro bodies have no visible associated pyroxenite.

These spatial and contact relationships suggest a genetic relationship between the gabbro and associated pyroxenite. This is further suggested by the presence of pyroxenite, mafic patches and layers in the gabbro.

The field relationship between Gabbroic and Ultramafic Suites

There are no obvious genetic ties between the rocks of the Gabbroic Suite and those of the Ultramafic Suite. There is no gradational contact or interlayering between them. The ultramafic rocks do not contain feldspar and gabbro does not contain identifiable olivine.

On the southeastern slope of Nadeau Hill, "olivine" pyroxenite and some dunite are exposed in several places near gabbro. Although the actual contact is drift-covered, there is no noticeable mineralogical or textural change approaching the contact from either side. Cooke (1937, p. 58) reports

"On the south side of Nadeau Hill pyroxenite is in contact with a large mass of gabbro and chilled over a wide zone ... approximately 100 to 200 feet. As the contact is approached, the pyroxenite becomes finer in grain ... The same change on approaching gabbro contacts was observed in pyroxenite on Lemay Hill and on the ridge north of it."

With one exception, the present author did not observe any conclusive evidence of chilling at any ultramafic/gabbro contact in either rock type. The exception is the gabbro exposure 1 km southeast of Peach Lake where chilled gabbro is in contact with serpentized, schistose dunite.

At several places, the gabbro body on the west side of Nadeau Hill is in fault contact with dunite. Immediately north of this gabbro body, dunite breccia is cemented by microgabbro. The microgabbro itself is not brecciated. Hence, the intrusion of the microgabbro must post-date the brecciation of the dunite. Further corroborating evidence is revealed in exposures on the southwest side of Nadeau Hill where abundant microgabbro veins cut dunite and cut and offset chromitite layers within it (Fig. 9).

The gabbro exposure 2 km southeast of Reed Hills is very informative. The gabbro is completely surrounded by pyroxene-rich ultramafic rocks and contains diabase dykes. There is no apparent chilling of either the gabbro or the ultramafic rock. The diabase dykes are confined to the gabbro, while discordant pyroxenite dykes in the ultramafic rocks do not cut the gabbro. It seems that this gabbro may be a xenolith and the above relationship is thought to indicate that it has been incorporated in a solid state by an ultramafic mass which was also solid.

At several points along the western cliff of Chalet Hill, serpentinite is in contact with the gabbro (Fig. 10). Wherever observed, the serpentinite seems to dip beneath the gabbro. This also appears to be true in exposures at the south end of the Peninsula of Breeches Lake (outside the map-area). The relationship is thought to indicate that the gabbro acted as a barrier to the intrusion of the ultramafic rock which, thus unable to intrude the gabbro, spread out beneath it.

There does not, therefore, appear to be any constant relationship between the rocks of the Gabbroic and Ultramafic Suites; each one intrudes the other. They do not appear to represent a single, simple differentiation sequence.

B. Petrography of the gabbro

Gabbro is extensively altered to uralite, chlorite, actinolite, green hornblende, clinozoisite, sericite and epidote. However, remnants of plagioclase are preserved. The plagioclase has the optical characteristics of basic andesine or labradorite and exhibits broken twin lamellae and undulatory extinction. No fresh pyroxene has been observed.

C. Chemistry of the gabbro

Three whole rock analyses and trace element analyses of five gabbro



Figure 10. Serpentinite (dark, lower part) - gabbro contact. The dunite is slightly schistose at the contact. No chilling effect has been observed.
(West cliff of Chalet Hill)

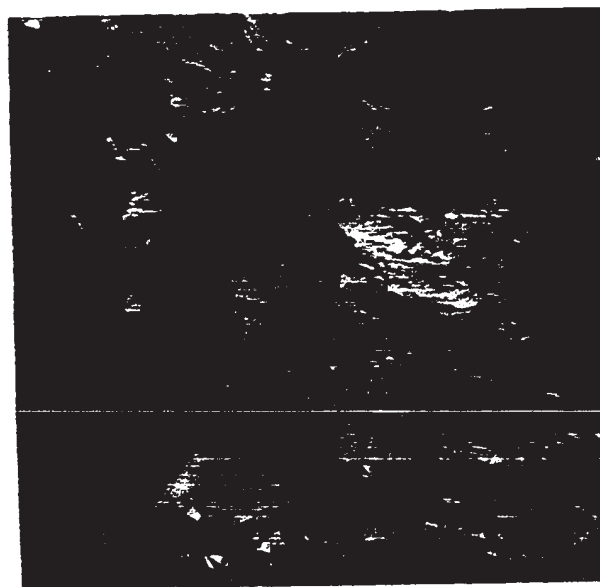


Figure 11. "Acidic" rock dyke of very irregular shape enclosing a peridotite block.
(West wall of Normandie Mine, third level)

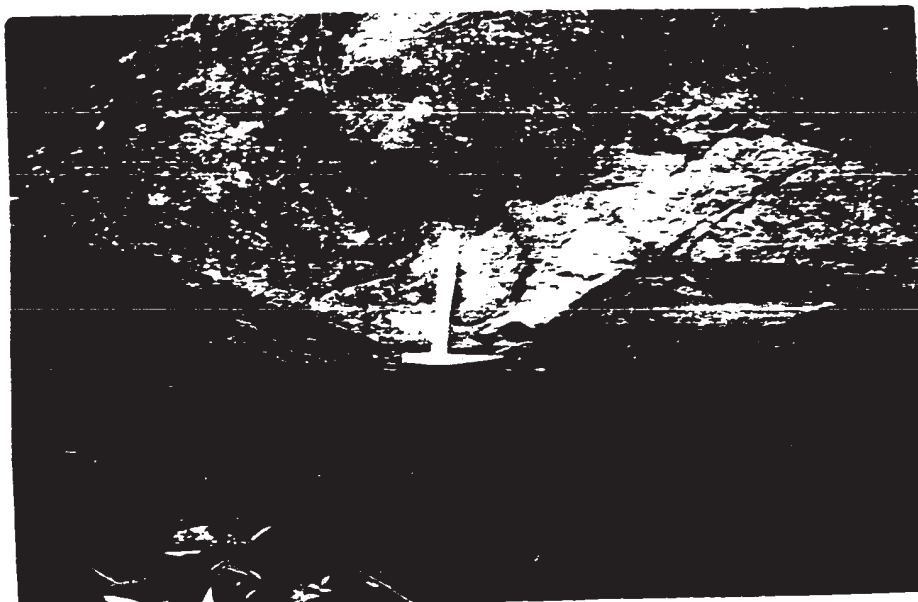


Figure 10. Serpentinite (dark, lower part) - gabbro contact. The dunite is slightly schistose at the contact. No chilling effect has been observed.
(West cliff of Chalet Hill)

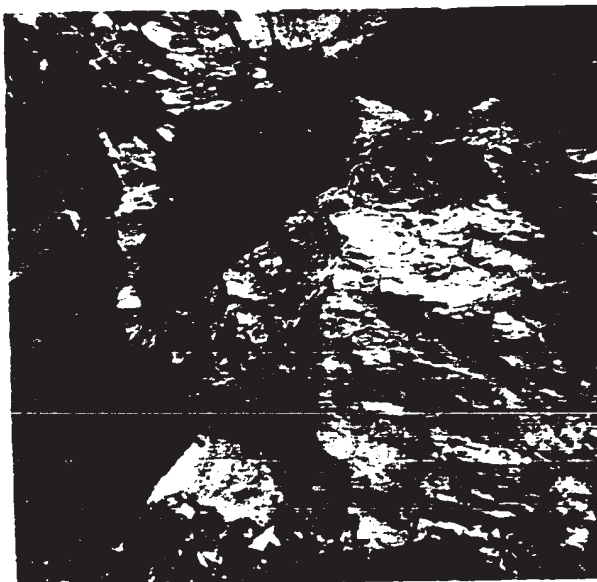


Figure 11. "Acidic" rock dyke of very irregular shape enclosing a peridotite block.
(West wall of Normandie Mine, third level)

samples are given in Table III A and Table IV respectively. Table IV also contains trace element analyses of one microgabbro sample. In Table III B whole rock analyses of basic pillow lava from and near the map-area are given for comparison with the gabbro analyses.

The gabbro samples K-6 and K-7 are rich in ferromagnesian minerals (>80% in both samples). Hence their higher than expected SiO_2 content is likely due to alteration and addition of Si during this alteration.

The analyses of gabbroic, ultramafic and volcanic rocks have been plotted in FeO-CaO-MgO and FeO- $\text{Na}_2\text{O}+\text{K}_2\text{O}$ -MgO triangular diagrams (Fig. 12 A and B respectively). The points are scattered and no differentiation trend is evident.

The gabbro contains similar amounts of SiO_2 to the lavas, while Al_2O_3 and CaO contents vary from one sample to the other in both groups of rocks. The gabbro is much poorer in TiO_2 , Na_2O , K_2O and much richer in MgO than the lavas (compare Table III A and B).

The chemical data thus indicate that the gabbro and lavas are compositionally different and that the former is not the plutonic equivalent of the latter. The data are inconclusive as to whether or not the gabbro is related to the lavas through a differentiation process which may have occurred prior to the intrusion of the gabbro.

The gabbro is poorer in Fe, Na, K, Ti, P and richer in Mg than average gabbro (Table III A) and gabbros believed to have differentiated from basalt (e.g. compare analysis 25-17 with analyses of gabbro from the map-area).

IV.3. "ACIDIC" ROCKS

All observed leucocratic rocks have been mapped as "acidic" rocks.

TABLE III A WHOLE ROCK ANALYSES (weight percent)

Locations are given on Map 2. For locations and descriptions, see Appendix I.
 Ser.D.: serpentized dunite, Ol.Py.: "olivine" pyroxenite, Orpy.: orthopyroxenite, Py.: pyroxenite.
 ----- Gabbroic Suite ----- K-6 K-7 K-20 Gabbro K-10 Py. K-9 Ol.Py. Orpy. K-12 Ser.D.
 ----- Ultramafic Suite ----- K-17

	Gabbro**	25-17* Gabbro	K-6 Melanogabbro	K-7 Gabbro	K-20 Gabbro	K-10 Py.	K-9 Ol.Py.	Orpy.	K-12 Ser.D.
SiO ₂	48.40	50.87	53.73	49.53	46.54	48.79	44.05	50.85	33.94
TiO ₂	1.60	1.59	0.03	0.03	0.02	0.04	0.03	0.02	0.23
Al ₂ O ₃	16.20	13.58	5.20	10.88	17.68	1.68	1.18	1.71	0.02
Fe ₂ O ₃	2.60	2.30	1.15	1.30	0.89	4.21	4.24	1.81	2.97
FeO	7.90	13.58	7.36	6.55	3.46	5.70	4.86	4.30	3.55
MnO	0.19	0.23	0.21	0.17	0.10	0.17	0.17	0.12	0.09
MgO	7.30	6.79	17.80	14.22	12.41	25.39	29.41	35.40	41.90
CaO	10.80	7.10	9.71	12.79	13.49	7.58	6.63	1.49	0.06
Na ₂ O	2.60	3.47	0.17	0.23	1.36	0.07	0.06	0.02	0.01
K ₂ O	0.70	0.39	0.03	0.04	0.13	0.04	0.02	0.02	0.03
P ₂ O ₅	0.26	0.11	n.d.	n.d.	n.d.	n.d.	n.d.	n.d.	n.d.
H ₂ O (+)	1.00	-	4.15	3.80	5.02	5.60	8.43	2.82	14.93
H ₂ O (-)	-	-	0.08	0.05	0.02	0.18	0.15	0.12	0.45
CO ₂	-	-	0.06	0.04	0.04	0.09	0.18	0.10	0.41
SO ₂	-	-	0.09	0.08	0.05	0.04	0.02	0.007	0.02
Cr ₂ O ₃	-	-	0.14	0.08	0.03	0.18	0.42	1.04	1.26
V ₂ O ₅	-	-	0.03	0.03	0.02	0.03	0.02	0.02	0.005
NiO	-	-	0.02	0.01	0.01	0.02	0.09	0.16	0.24
BeO	-	-	0.001	0.001	0.002	0.001	0.002	0.001	0.001
CuO	-	-	0.01	0.01	0.01	0.02	0.02	0.01	0.01
ZnO	-	-	0.01	0.01	0.01	0.01	0.01	0.01	0.01
PbO	-	-	0.001	0.001	0.001	0.001	0.001	0.001	0.001
Li ₂ O	-	-	0.009	0.006	0.003	0.002	n.d.	n.d.	n.d.
Total	99.55	100.01	99.92	99.79	100.27	99.84	99.88	100.03	100.14

* Gabbro: Munro Lake Sill (Differentiated basic sill), Lake Abitibi area, Ont., MacRae, 1969, p. 303.
 ** Average of 127 "superior" analyses of gabbro, collected from literature. Manson, 1967, p. 227.
 These two gabbro analyses from literature are included here for comparison with the present gabbro analyses.
 The present analyses were done by the Quebec Department of Natural Resources Laboratories.

TABLE III B

Whole rock chemical analyses of ultramafic rocks and mafic volcanic rocks from the map-area and its vicinity.

	420	423	424	ST-1	M-2-G-1	G-99	CD-132	L-BCM
	Dunite			Basic lava				
Pyrox.								
SiO ₂	46.30	38.24	38.16	44.75	53.60	43.25	48.15	47.00
TiO ₂	Trace	n.d.	n.d.	1.60	0.19	1.12	1.46	0.16
Al ₂ O ₃	2.58	0.70	0.63	18.30	10.70	14.30	13.50	12.65
Fe ₂ O ₃	3.45	3.50	3.32	8.57	0.75	2.55	1.47	2.42
FeO	3.57	4.25	4.76	5.05	5.97	6.89	11.73	5.73
Mn	-	-	-	0.25	0.52	0.25	0.24	0.19
MgO	23.18	41.92	41.84	4.34	5.39	8.10	7.22	9.65
CaO	15.20	0.65	0.68	8.28	8.72	12.99	11.77	11.42
Na ₂ O	0.15	0.20	0.20	4.38	1.98	2.28	4.66	2.08
K ₂ O	-	-	-	0.77	1.37	0.43	0.04	0.07
P ₂ O ₅	-	-	-	0.16	0.01	0.05	0.12	0.01
H ₂ O (+)	4.77	9.76	9.63	3.48	3.55	3.65	3.21	3.80
H ₂ O (-)	0.66	0.60	0.47	0.04	0.07	0.09	0.03	0.07
CO ₂	-	-	-	0.18	6.72	3.50	0.54	3.95
Total	99.86	99.85	99.69	100.15	99.54	99.45	100.14	99.26

420: Pyroxenite. Garthby Twp. R. II, Lot 40; Faessler, 1962, p. 87

423: Dunite. Irland Twp. R. II, Lot 28; Faessler, 1962, p. 87

424: Dunite. Irland Twp. R. VI, near Black Lake station; Faessler, 1962, p. 87

Unpublished analyses. Courtesy of R.Y. Lamarche. Analyst: Quebec Department of Natural Resources Lab.

St-1: Basic pillow lava; 2 km NE of Calapham Lake (outside the map-area)

M-2-G-1: Carbonatized basic pillow lava; 1 km NW of Coleraine

G-99: Basic volcanic rock; on the Highway, 1.5 km W of Lac Coullombe (outside the map-area)

CD-132: Basic pillow lava; Black Lake village, on the stream

L-BCM: Basic pillow lava. Sample is part of a pillow rich in chlorite, actinolite, epidote and calcite; $\frac{1}{2}$ km. W of British Canadian Mine

TABLE IV
WHOLE ROCK TRACE AND MINOR ELEMENT ANALYSES (in weight percent)
Locations of samples are indicated on Map 2. For locations and descriptions, see Appendix I.

Sample No.	Rock Suite	Rock type	Cu	Ni	Cr	V	Ti	Co	Mn	
K-5		Amphibolite	0.02	0.01	n.d.	0.048	0.84	0.003	0.1625	
K-13		Diabase	0.01	0.02	0.23	0.021	0.08	0.003	0.135	
K-2	Gabbro Suite	Microgabbro	0.02	n.d.	n.d.	0.008	0.05	0.002	0.081	
K-3		Melagabbro	0.01	0.02	0.27	0.015	0.09	0.003	0.108	
K-4		"	0.01	0.01	0.21	0.030	0.10	0.003	0.134	
K-6		"	0.01	0.02	0.23	0.013	0.09	0.005	0.0945	
K-7		Gabbro	0.01	0.01	0.16	0.018	0.09	0.003	0.117	
K-8		"	0.01	0.01	0.02	0.016	0.08	0.002	0.0875	
K-10			Pyroxenite (discord.)	0.02	0.02	0.24	0.022	0.08	0.003	0.122
K-9			Olivine Pyroxenite	0.01	0.03	0.33	0.014	0.06	0.007	0.142
K-16		Peridotite	0.01	0.24	0.19	0.005	0.05	0.007	0.0735	
K-22		"	0.004	0.21	0.34	0.006	0.004	-	0.062	
K-23		"	0.005	0.20	0.37	0.006	0.003	-	0.075	
K-30		"	0.001	0.22	0.40	0.002	0.003	-	0.054	
K-31		"	0.002	0.26	0.36	0.002	0.002	-	0.078	
K-32		"	0.002	0.23	0.33	0.007	0.004	-	0.049	
K-33		"	0.001	0.25	0.36	0.006	0.003	-	0.042	
K-17		Orthopyroxenite	0.01	0.14	0.61	0.011	0.05	0.003	0.090	
K-11		Dunite	0.01	0.13	0.98	0.006	0.05	0.008	0.077	
K-12		"	0.01	0.16	0.68	0.007	0.06	0.006	0.058	
K-24		"	0.002	0.36	0.25	0.005	0.002	-	0.050	
K-25		"	0.002	0.21	1.18	0.005	0.004	-	0.035	
K-26		"	0.005	0.21	0.71	0.002	0.012	-	0.046	
K-27		"	0.006	0.18	1.10	0.007	0.009	-	0.100	
K-1		Serpentinite	0.02	0.17	0.25	0.031	0.14	0.006	0.04	
K-28		Chromitite	0.005	0.09	-	0.080	0.045	-	0.200	
K-29		"	0.006	0.09	-	0.080	0.070	-	0.180	

K-1 to K-17: Analysed by the Quebec Department of Natural Resources Laboratories
K-22 to K-33: Analysed by X-Ray Laboratories, Don Mills, Ont.

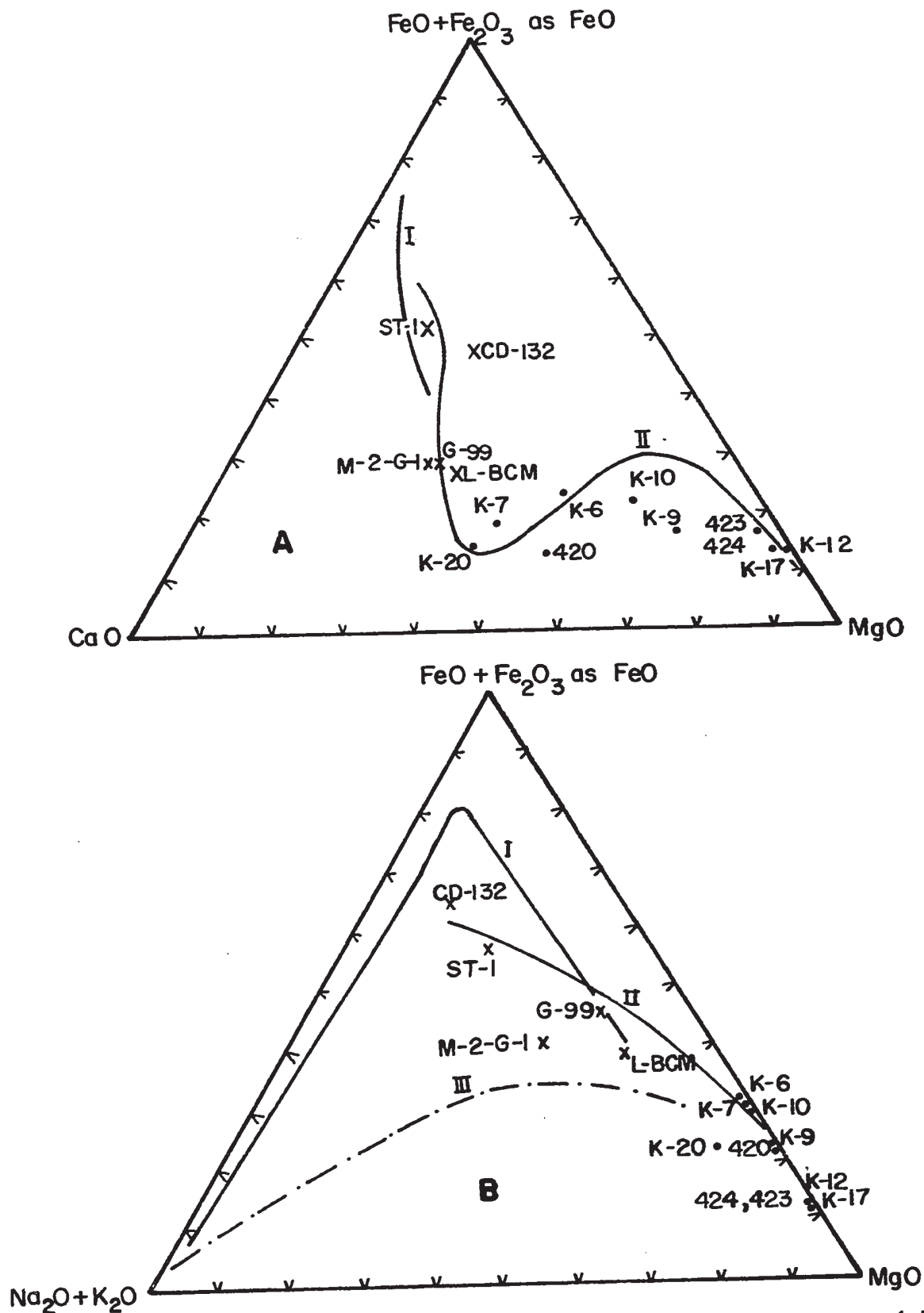


Figure 12. Plots of the whole rock analyses of phaneritic rocks (•) and aphanitic rocks (x) from the map-area.

I : Differentiation trend of the Skaergaard intrusion

II : Differentiation trend of the Munro Lake sill (MacRae, 1969)

III: Calc-alkaline trend (Thayer, 1967)

They occur as more or less rounded bodies or small, narrow dykes. Most of the dykes are irregular in shape (Fig. 11) and appear to be completely surrounded by ultramafic rocks, hence isolated from other "acidic" dykes. The "acidic" bodies are very numerous (not all are shown on the map) and they always occur within, or in contact with, the ultramafic rocks. Except for a few, all of them occur within dunite and peridotite.

"Acidic" rocks consist of varying proportions of quartz, alkali feldspars, biotite and/or muscovite and plagioclase. Granite, granodiorite, quartz monzonite and albitite are represented. In some bodies of "acidic" rock quartz was found to be secondary (Riordon, 1952) and the original rock appears to have been a syenite (Riordon, 1952). Locally, "acidic" rocks contain less common minerals such as phlogopite, garnet, chrome diopside, clinozoisite, epidote, wollastonite and vesuvianite. The "acidic" rocks are coarse to medium grained. The considerable length of many of the "acidic" dykes relative to their narrow width, and their irregular shape point to the high mobility of the magma from which they were formed. This magma was perhaps rich in water, as suggested by the pegmatitic nature of the "acidic" rocks.

The distribution of "acidic" rocks is irregular. While there are many sizable bodies of "acidic" rock in the peridotite of Murphy Hill and of Reed Hills, the large peridotite masses of Caribou Mountain, King Mountains, Quarry Hill and of Belmina Ridge are almost free of them, except along their margin. The "acidic" rocks appear to be most abundant in fault zones. At their contact with the "acidic" rocks, the ultramafic rocks are intensely serpentinized and frequently schistose. The schistosity could have developed during tectonic movements long after the intrusion of the "acidic" bodies.

The origin of "acidic" rocks is unknown. Olsen (1961) studied similar rocks in the Asbestos region and suggested that they are metasomatized gabbros and diorites. Metasomatism has presumably occurred during serpentinization of ultramafic rocks. Some "acidic" rocks closely resemble rodingites which have been considered (der Kaaden, 1971) as the result of metasomatism related to serpentinization of ultramafic rocks in a low-temperature and high-pressure environment.

IV.4. CONCLUSION

The contact relationship of the gabbro with the country rocks indicates that intrusion of some gabbro post-dates the deposition of the volcanic rocks. Some gabbro predates the deposition of "Coleraine Breccia" which probably is stratigraphically at the lower part of the volcanic pile; hence gabbro of different ages of intrusion seems to exist in the map-area.

Where observed, the gabbro is in intrusive contact with the meta-volcanic rocks. However, Lamarche (1971, oral comm.) observed gradational contacts between lavas and gabbro at Mount Louise (outside the map-area, 10 km south of Chalet Hill), hence some gabbroic rocks in the Serpentine Belt may represent differentiated flows.

The gabbro exhibits very rapid and considerable variation in grain size and composition. Disorderly mixing of fine-grained gabbro with coarser varieties is very common. This inhomogeneity might be interpreted to indicate that gabbroic rocks perhaps represent shallow intrusions within a mobile environment. The common occurrence of pegmatitic gabbro dykes within finer grained gabbro suggests that gabbroic magma was perhaps rich in water. Hence it is possible that alteration of the gabbro is partly the result of autometasomatism.

CHAPTER V

ULTRAMAFIC SUITE

V.1. INTRODUCTION

The Ultramafic Suite includes pyroxenite, "olivine" pyroxenite, "herzolite", peridotite, olivine orthopyroxenite, orthopyroxenite, dunite, serpentinite and chromitite (Table II, p. 18). Pyroxenite, "olivine" pyroxenite and "herzolite" occur interlayered with each other and form a group. Peridotite, olivine orthopyroxenite and orthopyroxenite occur together and form another group. Dunite is found within both groups. Chromitite occurs only in dunite.

Particular attention has been given to the internal structures, petrography and chemistry of the ultramafic rocks in the hope of determining their origin and mode of emplacement. All the minerals have been analysed with an electron microprobe analyser. The relevant data on procedure, estimated precision and accuracy and the details of the analyses are given in Appendix III. In the text only the mean composition of minerals is listed. The procedure used to calculate the mean composition is indicated in Appendix III. The locations of analysed samples are shown on Map 2 (back pocket).

Chromitite is described separately under "chromitite and chromite deposits" (Chapter VI).

V.2. PYROXENITE

The pyroxenite is usually coarsely granular and has a light brown- or dull grey-weathered surface. In the field, it is easily identified by its rough but regular surface which is very different from the mottled surface of "olivine" pyroxenite. The pyroxenite of the Ultramafic Suite can be distinguished from pyroxenite associated with gabbro by its lighter green crystals and its commonly finer grain size.

A. Field relationships

Two types of pyroxenite can be distinguished. The first type, which will be termed concordant, occurs interlayered with dunite, "herzolite" and "olivine" pyroxenite. The second, or discordant pyroxenite, forms veins and irregular patches.

Concordant pyroxenite

Pyroxenite interlayered with "olivine" pyroxenite has gradational contacts with the latter. Pyroxenite is usually the minor component of this association.

Pyroxenite-dunite and pyroxenite-"herzolite" interlayering is common and is well displayed by the exposures approximately 350 m north of the Hall Mine. The thickness of the layers varies from 4 mm to about 60 cm, individual layers are usually very constant in thickness. For instance, two pyroxenite layers, each 1 cm. thick and separated by a dunite layer also about 1 cm. thick, have been followed for 13 m. with only very slight variations in thickness. In general, the variation in thickness of most layers does not exceed a 2:1 ratio between thickest and thinnest parts. There is no apparent correlation between the thickness of adjacent dunite and pyroxenite layers (Figs. 13 and 14) and the

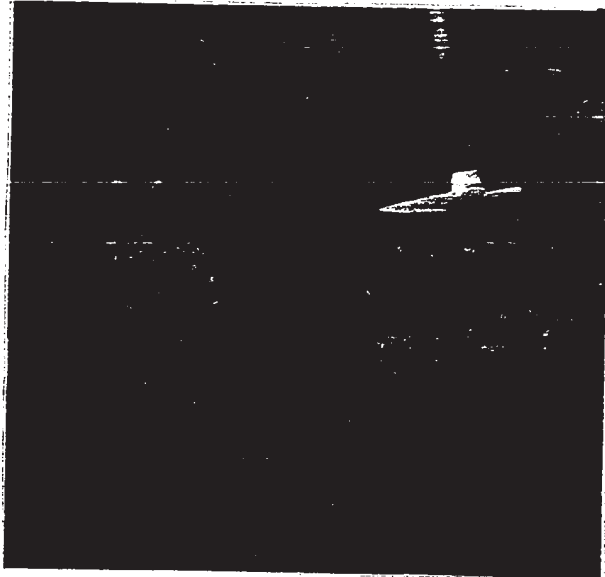


Figure 13. Dunite (light blue)-pyroxenite interlayering.
(South of Red Hills, 320 m north of Hall Mine)



Figure 14. Detail of the dunite (white)-pyroxenite (grey)
interlayering.
(Same location as Figure 13)

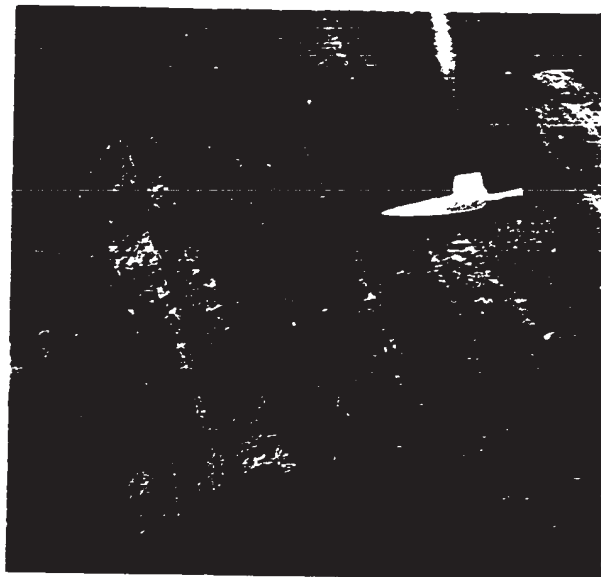


Figure 13. Dunite (light blue)-pyroxenite interlayering.
(South of Red Hills, 320 m north of Hall Mine)



Figure 14. Detail of the dunite (white)-pyroxenite (grey)
interlayering.
(Same location as Figure 13)

contacts are sharp. In detail, the contact between layers is irregular with clusters of pyroxene crystals entering the adjacent dunite layers or small tongues of the latter entering the pyroxenite layers.

Discordant pyroxenite

Discordant pyroxenite veins and patches are very common. The veins are from 1 to 50 cm thick and commonly are irregular in shape and of varying thickness. However, some veins have regular thickness and their boundaries, although undulating in detail, are quite straight (Fig. 15). These veins appear to have filled pre-existing fractures.

In places, the layered rocks have been brecciated and the blocks have been cemented by coarse, grey weathering pyroxenite (Figs. 16 and 18). The blocks are angular and the layering in adjacent blocks is not parallel. Hence, the layered rock was apparently fractured before or during the emplacement of discordant pyroxenite and the blocks have been moved, perhaps by the pyroxenite itself. Figure 17 shows a similar situation. However, here the blocks have been moved much less, since they almost fit together.

A chaotic mixture of dunite and pyroxenite, which will henceforth be referred to as dunite breccia, has been observed in several places, mostly near the contact of the Southern Dunite Zone with the Olivine Pyroxenite Zone. Roughly ellipsoidal and angular dunite blocks lie in a matrix of coarse-grained pyroxenite (Figs. 19 and 20). The size of the dunite blocks varies from about 150 cm long by 60 cm wide to small pieces 2 to 3 cm in size. They are usually randomly oriented, although at a few localities (e.g. on the southwest of the Hall Mine) they have an ill-defined parallel orientation. In places, such as Cloutier Hills,

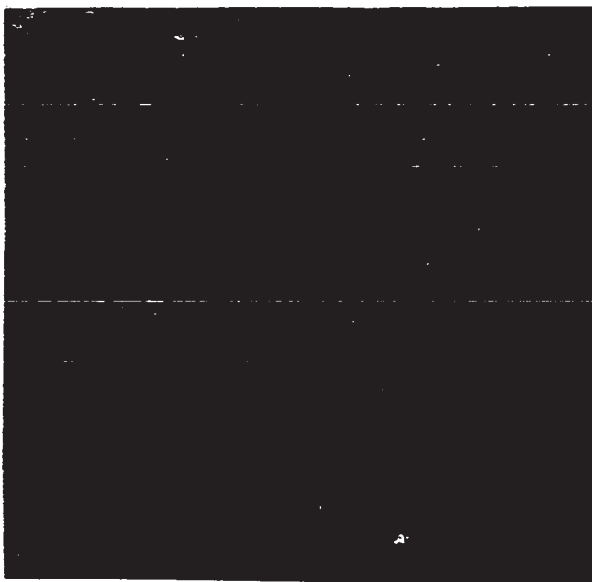


Figure 15. A dunite layer (light) in "olivine" pyroxenite has been cut and offset by a pyroxenite dyke (grey, parallel to the pencil).
(Southeast slope of Bengel Hill)



Figure 16. Brecciated, interlayered dunite-pyroxenite (grey). The pyroxenite layers are poorly defined and discontinuous. The space between the blocks is filled with coarse pyroxenite (dark, below the hammer). Note the non-parallel orientation of the layering in the different blocks.
(800 m northwest of Hall Mine, along the road)

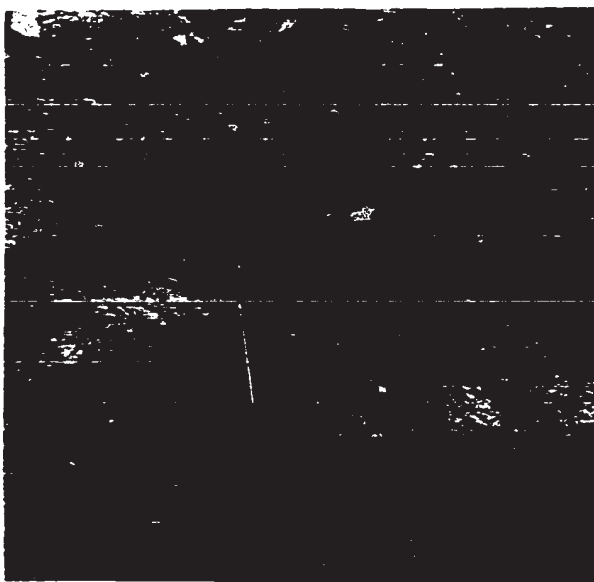


Figure 15. A dunite layer (light) in "olivine" pyroxenite has been cut and offset by a pyroxenite dyke (grey, parallel to the pencil).
(Southeast slope of Bengel Hill)

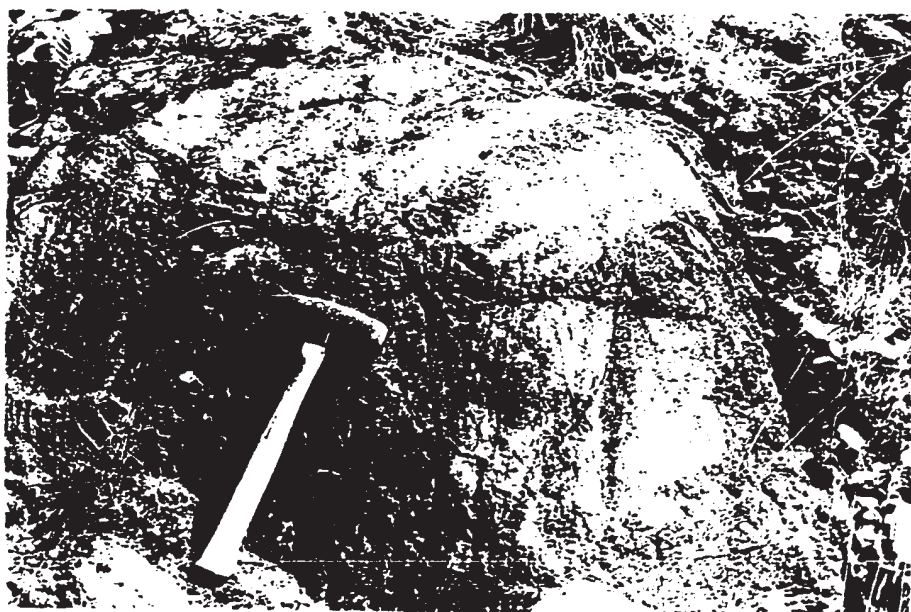


Figure 16. Brecciated, interlayered dunite-pyroxenite (grey). The pyroxenite layers are poorly defined and discontinuous. The space between the blocks is filled with coarse pyroxenite (dark, below the hammer). Note the non-parallel orientation of the layering in the different blocks.
(800 m northwest of Hall Mine, along the road)

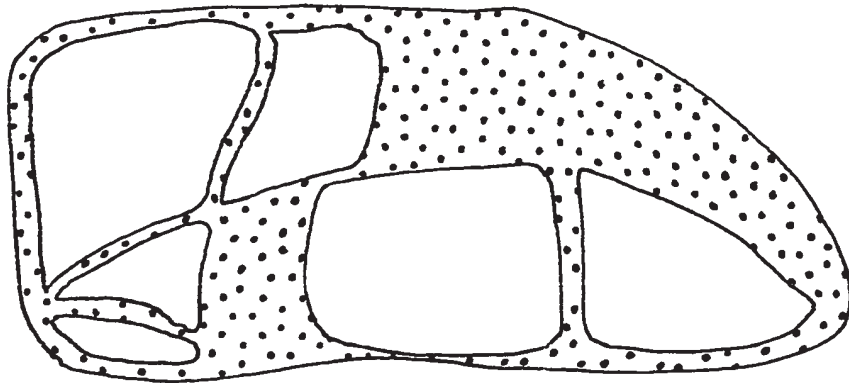


Figure 17. Dunite blocks in pyroxenite. Note the angular shape of the dunite blocks (white). The boundaries of dunite blocks more or less match. (West of Little Lake St. Francis)

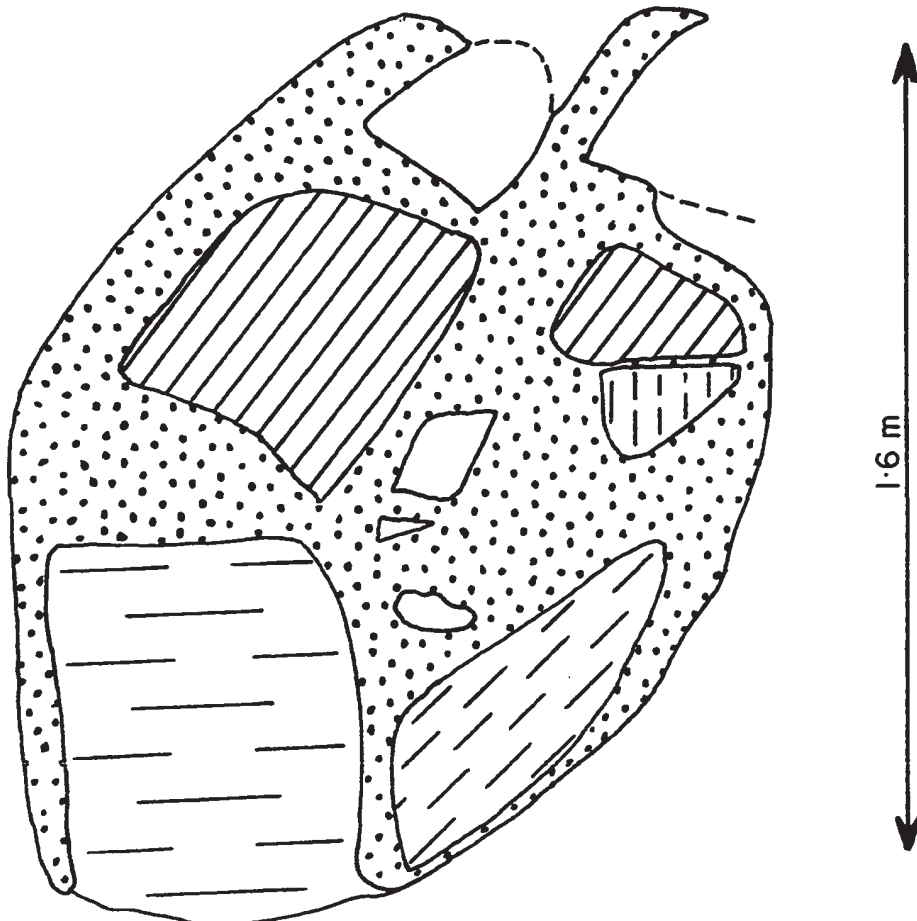


Figure 18. Breccia. Blocks of dunite (white) and dunite with pyroxenite layers (continuous and discontinuous lines, these lines show the orientation of the layers) in a pyroxenite matrix (stippled). (820 m. northwest of Hall Mine, along the road)

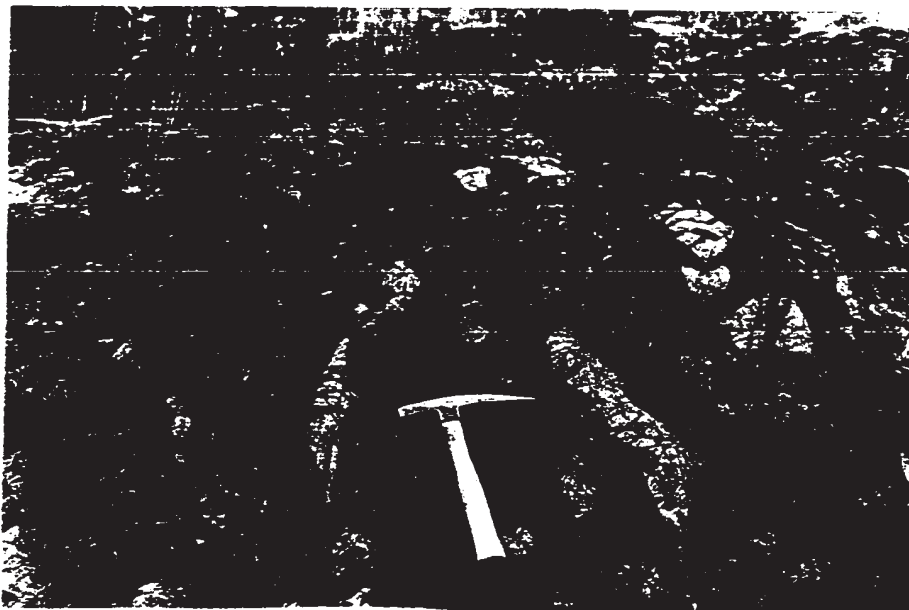


Figure 19. Dunite breccia. Dunite bodies (white) in pyroxenite. Note the angular shapes of the blocks. The blocks are cut by pyroxenite.
(West side of Nadeau Hill)

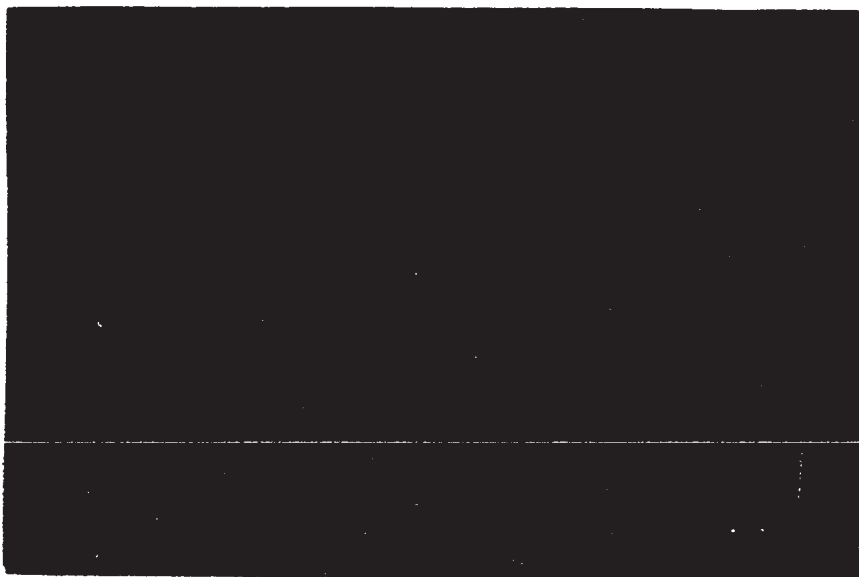


Figure 20. Eye-shaped dunite block (light-coloured) in coarse pyroxenite. The upper right part of the block seems to grade into pyroxenite (grey).
(130 m. west of Beebe Realty Chrome Prospects)



Figure 19. Dunite breccia. Dunite bodies (white) in pyroxenite. Note the angular shapes of the blocks. The blocks are cut by pyroxenite.
(West side of Nadeau Hill)



Figure 20. Eye-shaped dunite block (light-coloured) in coarse pyroxenite. The upper right part of the block seems to grade into pyroxenite (grey).
(130 m. west of Beebe Realty Chrome Prospects)

750 m northwest of Clay Lake, the proportion of dunite blocks is such that pyroxenite is only a minor component in the exposed rock.

B. Petrography

The pyroxenite consists of closely packed subhedral or anhedral crystals of pyroxene (Figs. 21 and 22). It is commonly coarsely granular, the grain size varying from 1 mm. to 6 cm. The orthopyroxene has the optical characteristics of bronzite and the clinopyroxene can be either diopside or augite, the former being commoner. The modal ratio of clino- to orthopyroxene ranges from about 50:50 to pure clinopyroxenite. Therefore, rock types such as websterite, bronzite-bearing clinopyroxenite and clinopyroxenite are represented. The discordant pyroxenite is commonly clinopyroxenite with rare orthopyroxene, whereas the concordant pyroxenite commonly contains an appreciable amount of orthopyroxene.

The tight packing of pyroxene crystals, with no interstitial space between them (Figs. 21 and 22), indicates extensive in situ growth or recrystallization. The clinopyroxene rarely contains small euhedral inclusions of orthopyroxene (Fig. 21); euhedral inclusions of clinopyroxene in orthopyroxene have also been observed. Thus, contemporaneous crystallization of both varieties of pyroxene is indicated. Orthopyroxene very rarely contains exsolution lamellae of clinopyroxene.

The pyroxenite is moderately altered and fractured. Orthopyroxene alters to serpentine and magnetite. Clinopyroxene alters to amphibole (hornblende and/or anthophyllite), epidote, talc and minor amounts of serpentine.



Figure 21. Photomicrograph: Pyroxenite composed of about 25% orthopyroxene, now mostly serpentinized (dark grey), and clinopyroxene. Note subhedral orthopyroxene inclusions in clinopyroxene (upper part of the figure). Sample No. 278 Crossed nicols, X 40

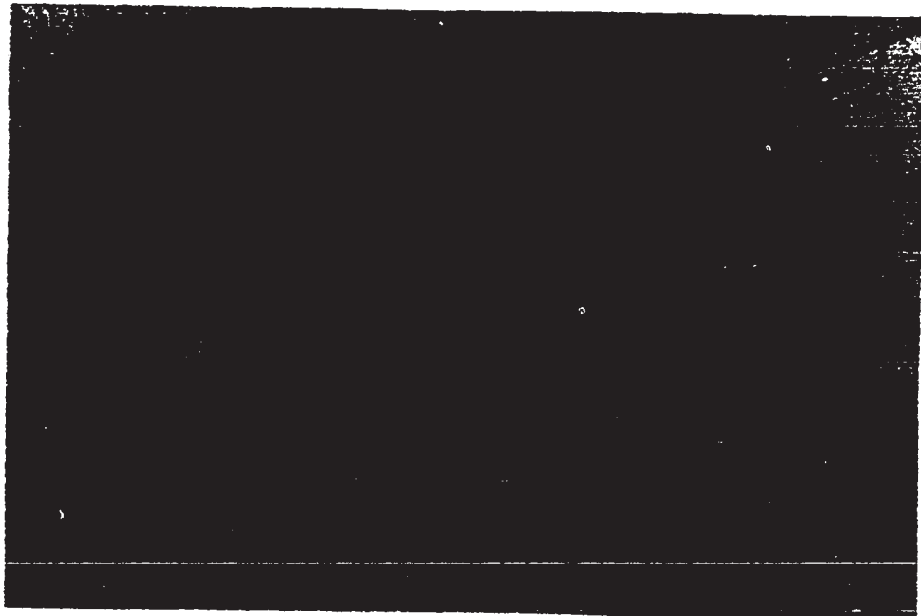


Figure 22. Photomicrograph: Pyroxenite, variety websterite. Serpentinized orthopyroxene (light) forms 25-30% of the rock. The remainder is clinopyroxene. Note that orthopyroxene is completely serpentinized while clinopyroxene is fresh. Clinopyroxene contains inclusions of orthopyroxene. Sample No. 279 Plane polarized light, X 40



Figure 21. Photomicrograph: Pyroxenite composed of about 25% orthopyroxene, now mostly serpentinized (dark grey), and clinopyroxene. Note subhedral orthopyroxene inclusions in clinopyroxene (upper part of the figure). Sample No. 278 Crossed nicols, X 40

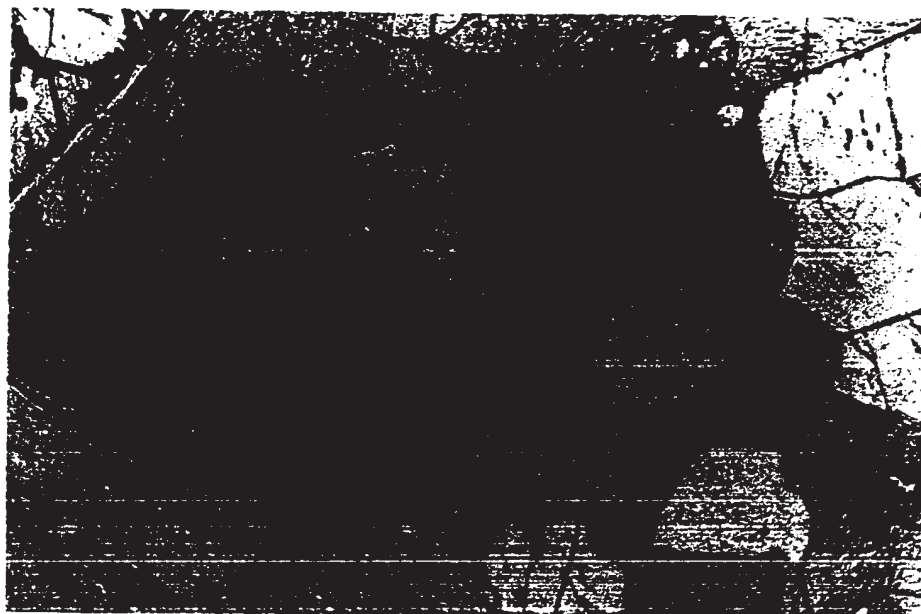


Figure 22. Photomicrograph: Pyroxenite, variety websterite. Serpentinized orthopyroxene (light) forms 25-30% of the rock. The remainder is clinopyroxene. Note that orthopyroxene is completely serpentinized while clinopyroxene is fresh. Clinopyroxene contains inclusions of orthopyroxene. Sample No. 279 Plane polarized light, X 40

C. Chemistry

The whole rock chemical analysis and the trace element analyses of one sample of discordant pyroxenite are listed in Table III A, p. 46 and Table IV, p. 48, respectively. Electron microprobe analyses of clinopyroxene in one sample of discordant pyroxenite (sample No. 444) and in two samples of concordant pyroxenite and an analysis of orthopyroxene in one sample of concordant pyroxenite are listed in Table V. These analyses confirm the bronzite composition of the orthopyroxene, whereas clinopyroxene has been found to be near the diopside-augite boundary. High Cr, low Al contents of pyroxenes and high Ca content of orthopyroxene are notable features in the analyses.

D. Discussion and conclusion

Perhaps the most significant point about pyroxenite is that it forms coarse pyroxenite dykes, irregular patches and cements breccias. To explain pyroxenite dykes, Bowen and Tuttle have suggested that silica saturated water vapor, streaming through a crack in dunite at temperatures above 650° C, would convert the wall rock to enstatite pyroxenite (Bowen and Tuttle, 1949, in Turner and Verhoogen, 1960, p. 316). The same process can presumably also operate in olivine-bearing ultramafic rocks other than dunite. However, in the discordant pyroxenite of the map-area, orthopyroxene is rare and chromite, which is present in the olivine-bearing rocks, appears to be absent from the pyroxenite (chromite should perhaps have survived the hydrothermal alteration). Furthermore, discordant pyroxenite is restricted to the Southern Assemblage, where clinopyroxene-rich rocks are prevalent, rather than occurring indiscriminantly in all the olivine-bearing rocks

TABLE V

Microprobe Analyses

Mean composition* of minerals in pyroxenite (Py.), "olivine" pyroxenite (Ol.Py.) and "herzolite" (Lhz.) of the ultramafic suite (in weight percent cations). Sample locations are indicated on Map 2.

Rock type and Sample No.	Mineral	Mg	Fe	Si	Al	Cr	Ca	Ni	End members Mole. %
Py. 39	Clinopyroxene	11.25	4.62	-	1.14	0.30	14.63	0.07	Wo _{40.1} En _{50.8} Fs _{9.1}
Py. 142	Clinopyroxene	11.33	5.24	-	1.15	0.25	14.73	0.04	Wo _{39.7} En _{50.2} Fs _{10.1}
Py. 142	Orthopyroxene	19.97	9.33	-	0.62	0.06	0.66	0.04	En _{83.1}
Py. 444	Clinopyroxene	11.58	4.96	-	1.12	0.25	14.43	0.07	Wo _{38.8} En _{51.5} Fs _{9.7}
Ol.Py. K-9	Clinopyroxene	10.58	3.89	24.30	1.22	0.21	16.02	-	Wo _{44.2} En _{48.1} Fs _{7.7}
Ol.Py. 189	Clinopyroxene	11.41	2.93	24.94	0.70	-	15.28	-	Wo _{42.2} En ₅₂ Fs _{5.8}
Lhz. 154	Clinopyroxene	12.16	4.34	25.11	0.95	-	12.42	-	Wo _{34.9} En _{56.3} Fs _{8.8}

Mean composition of accessory chromite - in weight percent cations

Rock type and Sample No.	Cr	Fe tot.	Fe ⁺²	Fe ⁺³	Mg	Al	Ti
Ol.Py. K-9	27.94	22.30	16.31	5.99	5.74	10.95	0.24
Ol.Py. 189	29.37	24.62	18.46	6.16	4.56	9.69	0.12
Lhz. 154	37.38	22.18	17.92	4.26	4.83	6.53	0.05
Lhz. 391	32.30	22.84	17.41	5.42	5.03	8.50	0.10

Fe⁺² and Fe⁺³ values have been calculated from total iron based on the assumption that chromite is stoichiometric.

* The analytical procedure, calculation of mean composition, precision, accuracy and detail of analyses are indicated in Appendix III.

of the map-area. It is therefore unlikely that discordant pyroxenite in the map-area has been formed by alteration of olivine-bearing rocks.

It is suggested here that the discordant pyroxenite has crystallized from an ultrabasic magma. The coarse grain size, even in very thin dykes, suggests that the magma was largely liquid during the injection.

V.3. OLIVINE PYROXENITE

A. Field relationships

"Olivine" pyroxenite occurs interlayered with "herzolite", pyroxenite and dunite. It grades into "herzolite" by a decrease in the pyroxene content and into pyroxenite by the disappearance of olivine. The thickness of layers varies from approximately 3 cm up to 3 m, the thickness of any given layer being variable (Figs. 23 and 24). The layer boundaries can be sharp, which is usually the case with dunite-"olivine" pyroxenite contacts, or gradational, which is often the case with "olivine" pyroxenite-"herzolite" contacts. Layers having one sharp and one gradational contact have been observed (Fig. 25). Frequently, a layer of homogeneous appearance exhibits subtle internal layering, which can be due either to slight changes in composition (Fig. 26) and/or grain size.

B. Petrography

Unlike pyroxenite, "olivine" pyroxenite is strongly altered, so that the original texture is obliterated. No fresh olivine remains; it is altered to serpentine. Orthopyroxene, in places still identifiable as bronzite, is also altered to serpentine. Diopside is also present but is largely altered to amphibole, epidote and serpentine.



Figure 23. Layering in "olivine" pyroxenite. The pyroxene-poor layers are light and the pyroxene-rich layers are grey. The layers are discontinuous and vary in thickness. The pyroxene-rich layer below the hammer is probably folded. (South slope of Nadeau Hill)

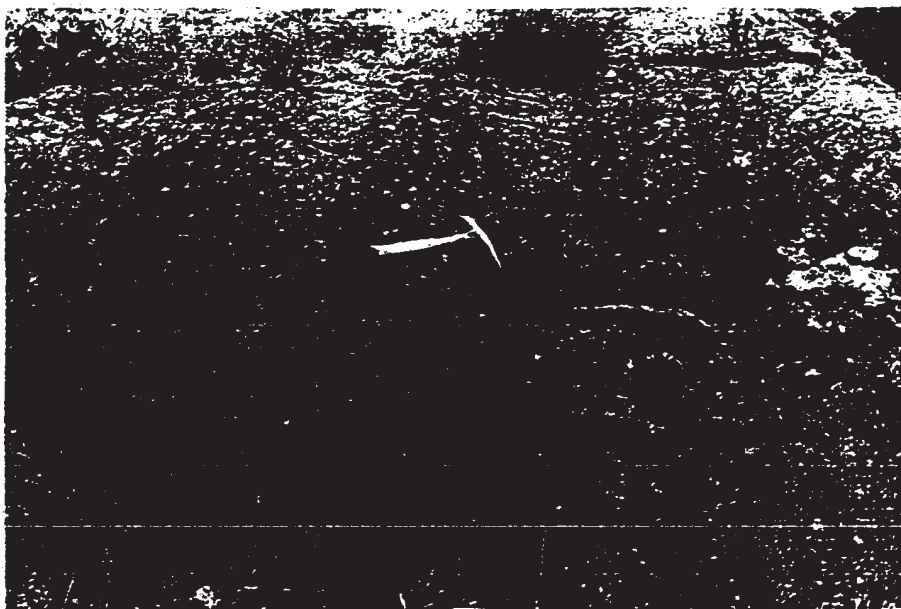


Figure 24. Layering in "olivine" pyroxenite. Pyroxene-poor layers are light and pyroxene-rich layers are darker. The layer below the hammer has a sharp boundary on one side (left) and a gradational boundary on the other side. (South slope of Nadeau Hill)



Figure 23. Layering in "olivine" pyroxenite. The pyroxene-poor layers are light and the pyroxene-rich layers are grey. The layers are discontinuous and vary in thickness. The pyroxene-rich layer below the hammer is probably folded. (South slope of Nadeau Hill)

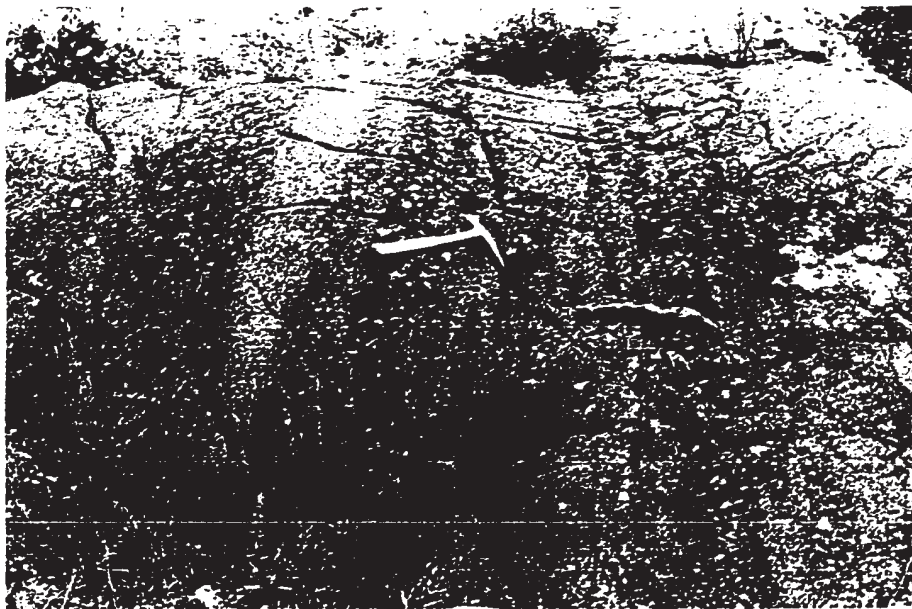


Figure 24. Layering in "olivine" pyroxenite. Pyroxene-poor layers are light and pyroxene-rich layers are darker. The layer below the hammer has a sharp boundary on one side (left) and a gradational boundary on the other side. (South slope of Nadeau Hill)

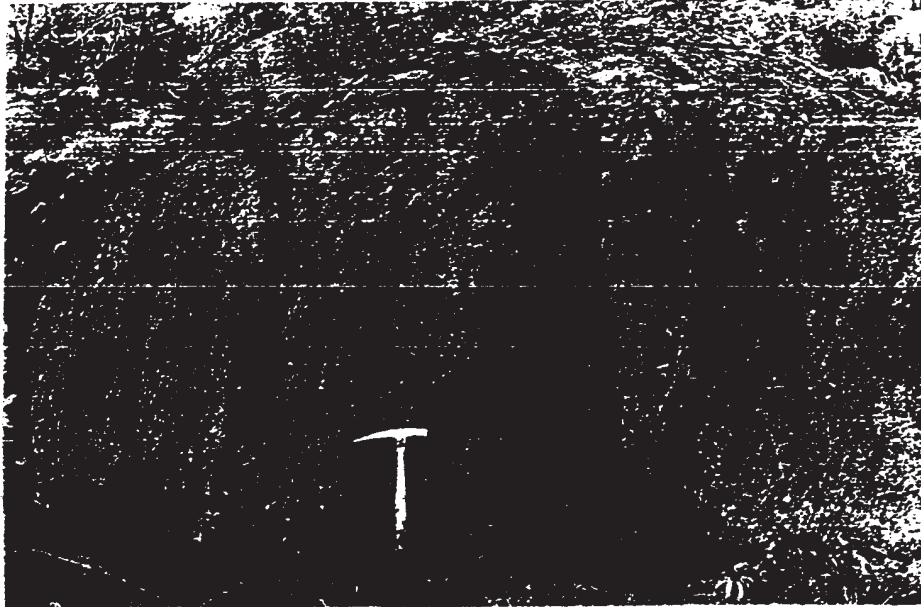


Figure 25. Layering in "olivine" pyroxenite. The layer (darker grey) in the centre of the figure is a pyroxenite layer with a sharp boundary at the right but a gradational one at the left.
(Top of Nadeau Hill)

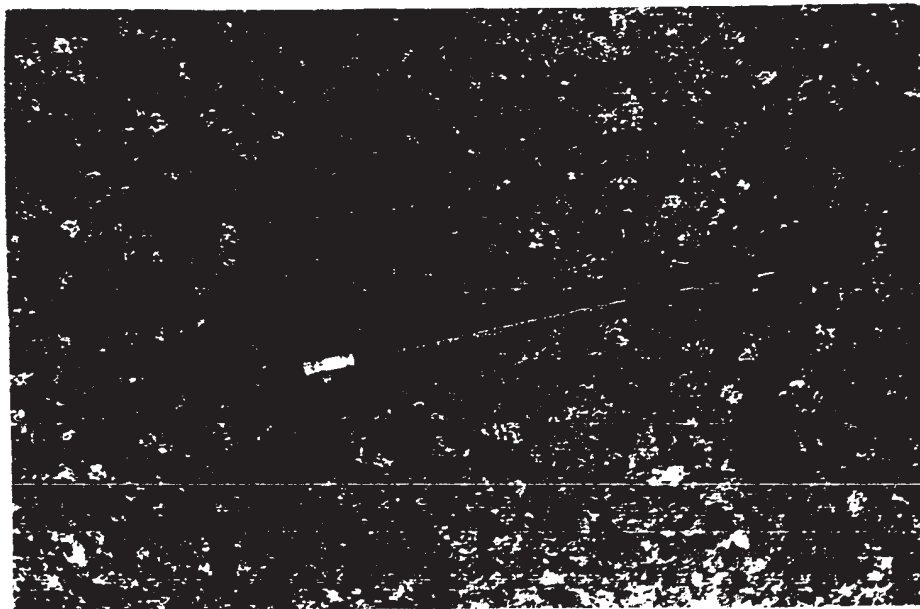


Figure 26. Internal layering in "olivine" pyroxenite. The difference of colour is due to slight compositional variation, the central part is poorer in pyroxene.
(South slope of Nadeau Hill)

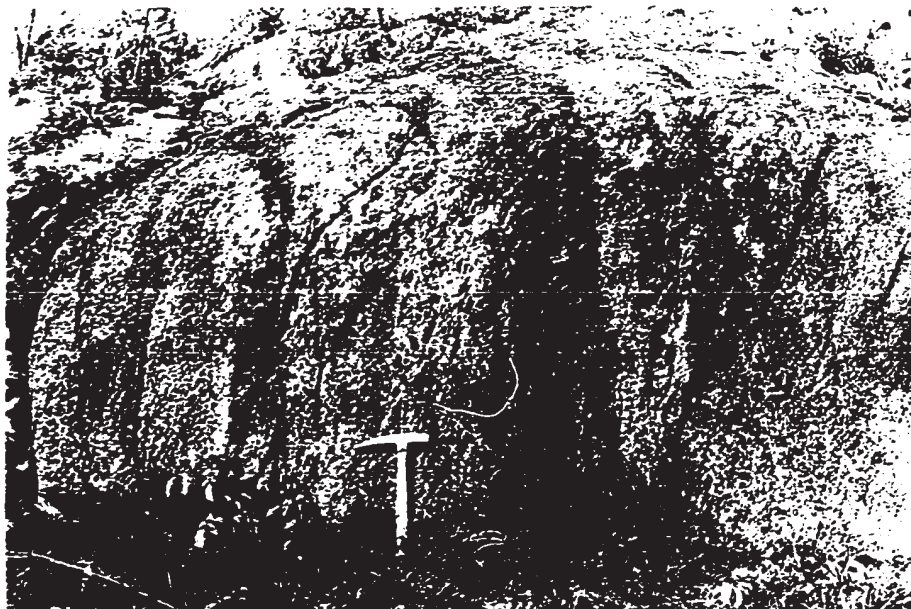


Figure 25. Layering in "olivine" pyroxenite. The layer (darker grey) in the centre of the figure is a pyroxenite layer with a sharp boundary at the right but a gradational one at the left.
(Top of Nadeau Hill)

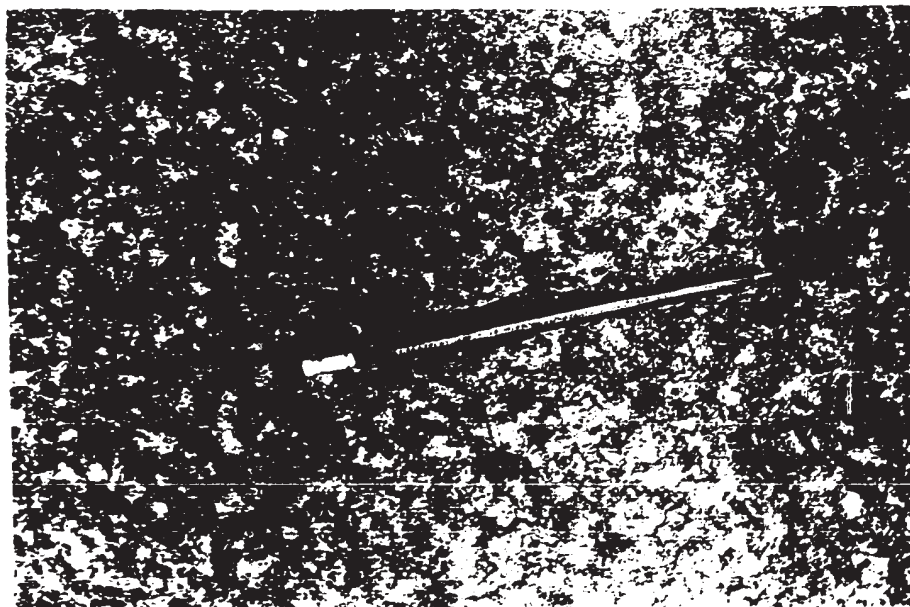


Figure 26. Internal layering in "olivine" pyroxenite. The difference of colour is due to slight compositional variation, the central part is poorer in pyroxene.
(South slope of Nadeau Hill)

Chromite is usually present as an accessory mineral and locally it can form up to 3% of the rock. The chromite grains commonly average 0.5 mm in size and are euhedral or subhedral; they are commonly rimmed by secondary magnetite and are moderately fractured.

C. Chemistry

Compared to pyroxenite, "olivine" pyroxenite is richer in Mg, Ni, Mn, Cr and Co and poorer in Al, Ca, Si, V and Ti (Table III A, p. 46, Table IV, p. 48). The high Mn value in "olivine" pyroxenite reflects the presence of chromite in which Mn is concentrated.

Electron microprobe analyses confirmed that the clinopyroxene is diopside (Table V), it is poorer in Fe than in the previously discussed pyroxenite of the Ultramafic Suite.

Chromite crystals are fairly homogeneous. However, electron microprobe analysis indicates small variations in composition. The most common variation is a very slight increase in Al from the centre toward the margin of the crystal and an accompanying decrease in Cr (Fig. 27). In some grains, there is a narrow marginal zone much richer in Al and poorer in Cr than the remainder of the grain (Fig. 27). Variation in Mg is more subtle, it decreases slightly toward the margin of the grains. It was expected that Fe would increase with decreasing Mg, but this variation has not been detected. Although the variations described above are common, they have not been detected in every grain.

V.4. LHERZOLITE

"Lherzolite" is strongly altered. No fresh olivine or orthopyroxene has been observed. Clinopyroxene is partially altered to amphibole and epidote. Secondary magnetite is abundant. "Lherzolite"

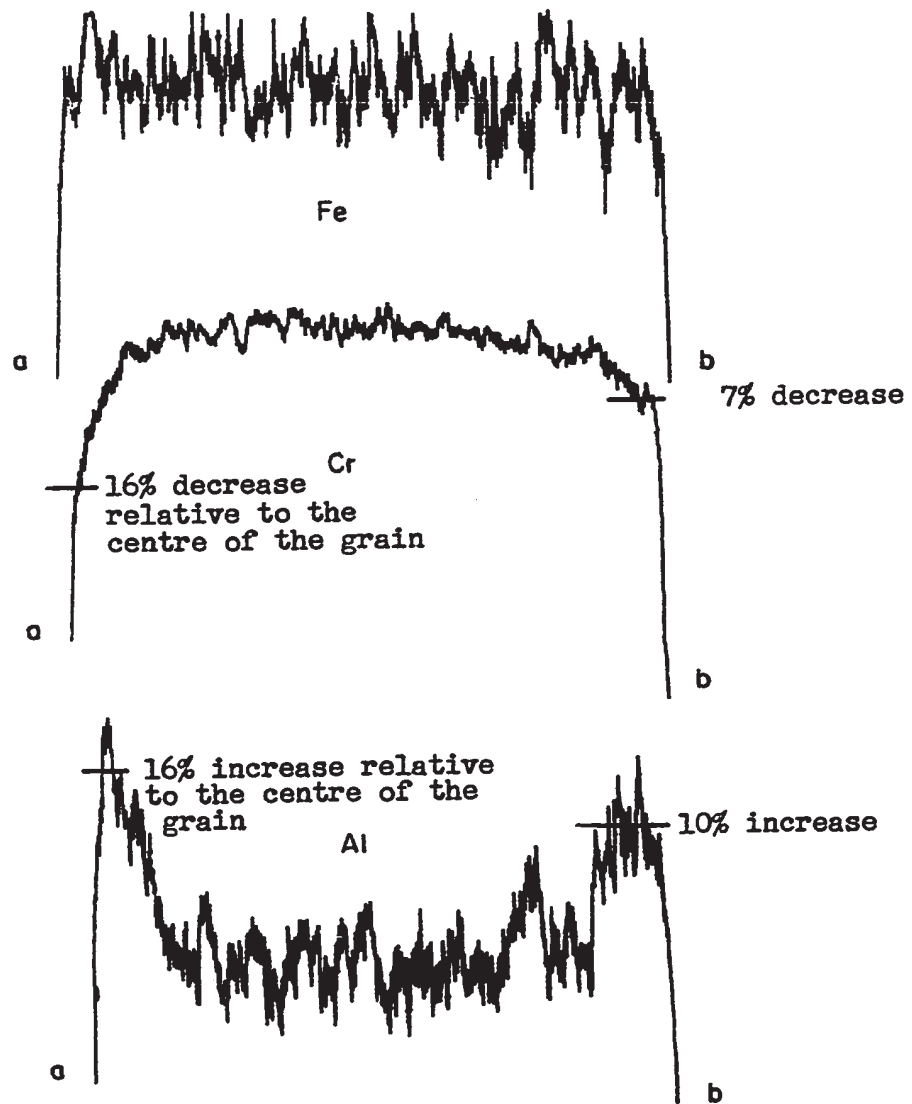


Figure 27. Zoning in chromite. Electron microprobe scanning profile showing variation of aluminum, chromium and iron in a chromite grain. Olivine pyroxenite, sample No. 189.
Photomicrograph: Reflected light, X 120

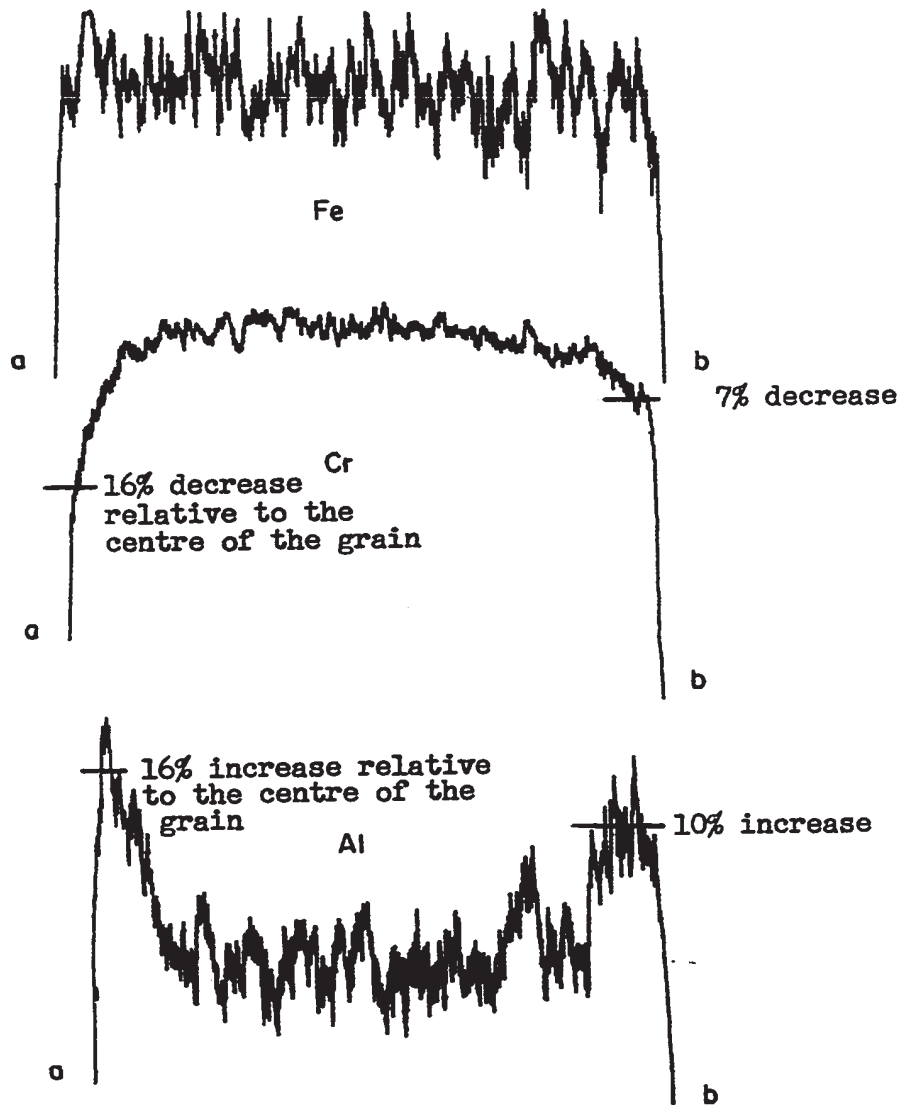


Figure 27. Zoning in chromite. Electron microprobe scanning profile showing variation of aluminum, chromium and iron in a chromite grain. Olivine pyroxenite, sample No. 189.
Photomicrograph: Reflected light, $\times 120$

is usually poor in accessory chromite (1%), however, a chromite content up to 5% has been observed in one section (sample No. 154). Chromite crystals are subhedral or euhedral and are usually below 1 mm in size.

The clinopyroxene is diopside, similar in composition (Table V) to that in "olivine" pyroxenite and pyroxenite. Chromite is rich in ferric iron and Ti and poor in Cr (Table V). It is similar in composition to the accessory chromite in "olivine" pyroxenite and exhibits similar zoning.

V.5. PERIDOTITE

Peridotite is dark green but weathers to a reddish-brown colour in which enstatite shows as brownish-golden crystals. Peridotite is the least serpentized ultramafic rock in the map-area. It is also the most abundant rock type in the map-area and elsewhere in the "alpine-type" peridotite belts of the world. Peridotite exhibits well-developed layering. It is closely associated with dunite and inter-layered with it.

A. Internal structures

Foliation, layering and interlayering with dunite are regional characteristics of the peridotite.

Foliation in peridotite

The foliation in peridotite results from the setting of pyroxene crystals in a plane; there is no preferred orientation within the plane. The foliation grades into layering by an increase in the proportion of pyroxene relative to olivine (Fig. 28).

Layering in peridotite

Four types of layering in peridotite are distinguished and three types are described below. The fourth type, dunite-peridotite interlayering, is discussed later, under "Dunite".

Type 1: The most common type of layering is produced by the interlayering of peridotite with varying pyroxene content or by the interlayering of olivine orthopyroxenite with peridotite. When the compositional difference between the layers is not great, the layers are not well defined and pyroxene-rich layers grade into normal peridotite (Fig. 29). With increasing pyroxene content, up to 95% or so, the pyroxene-rich layers become better defined and have sharp, planar boundaries (Figs. 30 and 31). The thickness of the layers varies from 1 to 25 cm and they are remarkably continuous. Elongated lenses, approximately 3 cm thick, of pyroxene-rich peridotite, are exposed along one horizon for 160 m, the full extent of an exposure. Differential weathering of serpentinized olivine and pyroxene has resulted in low-surface relief for the pyroxene-rich layers, thus accentuating the layering effect in exposure. Layering of this type is commonly exhibited in the Caribou Mountain exposures.



Figure 28. Foliation in peridotite. The central band of pyroxene clusters (parallel to the pencil) is an intermediate situation between foliation and layering.
(Top of Caribou Mountain)



Figure 29. Pyroxene-rich layers in peridotite (type 1 layering). The layers are discontinuous and their boundaries are ill defined.
(Same location as figure 28)

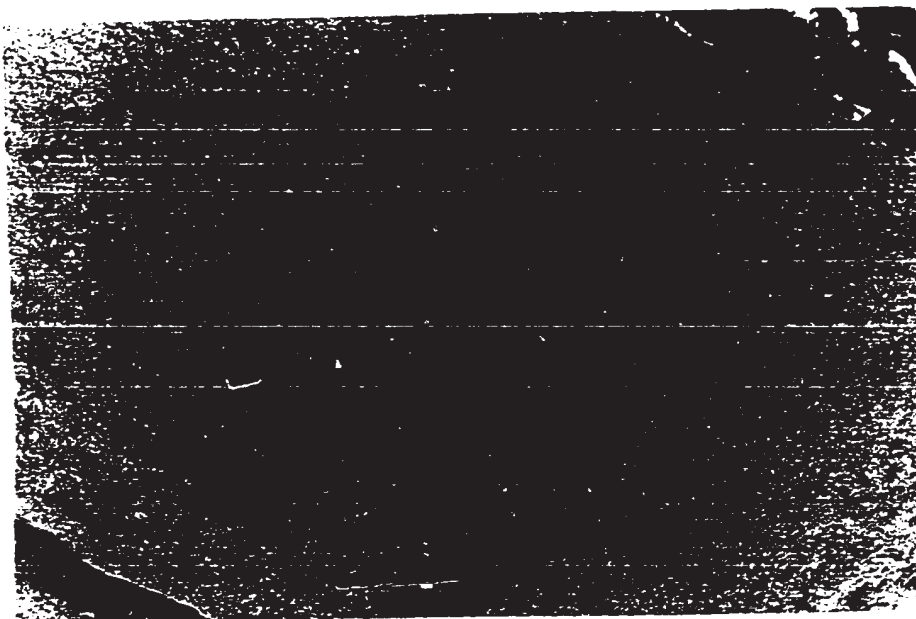


Figure 28. Foliation in peridotite. The central band of pyroxene clusters (parallel to the pencil) is an intermediate situation between foliation and layering.
(Top of Caribou Mountain)



Figure 29. Pyroxene-rich layers in peridotite (type 1 layering). The layers are discontinuous and their boundaries are ill defined.
(Same location as figure 28)

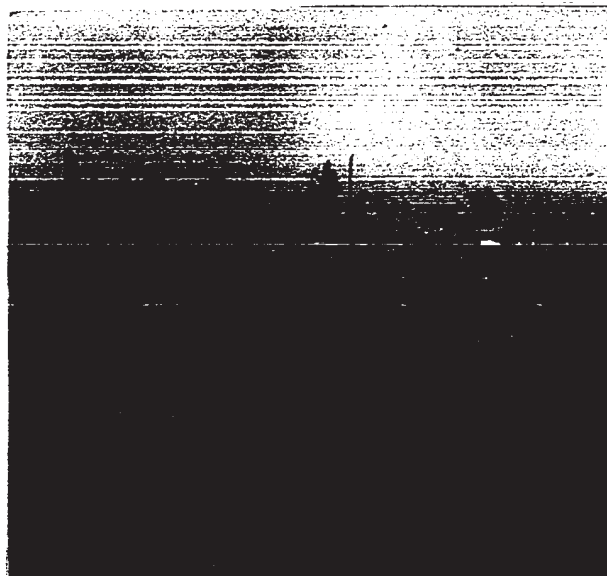


Figure 30. Olivine orthopyroxenite layers in peridotite (type 1 layering). Olivine orthopyroxenite layers have been deeply eroded (centre). The thick layer toward the right of the figure is an orthopyroxenite layer.
(Top of Caribou Mountain)



Figure 31. Olivine orthopyroxenite layers (dark) interbanded with peridotite (type 1 layering).
(Top of Caribou Mountain)



Figure 30. Olivine orthopyroxenite layers in peridotite (type 1 layering). Olivine orthopyroxenite layers have been deeply eroded (centre). The thick layer toward the right of the figure is an orthopyroxenite layer.
(Top of Caribou Mountain)

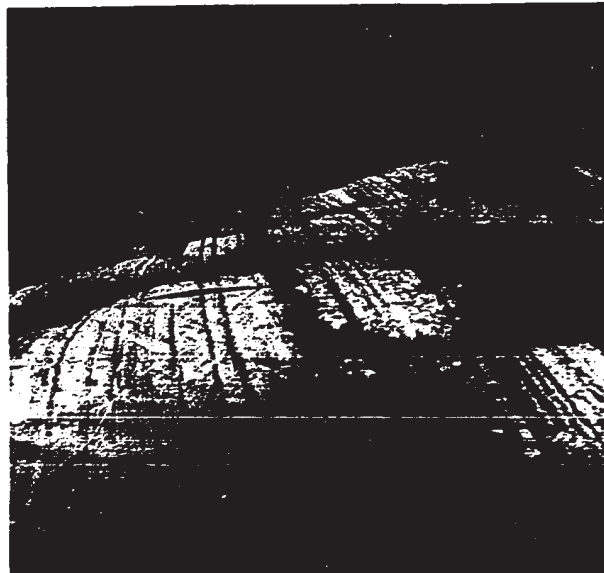


Figure 31. Olivine orthopyroxenite layers (dark) interbanded with peridotite (type 1 layering).
(Top of Caribou Mountain)

Type 2: Orthopyroxenite-peridotite layering. This type of layering is quite similar to type 1 but differs in that the pyroxene-rich layers are olivine-free orthopyroxenite. The contacts of the pyroxenite layers with peridotite are sharp and there is no noticeable variation of the pyroxene content in the peridotite approaching an orthopyroxenite layer. The orthopyroxenite layers in peridotite are mostly much less regular than the layers of type 1 layering. Although numerous pyroxenite layers are continuous over 50 to 100 m., many are discontinuous and consist of a series of small lenses from 3 cm. to 3 m long (Figs. 32 and 33). Even many of the less continuous layers exhibit rapid and considerable variation in thickness. Orthopyroxenite-peridotite layering is common on Belmina Ridge, Caribou Mountain and to a lesser degree on Quarry Hill.

Type 3: Thin dunite layers in peridotite. Locally, close inspection of apparently homogeneous peridotite reveals the presence of thin dunite layers a few mm. thick (Fig. 34). This type of layering is common on King Mountains and Caribou Mountain.

B. Petrography

Peridotite consists of interlocking grains of olivine and orthopyroxene, now partially serpentinized, and accessory chromite (Fig. 35). Although clinopyroxene exsolution lamellae in orthopyroxene are common,



Figure 32. Orthopyroxenite layers (dark grey) in peridotite (type 2 layering). The orthopyroxenite layers are discontinuous. (Belmina Ridge)



Figure 33. Orthopyroxenite layers in peridotite (type 2 layering). The lower layer is very variable in thickness. (Top of Quarry Hill)

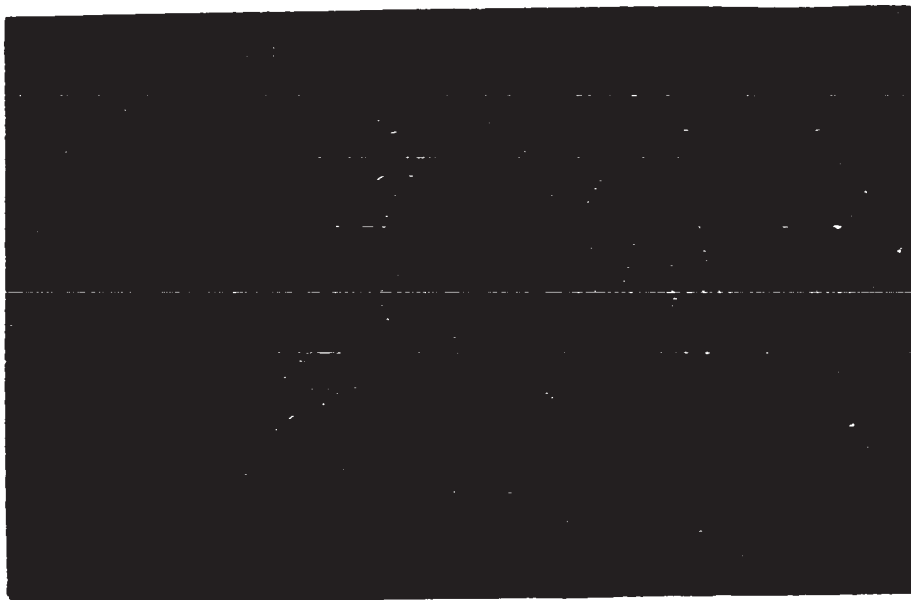


Figure 32. Orthopyroxenite layers (dark grey) in peridotite (type 2 layering). The orthopyroxenite layers are discontinuous. (Belmina Ridge)

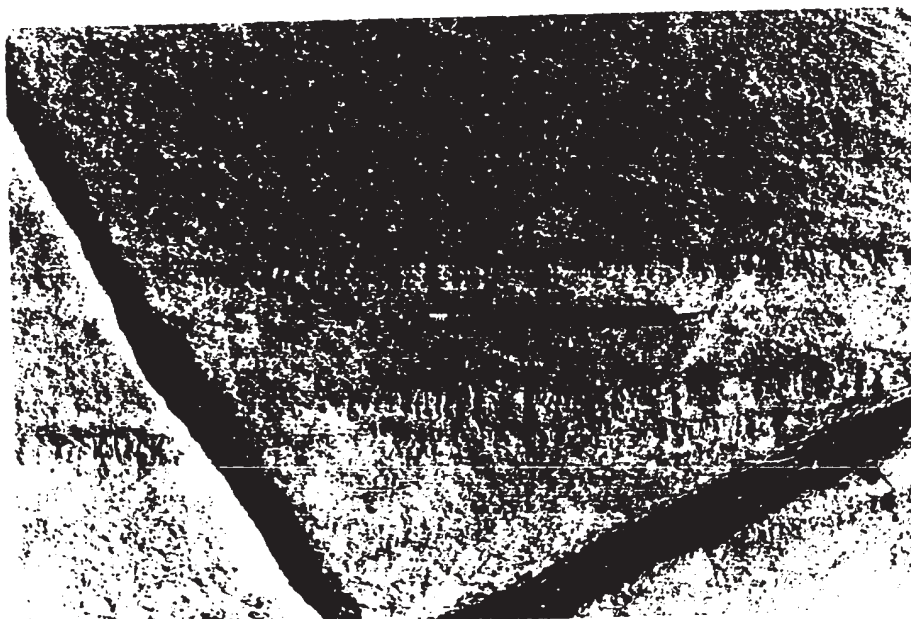


Figure 33. Orthopyroxenite layers in peridotite (type 2 layering). The lower layer is very variable in thickness. (Top of Quarry Hill)



Figure 34. Thin dumite layers in peridotite (type 3 layering).
(King Mountains)

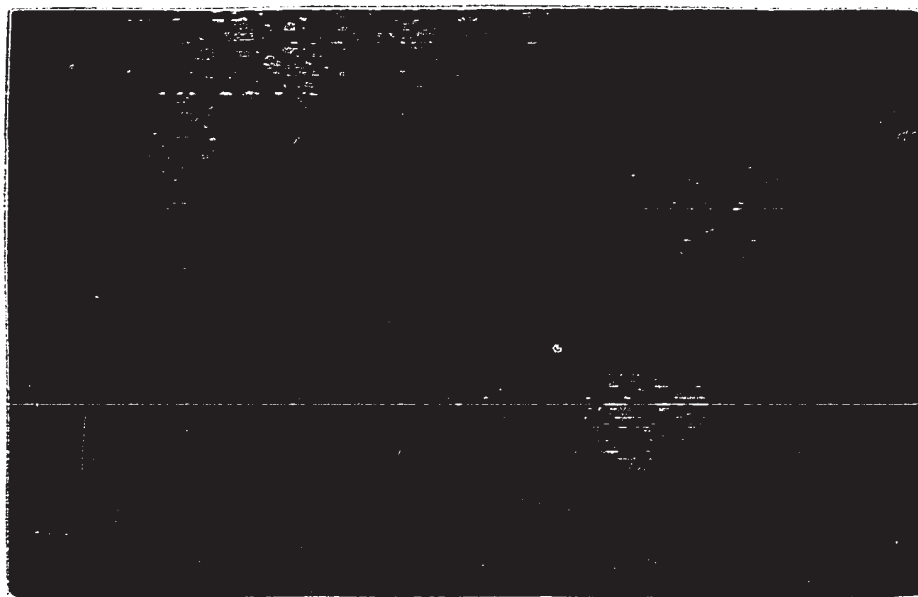


Figure 35. Photomicrograph: Mosaic texture of peridotite
Sample No. 218
Crossed nicols, approximately X 20

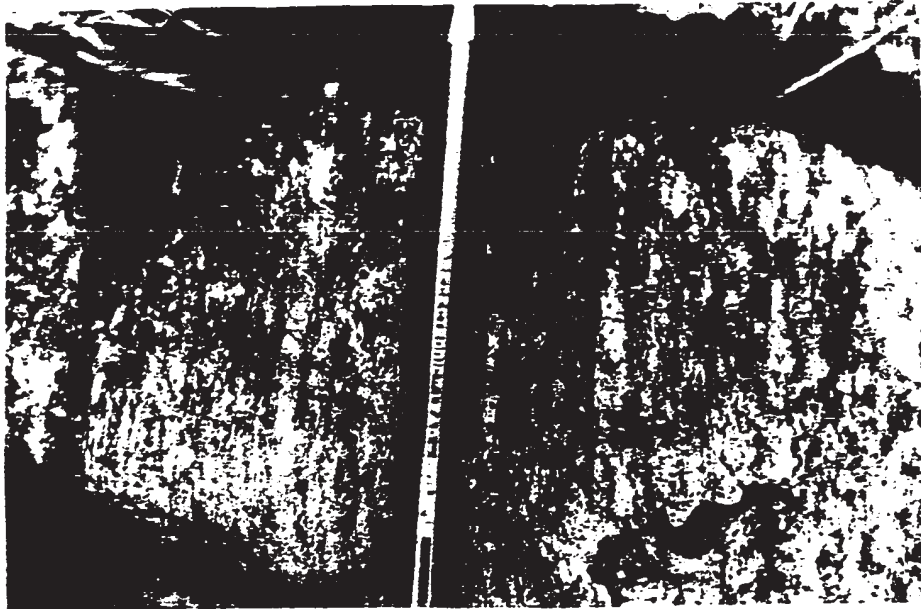


Figure 34. Thin dunite layers in peridotite (type 3 layering).
(King Mountains)

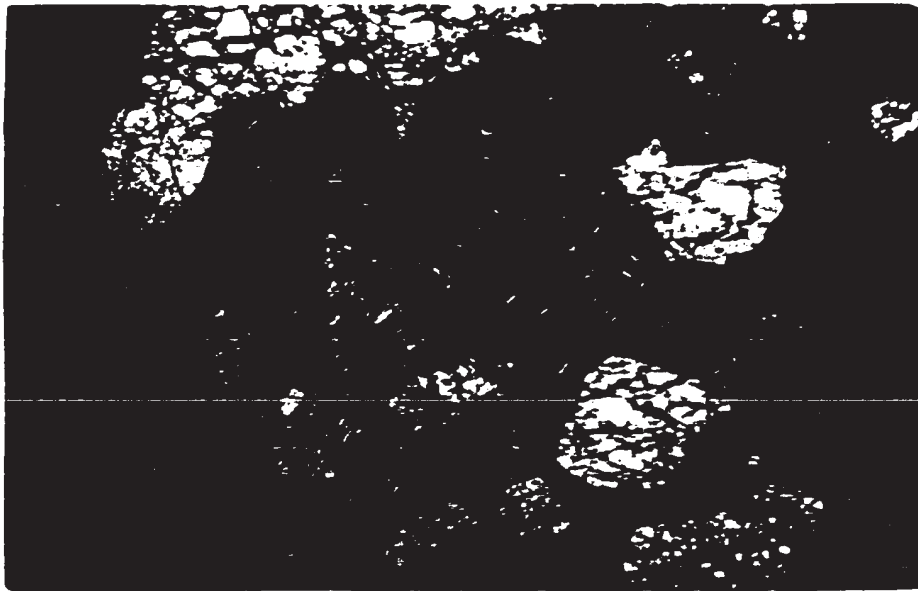


Figure 35. Photomicrograph: Mosaic texture of peridotite
Sample No. 218
Crossed nicols, approximately X 20

individual crystals of clinopyroxene appear to be exceedingly rare; when they occur, they are diopside and interstitial. The orthopyroxene is enstatite, the average enstatite content for the entire peridotite mass of the area is estimated to be 15%. Chromite is irregular in shape and forms 0.5 to 2.5% of the peridotite. The textural characteristics of constituent minerals are described below.

Olivine

Olivine is commonly anhedral, rarely subhedral. The boundaries between adjacent olivine grains can be straight (Fig. 36) or curved and irregular, the grains are usually interlocking and even without pyroxene and chromite they would have formed a largely self-supporting rock. The average grain size of olivine is about 1.5 mm.

No zoning has been detected in olivine. Olivine very rarely contains chromite as inclusion but occurs very commonly as euhedral or subhedral inclusions in chromite. It never contains pyroxene as inclusion but commonly occurs as inclusions in pyroxene. In some serpentinized olivine grains, minute inclusions of a needle-like, unidentified mineral (hematite?), showing a preferred orientation, are observed.

Locally, a mosaic of randomly oriented, very small olivine crystals occurs interstitial to large grains (Fig. 37). This texture is thought to be due to recrystallization. Recrystallization of this type is not common.

Olivine alteration products are serpentine (mainly antigorite), brucite and magnetite. The mode of serpentinization is described in Chapter VII.



Figure 36. Photomicrograph: Straight boundaries of olivine crystals in peridotite. Olivine crystals are intensely fractured. Sample No. 221. Crossed nicols, X 120



Figure 37. Photomicrograph: Recrystallized (?) olivine. Peridotite, Sample D. Crossed nicols, X 120

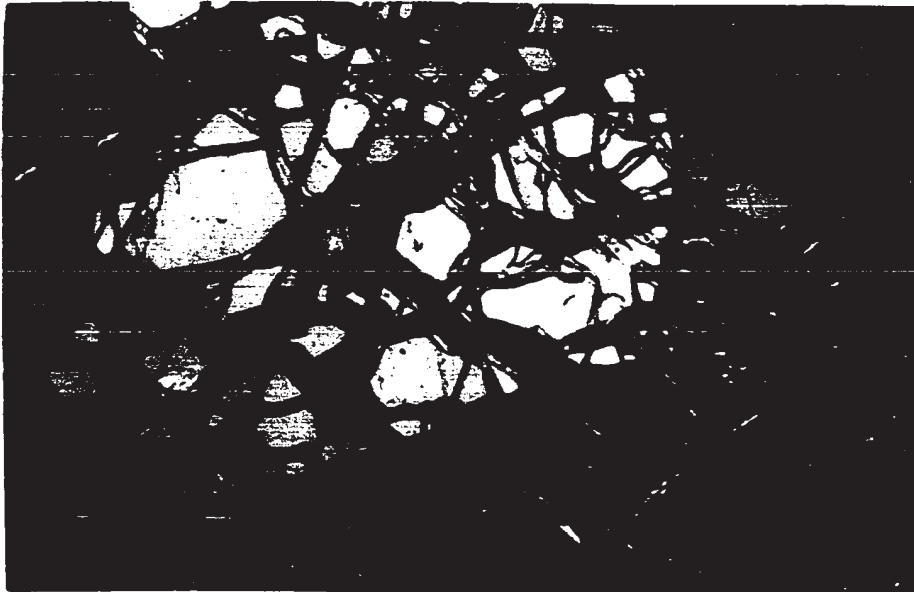


Figure 36. Photomicrograph: Straight boundaries of olivine crystals in peridotite. Olivine crystals are intensely fractured. Sample No. 221
Crossed nicols, X 120

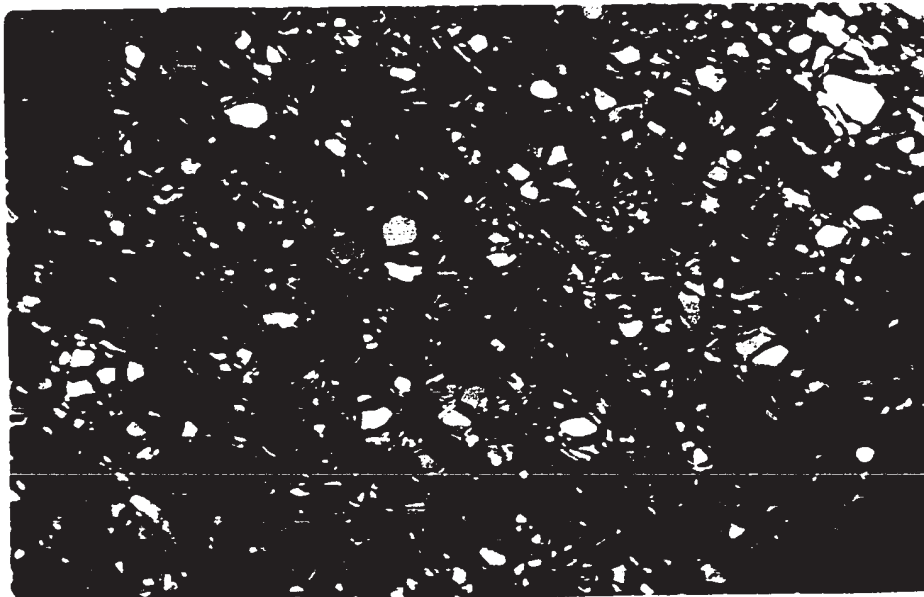


Figure 37. Photomicrograph: Recrystallized (?) olivine. Peridotite, Sample D
Crossed nicols, X 120

Olivine grains are fractured (Fig. 36) and commonly exhibit undulatory extinction together with deformation lamellae. A few measurements on deformation lamellae indicate that they are parallel to (100). The difference of extinction angle between lamellae within a deformed olivine grain rarely exceeds 12° , and the highest observed value is 15° . No systematic study of deformation features has been undertaken.

Challis (1967) proposed that deformation lamellae in olivine are due to stresses imposed by mutual interference of olivine crystals during growth. On the other hand, Raleigh (1967) suggested that the lamellae arise from deformation of previously formed crystals. He obtained, experimentally, deformation lamellae similar to those in naturally deformed olivine, at temperatures of 1000°C and above. Undulatory extinction has been produced by deformation above 450°C .

Orthopyroxene

The orthopyroxene in peridotite is enstatite. In thin section, enstatite can be recognized even when serpentinized, since the serpentine derived from enstatite is flaky and does not form the concentric rims typical of serpentine derived from olivine.

Enstatite is mostly anhedral, rarely subhedral. The grain size varies from 0.2 mm to 3 cm with an average of approximately 2 mm. Enstatite has interlocking boundaries with olivine and chromite. It commonly contains olivine and chromite as inclusions (Fig. 38) but has not been observed included in either of these latter minerals. This suggests that enstatite began to crystallize when the crystallization of olivine and chromite had ceased and that it crystallized from an interstitial liquid while in situ overgrowth of olivine and chromite was



Figure 38. Photomicrograph: Subhedral chromite grain (black, middle of the figure) included in enstatite. The chromite contains two olivine inclusions.
Peridotite, Sample No. 87
Crossed nicols, X 40

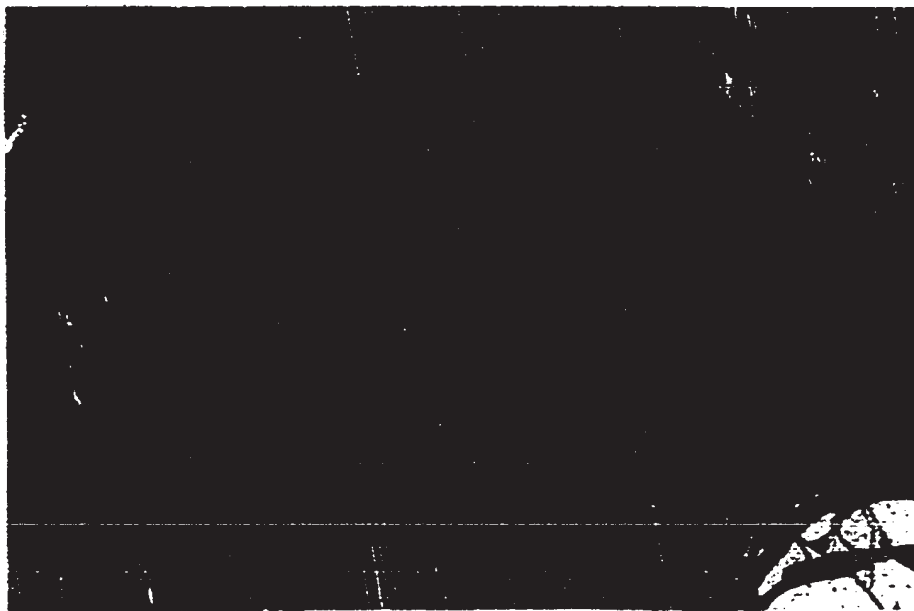


Figure 39. Photomicrograph: Regular, continuous exsolution lamellae of clinopyroxene in enstatite. Note that the exsolution lamellae are less affected by serpentinization; they cross serpentine veins by only negligible weakening.
Peridotite, Sample No. 221
Crossed nicols, X 120



Figure 38. Photomicrograph: Subhedral chromite grain (black, middle of the figure) included in enstatite. The chromite contains two olivine inclusions.
Peridotite, Sample No. 87
Crossed nicols, X 40

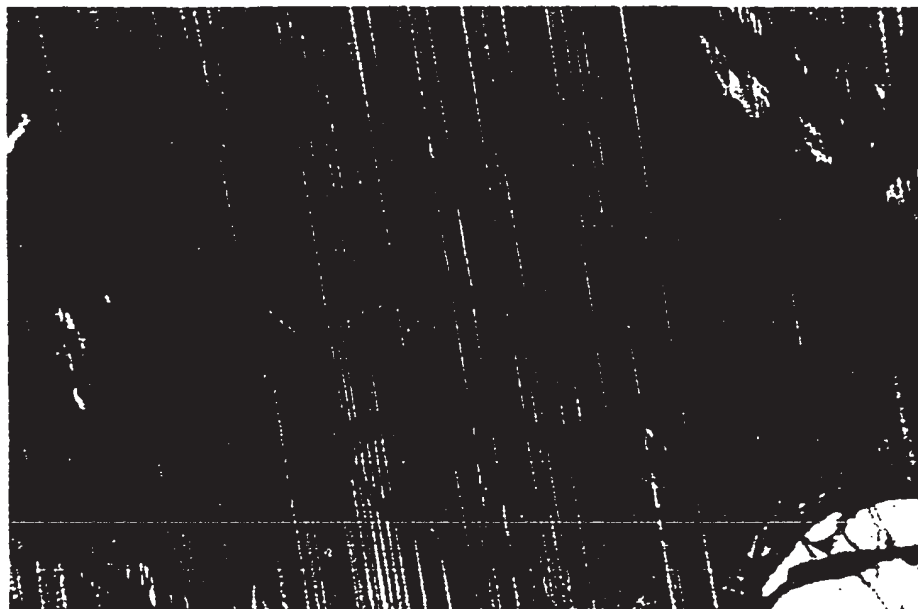


Figure 39. Photomicrograph: Regular, continuous exsolution lamellae of clinopyroxene in enstatite. Note that the exsolution lamellae are less affected by serpentinization; they cross serpentine veins by only negligible weakening.
Peridotite, Sample No. 221
Crossed nicols, X 120

continuing. However, enstatite does not seem to be an interstitial mineral and pyroxene rimming olivine is lacking. Therefore, it is concluded that enstatite crystallized, in the main, contemporaneously with olivine and chromite, but for some reason enstatite crystals did not nucleate olivine or chromite crystals.

Enstatite commonly exhibits abundant exsolution lamellae of clinopyroxene (Figs. 39, 40 and 41), which has the optical characteristics of diopside. The lamellae are usually less than 0.01 mm thick and spaced 0.1 to 0.006 mm apart, and as many as 90 lamellae have been observed within 1 mm. They are continuous throughout almost the whole length of the pyroxene crystal (Fig. 39) and parallel to (100) of the host enstatite. Hess (1960) applied the term "Pyroxene of Bushveld type" to orthopyroxene containing clinopyroxene exsolution lamellae parallel to (100).

Thicker, discontinuous lamellae of diopside are also common (Figs. 40 and 41). The result of an electron microprobe analysis of one of these lamellae, in weight per cent oxide, is : CaO:26.80, MgO:19.89, SiO₂:49.15, FeO:1.92, Al₂O₃:1.52, CrO:0.53, thus confirming that the material is diopside. The thickness of these lamellae varies from 0.05 to 0.003 mm and their length is less than 0.2 mm. They are irregularly spaced, there can be as many as 20 exsolution lamellae per mm or only a few. All the exsolution lamellae within one enstatite grain have the same crystallographic orientation. Toward the margins of the host enstatite crystal, the diopside lamellae usually pinch out or become thinner and less abundant (Fig. 41). Jackson (1961, p. 18) observed similar exsolution lamellae in the pyroxenes of the Stillwater Complex. He suggested that the reduction in number and size of the

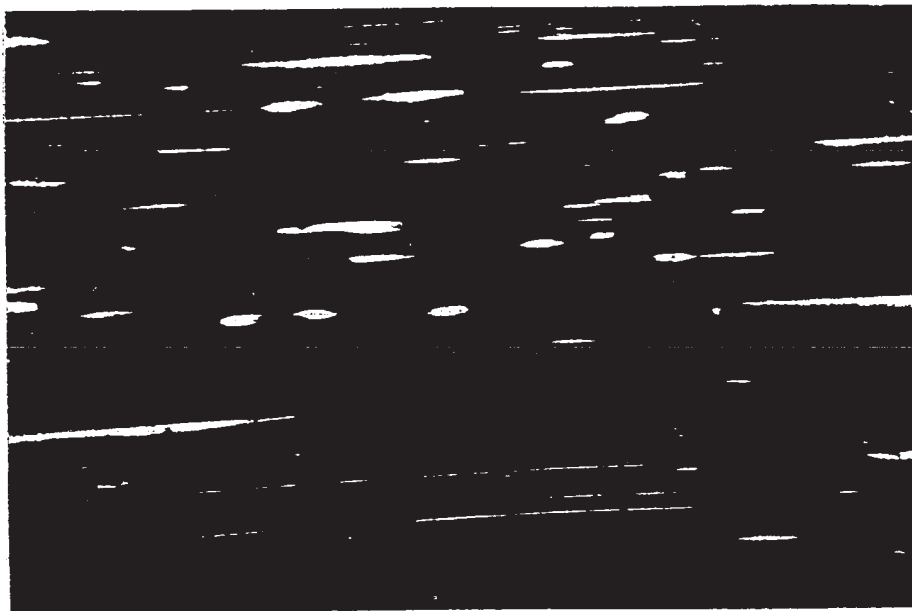


Figure 40. Photomicrograph: Thick, discontinuous exsolution lamellae (white) of diopside and thin, continuous ones in enstatite. The thin and thick lamellae are optically parallel to each other and parallel to (100) of enstatite. Peridotite, Sample No. 556
Crossed nicols, X 120

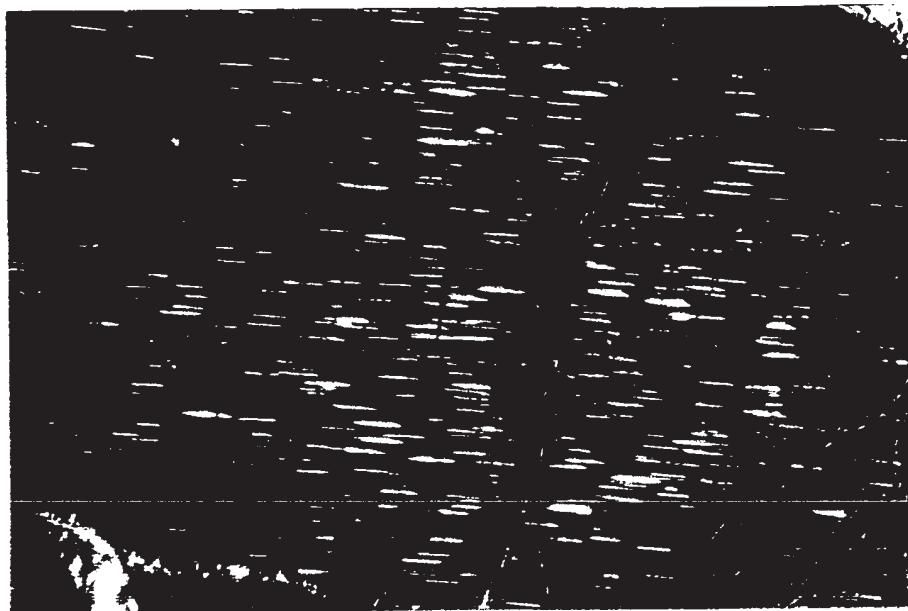


Figure 41. Photomicrograph: Thick, discontinuous exsolution lamellae of diopside in enstatite. Note that the exsolution lamellae are less frequent toward the margin of the grain than toward the centre. Peridotite, Sample No. 554
Crossed nicols, X 40

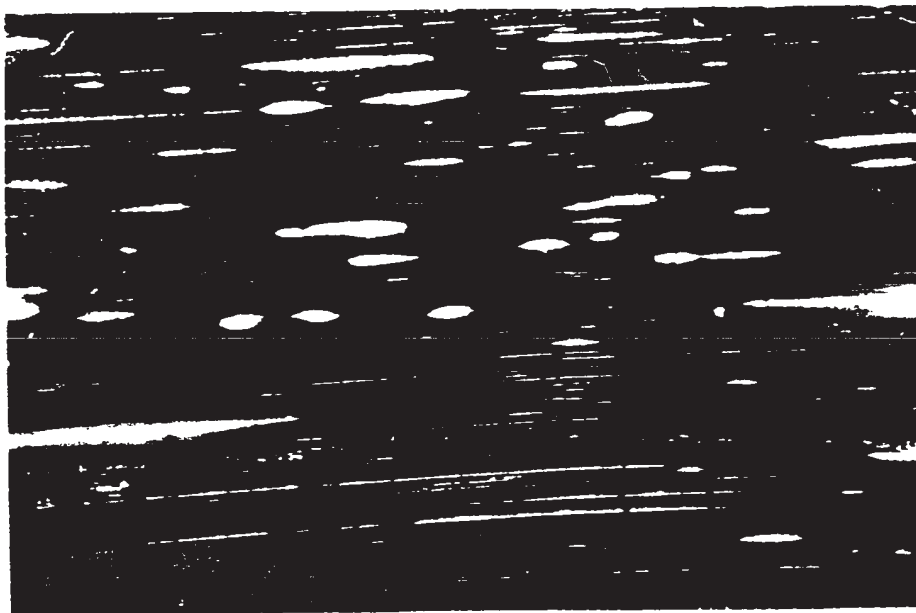


Figure 40. Photomicrograph: Thick, discontinuous exsolution lamellae (white) of diopside and thin, continuous ones in enstatite. The thin and thick lamellae are optically parallel to each other and parallel to (100) of enstatite. Peridotite, Sample No. 556
Crossed nicols, X 120

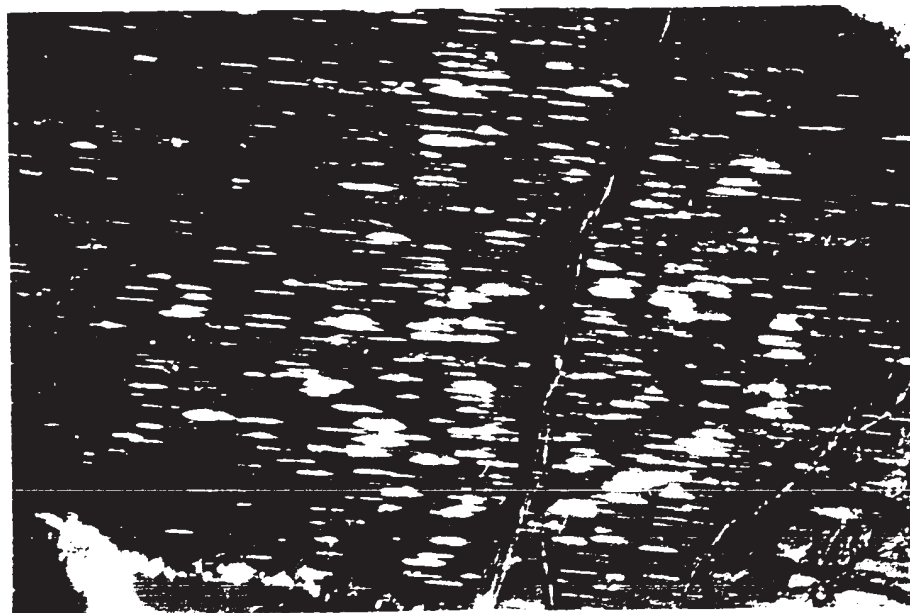


Figure 41. Photomicrograph: Thick, discontinuous exsolution lamellae of diopside in enstatite. Note that the exsolution lamellae are less frequent toward the margin of the grain than toward the centre. Peridotite, Sample No. 554
Crossed nicols, X 40

exsolution lamellae near the grain boundaries might be caused by the migration of Ca near the original grain boundaries during exsolution. Based on this assumption, he further concluded that the exsolution occurred after crystallization of much of the interstitial magma.

The proportion of exsolved diopside to the host enstatite has been estimated for a number of grains by counting the lamellae and measuring their average thickness. Enstatite contains from nil to 20% by volume of exsolved diopside. In view of the small difference in density between diopside and enstatite, the per cent volume can be equated to mole per cent.

Study of the synthetic system diopside-enstatite suggests that the enstatite structure cannot accommodate more than 10 mole per cent diopside at any temperature (Boyd and Schairer, 1964). However, protoenstatite can accommodate up to 24 mole per cent diopside at 1386° C; this amount decreases rapidly to 5% at 1100° C, the inversion point from protoenstatite to $En_{90}Di_{10}$. It is therefore concluded that at least some of the enstatite in the peridotite crystallized initially as protoenstatite and that the crystallization of this latter began at some temperature higher than 1250° C.

In very few cases, the enstatite grains show twinning and reorientation of the lamellae at the twin plane (Fig. 42). In other cases, the pyroxene grains are deformed and show curved lamellae and undulatory extinction (Fig. 43). Deformation lamellae occur but are not common.

Clinopyroxene

Clinopyroxene rarely occurs as separate grains. When it does, it is diopside and similar in composition to the previously described exsolu-

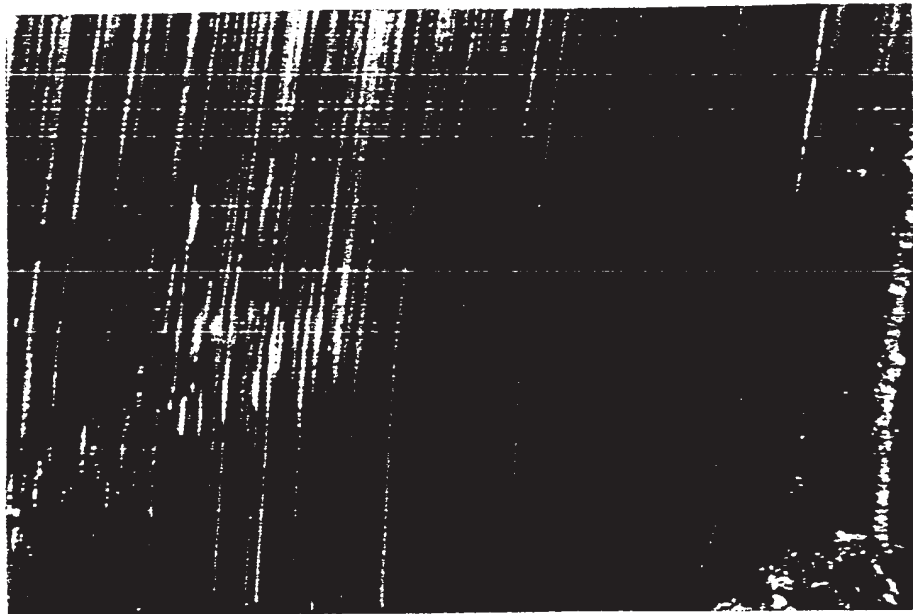


Figure 42. Photomicrograph: Exsolution lamellae bent by the twinning of enstatite. Peridotite, Sample No. 556
Crossed nicols, X 40

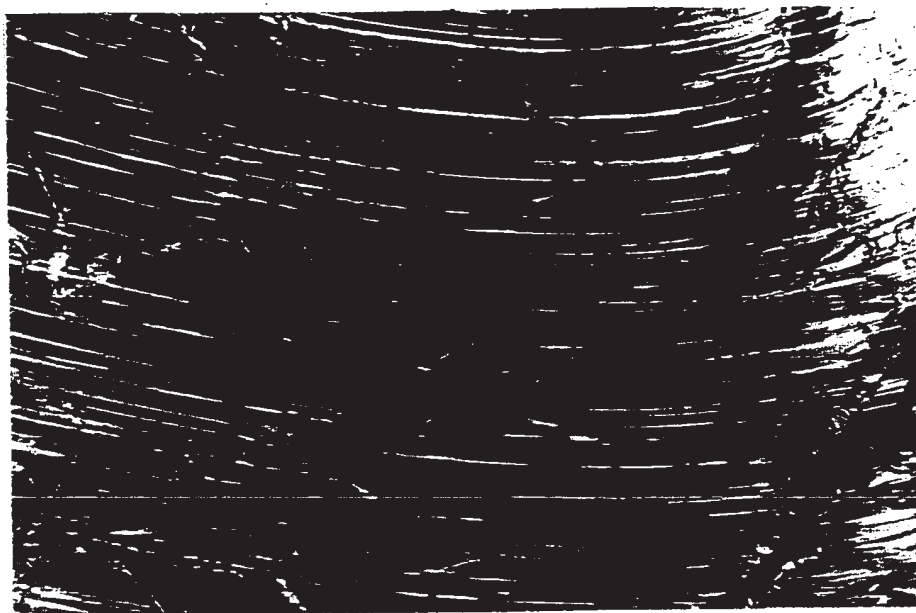


Figure 43. Photomicrograph: Bent exsolution lamellae in deformed enstatite. The enstatite grain exhibits twinning (right of the figure) and undulatory extinction. Peridotite, Sample A
Crossed nicols, X 40

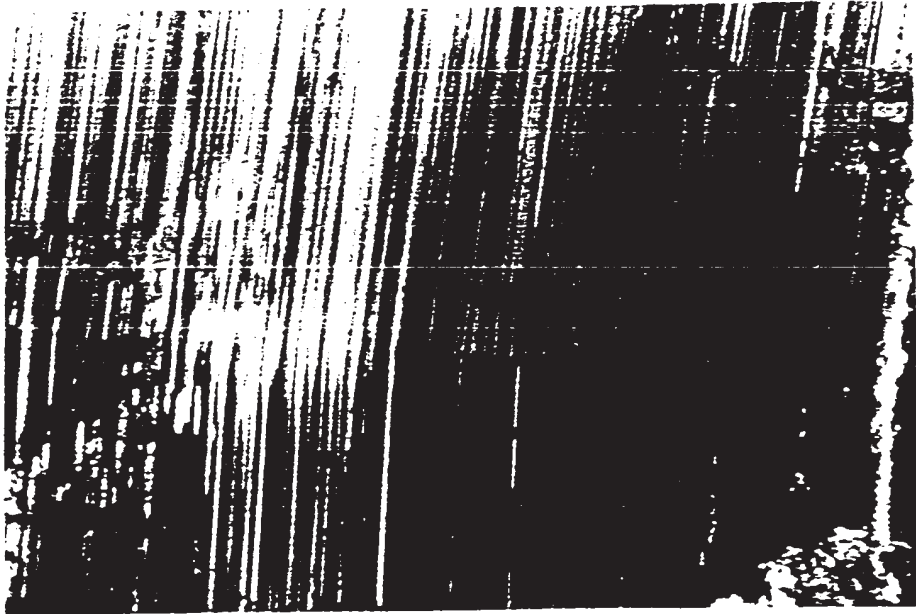


Figure 42. Photomicrograph: Exsolution lamellae bent by the twinning of enstatite. Peridotite, Sample No. 556
Crossed nicols, X 40

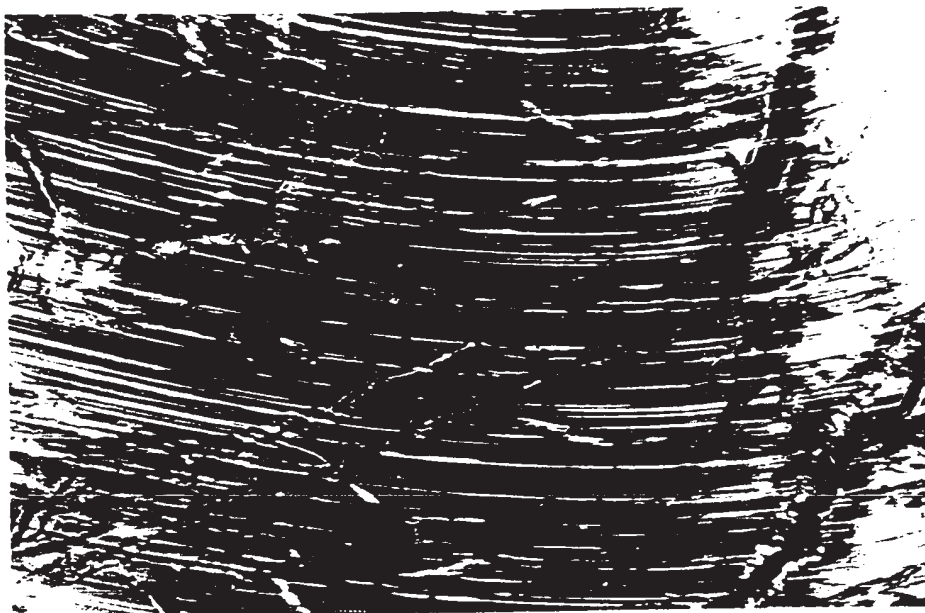


Figure 43. Photomicrograph: Bent exsolution lamellae in deformed enstatite. The enstatite grain exhibits twinning (right of the figure) and undulatory extinction. Peridotite, Sample A
Crossed nicols, X 40

tion lamellae. The grains are interstitial and appear to have crystallized later than orthopyroxene and olivine.

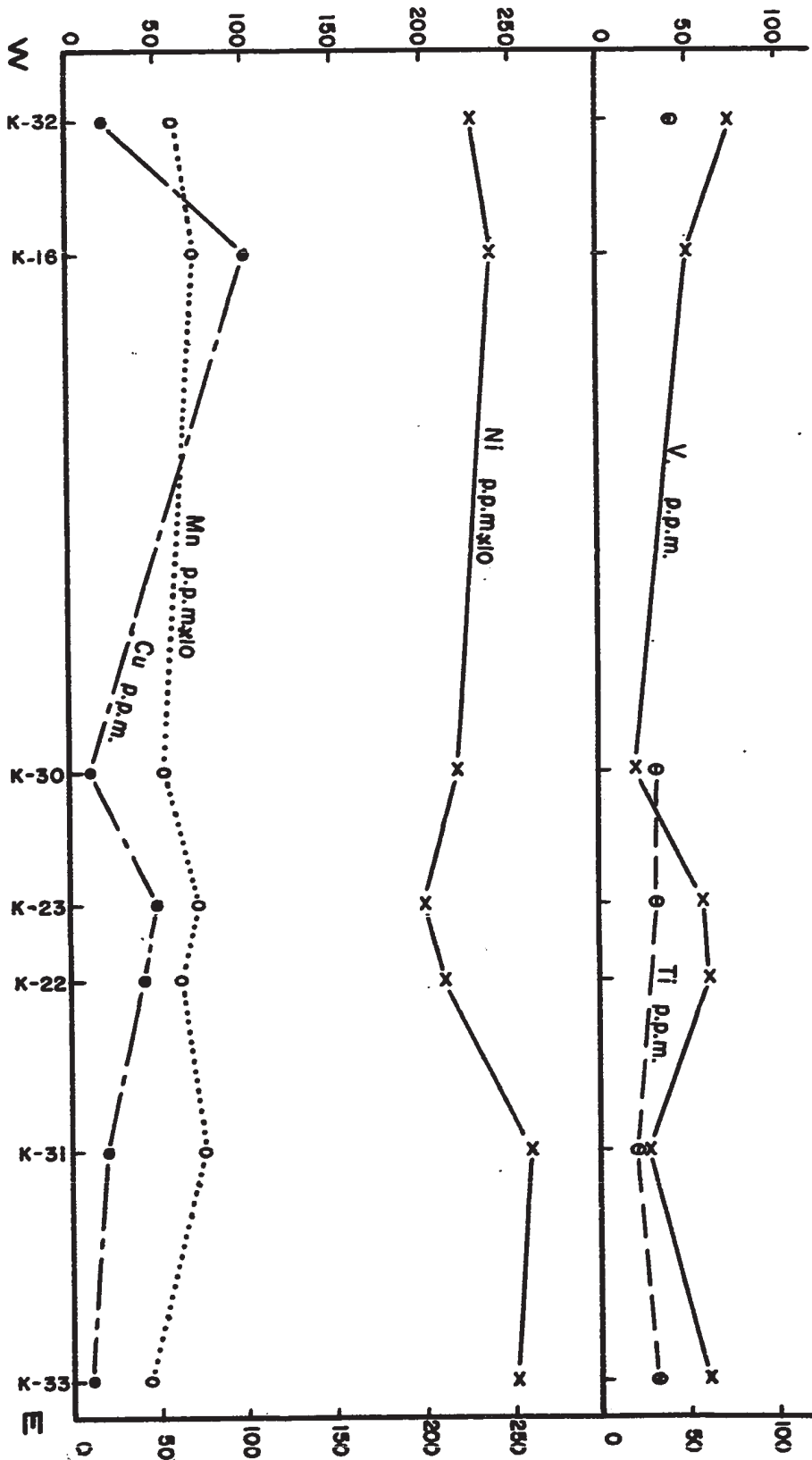
Chromite

Chromite occurs as an accessory mineral in peridotite. It is commonly anhedral and moderately fractured. Chromite may contain olivine inclusions and rarely occurs as inclusions in olivine, thus olivine and chromite must have crystallized contemporaneously. Chromite is also commonly included in orthopyroxene but never contains orthopyroxene inclusions.

C. Chemistry

Trace and minor element analyses of seven peridotite samples are listed in Table IV. These peridotite samples have been taken along a 10 km. east-west traverse on Caribou Mountain, across the general strike of layering in the peridotite (see Fig. 5, p. 27). The analyses show small variations (except for Cu) and a lack of any regular trend (Fig. 44). For instance, the Ni content of peridotite varies only from 2000 ppm to 2600 ppm. This variation is very small compared with the variations observed in stratiform complexes. In the Muskox intrusion, for example, the Ni content of 95 m thick "dunite" layers decreases by more than half from the bottom to the top of layers (Irvine and Smith, 1967).

No zoning has been detected in olivine, and the composition of olivine shows little variation within a sample (see Appendix III). The Ni content is high (0.25 to 0.38%). Olivine is usually richer in Fe (Fig. 45) at the west of Caribou Mountain than on Quarry Hill and,



Horizontal scale 1:50,000

Figure 44. Trace element variations in peridotite

although it is not very regular, there is a decrease in the Fo content of olivine from west to east. However, the variation in the Fo content of olivine does not exceed 1.5 mole per cent. Rapid and considerable compositional variations like those observed in some stratiform complexes are lacking.

Analyses of enstatite from peridotite are presented in Table VI D. There is no correlation between the En content of orthopyroxene and the Fo content of coexisting olivine (Fig. 45). This is perhaps due to the differing amount of exsolved diopside initially contained in the orthopyroxene structure. Orthopyroxene in peridotite has a much higher Mg/Fe ratio than the orthopyroxene in pyroxenite, while clinopyroxene in peridotite is considerably poorer in Fe and, oddly enough, much poorer in Mg and richer in Ca than the same mineral in clinopyroxene-rich rocks ("lherzolite", "olivine" pyroxenite, pyroxenite) (compare Table V, p. 62 and Table VI).

Accessory chromite in peridotite exhibits considerable compositional variation from one sample to another but is fairly constant within each sample. Zoning in the chromite grains is poorly developed and the concentration of Al in the marginal zone is less marked than in accessory chromite in "lherzolite" or "olivine" pyroxenite. Accessory chromite from King Mountains and from the west side of Caribou Mountain is richer in Al and Mg and poorer in Cr than that from Quarry Hill and Murphy Hill. Accessory chromite in peridotite is richer in Mg and much poorer in Fe and Ti than accessory chromite in "lherzolite" and "olivine" pyroxenite (Fig. 64, p. 118 and Fig. 65, p. 119). This is consistent with the iron-rich nature of these latter two rock types compared with peridotite.

TABLE VI
Microprobe Analyses
Mean composition¹ of minerals in peridotite, olivine orthopyroxenite and orthopyroxenite

A) Accessory chromite in peridotite and olivine orthopyroxenite* ($\pm 60\%$ orthopyroxene)

Sample No.	Cr	Fe tot.	Cations wt. %				Al	Ti
			Fe ⁺²	Fe ⁺³	Mg	Ti		
A	18.20	11.34	7.42	3.92	10.79	21.97	0.14	
B	23.70	12.10	9.97	2.13	9.89	18.03	0.02	
C	30.43	12.83	10.81	2.02	8.57	12.64	0.03	
D	18.58	10.58	6.77	3.81	11.48	20.50	0.08	
E	19.25	11.36	8.56	2.80	10.48	20.19	-	
F	25.98	13.38	10.75	2.63	9.58	16.74	0.03	
G	33.71	14.33	13.71	0.62	6.98	10.62	-	
H	24.30	12.58	8.38	4.20	10.17	16.09	0.04	
I	29.04	13.47	10.28	3.19	8.97	13.22	0.05	
K-57*	29.73	15.40	12.88	2.52	7.75	13.07	0.02	
K-58	39.88	17.00	16.83	0.17	5.60	7.77	0.09	
48	30.97	14.32	10.29	4.03	9.50	12.95	0.09	
56	35.34	18.15	16.08	2.07	5.82	9.04	-	
58	31.56	19.33	16.25	3.08	4.39	7.50	0.03	
65	31.15	17.17	14.26	2.91	5.96	9.93	0.03	
72	32.15	15.58	12.16	3.42	7.38	9.77	0.10	
87	29.72	15.60	13.08	2.52	8.28	14.12	0.11	
218	39.32	14.99	13.87	1.12	7.09	8.24	0.05	
221	28.39	16.38	13.69	2.69	7.55	13.81	0.21	
225	28.67	14.32	11.93	2.39	8.17	12.59	-	
258	32.85	16.08	14.51	1.57	6.18	9.88	0.02	
366	23.41	10.69	8.56	2.13	10.28	18.17	0.04	
476	19.69	13.09	7.88	5.21	9.70	16.35	0.04	

¹ The analytical procedure, calculation of mean composition, the precision, accuracy and detail of analyses are indicated in Appendix III.
Fe⁺² and Fe⁺³ values have been calculated from total iron.

TABLE VI (continued)

B) Olivine in peridotite and olivine orthopyroxenite*

Sample No.	Cations wt.%				Mole.%Fo.
	Mg	Fe	Ni	Si	
A	29.97	7.14	0.35	18.67	90.5
C	28.00	7.33	0.26	18.92	89.7
D	29.07	7.41	0.38	19.41	90.0
E	28.80	7.32	0.26	18.44	90.0
G	27.00	7.61	0.30	18.77	89.0
I	27.67	7.45	0.26	19.60	90.3
K-57*	30.40	7.53	0.32	18.59	90.8
K-58	29.50	7.85	0.30	18.68	90.6
48	29.96	7.11	0.37	18.87	90.5
56	29.75	7.30	0.26	19.21	90.3
65	29.60	7.08	-	18.18	90.5
72	30.61	7.52	-	18.61	90.3
87	29.80	7.62	-	18.63	89.9
218	30.09	7.05	0.25	17.85	90.6
221	29.21	6.74	-	18.86	90.8
225	30.48	7.25	-	18.40	90.5
258	29.05	7.38	-	19.00	89.9
366	29.13	7.48	0.27	19.60	89.9
476	29.73	7.59	-	18.70	90.0
554	30.37	7.24	-	19.13	89.9

C) Clinopyroxene in peridotite and orthopyroxenite

Sample No.	K-58	221
Rock type	Orthopyroxenite (layer)	Peridotite
	10.95	10.11
Mg	2.10	1.50
Fe	25.35	24.59
Si	0.49	0.95
Al	0.15	0.20
Cr	17.55	18.75
Ca		
End members	Wo _{47.6} En _{48.4} Fs ₄	Wo _{51.3} En _{45.7} Fe ₃
Mole. %		

Samples No. K-58 and No. 221 are located 5 km. apart from each other (see Map 2).

Locations of all samples in Table VI are indicated on Map 2.

TABLE VI (continued)

D) Orthopyroxene in peridotite, olivine orthopyroxenite* and orthopyroxenite (K-58, 554)

(K-58: Orthopyroxenite layer, 554: Orthopyroxenite vein)

Sample No.	Cations wt. %										Mole. % En.
	Mg	Fe	Si	Al	Cr	Ca	Ni				
A	21.08	3.98	26.66	0.98	0.16	0.21	0.03				92.8
C	21.58	3.84	27.14	0.69	0.19	0.38	-				92.8
D	21.08	3.90	26.97	0.94	0.12	0.31	0.06				92.5
E	20.92	3.87	27.18	1.00	0.17	0.36	-				92.6
G	22.50	3.51	27.73	0.51	0.11	0.18	-				93.6
I	21.63	3.87	27.63	0.47	-	-	-				92.8
K-57*	21.58	3.95	26.91	0.62	0.19	0.57	-				92.6
48	21.14	3.71	27.37	0.56	0.15	0.42	-				92.9
56	22.82	3.99	-	0.56	0.15	0.42	0.11				93.0
65	21.21	3.91	27.30	0.46	0.14	0.46	-				92.6
87	19.64	3.89	28.48	0.61	0.19	0.41	-				92.1
218	21.31	3.73	27.02	0.38	0.14	0.36	-				92.9
221	20.78	4.68	26.69	0.85	0.32	0.67	-				91.1
225	19.85	4.35	28.00	0.66	0.17	0.59	-				91.3
258	19.32	4.10	27.94	0.49	0.18	0.41	-				91.5
366	19.51	3.96	27.33	0.93	-	-	-				91.9
476	20.53	3.96	28.92	1.12	0.14	0.24	-				92.3
K-58	21.14	4.58	26.88	0.27	0.05	0.61	-				91.4
554	21.09	5.10	25.89	0.53	0.38	0.60	-				90.1

Samples No. K-58 and No. 554 both contain peridotite and orthopyroxenite.

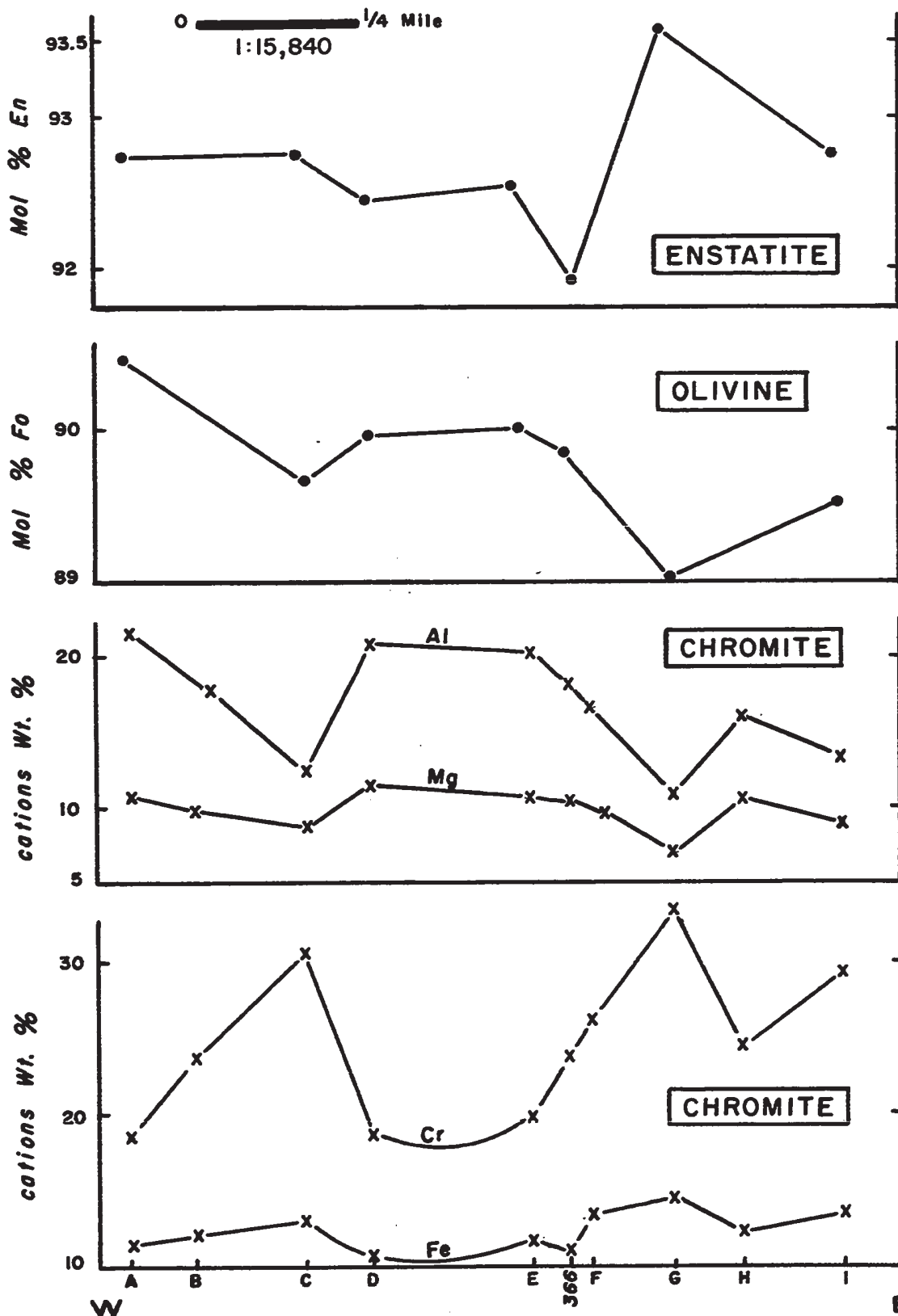


Figure 45. Compositional variations in coexisting olivine, orthopyroxene and chromite in peridotite of Caribou Mountain.

Since three of the most important minerals of the ultramafic rocks, namely olivine, orthopyroxene and chromite coexist in the peridotite, variation diagrams have been made. In all diagrams mean compositions have been used. The variation diagrams did not yield conclusive information concerning the degree of equilibrium between the coexisting phases.

There is a positive correlation between the Mg content of chromite and the Fo content of olivine (Fig. 45). There is no correlation between $Mg/Mg+Fe^{++}$ or $Mg/Mg+Fe_{total}$ ratios in chromite and the $Mg/Mg+Fe^{++}$ ratio in the coexisting olivine. The Fo content of olivine does not correlate with the En content of coexisting orthopyroxene.

The Al content of orthopyroxene increases with increasing Al content of the coexisting chromite (Fig. 46). There is no correlation between $Mg/Mg+Fe^{++}$ or $Mg/Mg+Fe_{total}$ ratios in chromite and $Mg/Mg+Fe^{++}$ ratios in coexisting orthopyroxene.

Irvine (1965) contoured the spinel triangular prism of composition by theoretical surfaces joining spinel compositions that may, at a given temperature and pressure, coexist in equilibrium with olivine or pyroxene having specific MgO/FeO ratios. According to Irvine (1965), if spinel, olivine and orthopyroxene coexist and are in equilibrium, the chemical potentials of MgO and FeO are fixed along these surfaces which, therefore, are referred to as equipotential surfaces. The traces of the equipotential surfaces on the faces of the spinel compositional prism are equipotential lines (Irvine, 1965).

An attempt has been made to contour the composition of accessory chromite in the peridotite according to Fo and En contents of coexisting olivine and orthopyroxene respectively. The trend of the equipotential lines for $\ln K_e = 4$ (where K_e is the equilibrium constant for the reaction $MgCr_2O_4 +$

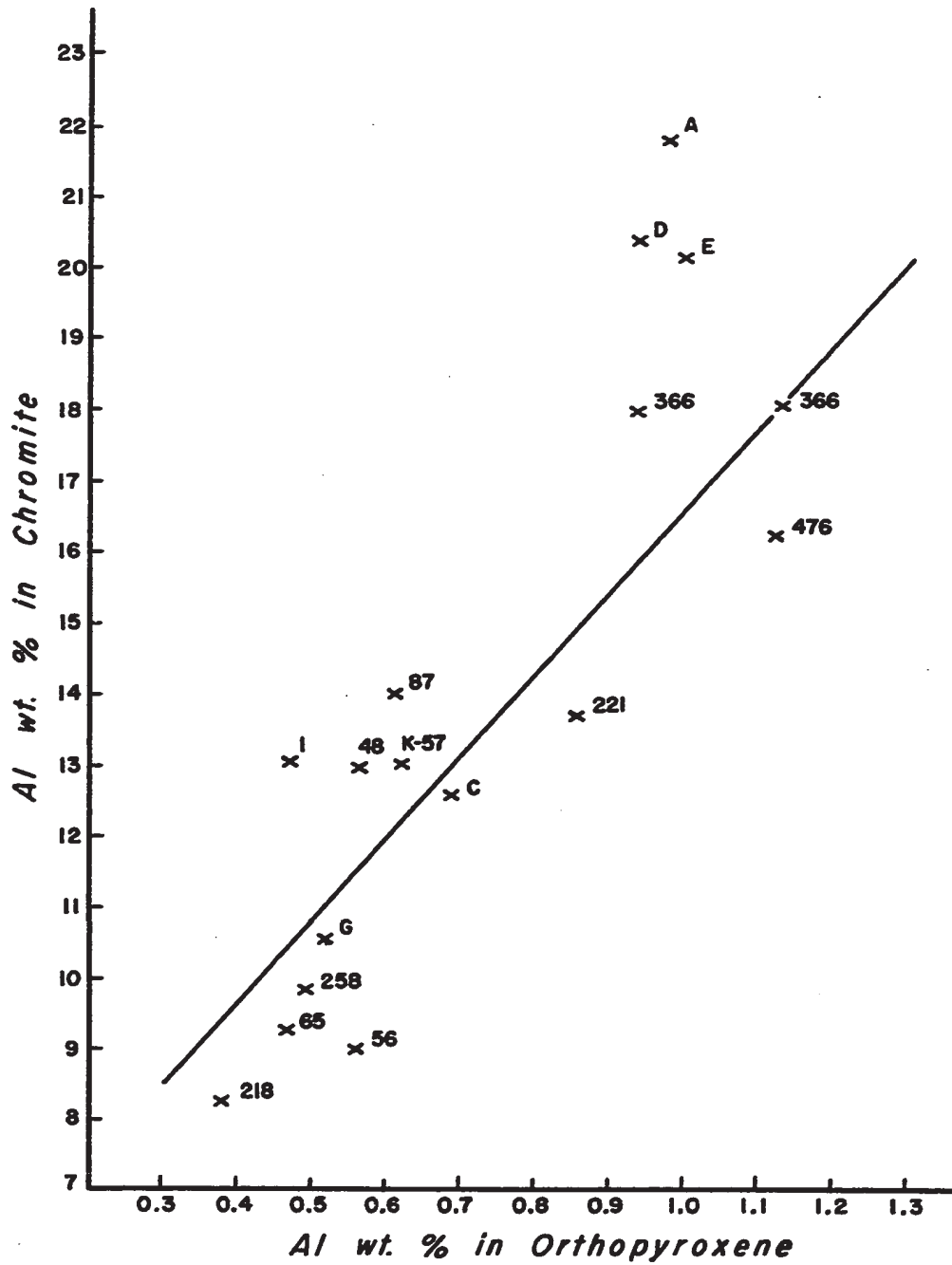


Figure 46. Aluminum content of coexisting enstatite and chromite in peridotite and olivine orthopyroxenite (Sample No. K-57).

$\text{FeAl}_2\text{O}_4 \rightleftharpoons \text{FeCr}_2\text{O}_4 + \text{MgAl}_2\text{O}_4$) given by Irvine (1965, Fig. 7, p. 663) was used as the trend of eventual contours. The $\ln K_e$ values for chromite - orthopyroxene and chromite - olivine pairs were estimated using relationships developed by Irvine (1965, equations 15 and 16, p. 660) and subject to the same assumptions, that is, phases in each pair formed together in equilibrium at a temperature where they behaved as ideal solutions. Plots to estimate $\ln K_e$ values are given in the Appendices. It was not possible to thus contour the chromite compositions. This may be due to non-equilibrium between the phases, to analytical errors or different temperatures of formations of the phases.

The plots of distributions of elements, discussed above, between coexisting chromite, olivine and orthopyroxene are inconclusive concerning their degree of equilibrium. This point is further discussed below, under "Discussion".

D. Discussion

In the peridotite of the map-area the Mg/Fe ratio is consistently higher in orthopyroxene than in coexisting olivine (Table VI B and D, compare the Fo content of olivine with the En content of orthopyroxene). This is in contrast to stratiform complexes where the Mg/Fe ratio in olivine is equal to or higher than the same ratio in the coexisting orthopyroxene (Fig. 47).

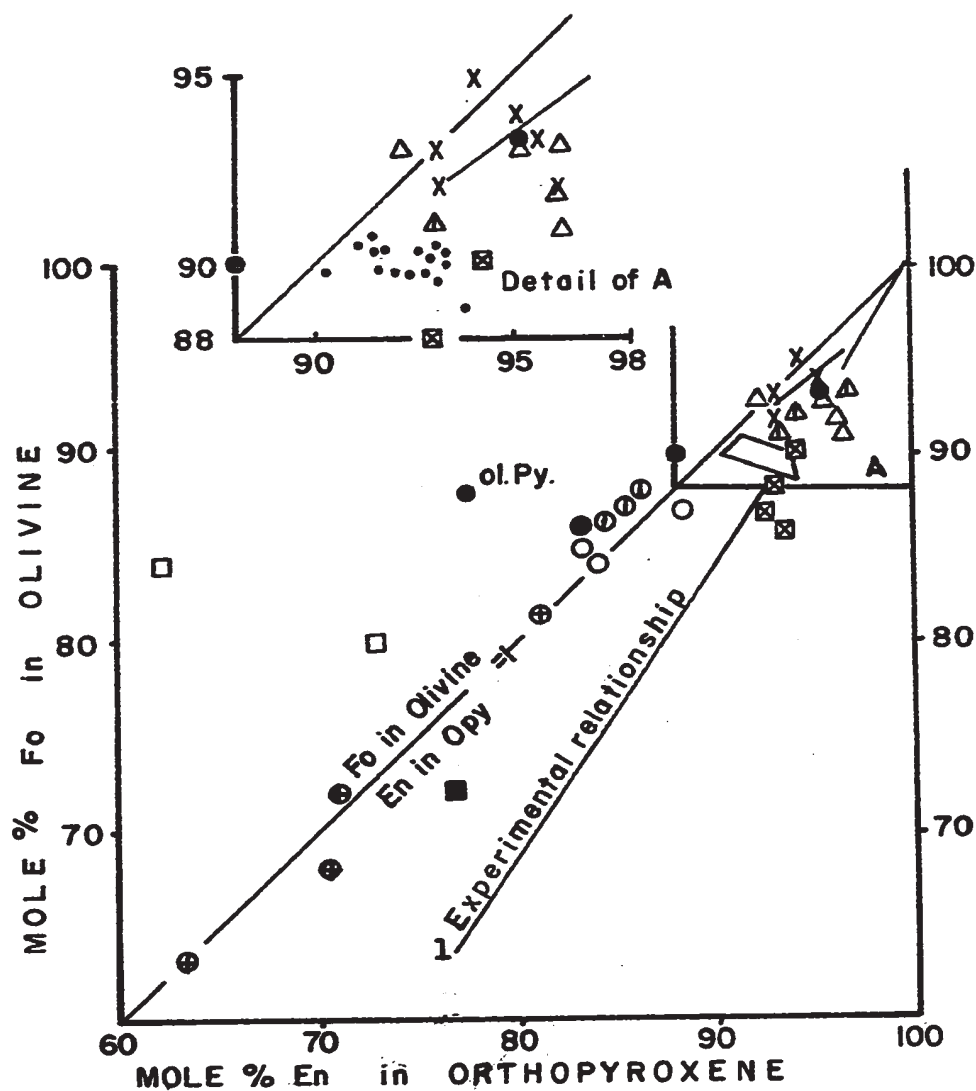
Experimental work in the system MgO-FeO-SiO_2 (Bowen and Schairer, 1935, op. cit. in O'Hara, 1963) showed that at equilibrium the Mg/Fe ratio in olivine is lower than in the coexisting Ca-poor pyroxene. Although the experiments involved clinopyroxene and olivine rather than orthopyroxene and olivine, the authors of these experiments have

argued that the clino-ortho inversion in the hypersthene will not influence the distribution of Fe^{++} and Mg between the phases involved.

O'Hara (1963) discussed the distribution of Fe^{++} and Mg between coexisting olivine and orthopyroxene in igneous and metamorphic rocks and in meteorites. Comparing the Mg-Fe distribution in natural assemblages with the experimental results, he concluded that equilibrium between coexisting olivine and orthopyroxene is rarely attained in nature. O'Hara (1963, 1967a) has reported that garnet peridotites, Pyrenean spinel lherzolites, peridotite nodules in kimberlite and chondritic meteorites contain olivine with a Mg/Fe ratio equal to or lower than the ratio in coexisting orthopyroxene. He suggested that olivine-orthopyroxene pairs in these rocks probably represent or approach true equilibrium.

The compositions of coexisting olivine and orthopyroxene from several igneous bodies and from a metamorphic rock, together with the experimental relationship are shown in Fig. 47. Except for the data from the present map-area and the Bay of Islands Complex, the mineral compositions have been taken from O'Hara (1963). The olivine and orthopyroxene compositions from the Bay of Islands Complex are from Smith (1958). The compositions of some olivine-orthopyroxene pairs from the peridotite of the map-area plot among those from equilibrium assemblages (Fig. 47), hence the peridotite perhaps represents an equilibrium assemblage.

The effects of temperature and pressure on the Mg-Fe distribution between olivine and coexisting orthopyroxene are not well known. According to Bartholomé (1962), with increasing temperature of equilibration the Fe content of olivine increases with respect to ortho-



- Harzburgite and olivine pyroxenite (Ol.Py.), Great Dyke, Rhodesia
- Harzburgite, Stillwater Complex, Montana (⊙: plot of more than one sample)
- ⊕ Skaergaard, Greenland
- Basalt, Hawaii
- △ Harzburgite and garnet harzburgite xenoliths in kimberlites (▲: plot of more than one sample)
- × Garnetiferous harzburgite in gneissic terrains, Norway
- ⊠ Lherzolite, Lherz (Pyrenees) and garnet lherzolite, Bellinzona, Switzerland
- Pyroxene-granulite, Eilean Carach, Ardnamurchan
- ⊖ Range of composition of coexisting olivine and orthopyroxene in harzburgite from the Bay of Islands Complex, Canada
- Peridotite (harzburgite) from the Thetford-Black Lake Area, Quebec

Figure 47. Compositions of coexisting orthopyroxene and olivine in ultramafic and mafic igneous rocks and in a pyroxene granulite. Line denoted 1 is the experimental relationship for the Mg-Fe distribution between coexisting olivine and orthopyroxene.

pyroxene. The plots of compositions of naturally occurring olivine-orthopyroxene pairs presented by O'Hara (1963) and those in Fig. 47 suggest that pressure increase perhaps increases the Fe^{++} concentration in olivine relative to orthopyroxene. If this is true, the data presented in Fig. 47 can be interpreted consistently. In rocks believed to have formed at high pressure (e.g. garnet peridotites, granulite, etc.) the Mg/Fe ratio in olivine is lower than the same ratio in coexisting orthopyroxene, whereas the reverse is observed for low-pressure assemblages (e.g. basalt, stratiform complexes).

Bartholomé (1962) suggested that the equilibrium constant K_T $(\text{Fe}^{++}/\text{Mg})_{\text{ol}} / (\frac{\text{Fe}^{++}}{\text{Mg}})_{\text{opx}}^2$ is temperature dependent and his plot of K_T versus temperature is shown in Fig. 48. The equilibrium constants for the olivine-orthopyroxene pairs from the peridotite of the map-area are listed in Table XIII and the range is plotted on Bartholomé's curve (Fig. 48). This suggests temperatures of equilibration between 1350° and 1750°C. Bartholomé emphasized that his curve is a first approximation based on the assumption of equilibrium and ideality of the solutions, hence the above temperature range is approximate. Nevertheless, one might postulate that the temperature of equilibration of olivine-orthopyroxene in peridotite was in the range 1500 to 1600°C.

It is therefore suggested that the peridotite in the map-area perhaps represents a high-temperature and/or high-pressure equilibrium assemblage.

Aluminum-rich accessory chromite in peridotite

The peridotite contains accessory chromite which, locally, is rich in Al (17 to 21% Al), whereas the Al content of accessory chromite from

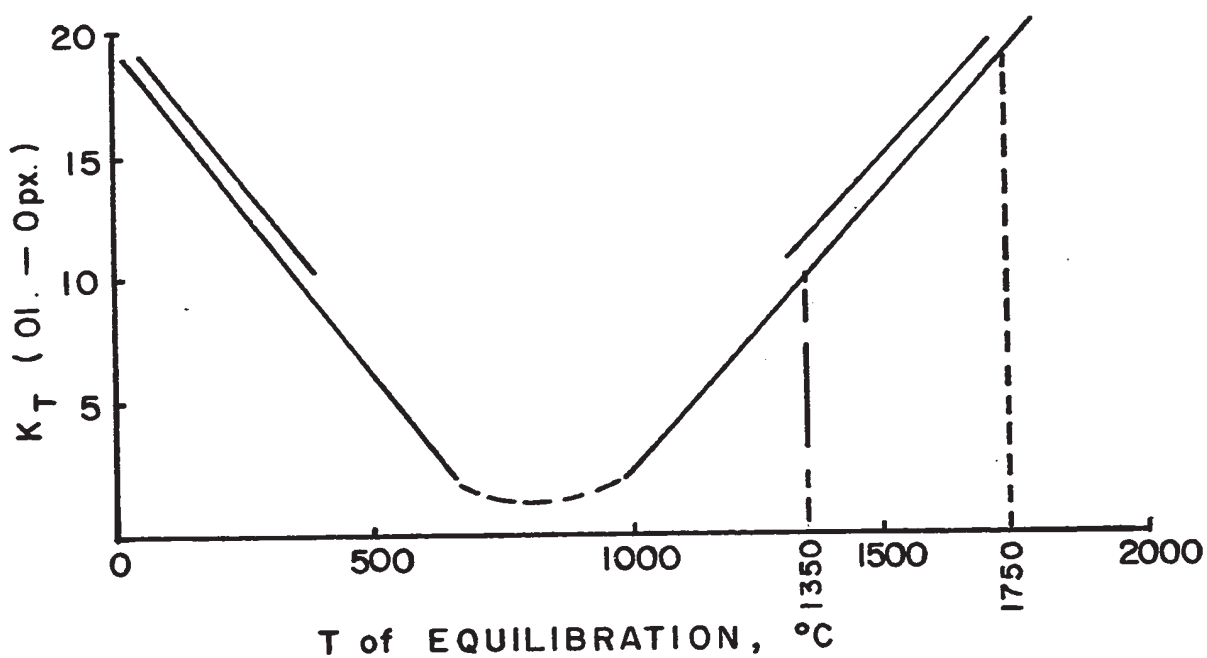


Figure 48. Variations of equilibrium constant K_T (ol-opx) versus temperature of equilibration for olivine-orthopyroxene pairs in the peridotite (after Bartholomé, 1962). The K_T values are listed in Table XII in the Appendices and their range is plotted on the above curve (the two short bars).

most peridotite samples ranges from 7.5 to 14% (Table VI A).

Green (1967) has proposed a metamorphic origin for the aluminous spinel from both the Lizard and Tinaquillo ultramafic bodies. He suggested that the spinel is formed from elements released during recrystallization of aluminous enstatite. The possibility of a similar origin for the Al-rich chromite in the peridotite has not been overlooked. However, it is believed, for the following reasons, that such a metamorphic origin is unlikely for the Al-rich chromite. Firstly, enstatite coexisting with Al-rich chromite is not depleted in Al and Cr relative to enstatite coexisting with Al-poor chromite. On the contrary, the Al content of enstatite increases with increasing Al content of coexisting chromite (Fig. 46). Secondly, enstatite in the peridotite of the map-area is an unlikely source of Al, since it is low in Al. Furthermore, the orthopyroxene was probably never rich in Al, since it contains abundant diopside exsolution lamellae; experiments have shown that increasing Al content of coexisting diopside and enstatite results in a continuous decrease of their mutual solubility (MacGregor, 1967). Thirdly, there is no correlation between the amount of enstatite in the rock and the Al content of chromite, and chromite compositions are fairly homogeneous within a sample. Therefore, it is unlikely that there are two generations of chromite, one originating by magmatic processes, the other by metamorphism.

It is therefore concluded that the compositional variations of accessory chromite in peridotite are due, in the main, to primary magmatic crystallization and reaction. The large variation in the Cr/Al ratio of accessory chromite in peridotite can be explained in two ways.

Firstly, it can be due to the reaction of settled chromite crystals with an aluminous interstitial liquid. Irvine (1966) suggested that, at high pressure, an interstitial liquid of basaltic composition in an olivine cumulate crystallizes aluminous spinel and pyroxene rather than plagioclase. Pressure should perhaps favour the entry of Al into the spinel structure rather than into the pyroxene, since the former is a much denser phase. Therefore, a peridotite with Al-rich chromite could result where an aluminous interstitial liquid has stayed long enough to react with chromite.

Secondly and more probably, the Cr/Al variations of accessory chromite in peridotite are perhaps due to magmatic differentiation, this would explain the increase in the Cr/Al ratio from west to east in the Peridotite Body. This would also explain the parallel changes in the composition of chromite and coexisting olivine (Fig. 45, p. 89). Figure 45 suggests a somewhat cyclic variation in composition of chromite and olivine, the cycles being about 650 m thick. If it is assumed that the beginning of the cycle is marked by the high Fo content of olivine, the stratigraphic top of the cycles is to the east. Thus, the Cr and Fe contents of chromite increase, whereas the Mg and Al contents decrease upwards within each cycle. The Al content of orthopyroxene also decreases from the bottom to the top of a cycle.

V.6. OLIVINE ORTHOPYROXENITE

Olivine orthopyroxenite occurs as layers in peridotite (Figs. 30 and 31, p. 71) and grades into it by an increase in the olivine/orthopyroxene ratio.

Olivine orthopyroxenite consists of interlocking, anhedral to subhedral crystals of orthopyroxene, olivine, accessory chromite and rare

interstitial clinopyroxene. The constituent minerals of one olivine orthopyroxenite sample (K-57) have been analysed and have been found to be similar in composition to those in peridotite. These mineral analyses are listed with those of the same minerals in peridotite and orthopyroxenite (Table VI).

V.7. ORTHOPIYROXENITE

Orthopyroxenite occurs in peridotite as layers (Figs. 32 and 33, p. 73), as coarse-grained veins 1 to 20 cm thick (Figs. 49 and 50) and as isolated pods from 3 cm to 1 m in length (Fig. 51). Layers of this rock are common on Caribou Mountain and less common elsewhere, whereas pods are rare and occur mostly in the Belmina Ridge peridotite. Although orthopyroxenite veins cut small dunite layers and bodies in peridotite, none have been observed cutting a major dunite body either in peridotite or in dunite zones.

Orthopyroxenite consists almost entirely of enstatite (Fig. 52) with rare olivine, interstitial diopside, amphibole and seldom chromite. The enstatite crystals are subhedral or anhedral and are about 5 mm. in average grain size, thus coarser than pyroxene in peridotite. Many orthopyroxene crystals contain exsolution lamellae of diopside, which can form as much as 16 volume per cent of the host. Enstatite grains are commonly rimmed by thin carbonate-brucite-serpentine veinlets. Orthopyroxenite is only moderately altered to serpentine and amphibole.

The enstatite in orthopyroxenite layers is similar in composition to that in peridotite (Table VI D, p. 88). The enstatite in orthopyroxenite veins is somewhat richer in Fe (sample No. 554, Table VI D) and one analysis (see p. 243, anal. 554-5) indicates the presence of bronzite in these veins.



Figure 49. Coarse-grained orthopyroxenite veins (light coloured) in peridotite.
(Along Highway 1, beside Lake Asbestos Mine)



Figure 50. The exposed face of a planar orthopyroxenite vein in peridotite. A vein branches (lower part of the figure) from the main one. The whitish spots are reflections from cleavage surfaces of pyroxene grains. Keys show scale.
(Same location as figure 49)

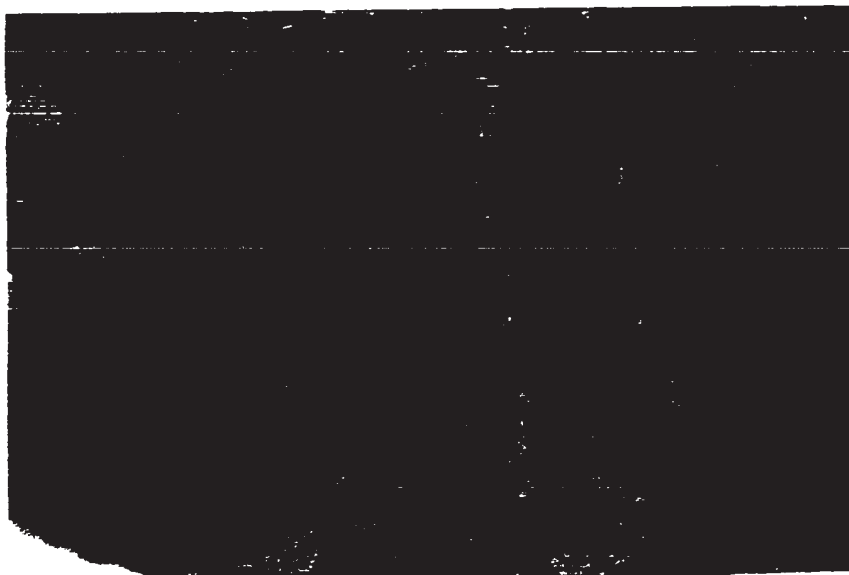


Figure 49. Coarse-grained orthopyroxenite veins (light coloured) in peridotite.
(Along Highway 1, beside Lake Asbestos Mine)

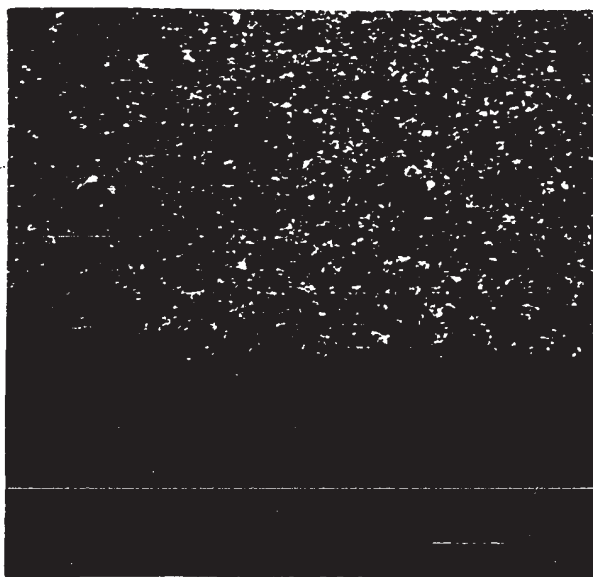


Figure 50. The exposed face of a planar orthopyroxenite vein in peridotite. A vein branches (lower part of the figure) from the main one. The whitish spots are reflections from cleavage surfaces of pyroxene grains. Keys show scale.
(Same location as figure 49)



Figure 51. Orthopyroxenite pod in peridotite.
(Belmina Ridge)

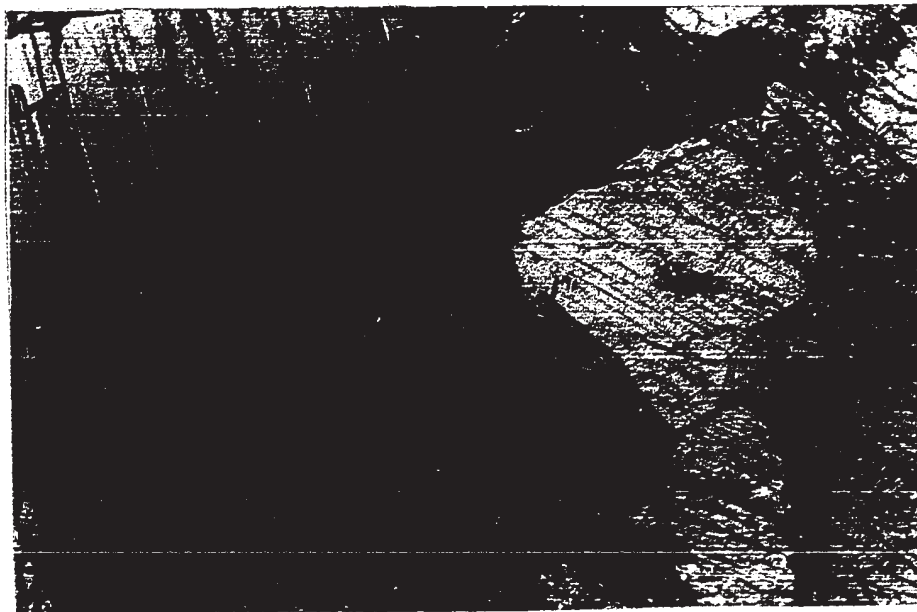


Figure 52. Photomicrograph: Anhedral enstatite grains in an orthopyroxenite vein in peridotite. Orthopyroxene grains are tightly packed. The little intergranular space left is occupied by olivine and amphibole.
Orthopyroxenite, Sample No. 556
Crossed nicols, X 40

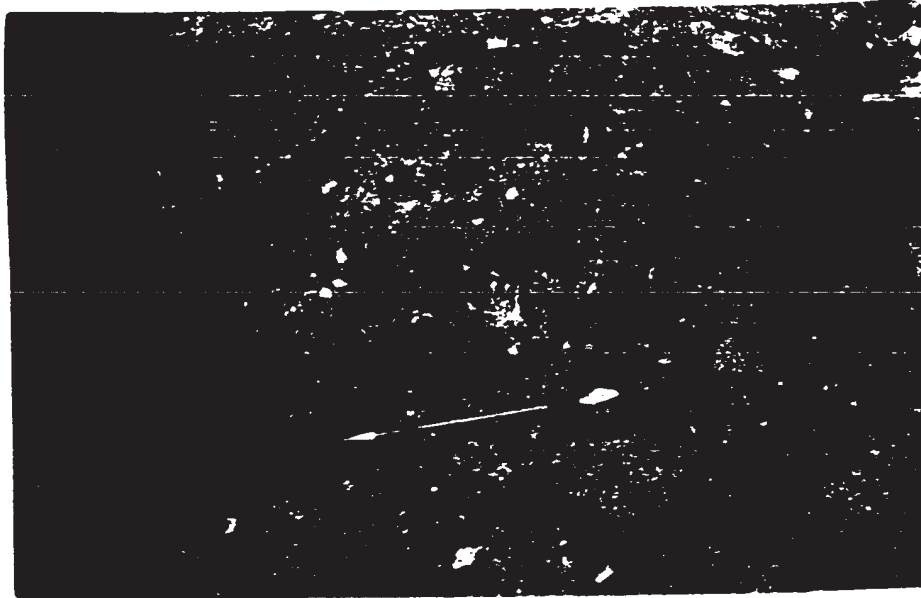


Figure 51. Orthopyroxenite pod in peridotite.
(Belmina Ridge)



Figure 52. Photomicrograph: Anhedral enstatite grains in an orthopyroxenite vein in peridotite. Orthopyroxene grains are tightly packed. The little intergranular space left is occupied by olivine and amphibole.
Orthopyroxenite, Sample No. 556
Crossed nicols, X 40

It is suggested that the orthopyroxenite veins have resulted from injection of a largely liquid, residual, ultramafic magma rather than having been formed by metasomatism of olivine-bearing rocks, as has been proposed by other workers (Bowen and Tuttle, 1949, in Turner and Verhoogen, 1960, p. 316), the same hypothesis was advanced for the discordant pyroxenite (p. 61). If the orthopyroxenite veins had been formed by metasomatism of peridotite, chromite would probably have survived the process, however, chromite is rare. Further, if metasomatism had occurred, one would expect to find partially replaced olivine or olivine rimmed by pyroxene; such textures have not been observed. The contacts of the veins with peridotite are sharp. Abundant diopside exsolution in the enstatite of these veins suggests a high temperature of formation (see p. 81). Orthopyroxenite veins are restricted to peridotite and do not occur in other olivine-rich rocks of the map-area. Therefore, a metasomatic origin for orthopyroxenite veins appears unlikely.

The coarse grain size of orthopyroxenite veins suggests a largely liquid injection. It is likely that they were injected prior to complete solidification (or subsequent to partial melting) of the peridotite. Orthopyroxene in the veins is richer in Fe than the same mineral in the adjacent peridotite and this is consistent with somewhat later formation of the veins.

V.8. DUNITE

This is a dark green rock on the fresh broken surface and brownish, grey or white on the weathered surface. The white colour is due to weathering of the intensely serpentinized rock.

A. Field relationships

Dunite occurs throughout the ultramafic intrusion. It forms extensive zones and is interlayered with peridotite, pyroxenite, "olivine" pyroxenite, "lherzolite" and chromitite. Dunite also occurs in peridotite as small discordant lenses, irregular masses and as large bodies which commonly carry chromite deposits. Chromitite-dunite interlayering is described under "Chromitite and chromite deposits" (Chapter VI). Dunite grades into chromitite and the division (Table II, p. 18) is an arbitrary one. The rock, consisting of dunite blocks set in a mass of pyroxenite, is referred to as dunite breccia and has been described earlier.

Dunite-peridotite interlayering

Dunite layers in peridotite are very abundant. They vary in thickness from a few mm to 3 m and are generally continuous. At the top of Caribou Mountain, a dunite layer has been followed for 125 m, the full extent of the exposure. The contacts are usually sharp and straight (Figs. 53 and 54). There is no noticeable variation in the pyroxene content of the peridotite approaching a dunite layer. In places, discordant offshoots of dunite branch from the dunite layer into the peridotite. Chromite in the dunite layers usually forms clusters rather than isolated grains.

Dunite bodies and discordant dunite dykes in peridotite

As well as the regular dunite layers described above, peridotite contains numerous bodies, the size of which varies from 10 cm pods (Fig. 55) to areas tens of meters in extent. By far the greater majority of these bodies are elongated, parallel or subparallel to the layering

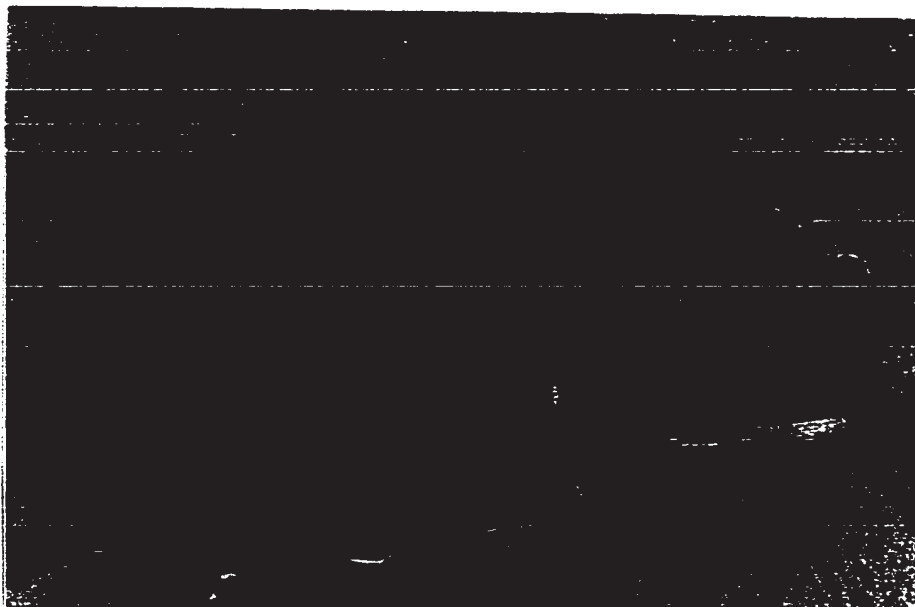


Figure 53. Dunite layer (white, at the centre) in peridotite. The dunite layer has straight, sharp boundaries. (West slope of Caribou Mountain)

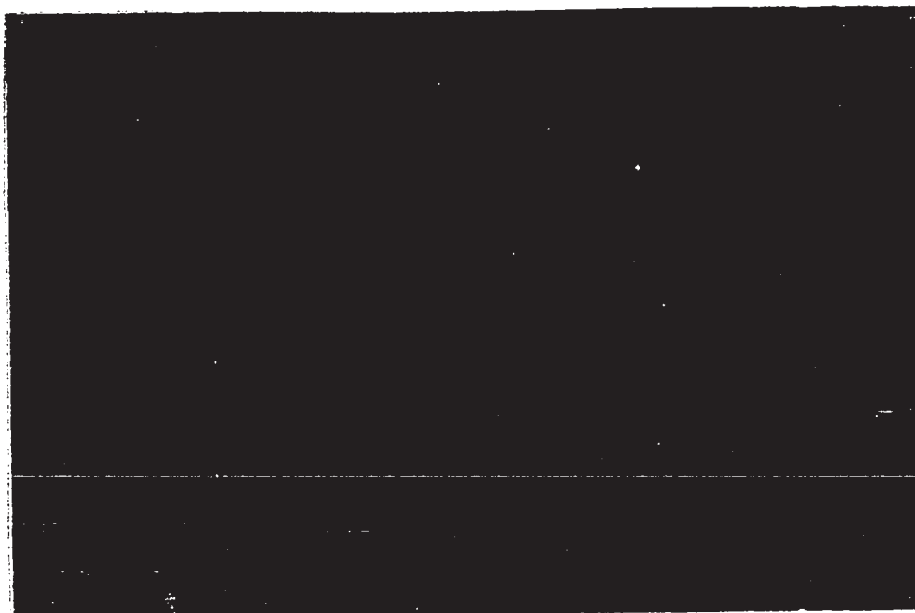


Figure 54. Dunite layer in peridotite. The black spots in the dunite layer are chromite crystals and clusters. (Top of Quarry Hill)

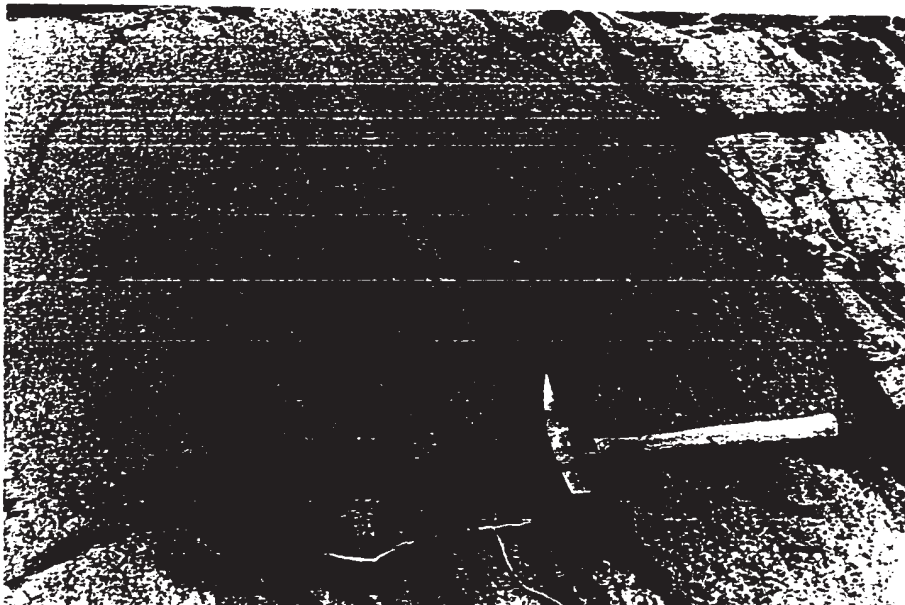


Figure 53. Dunite layer (white, at the centre) in peridotite. The dunite layer has straight, sharp boundaries. (West slope of Caribou Mountain)



Figure 54. Dunite layer in peridotite. The black spots in the dunite layer are chromite crystals and clusters. (Top of Quarry Hill)

A. Field relationships

Dunite occurs throughout the ultramafic intrusion. It forms extensive zones and is interlayered with peridotite, pyroxenite, "olivine" pyroxenite, "herzolite" and chromitite. Dunite also occurs in peridotite as small discordant lenses, irregular masses and as large bodies which commonly carry chromite deposits. Chromitite-dunite interlayering is described under "Chromitite and chromite deposits" (Chapter VI). Dunite grades into chromitite and the division (Table II, p. 18) is an arbitrary one. The rock, consisting of dunite blocks set in a mass of pyroxenite, is referred to as dunite breccia and has been described earlier.

Dunite-peridotite interlayering

Dunite layers in peridotite are very abundant. They vary in thickness from a few mm to 3 m and are generally continuous. At the top of Caribou Mountain, a dunite layer has been followed for 125 m, the full extent of the exposure. The contacts are usually sharp and straight (Figs. 53 and 54). There is no noticeable variation in the pyroxene content of the peridotite approaching a dunite layer. In places, discordant offshoots of dunite branch from the dunite layer into the peridotite. Chromite in the dunite layers usually forms clusters rather than isolated grains.

Dunite bodies and discordant dunite dykes in peridotite

As well as the regular dunite layers described above, peridotite contains numerous bodies, the size of which varies from 10 cm pods (Fig. 55) to areas tens of meters in extent. By far the greater majority of these bodies are elongated, parallel or subparallel to the layering

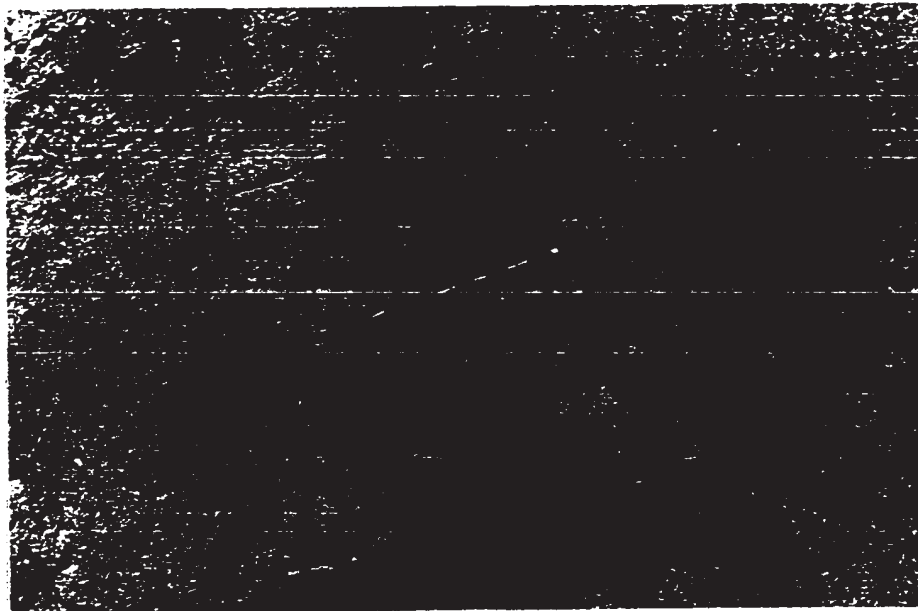


Figure 55. A layer and a pod (right) of dunite (lighter grey) in peridotite.
(West slope of Caribou Mountain)



Figure 56. A dunite layer in peridotite, slightly offset by a fracture. Two apophyses separate from the layer to join again (above the compass) enclosing a peridotite island.
(On Highway 1, beside Lake Asbestos Mine)

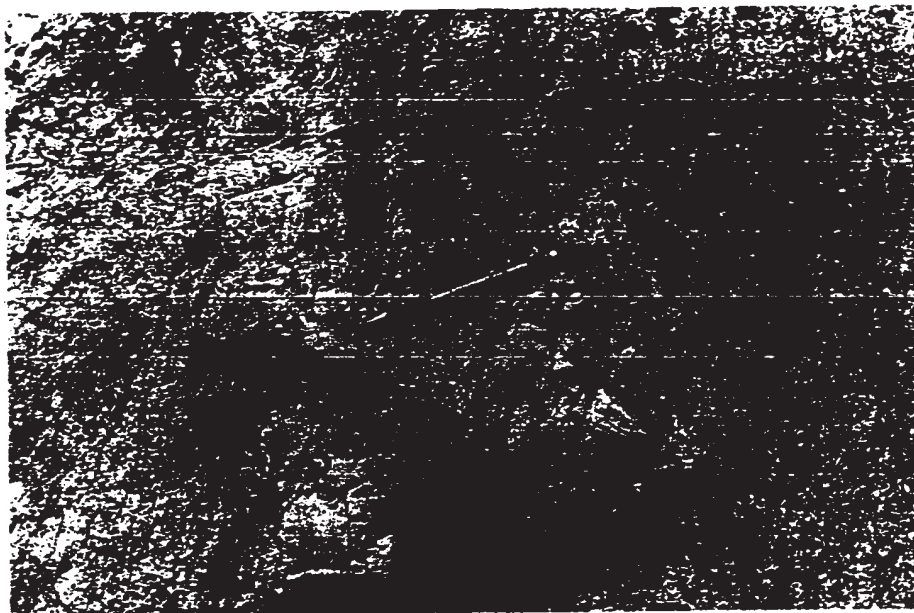


Figure 55. A layer and a pod (right) of dunite (lighter grey) in peridotite.
(West slope of Caribou Mountain)



Figure 56. A dunite layer in peridotite, slightly offset by a fracture. Two apophyses separate from the layer to join again (above the compass) enclosing a peridotite island.
(On Highway 1, beside Lake Asbestos Mine)

in the adjacent peridotite, and they are therefore intermediate between dunite layers and discordant dunite dykes. Anasthomosing dunite veins (Fig. 56) and dykes branching from pod-like or irregular bodies (Fig. 57) occur. The great majority of observed contacts are sharp, only rarely are they gradational, any gradation taking place over 1 cm. or less. The contacts can be curved, irregular, wavy and/or inter-fingering (Fig. 58). There is no observable variation in the pyroxene content of peridotite approaching discordant dunite bodies. The foliation in peridotite has not been observed to be disturbed around discordant dunite bodies. The chromite in these dunite dykes is clustered, and in some of them it is concentrated in the middle of the dyke to form a central string. Although discordant dunite is most conspicuous in peridotite, it also occurs in the Olivine Pyroxenite Zone.

Many of the bigger dunite bodies in peridotite contain chromite deposits. These dunite bodies are usually lenses, elongated parallel to the layering in the adjacent peridotite. The banding in the chromite is also parallel to the elongation of the enclosing dunite body. However, a number of dunite bodies are irregular in form or rounded.

B. Petrography

With the exception of the dunite bodies within peridotite, dunite is always completely serpentized, unlike the peridotite which is, in the main, only moderately serpentized. Alteration minerals in dunite include antigorite, brucite, chlorite, magnetite and, in later cross-cutting veinlets, talc, chrysotile and carbonate.

In serpentized dunite, the grain boundaries of olivine can still be inferred and the average grain size is about 2 mm, coarser than the

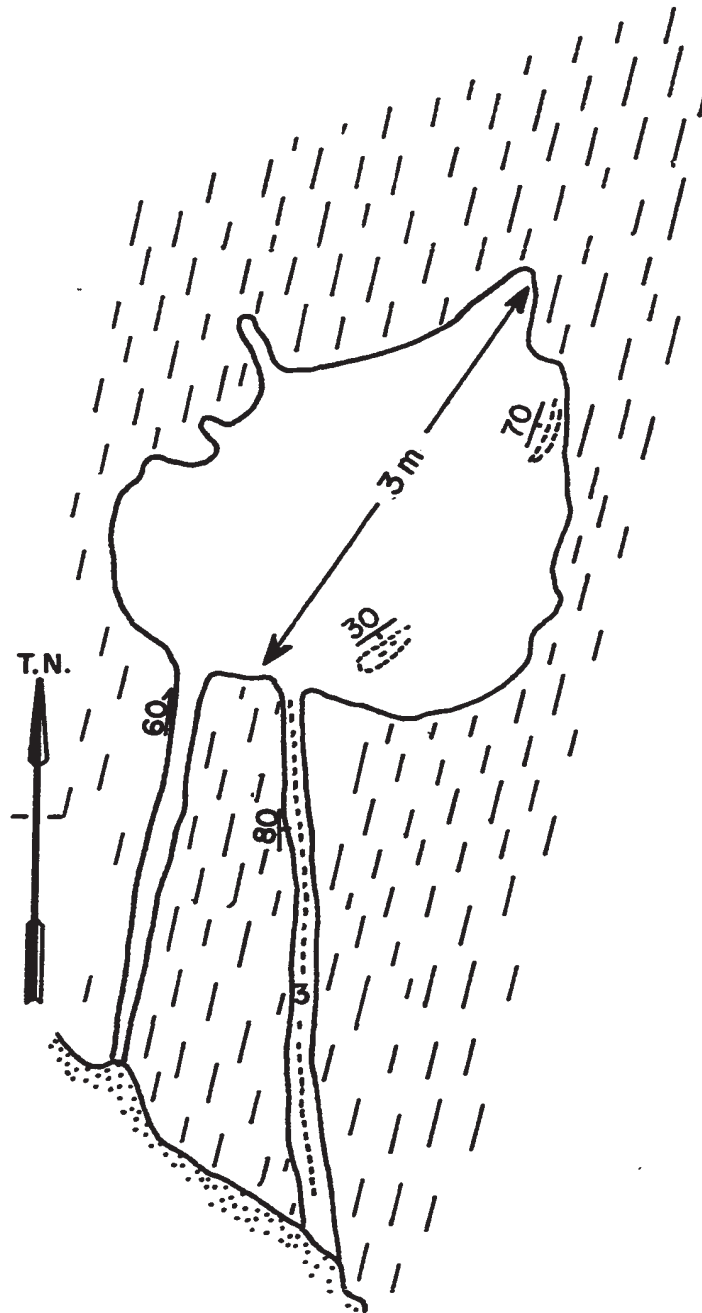


Figure 57. A dunite pod with discordant apophyses in peridotite. There is no noticeable disturbance of the foliation in the peridotite approaching the dunite pod. A string of chromite grains can be observed in the apophysis (dotted line). The thin ill-defined chromite layering in dunite varies in strike and dip.
(west slope of Caribou Mountain)



Figure 58. Dunite (D) in peridotite (P). Note the interfingering dunite-peridotite boundary. The large-scale relationship of the Northern Dunite Zone with the Peridotite Body is probably similar to that seen here. (On Highway 1, beside Lake Asbestos Mine)



Figure 59. Photomicrograph: Magnetite (light) rimming chromite grains (light grey). The magnetite also fills fractures in the chromite. Dunite, Sample No. 150 Reflected light, X 50

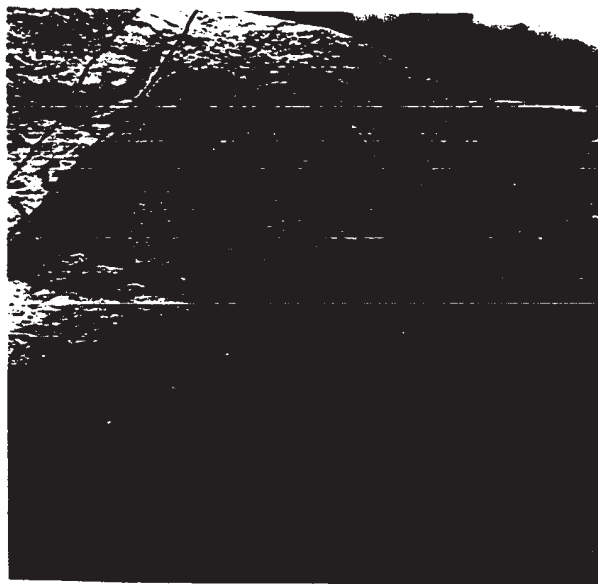


Figure 58. Dunite (D) in peridotite (P). Note the interfingering dunite-peridotite boundary. The large-scale relationship of the Northern Dunite Zone with the Peridotite Body is probably similar to that seen here. (On Highway 1, beside Lake Asbestos Mine)

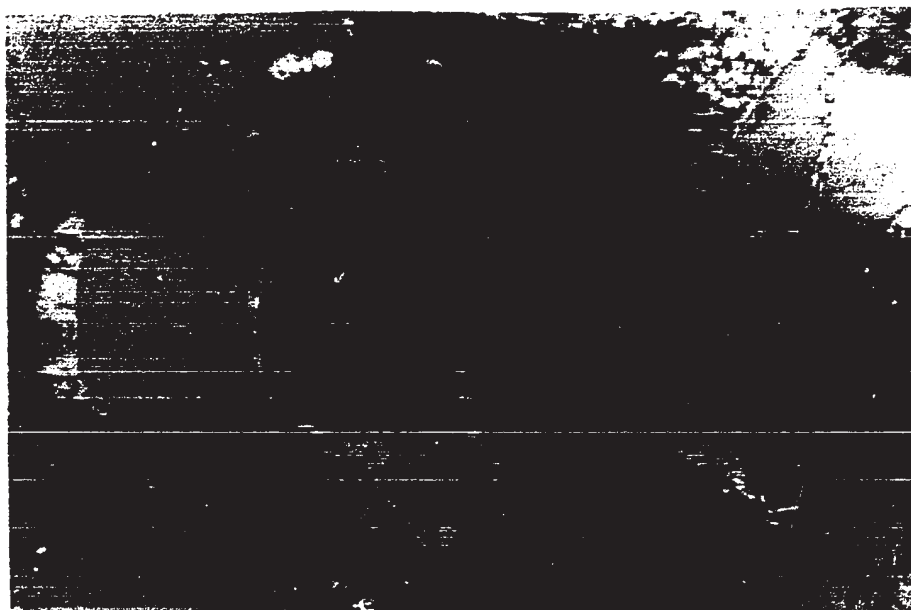


Figure 59. Photomicrograph: Magnetite (light) rimming chromite grains (light grey). The magnetite also fills fractures in the chromite. Dunite, Sample No. 150 Reflected light, X 50

olivine in peridotite. The average chromite content of dunite is about 2.5 to 3% and it seems to remain constant over large areas. The accessory chromite tends to be more euhedral in shape than the accessory chromite in peridotite. Chromite grains are fractured and fractures are filled with magnetite or magnetite + serpentine. Many chromite grains are rimmed by secondary magnetite (Fig. 59).

C. Chemistry

The trace element content of dunite varies considerably (Table IV, p. 48). This variation is attributed largely to the variable degree of alteration of dunite.

All the dunite samples from which olivine has been analysed are from chromitite-bearing dunite bodies in peridotite. The olivine in these bodies is consistently poorer in Fe than the same mineral in the adjacent peridotite (Fig. 60).

Except for the dunite in the Olivine Pyroxenite Zone and dunite layers and small bodies in peridotite, the accessory chromite in dunite is of similar composition throughout the map-area (Table VII). The accessory chromite in dunite within the Olivine Pyroxenite Zone is characterized by much higher Fe, Al and Ti contents and a lower Cr content compared with accessory chromite in dunite elsewhere. This composition is similar to that of the accessory chromite in "lherzolite" and "olivine" pyroxenite.

It is noteworthy that accessory chromite in a dunite layer in peridotite is similar in composition to the accessory chromite in the adjacent peridotite (Fig. 62, p. 116, Fig. 63, p. 117 and Fig. 64, p. 118). The accessory chromite from large dunite bodies in peridotite is similar in composition to the same mineral in both the Northern and

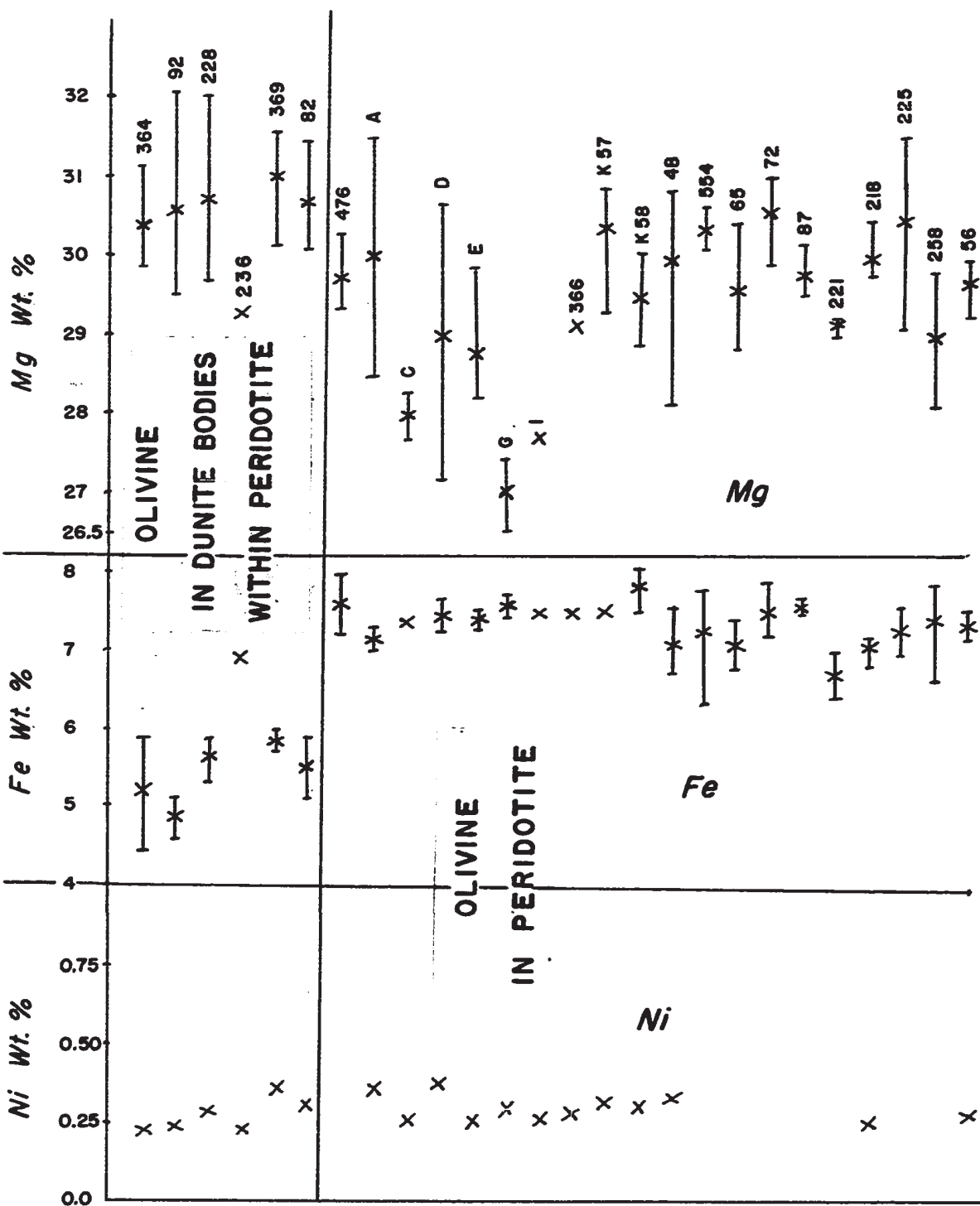


Figure 60. Magnesium, iron and nickel contents of olivine in peridotite and in dunite bodies within peridotite. Vertical bars: range of variation in each sample. X: average value of all analyses for each sample.

TABLE VII

Mean composition¹ of minerals in dunite
Microprobe Analyses
Cations wt.%

A) Olivine in dunite bodies in peridotite

Sample No.	Mg	Fe	Ni	Si	Ca	Mole.%Fo.
82	30.64	5.56	0.30	19.09	-	92.6
92	30.29	4.86	0.24	19.21	0.35	93.6
228	30.64	5.64	0.28	19.25	-	92.6
236	29.24	6.91	0.22	19.32	-	90.6
364	30.40	5.21	0.23	19.06	0.26	93.0
369	31.00	5.83	0.34	19.22	-	92.4

B) Accessory chromite in dunite

Sample No.	Cr	Fe tot.	Fe ⁺²	Fe ⁺³	Mg	Al	Ti
K-61	38.53	22.21	19.69	2.52	3.64	5.85	0.08
N-6*	37.80	14.73	11.37	3.36	7.75	6.93	0.05
27	36.36	18.38	14.36	4.03	6.32	6.98	0.14
28	36.84	18.06	14.53	3.53	6.44	7.43	0.15
30	38.47	17.65	13.23	4.42	7.27	6.74	0.10
31	37.75	18.20	17.08	1.12	4.93	7.26	0.11
35	39.60	13.55	9.29	4.26	9.21	7.70	0.12
41	38.31	20.45	18.04	2.41	4.82	6.08	0.11
42	34.11	21.65	15.77	5.88	5.27	6.38	0.14
47	36.10	14.42	12.74	1.68	6.19	6.42	0.09
57**	31.75	19.53	13.99	5.54	6.09	7.92	0.22
61	38.35	17.48	17.03	0.45	4.14	5.49	0.06
116	35.24	19.09	16.57	2.52	4.77	7.03	0.07
138***	36.57	24.91	19.53	5.38	3.26	4.46	0.10
161***	26.10	25.91	16.12	8.79	4.56	10.81	-0.19
228*	37.60	15.43	14.25	1.18	6.60	8.28	0.09
236**	38.98	19.82	18.59	1.23	3.80	5.52	0.06
364*	37.78	15.71	9.77	5.94	8.58	6.02	0.07
369*	40.42	16.60	15.37	1.23	5.79	6.09	0.07
380	38.31	17.08	14.67	2.41	5.93	6.38	0.09

* Accessory chromite in chromitite-bearing dunite bodies in peridotite.

** Accessory chromite in dunite layer (57) and dunite body (236) in peridotite.

*** Accessory chromite in dunite associated with clinopyroxene-rich rocks.

1 The analytical procedure, calculation of mean composition, the precision, accuracy and detail of analyses are indicated in Appendix III. Fe⁺² and Fe⁺³ have been calculated from total iron values. Locations of samples are indicated on Map 2.

Southern Dunite Zones but quite different from the accessory chromite in peridotite.

Zoning in chromite is generally weakly developed, although a thin Al-rich marginal zone is well developed in some grains (Fig. 61). This type of zoning is less common and usually less well defined in the accessory chromite in dunite than in other rocks.

D. Discussion

Dunite layers in peridotite are parallel to other types of layering in this rock and the accessory chromite in the layers is similar in composition to the accessory chromite in the peridotite. It is therefore reasonable to conclude that the dunite layers have differentiated from the same material as the peridotite.

Discordant dunite veins and lenses have been observed and described from alpine-type peridotites in many localities as well as from layered complexes. Bowen and Tuttle proposed that they have been formed by desilification of pyroxene-bearing ultramafic rocks, by silica deficient solutions (Bowen and Tuttle, 1949, in Turner and Verhoogen, 1960, p. 316). Lipman (1964, p. 213) demonstrated a metasomatic replacement origin for similar discordant dykes in an ultramafic body from the Klamath Mountains of California. He showed that preferred orientation of olivine in the host rock continued through dunite dykes. Burch (1968) described discordant dunite bodies in the peridotite mass of Burro Mountain (California) and suggested that they have been formed by metamorphic differentiation aided by metasomatism.

The discordant dunite bodies in the peridotite of the map-area do not seem to have originated by either metamorphic differentiation or

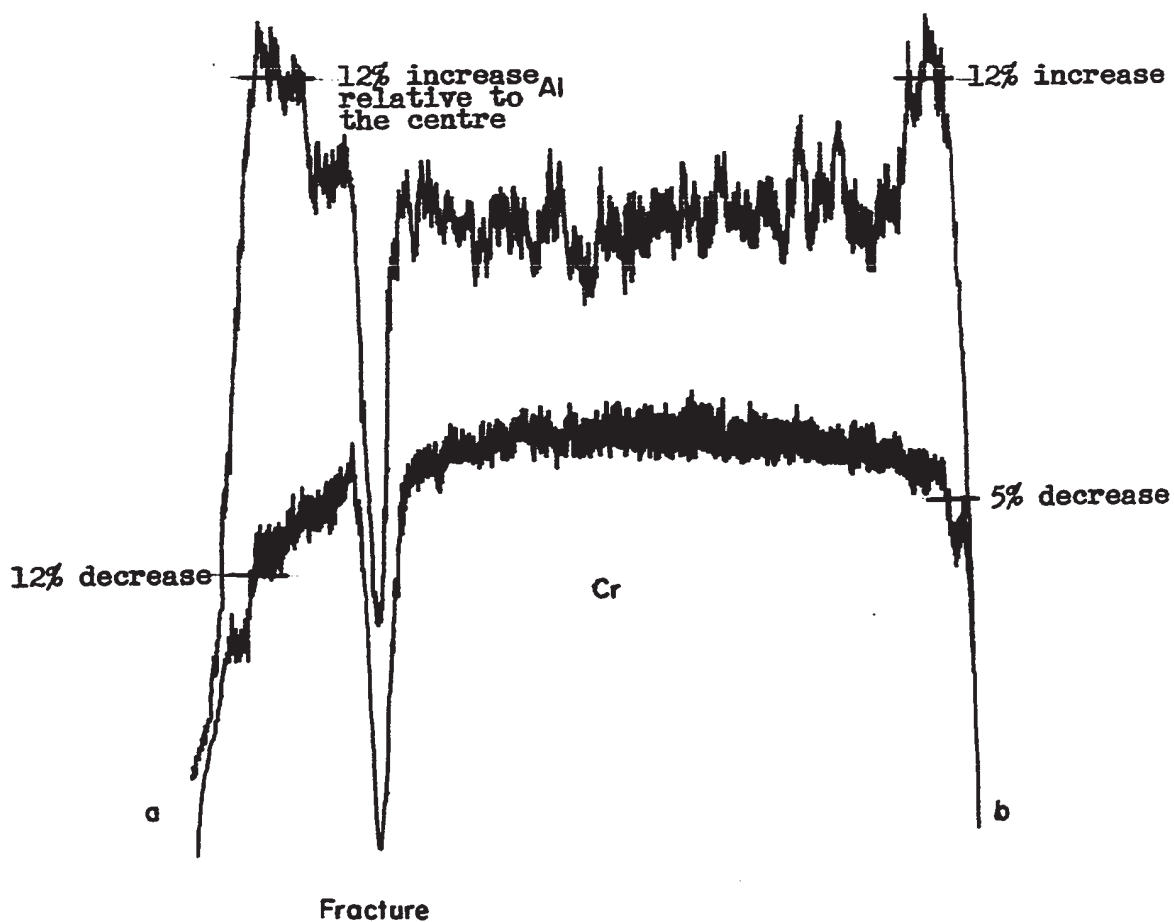


Figure 61. Zoning in chromite. Electron microprobe scanning profile showing variation of chromium and aluminum. Dunite, sample No. 116. Photomicrograph: Reflected light, X 120

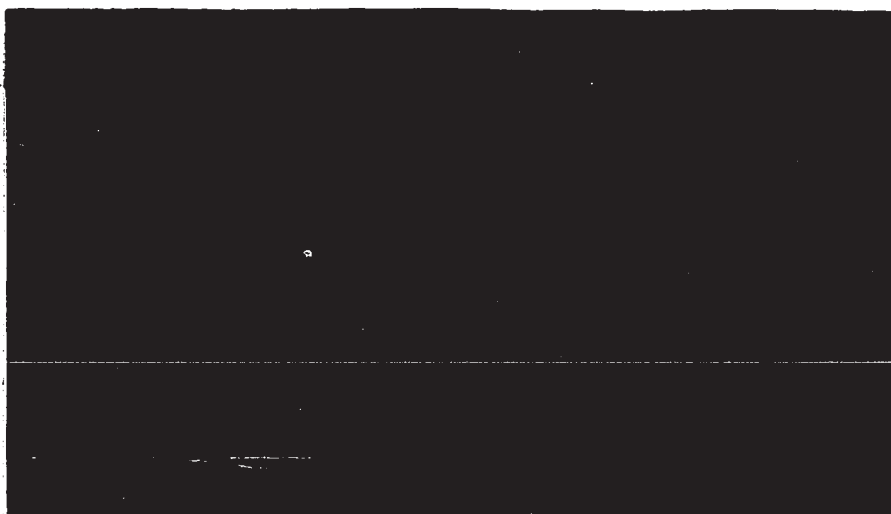
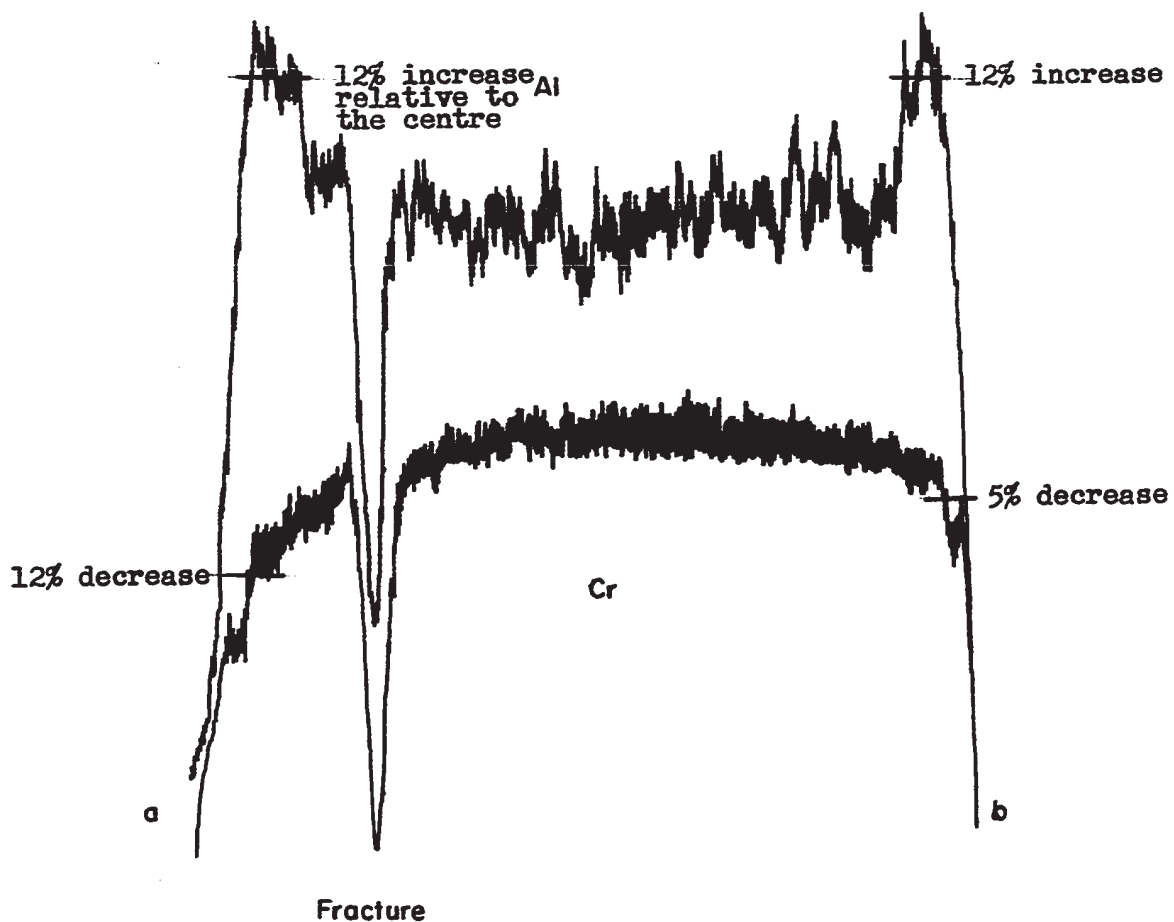


Figure 61. Zoning in chromite. Electron microprobe scanning profile showing variation of chromium and aluminum. Dunite, sample No. 116. Photomicrograph: Reflected light, X 120

metasomatism. No pyroxene enrichment, which could be related to a metamorphic differentiation process, has been observed around the discordant dunite bodies and dykes. In a metasomatic process one would expect to see some partly replaced pyroxene, rimmed by olivine; this has not been observed. The occurrence of discordant dunite bodies in clinopyroxene-rich rocks is particularly difficult to explain, since it is unlikely that olivine could have been generated from calcic pyroxene. It is therefore suggested that the discordant dunite bodies are the result of deformation prior to the complete solidification of the rock and that they represent injections from layers of dunite into the host rock. This would explain the presence of all types of dunite bodies from cross-cutting dykes to subconcordant dunite bodies to layers.

Many of the large dunite bodies in peridotite contain or contained chromitite. The accessory chromite in these dunite bodies is similar in composition to the accessory chromite in the Northern and Southern Dunite Zones but quite different from that in the adjacent peridotite (Figs. 62, 63, 64 and 65). The chromite of chromitite in the dunite bodies and dunite zones has also similar composition. Furthermore, the olivine in these dunite bodies is consistently poorer in Fe than the same mineral in the adjacent peridotite (Fig. 60). It is therefore suggested that the large dunite bodies in peridotite represent xenoliths initially belonging to dunite zones rather than being local differentiates.

V.9. SERPENTINITE

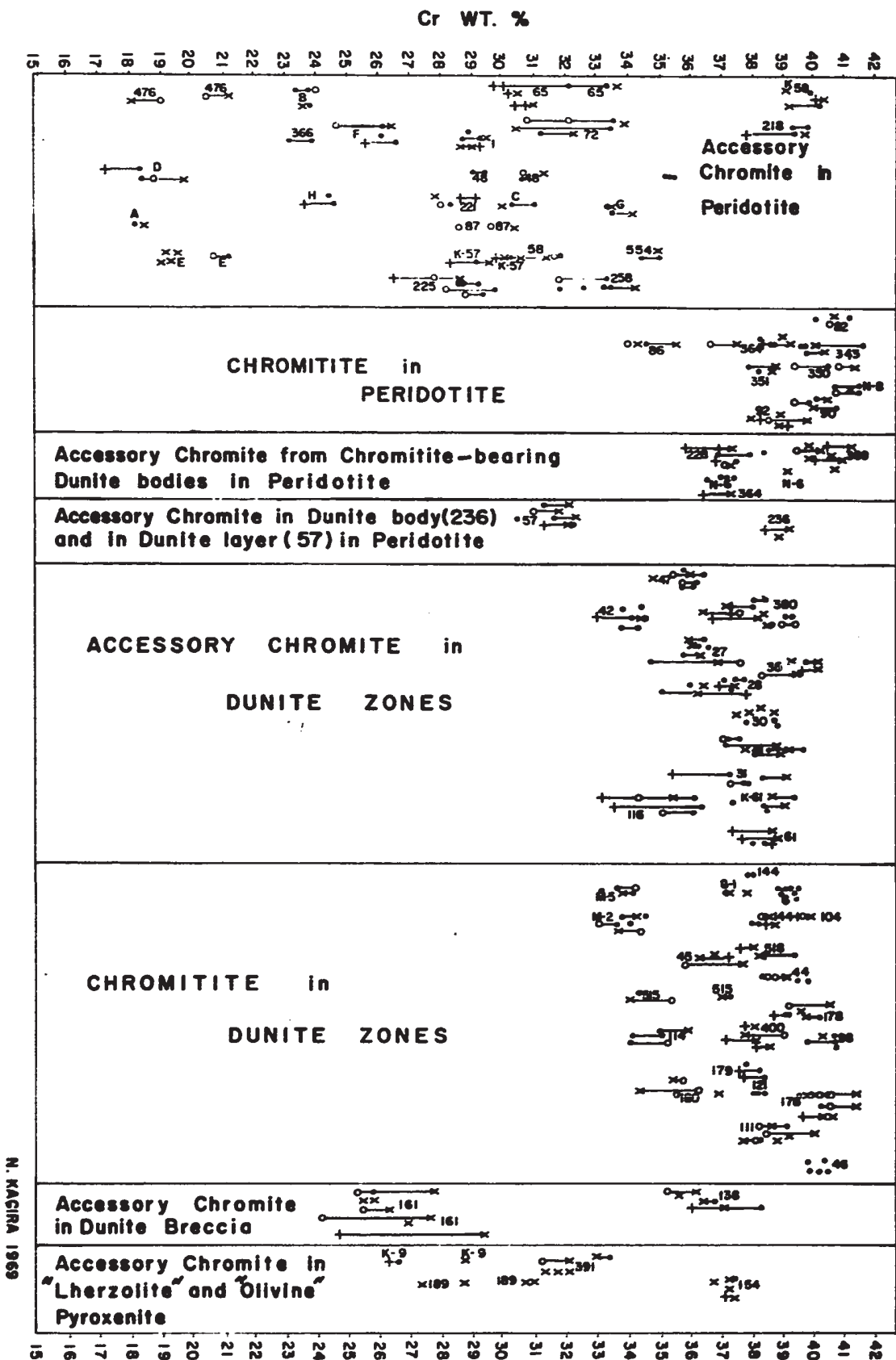
Serpentinite consists of a mixture of serpentine, brucite, talc, magnetite, and a small amount of chromite. Olivine serpentized in

EXPLANATION FOR FIGURES 62 TO 65

The chromite has been divided into eight groups on the basis of host rock type, chromite concentration and geological setting. The analyses have been made with an electron microprobe. The analyses belonging to one crystal are linked by a line. A different symbol is used for the analyses at the centre, anhedral margin, euhedral margin or at an intermediate point between the centre and the margin of the grain. These designations are very approximate and refer to the two-dimension section of chromite crystals rather than to the crystals in three dimensions. All the analyses from a sample are grouped. Because of superposition and other drafting difficulties, some analyses do not appear on the Figures.

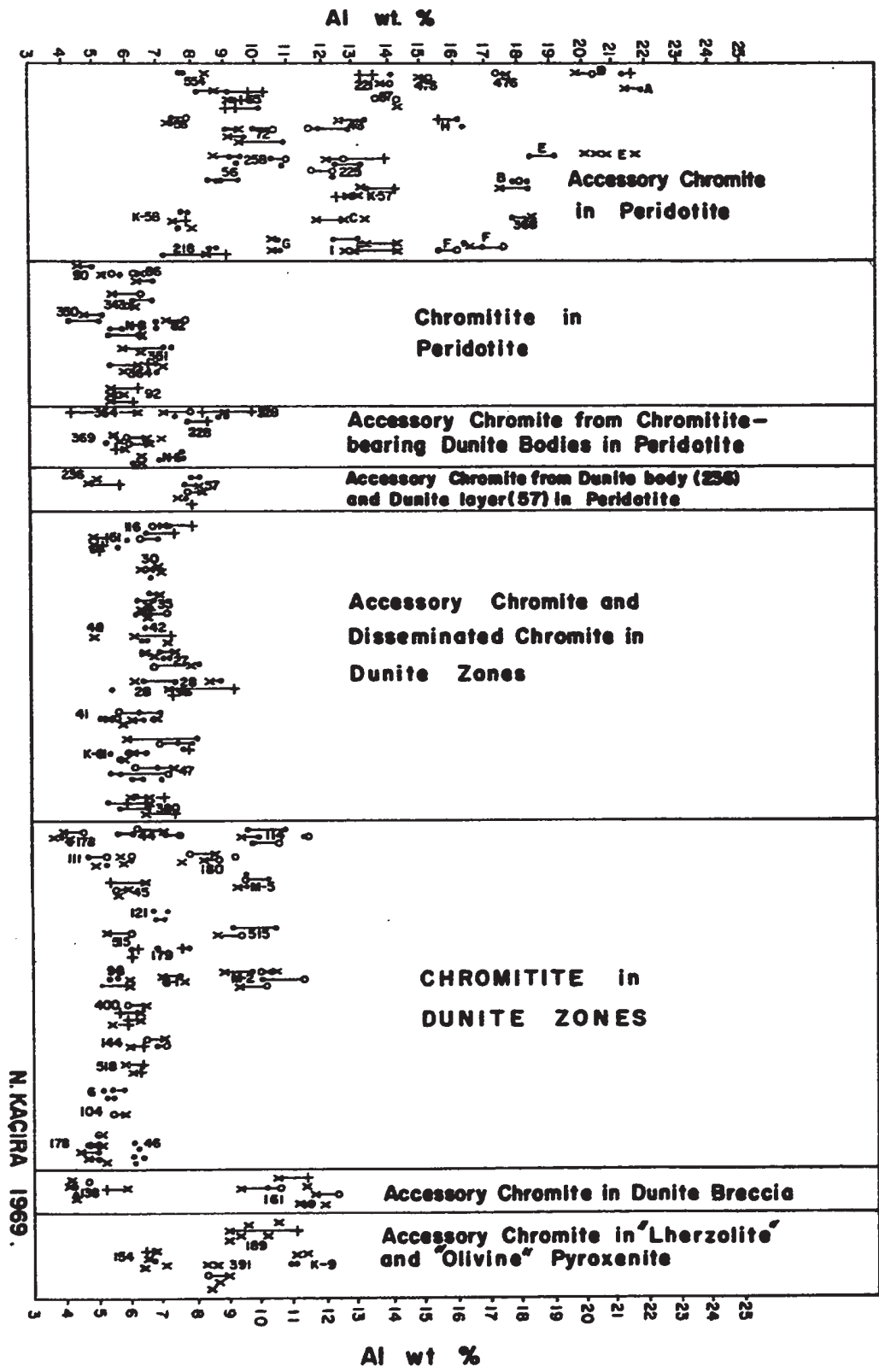
Approximate positions of analysed spots on the thin section of the grains:

- x near the centre of the grain
- + near the euhedral or subhedral margin of the grain
- o near the anhedral margin of the grain
- intermediate location between centre and margin of the grain



N. KAGIRA 1969

Figure 62. Chromium content of chromite



N. KACIRA 1969.

Figure 63. Aluminum content of chromite

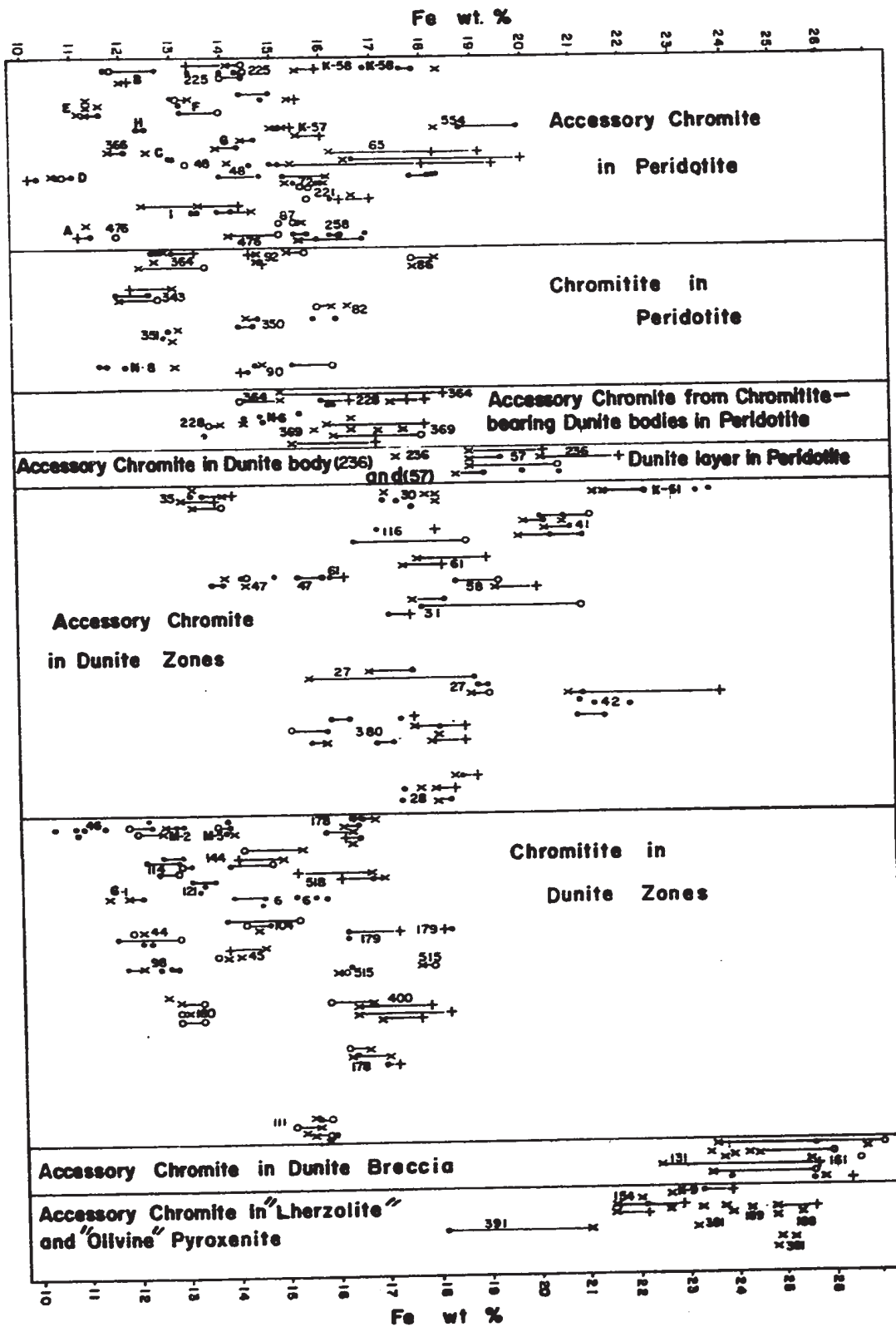


Figure 64 . Total iron content of chromite

concentric rings was not observed in serpentinite. This indicates either a strong post-serpentinization deformation or an intense serpentinization, which obliterated the original alteration texture, or both. A very fine-grained mixture of chromite and magnetite filling a fracture or vein about 0.3 mm. wide has been observed. This perhaps resulted from the dissolution and redeposition of chromite.

V.10. DISCUSSION

The ultramafic rocks in which the original texture has not been obliterated by alteration exhibit an interlocking or mosaic texture. Grains are anhedral or subhedral and are tightly packed. With the exception of clinopyroxene in peridotite, no interstitial mineral has been observed. Grains are strongly fractured and exhibit deformation lamellae and undulatory extinction.

Some textural features of the ultramafic rocks are very likely of primary magmatic origin. For instance, many chromite grains contain irregularly shaped islands of olivine (Fig. 66) which, it is thought, represent intersections of deep embayments at the plane of the thin section rather than inclusions. This, and the irregular shape (Figs. 66 and 67) of many chromite grains could be due to a combination of magmatic corrosion, in situ growth and mutual interference of adjacent crystals.

A common textural feature is that of a chromite crystal occurring at the boundary between two or more olivine grains and penetrating each of them (Fig. 68). Such a relationship could have resulted from in situ growth of olivine crystals around the chromite or from boundary mig-

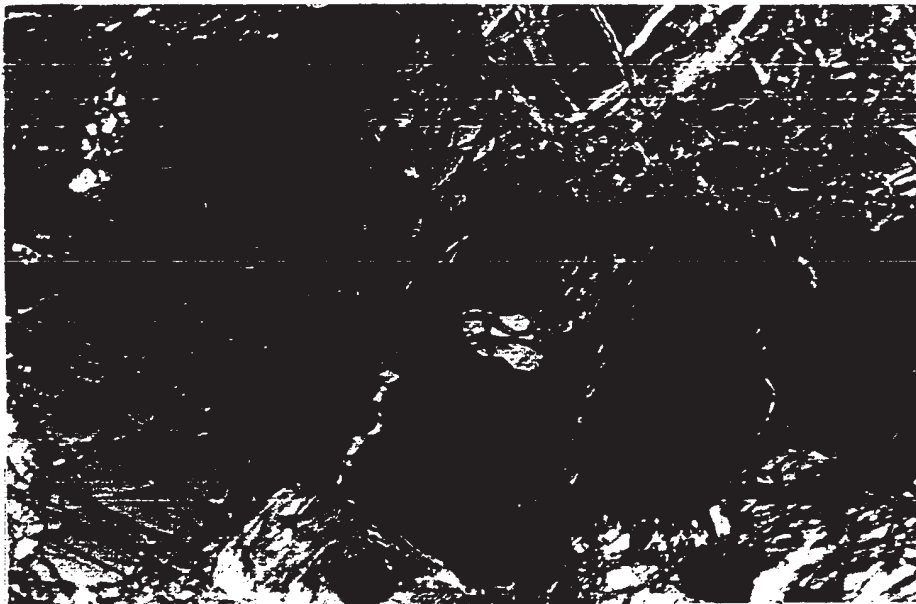


Figure 66. Photomicrograph: Irregularly shaped chromite (black). The partly serpentinized olivine island in chromite probably represents a section through an embayment rather than an inclusion.
Peridotite. Sample No. 218
Plane polarized light, X 40

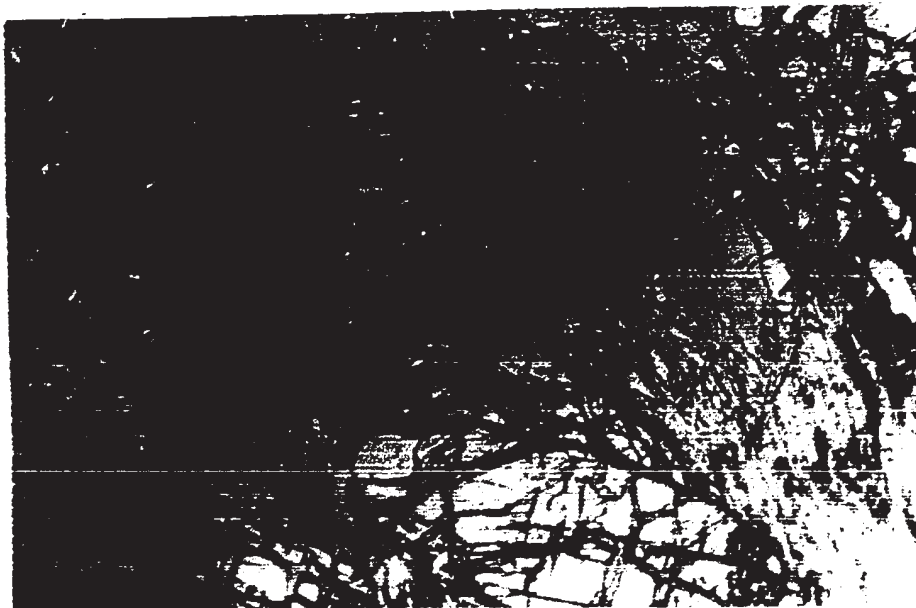


Figure 67. Photomicrograph: Irregularly shaped chromite (black) in peridotite. Sample No. 554
Plane polarized light, X 40

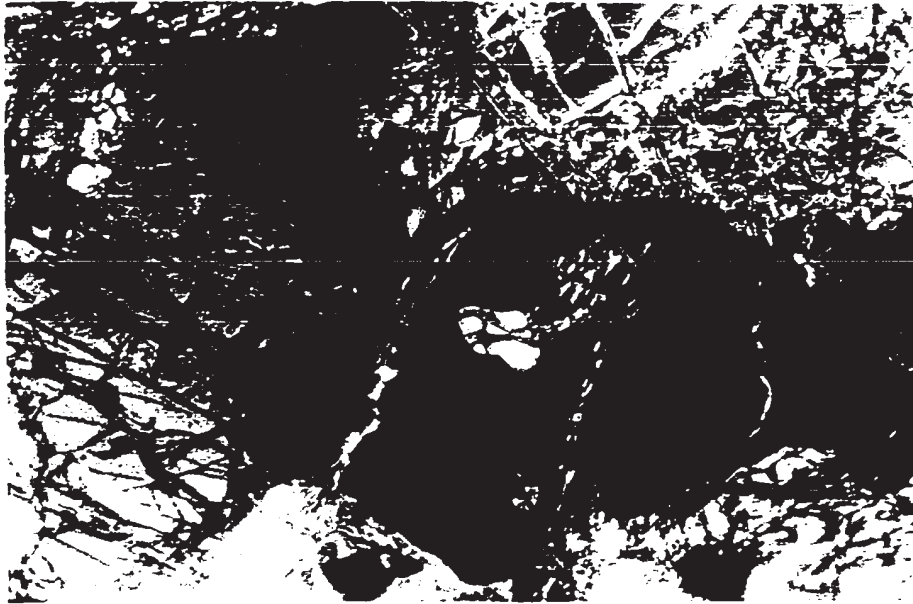


Figure 66. Photomicrograph: Irregularly shaped chromite (black). The partly serpentinized olivine island in chromite probably represents a section through an embayment rather than an inclusion.
Peridotite. Sample No. 218
Plane polarized light, X 40

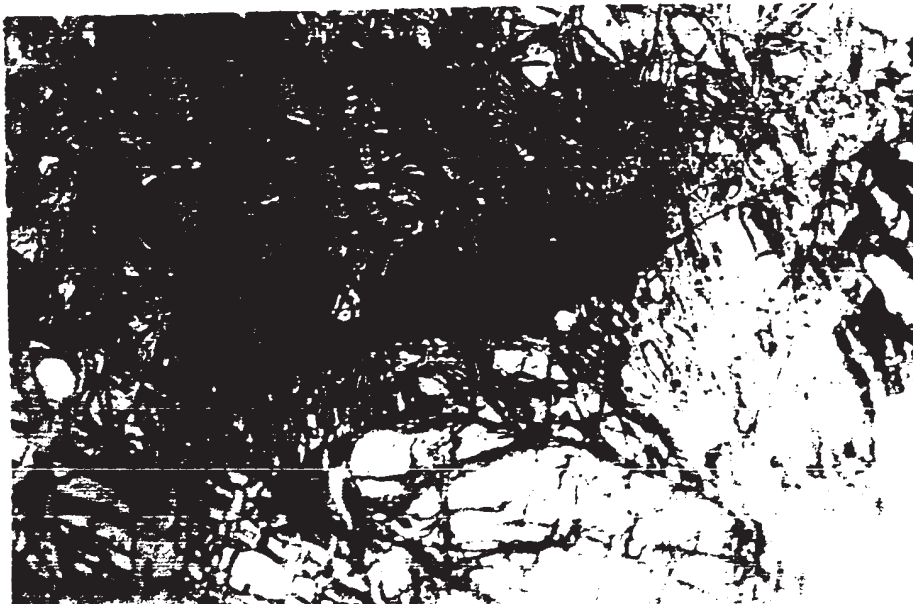


Figure 67. Photomicrograph: Irregularly shaped chromite (black) in peridotite. Sample No. 554
Plane polarized light, X 40



Figure 68. Photomicrograph: Chromite grain (black, centre of the figure) across the boundary between two olivine grains. The chromite grain contains an olivine inclusion. Peridotite. Sample G
Crossed nicols, X 40



Figure 69. Photomicrograph: Irregularly shaped chromite (black) Peridotite, Sample No. 225
Crossed nicols, X 40

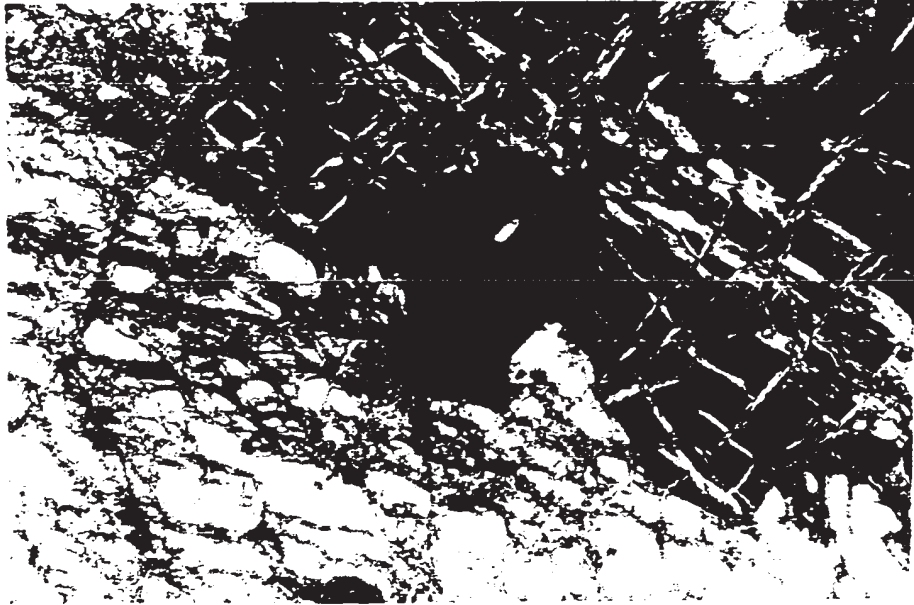


Figure 68. Photomicrograph: Chromite grain (black, centre of the figure) across the boundary between two olivine grains. The chromite grain contains an olivine inclusion. Peridotite. Sample G
Crossed nicols, X 40



Figure 69. Photomicrograph: Irregularly shaped chromite (black) Peridotite, Sample No. 225
Crossed nicols, X 40

ration due to recrystallization of olivine. A variation of the above texture is observed where a chromite crystal has ragged boundaries as well as euhedral boundaries with the surrounding olivine grains (Fig. 69). This perhaps represents either mutual interference of olivine and chromite during in situ growth or magmatic corrosion of certain faces of formerly euhedral chromite grains.

Identifiable recrystallization textures are rare in the ultramafic rocks. With the exception of serpentinite, in the rocks under study the fragile serpentinitization textures are not deformed and secondary magnetite is not fractured. These data suggest that no metamorphic recrystallization and no penetrative deformation occurred within the stability range of serpentine ($< 600^{\circ}\text{C}$). Recrystallization presumably heals fractures, obliterates previous deformation lamellae and undulatory extinction and causes preferred orientation of minerals (Ragan, 1967). The presence of common deformation lamellae and undulatory extinction interpreted in the light of experimental data (Raleigh, 1967) suggest that recrystallization, if it occurred, occurred at high temperatures, probably above 1000°C . The effects of such a possible recrystallization are not conspicuous in the texture of the ultramafic rocks. Nevertheless, it is possible that recrystallization at high temperatures may have contributed to the formation of mosaic texture in the ultramafic rocks.

All the ultramafic rocks are coarsely granular, suggesting that their crystallization proceeded slowly. The absence of detectable zoning in olivine and pyroxene also suggests slow cooling and very slow changes in the composition of the magma. Chromite was apparently the only mineral sensitive enough to register the slow compositional

variation. It is therefore reasonable to infer that the ultramafic rocks crystallized at depth and from a magma body either very large in volume and/or near their own composition.

The distribution of some trace elements shows considerable variation between different rock types (Table IV, p. 48). The abundance of Cr is directly related to the abundance of chromite and pyroxene. The Co content appears to vary with the amount of olivine present. Titanium is low in peridotite and reaches a maximum in pyroxenite. Vanadium and Mn increase from dunite to pyroxenite.

Within a given rock type there is also considerable variation in the distribution of some trace elements. This may be due in part to variation in the degree of alteration. It is notable that the Ni content shows little variation within a rock type.

In Fig. 70 the ranges of compositions of olivine and orthopyroxene from the ultramafic rocks of the map-area are compared with the compositions of the same minerals from ultramafic portions of some stratiform complexes, ultramafic rocks of orogenic belts, peridotite nodules in basalt and from harzburgite xenoliths in kimberlites. Olivine and orthopyroxene compositions from stratiform complexes partly overlap the compositions of olivine and orthopyroxene from other ultramafic rocks and extend to less magnesian compositions. Except for olivines and orthopyroxenes from basaltic differentiates, these two minerals have similar compositions in all other rocks, shown in Fig. 70. This perhaps indicates the similarity of the sources of these rocks.

The Ca content of orthopyroxenes in the ultramafic rocks under study varies from 0.18 to 0.67%; most values are within the range 0.20 to 0.50% Ca (Tables V, p. 62 and VI.D, p. 68). These values are

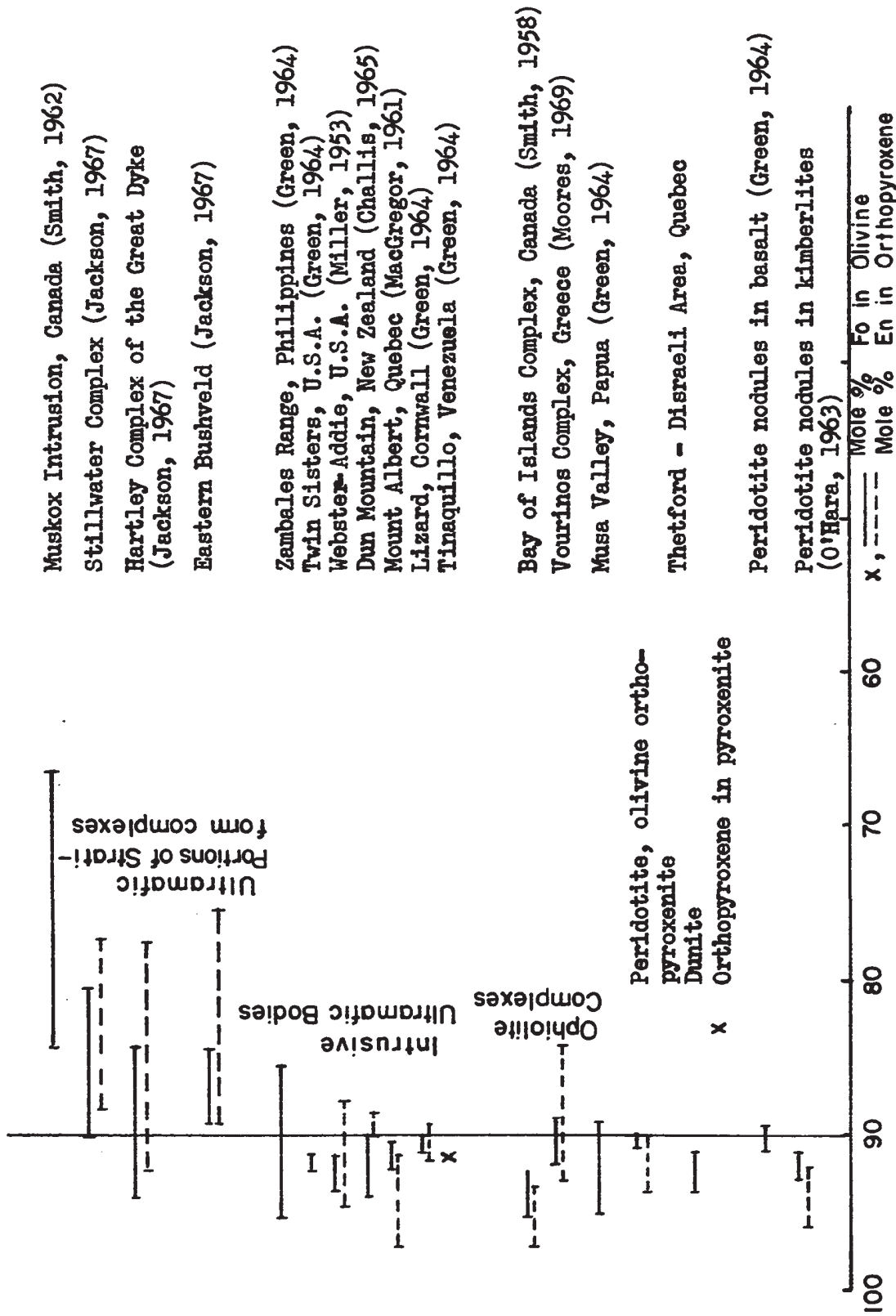


Figure 70. Ranges of Fo and En contents of olivine and coexisting orthopyroxene respectively from ultramafic rocks. The references are the sources of the plotted analyses.

distinctly lower than the 0.96 to 1.36% Ca range of orthopyroxenes from the stratiform complexes of Great Dyke, Bushveld and Stillwater (Hess, 1960). Hess (1960) has compiled the CaO contents of enstatites from "calcium-poor ultramafic magma series" which include alpine-type ultramafic rocks. The Ca values calculated from CaO contents listed by Hess are low and except for one, all are within the range 0.16 to 0.7% Ca. The range of Ca contents given by Ross et al. (1954, op. cit. in Green, 1964) for enstatites in "intrusive dunites" is 0.42 to 1%. These ranges of Ca contents are similar to that of orthopyroxene in the map-area.

The Ca content of orthopyroxene has been interpreted as a qualitative temperature indicator, although the parent magma composition is also important (Hess, 1960). The occurrence of abundant diopside exsolution lamellae in the orthopyroxene of the map-area is evidence of the decreasing solubility of Ca in this mineral with falling temperature. In spite of the calcic nature of "herzolite" and pyroxenite, the orthopyroxene in these rocks exhibits much less exsolution than the same mineral in peridotite, perhaps indicating a relatively lower temperature of crystallization of orthopyroxene in clinopyroxene-rich rocks.

The effect of pressure on the solubility of Ca in orthopyroxenes is uncertain (Green, 1964). Dissolution of Ca in the orthopyroxene structure results in an increase of the cell volume of this mineral (Deer et al., 1963, v. 2, p. 12); hence with increasing pressure at constant temperature the solubility of Ca might be expected to decrease. The comparison of the system $\text{MgSiO}_3\text{-CaMgSi}_2\text{O}_6$ at 1 kb (Boyd and Schairer, 1964) with the same system at 30 kb (Davis and Boyd, 1966, op. cit. in Boyd, 1966) shows that pressure increase results in a marked decrease in the solubility of Ca in Ca-poor pyroxenes. In the rocks under study the

orthopyroxene was probably saturated with Ca at the time of its crystallization (see p. 81). However, the orthopyroxene from the map-area contains distinctly less Ca than those from layered complexes and high-temperature volcanic orthopyroxenes (the range 1.15 to 1.9% Ca has been given by Kuno, 1954, op. cit. in Green, 1964). One might speculate that the ultramafic rocks under study crystallized under high pressure and that with falling temperature Ca was more thoroughly exsolved from the orthopyroxene than it would have been in the lower pressure environment of stratiform complexes and volcanic rocks.

Green (1964) has compiled the Cr_2O_3 and Al_2O_3 contents of orthopyroxenes from stratiform complexes, peridotite nodules in basalt and from the "intrusive" peridotites (e.g. Twin Sisters, Webster-Addie and Dawros) of orogenic belts. The Cr content of the orthopyroxene in the map-area (0.05 to 0.38% Cr) is similar to the Cr contents of orthopyroxenes from stratiform complexes and from "intrusive" peridotites. However, the range of Cr content in the orthopyroxene of the map-area is distinctly lower than that of orthopyroxenes from peridotite nodules in basalt (0.25 to 0.7% Cr).

The orthopyroxene in the map-area contains 0.27 to 1.12% Al. Comparison with Green's (1964, Fig. 8, p. 153) compilation of Al_2O_3 contents in orthopyroxenes shows that the orthopyroxene in the map-area contains similar amounts of Al as those from stratiform complexes, "intrusive" peridotites and from volcanic rocks. The Al content (0.37 to 0.74%) of orthopyroxenes from the Vourinos Complex, Greece (Moores, 1969) is within the range of Al content of the same mineral from the map-area.

Kushiro (1965, op. cit. in MacGregor, 1967) showed that on the diopside - anorthite join the solubility of Al_2O_3 in diopside increases

with increasing pressure. Al enrichment of enstatite with increasing pressure can be inferred by analogy. However, in the presence of spinel, the Al_2O_3 content of pyroxene will decrease with increasing pressure at constant temperature (MacGregor, 1967). Thus, if the ultramafic rocks in the map-area crystallized under relatively high pressures, as suggested earlier, the low Al content of orthopyroxene might be due to the presence of chromite and/or to the Al-poor nature of the parent magma. The low Al content of chromite (Chapter VI) and of pyroxene in pyroxenite (without chromite) suggests that the parent magma was poor in Al.

Clinopyroxene in all the rocks under study is richer in Cr than coexisting orthopyroxene. Clinopyroxene in pyroxenite is richer in Al than coexisting orthopyroxene. These characteristics perhaps explain the absence of chromite in pyroxenite and the absence of chromite in the pyroxene-bearing rocks in the map-area. During crystallization of these rocks, the incorporation of Al and Cr into the pyroxene structure depleted the liquid in these two elements, hence decreased the crystallization of chromite.

The distribution coefficient of Fe^{++} $K_{\text{Fe}} = (\text{Fe}^{++}/\text{Mg})_{\text{Opx}} (\text{Mg}/\text{Fe}^{++})_{\text{Cpx}}$ for the orthopyroxene-clinopyroxene pair has been calculated in three samples. The K_{Fe} value is 1.07 in pyroxenite (sample 142), 1.12 in orthopyroxenite (sample K-58) and 1.51 in peridotite (sample 221). In both peridotite and orthopyroxenite, clinopyroxene is interstitial and might have crystallized at a different temperature than orthopyroxene and/or might not be in equilibrium with this latter. Kretz (1961, op. cit. in Green, 1964) and Bartholomé (1961) have shown that in pyroxene granulites and assemblages crystallizing at metamorphic temperatures

$K_{Fe} = 1.8$ and $= 1.4$ in those crystallizing from a basic magma, while in peridotite nodules in basalt $K_{Fe} = 1.2$ to 1.3 . Kretz (1961, op. cit. in Green, 1964) considers that the effects on K_{Fe} of minor constituents and of pressure are negligible in comparison with temperature effects. Although O'Hara (1967b) has challenged Kretz's opinion concerning the effect of minor constituents on K_{Fe} , this coefficient appears to be a reasonable qualitative indicator of temperature of equilibration. The K_{Fe} value (1.07) for the clinopyroxene-orthopyroxene pair in pyroxenite suggests that the pyroxenite in the map-area has crystallized at much higher temperatures than basaltic differentiates. The same conclusion is not extended to orthopyroxenite, because assumption of equilibrium crystallization of interstitial clinopyroxene and coexisting orthopyroxene will probably be incorrect.

Boyd (1966) has related the composition of clinopyroxenes crystallized in equilibrium with coexisting orthopyroxene to their temperatures of crystallization. The relevant relationship is shown in Fig. 71 taken from Boyd (1966, Fig. 19). Although not stated by Boyd, this figure is presumably based on the shape of diopside (En) solvus in the system $MgSiO_3$ - $CaMgSi_2O_6$ at high pressure. However, pressure seems to have little effect on the solubility of $MgSiO_3$ in diopside, but the effects of minor constituents (e.g. Al, Fe^{+3} , Cr) are unknown (Boyd, 1966). The mean compositions of clinopyroxenes from the rocks under study have been plotted in this figure (Fig. 71). Equilibrium crystallization of clinopyroxene with coexisting orthopyroxene is assumed. The suggested temperatures of crystallization of clinopyroxenes in "herzolite", "olivine" pyroxenite and pyroxenite are in the range 1300 to 1450°C. These temperatures are in agreement with the high temperature that may

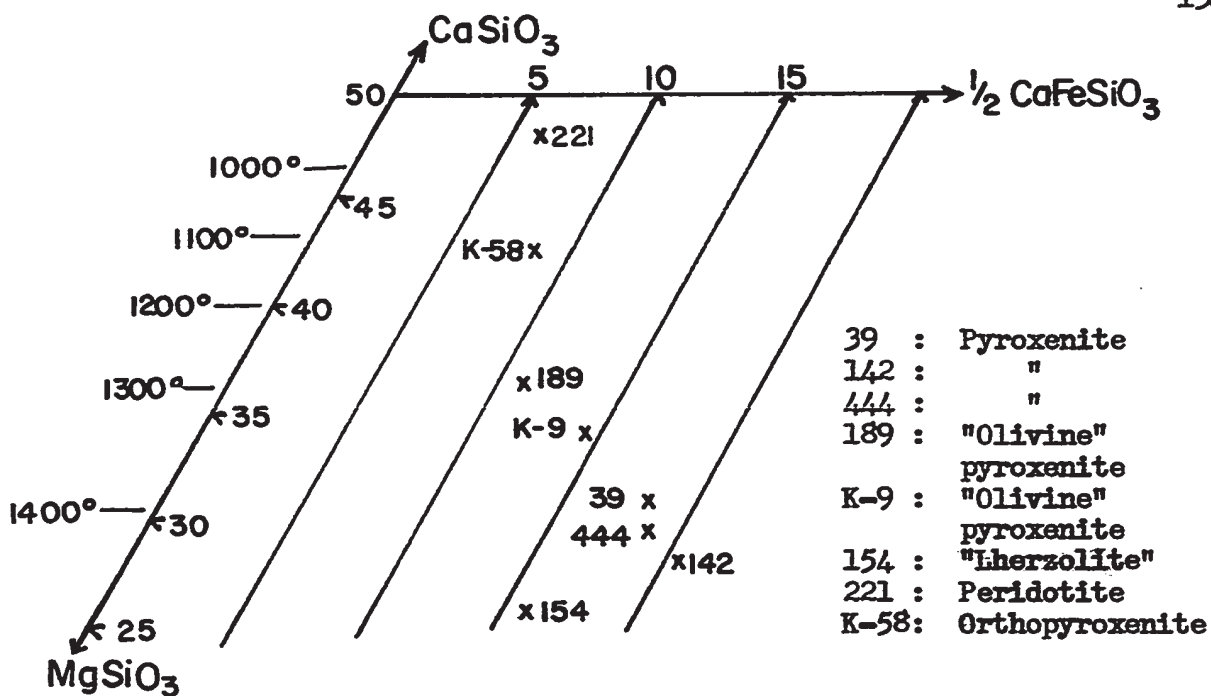


Figure 71. Compositions of clinopyroxenes coexisting with orthopyroxene versus temperature of crystallization (after Boyd, 1966)

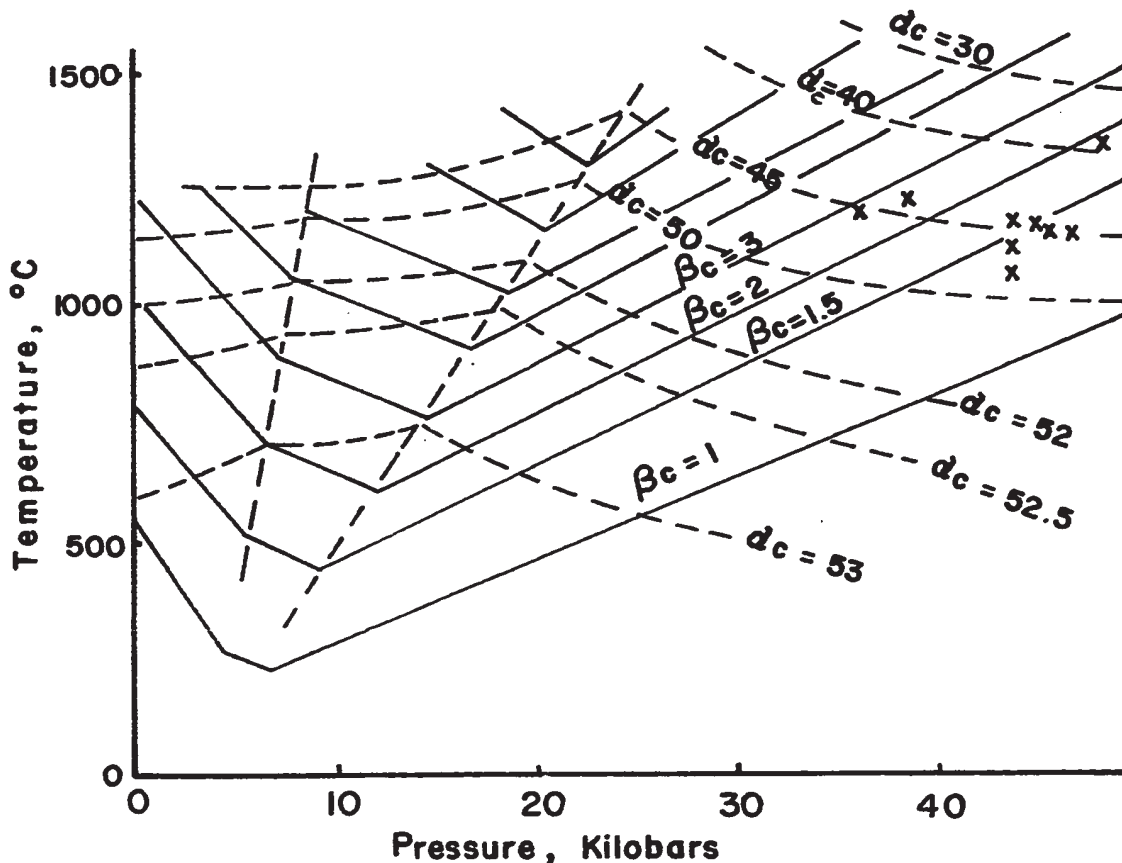


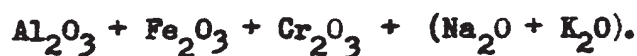
Figure 72. Variation of compositions of clinopyroxenes from "Iherzolite" (154) and "olivine" pyroxenite (189, K-9) versus temperature and pressure of formation of these rocks (after O'Hara, 1967b).

be inferred from the K_{Fe} value in pyroxenite (sample 142), discussed earlier.

O'Hara (1967b) has devised a petrogenetic grid using two compositional parameters of clinopyroxenes coexisting with orthopyroxene and olivine in an Al_2O_3 -saturated environment. The two parameters are;

$$\alpha = \frac{\text{wt.}\% \text{ CaSiO}_3}{\text{wt.}\% (\text{CaSiO}_3 + \text{MgSiO}_3)} \quad \text{and} \quad \beta = \frac{\text{wt.}\% \text{ Al}_2\text{O}_3}{\text{wt.}\% (\text{CaSiO}_3 + \text{MgSiO}_3 + \text{Al}_2\text{O}_3)}$$

where Al_2O_3 is equivalent, by convention (O'Hara, 1967b) to



Among the rocks from which clinopyroxenes have been analysed, only "lherzolite" (sample 154) and "olivine" pyroxenite (samples 189 and K-9) can perhaps be assumed to satisfy the requirements stated above for the applicability of O'Hara's grid. The present clinopyroxene analyses are incomplete in that only Fe_{total} is available and Mn, Na and K have not been analysed. No Cr analysis is available for the sample 189. Nevertheless, α and β parameters of clinopyroxenes in "lherzolite" and "olivine" pyroxenite have been calculated using O'Hara's (1967b) convention and are given in Table XII in the Appendices.

The plot of clinopyroxene compositions on O'Hara's grid is shown in Fig. 72. The plots suggest pressures of equilibration in the range 35 to 50 kb and temperatures in the range 1100 to 1400°C; essentially the same conditions of equilibration as for peridotite nodules in kimberlites (O'Hara, 1967b, Fig. 12.6). If allowance were made for the probable amounts of Fe_2O_3 , Cr_2O_3 (in sample 189), MnO, Na_2O and K_2O , this would probably shift the plots to slightly higher temperatures and lower pressures. However, in all probability, the data would then plot in the range

1200 to 1500° C, 30 to 40 kb, thus well within the garnet peridotite field.

The range of pressures of equilibration of the "herzolite and "olivine" pyroxenite, suggested by O'Hara's grid, is too high in comparison with the pressure ranges inferred (O'Hara, 1967b, Fig. 12.6) for similar ultramafic rocks in orogenic belts elsewhere. It is possible that the assemblages used in Fig. 72 do not satisfy one or more of the conditions for the applicability of O'Hara's grid.

V.11. CONCLUSION

Dunite dykes and discordant dunite are thought to represent injections of dunitic crystal mush. The pyroxenite and orthopyroxenite dykes are believed to have formed by liquid injections, hence perhaps constitute evidence for the existence of the ultramafic magma.

The Mg/Fe ratios in orthopyroxene and olivine from the map-area are similar to those of the same mineral from alpine-type ultramafic rocks, intrusive peridotites (e.g. Mount Albert, Lizard intrusion), peridotite nodules in basalt and kimberlites and from ultramafic rocks of ophiolite complexes. The Cr, Al and Ca contents of the orthopyroxene from the map-area are similar to those of orthopyroxenes from most ultramafic rocks in orogenic belts elsewhere. The mineral chemistry suggests similar sources for these rocks and appears to be independent of their mode of emplacement.

All the available evidence points to high temperatures of crystallization of the ultramafic rocks. Slow cooling and slow rate of settling of crystals are inferred. The compositions of minerals in the ultramafic rocks suggest relatively high pressure of equilibration. Attempt to quantify pressure of equilibration by using O'Hara's grid yielded improbably high pressures and is considered inconclusive.

CHAPTER VI

CHROMITITE AND CHROMITE DEPOSITS

VI.1. INTRODUCTION

Most of the major chromite deposits which have been commercially explored in southern Quebec are within the map-area and all of them have been visited by the writer. The Sterrett Mine in Cleveland Township, some 100 km south-southeast of the map-area, is included in this study because of its large size.

With only three exceptions, all the chromitite mined in the area was excavated from open pits. Most of these pits are now full of water and thus only partially accessible for examination. However, their distribution, apparent shape, size and orientation are readily observable and yield interesting information. The quality and characteristics of extracted chromitite can be deduced by examining the waste. All the chromite workings and all the observed chromitite are in dunite. The dunite body itself can be entirely surrounded by peridotite but only dunite contains chromitite.

In this chapter the structures and petrography of chromitite, the chemistry of chromite in chromitite and the distribution and characteristics of chromite workings are described. Since chromite workings are former chromite deposits, the distribution and characteristics of

concealed chromite deposits can perhaps be inferred from the study of chromite workings.

It is apparent that there are quite definite relationships between the structure of chromitite and the inferred shape and size of the deposits. Furthermore, the geological setting of chromite workings seems to have a bearing on the structure of chromitite which occurs in them and hence on the shape of the former chromite orebodies.

VI.2. STRUCTURES OF CHROMITITE

For the purpose of description, the structures observed in chromitite have been divided into four groups. The division between banded chromitite and schlieren is arbitrary.

Banded chromitite

The interlayering of dunite with chromitite is the most common structure. The chromitite bands have an average thickness of 1 to 5 cm but vary from being only one grain size thick (i.e. < 2 mm) to 20 cm. One exceptional band, exposed in Belanger pit, is 1 m thick.

Throughout the map-area, chromitite layers are commonly less continuous and more variable in strike and dip than silicate rock layers. Massive chromitite ($> 90\%$ chromite) layers are usually short and variable in strike and dip. Their thickness varies rapidly, they disappear by pinching out and commonly do not reappear along their strike direction. Their contact with dunite is sharp (Fig. 73) and dunite around them is commonly poor in accessory chromite. Chromitite layers with low chromite content (35-65% chromite) are usually several tens of meters long, have fairly constant thickness (Figs. 74 and 75) and more regular strike and dip than massive chromitite layers. The chromitite layers



Figure 73. Coarse, massive chromitite layer. Note sharp contacts with serpentinized dunite. Transverse fracture system is interpreted as representing the beginning of "Pull-apart" texture. Serpentine within the ore is bleached white. (From the tailing of Caribou deposit)



Figure 74. Chromitite with low chromite content (dark grey) inter-layered with dunite. (Bélanger pit, 350 m west of Caribou Lake)

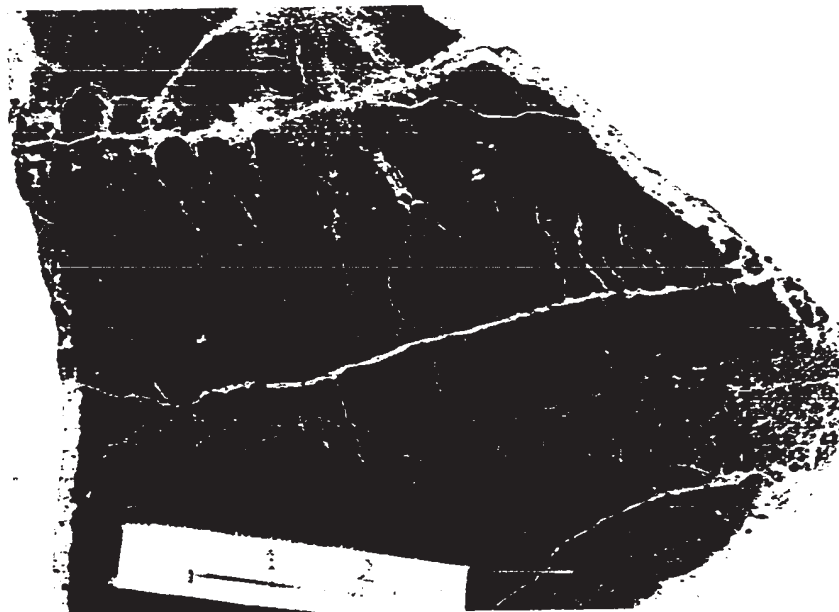


Figure 73. Coarse, massive chromitite layer. Note sharp contacts with serpentinized dunite. Transverse fracture system is interpreted as representing the beginning of "Pull-apart" texture. Serpentine within the ore is bleached white. (From the tailing of Caribou deposit)

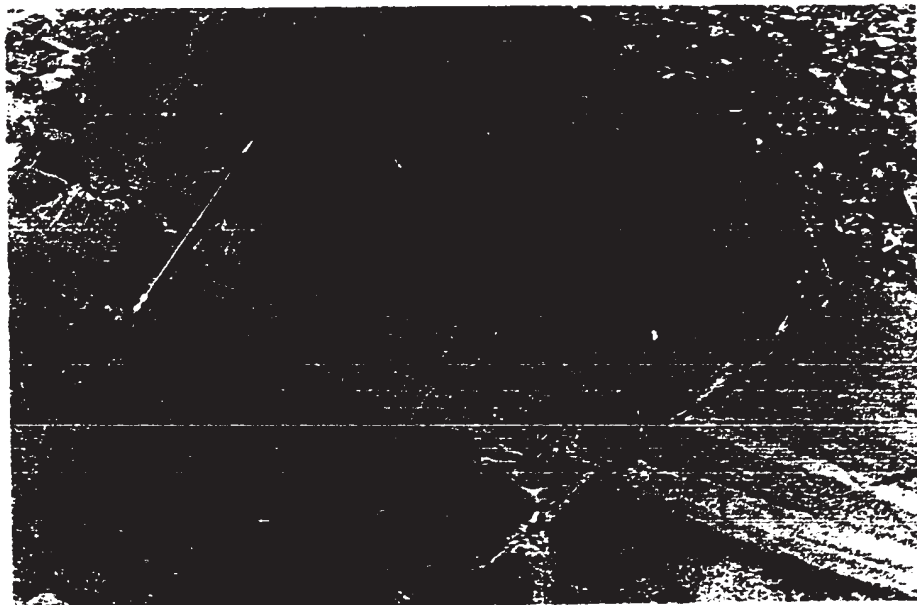


Figure 74. Chromitite with low chromite content (dark grey) inter-layered with dunite. (Bélanger pit, 350 m west of Caribou Lake)

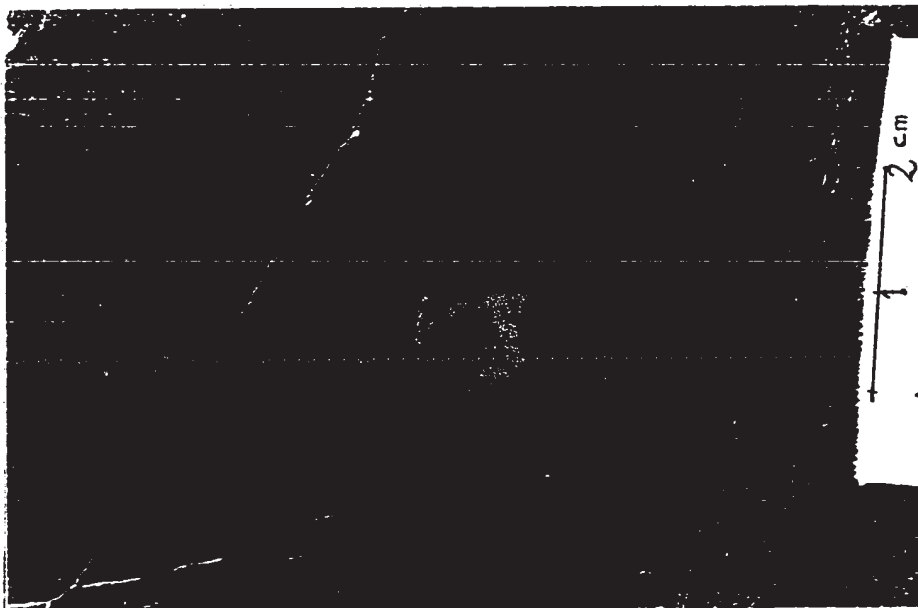


Figure 75. Detail of chromitite-dunite interlayering. Chromitite is light grey.
(From a chromite working on Brousseau Hill)

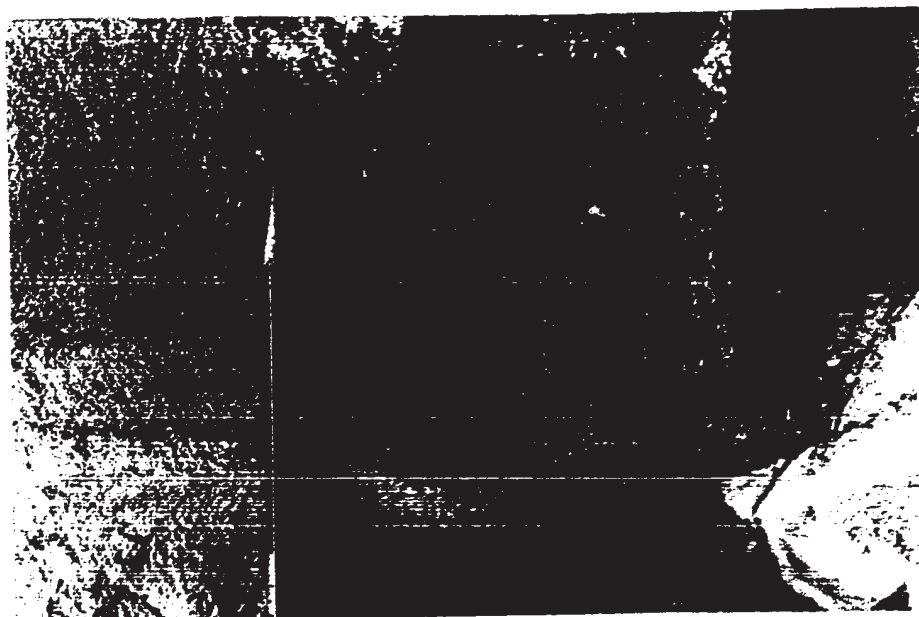


Figure 76. Chromitite layer with low chromite content. The layer has one sharp surface (lower part of the figure), while the other side is very gradational.
(Bélanger pit)

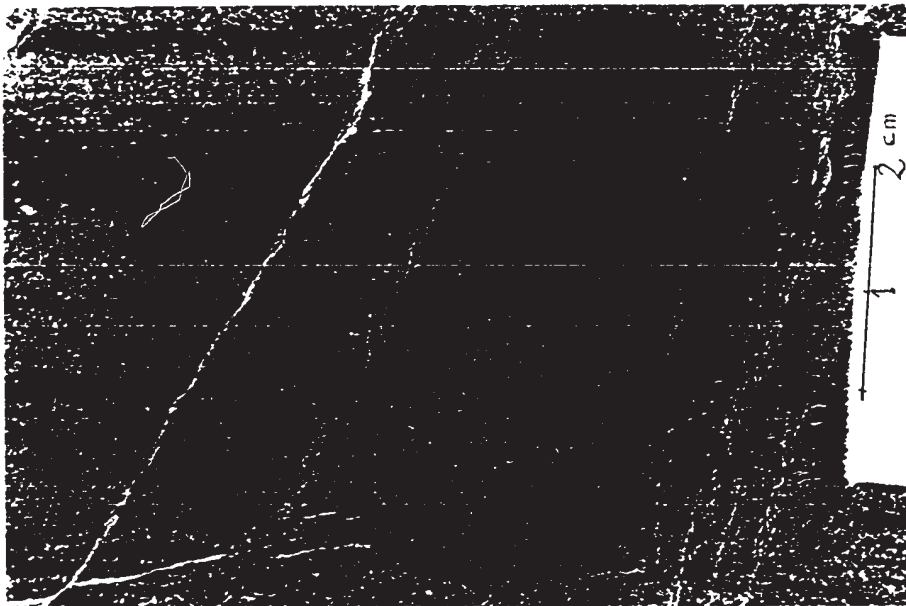


Figure 75. Detail of chromitite-dunite interlayering. Chromitite is light grey.
(From a chromite working on Brousseau Hill)

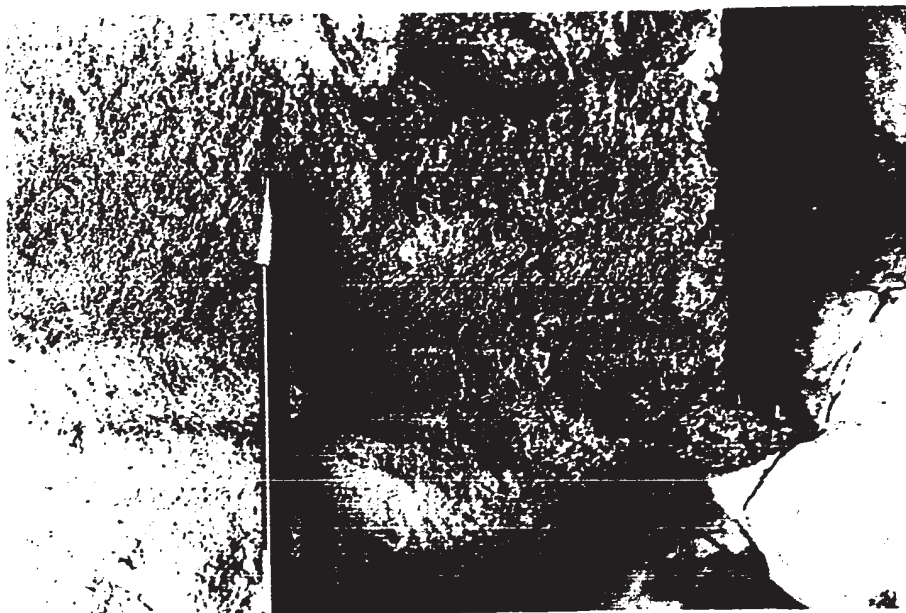


Figure 76. Chromitite layer with low chromite content. The layer has one sharp surface (lower part of the figure), while the other side is very gradational.
(Bélanger pit)

with low chromite content disappear by pinching out, usually to reappear along their strike direction. Chromitite layers with high chromite content (65 to 90% chromite) are intermediate in nature between the two types of layers described above.

No well-defined graded bedding has been observed in banded chromitite, the best possible example is that illustrated by Fig. 76 which shows a band with one sharp side, while the other is gradational. No inference of "stratigraphic top" has been made from such features.

Nodular chromitite

Nodular chromitite consists of ellipsoidal nodules whose long axes are from about 4 mm. to 3 cm in length. Most nodules are oriented with their long axis parallel to the elongation of the deposit in which they occur. The best developed nodular chromitite has been called "grape ore" and consists of nodules 1 to 3 cm in diameter (Figs. 77 and 78). Usually the surface of nodules is smooth. Fracturing is always present in chromitite of this type, and in some cases there is a roughly orthogonal fracture pattern with one set of fractures perpendicular to the long axis of the nodules. Nodular chromitite forms lenticular bodies and bands parallel or subparallel to the other types of chromitite bands in dunite (Figs. 79 and 80). With one exception, all the observed nodular chromitite occurs in dunite bodies within peridotite, and almost every chromitite-bearing dunite body within peridotite has some nodular chromitite. The exception is in the American Chrome Company's deposits, south of Morin Hill, which are in the Southern Dunite Zone and contain nodular chromitite.

Nodular chromitite appears to be chemically homogeneous. The

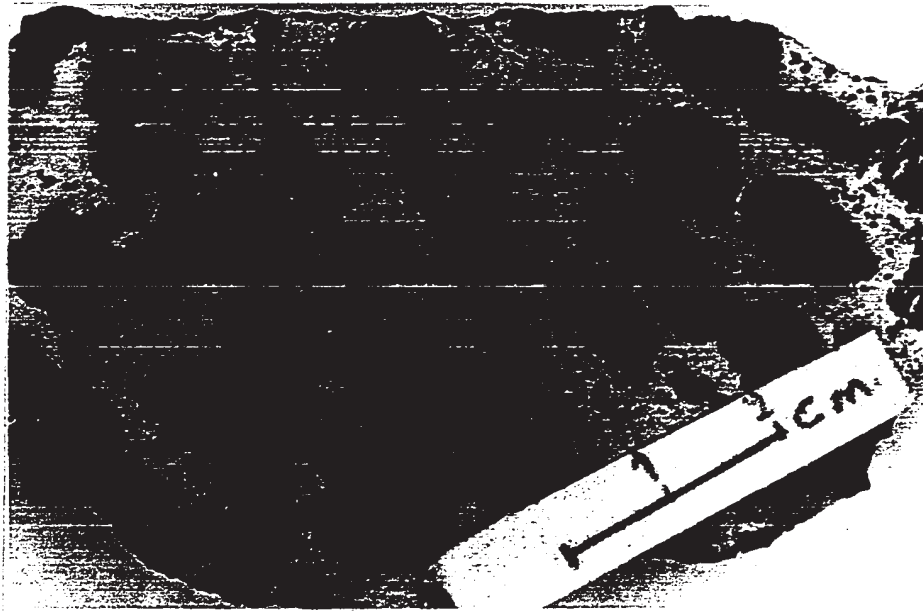


Figure 77. Nodular chromitite, variety "grape ore" (dark grey) in serpentinized dunite. Small chromite grains in the matrix appear to be pieces from the "grapes" of chromitite. Sample No. 371
(Ross Lot, along the road from B.C. Asbestos Mine to Caribou Lake)

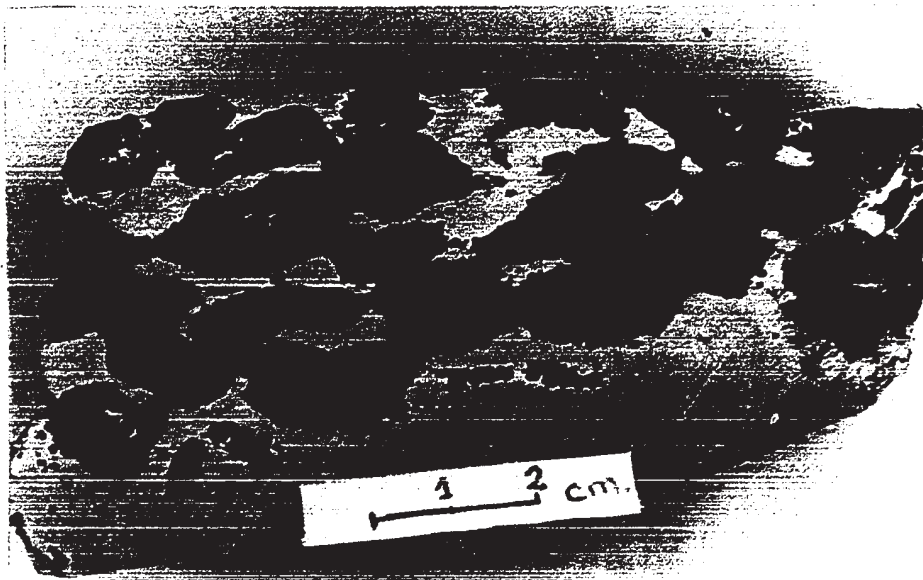


Figure 78. Nodular chromitite, variety "grape ore". The chromitite nodules exhibit a preferred orientation with their long axes parallel to the elongation of the deposit. Sample No. 371
(From a chromite working at the top of Caribou Mountain)

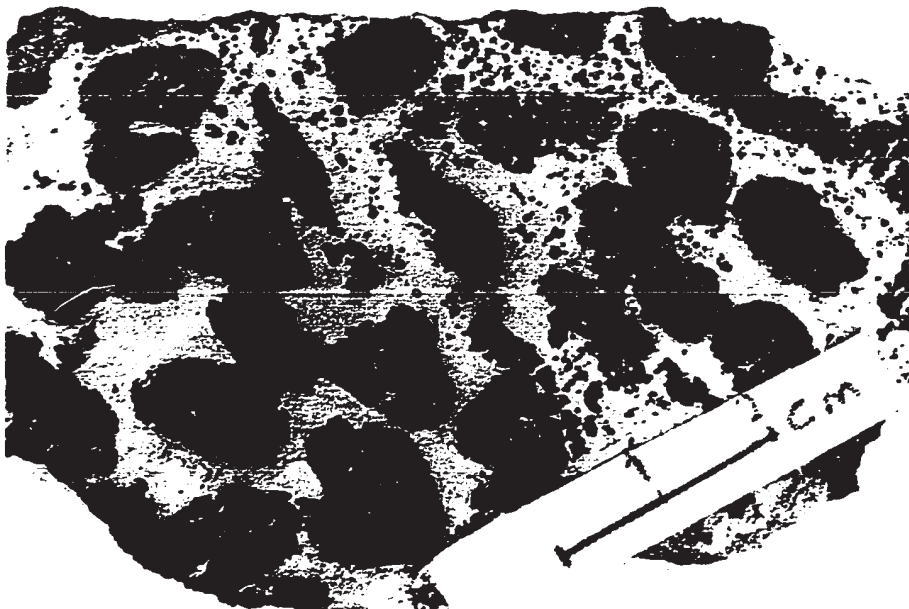


Figure 77. Nodular chromitite, variety "grape ore" (dark grey) in serpentinized dunite. Small chromite grains in the matrix appear to be pieces from the "grapes" of chromitite. Sample No. 371 (Ross Lot, along the road from B.C. Asbestos Mine to Caribou Lake)



Figure 78. Nodular chromitite, variety "grape ore". The chromitite nodules exhibit a preferred orientation with their long axes parallel to the elongation of the deposit. Sample No. 371 (From a chromite working at the top of Caribou Mountain)

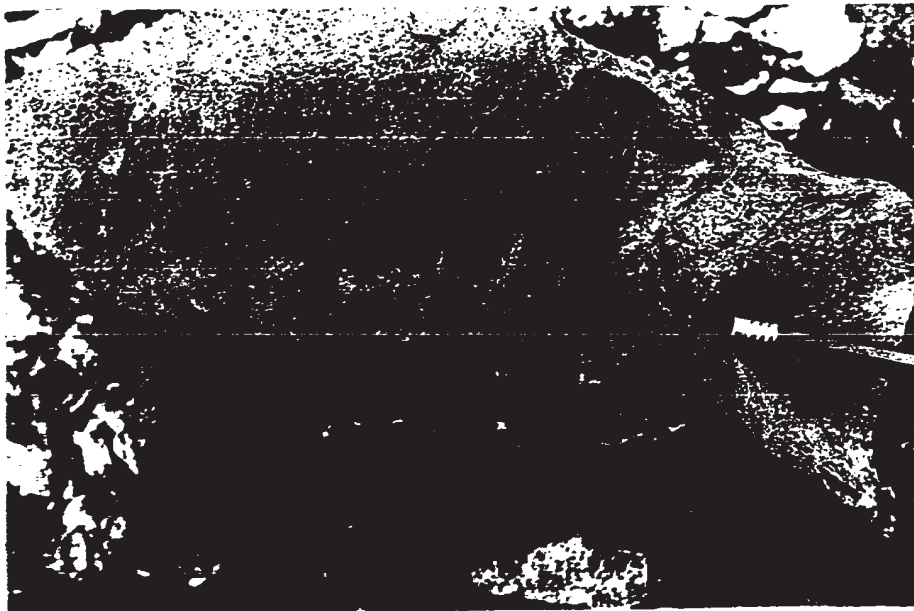


Figure 79. Ill-defined layering of "grape ore" now largely deformed. The upper layer has one sharp surface, while the other is gradational. (Ross Lot, along the road from B.C. Asbestos Mine to Caribou Lake)

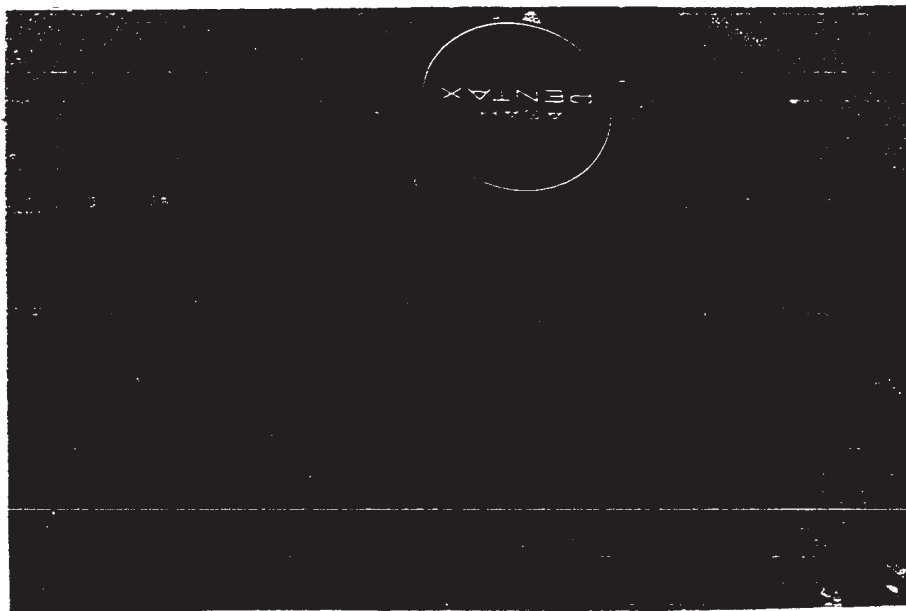


Figure 80. Fine layering of chromite ore (dark grey) with occasional "grapes" of chromitite (below the objective cover). (American Chrome Company's Pits, south of Morin Hill)



Figure 79. Ill-defined layering of "grape ore" now largely deformed. The upper layer has one sharp surface, while the other is gradational. (Ross Lot, along the road from B.C. Asbestos Mine to Caribou Lake)



Figure 80. Fine layering of chromite ore (dark grey) with occasional "grapes" of chromitite (below the objective cover). (American Chrome Company's Pits, south of Morin Hill)

nodules commonly contain olivine inclusions. It has not been determined whether the nodules are agglomerations of several crystals, since an entire nodule appears now as a continuous mass. They are, most likely, an agglomeration of several crystals similar to other chromitite pods and clusters.

Nodular chromitite is common in the map-area and appears to be quite common in alpine-type chromite deposits elsewhere (Thayer, 1960). It has not been described from chromite deposits of stratiform complexes. Until recently, nodular chromitite was almost unanimously considered to be a corrosion feature, supposedly resulting from the corrosion of fragments which were broken off from larger chromitite masses. Donath (1931, in Williamson, 1933, p. 77), who was first to suggest an origin by corrosion, pointed out that a spherical form has the lowest surface to volume ratio and thus offers the greatest resistance to corrosive agents. However, this origin for chromitite nodules is not entirely satisfactory when applied to the rocks under study, for the following reasons: The chromitite nodules occur in layers which are parallel to the other types of layering and they are not randomly distributed as fragments might be. There is not always massive chromitite near the nodular chromitite from which it might have been derived by fragmentation. The nodules always consist of massive chromitite (95% chromite), it would be fortuitous if only massive chromitite underwent fragmentation and subsequent corrosion. Hence, although it is conceivable that some chromitite nodules could have been formed by the corrosion of the fragments, this does not seem to have been the main process. There appear to be three alternatives:

- (1) Formation of nodules by rolling: The chromite grains could roll down a slope during crystal settling and agglomerate with other chromite

grains to form a ball. This is the way Borchert (1964) explains massive chromitite pockets, lenses, etc. Although he does not refer particularly to nodular chromitite, his idea is applicable to this case.

(2) Formation of nodules "suspended" in the magma: Thayer (1969a) believes that chromitite nodules formed by agglomeration of chromite crystals around a nucleus (olivine or chromite) suspended in the magma. He states (p. 139) "The intact forms and packing structure of many nodules show that they were rigid and fully grown before they piled up." He suggests that the massive nature of chromitite nodules resulted from extensive postcumulus growth. He further reports sedimentary bedding and size sorting of chromitite nodules in the Guillermina Mine, Cuba, definitely pointing to gravity as a process of settling of nodules.

(3) Separation of an immiscible chromite-rich liquid: This is thought to be the most likely process for the formation of nodular chromitite in the rocks under study. Liquid immiscibility has already been proposed by Shams (1964) in connection with chromitite nodules from chromite deposits in the Hindubagh district, W. Pakistan. Chromitite nodules in the map-area are also thought to have been formed by liquid immiscibility. In the synthetic system $\text{Cr}_2\text{O}_3 - \text{MgO} - \text{SiO}_2$, there are two immiscible liquid phases, one is rich in silica, the other intermediate in composition between SiO_2 and the other two end members (Keith, 1954). The immiscibility occurs at a very low normative chromite concentration. The following statement concerning Fisher's experiment on chromite immiscibility is taken from Shams (1964, p. 1346):

"He observed that all melts made from a mixture of gabbro with 2.5, 5 and 10 per cent chromite separated into two immiscible liquids at 1400°C , one rich and the other poor in chromium. He further observed that the chromium-rich melts crystallized into mixtures of chromite and olivine."

A chromite melt is known to have very high viscosity and high surface tension. Therefore, a drop of this melt would assume a more or less rounded shape. The fact that chromite crystals at the margin of the nodules do not have euhedral boundaries can be explained by corrosion of the initial segregations. The preferred orientation of nodules could result from flow.

As already noted, although common, nodular chromitite is not quantitatively important in the map-area. Therefore, liquid immiscibility is probably of minor importance in the formation of chromite deposits. However, the important implication is that each of these three outlined processes requires an entirely or largely liquid original magma.

Pencil-shaped concentrations, chromitite pods and schlieren

The shapes of many chromite concentrations are extremely variable. Three main types are recognized, namely pencil-shaped concentrations, pods and schlieren. The pencil-shaped concentrations are mostly a few centimeters long and 1 to 2 cm thick (Fig. 81). The chromitite pencils often exhibit fractures perpendicular to their length, this has been named "pull-apart texture" by Thayer (1964) and is supposedly due to the stretching of the chromitite mass during flow.

The chromitite pods are irregular in shape. They are from a few centimeters to 20 cm in length and are mainly massive or contain a high percentage of chromite. Chromitite schlieren have usually high chromite content (>65% chromite), and they disappear by pinching out (Fig. 82). The length of schlieren varies from about 10 cm to several meters.

Most of the schlieren are probably the remnants of former chromitite layers which have been disjointed by deformation. It is very likely

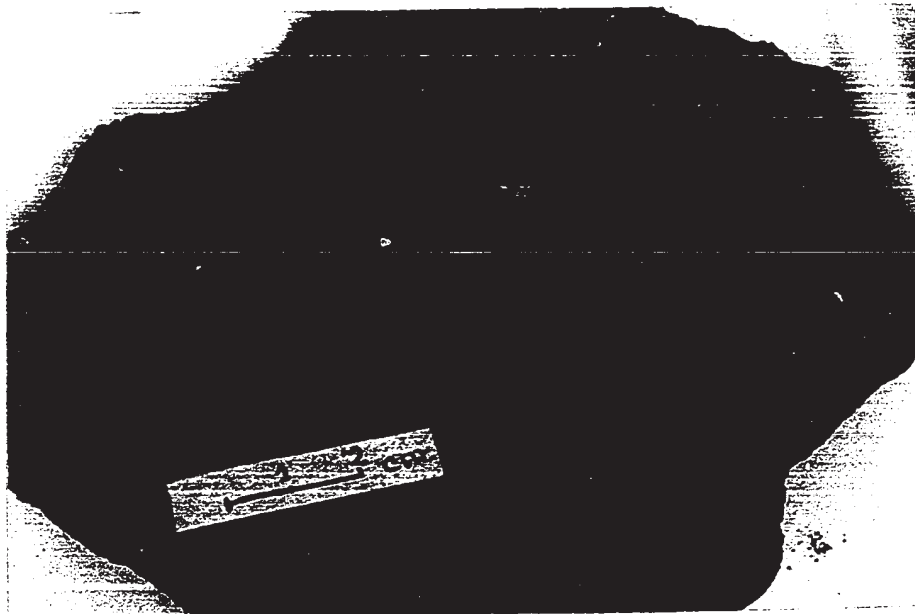


Figure 81. Pencil-shaped concentrations (dark grey) in serpentinized dunite.
(From a deposit on the north slope of Quarry Hill)

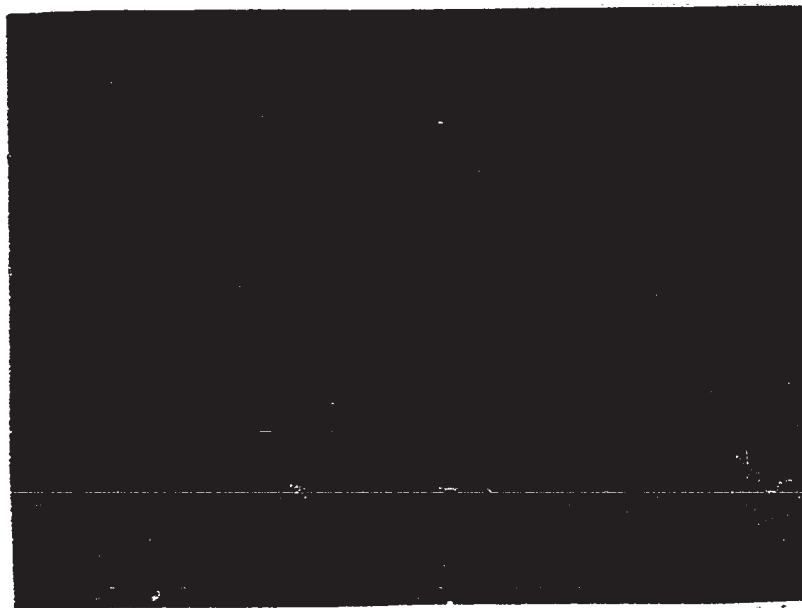


Figure 82. Chromitite schlieren and lenses (dark grey) in dunite.
The schlieren and lenses exhibit the same discontinuity
in the third dimension.
(From the tailing of the Greenshields deposit)



Figure 81. Pencil-shaped concentrations (dark grey) in serpentinized dunite.
(From a deposit on the north slope of Quarry Hill)

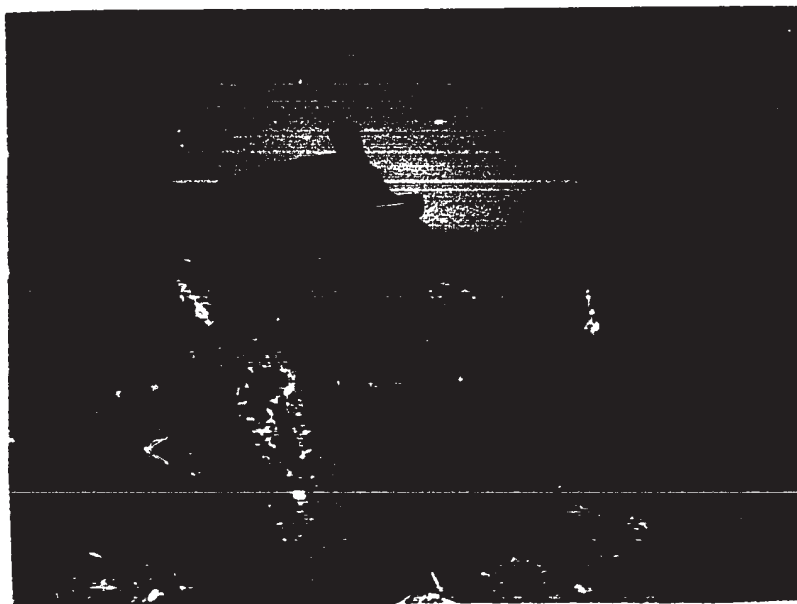


Figure 82. Chromitite schlieren and lenses (dark grey) in dunite.
The schlieren and lenses exhibit the same discontinuity
in the third dimension.
(From the tailing of the Greenshields deposit)

that chromitite with high chromite content would be more competent and much more severely disjointed during this deformation than chromitite with a lower amount of chromite. This would explain the usually chromite-rich nature of the schlieren.

The chromitite pods and pencil-shaped masses might also be fragments of formerly larger chromite concentrations. They might also have been formed by the local concentration of a chromite-rich liquid as postulated for the nodular chromitite.

Chromitite veins and chromitite with "chain structure"

Chromitite veins consist of massive chromitite or chromitite with high chromite content. The veins crosscut each other to form an intricate stockwork isolating islands of serpentinized dunite (Figs. 83 and 84). Toward the margins of the veins, the granular nature of this chromitite and the euhedral and subhedral shape of the crystals can be seen in hand specimen. From their appearance it would seem that chromitite veins have resulted from injection of a chromite crystal mush or a chromite-rich liquid into partly solidified dunite; subsequent secondary growth of chromite crystals having resulted in the expulsion of the silicate component, if present. Because of its peculiarities, the origin of chromitite veins is discussed in some detail later in this chapter.

Locally, euhedral and subhedral chromite crystals surround olivine grains (Figs. 84, 85 and 86). The chromite grains are in contact with each other. Jackson (1961) observed an identical structure which he called a "chain structure" in the Stillwater Complex and claimed it was the result of contemporaneous gravity settling of olivine and chromite crystals modified by in situ growth. Thayer (1969a) believes that this



Figure 83. Chromitite veins (light grey). The granular nature of this ore can be seen in hand specimen. (Hall Mine)

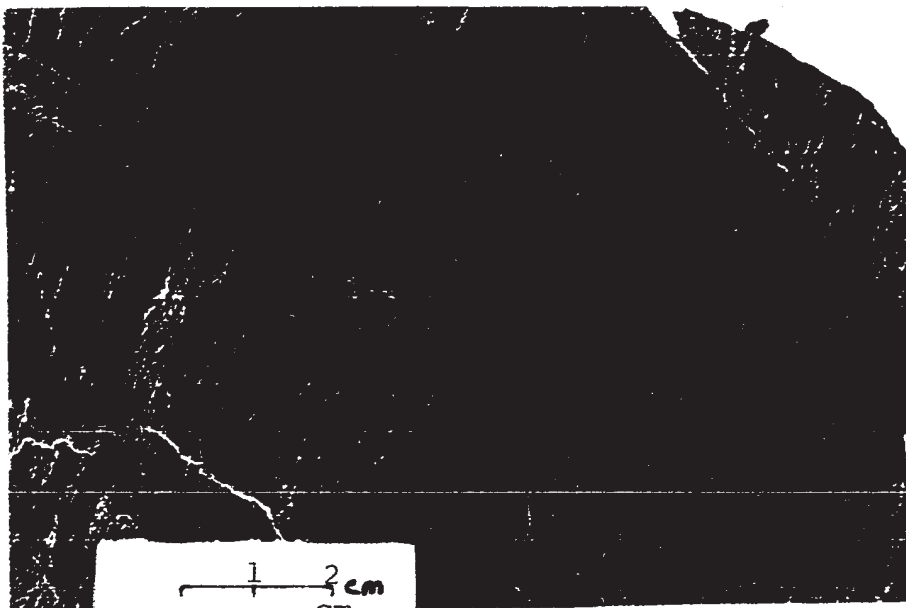


Figure 84. Chromitite in veins (light grey) grading into chromitite with "chain structure". (Hall Mine)

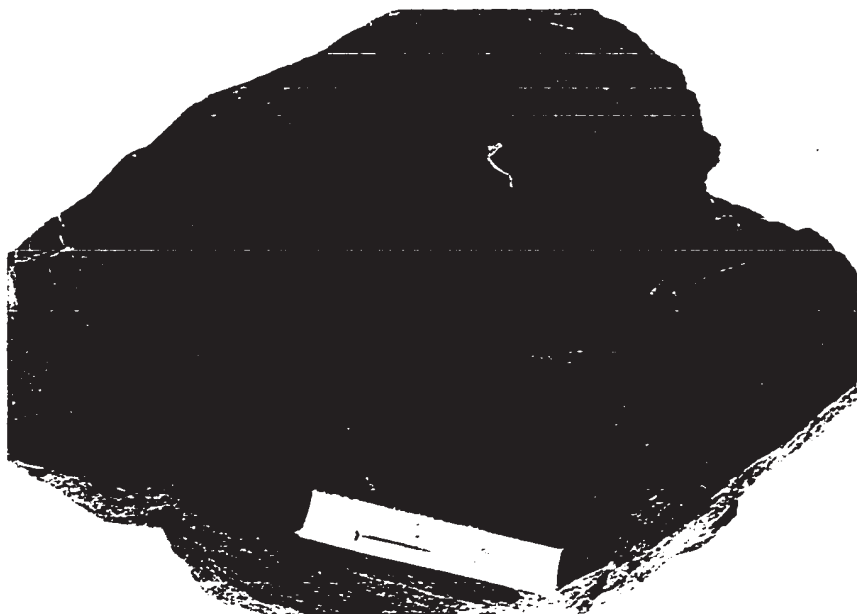


Figure 83. Chromitite veins (light grey). The granular nature of this ore can be seen in hand specimen. (Hall Mine)

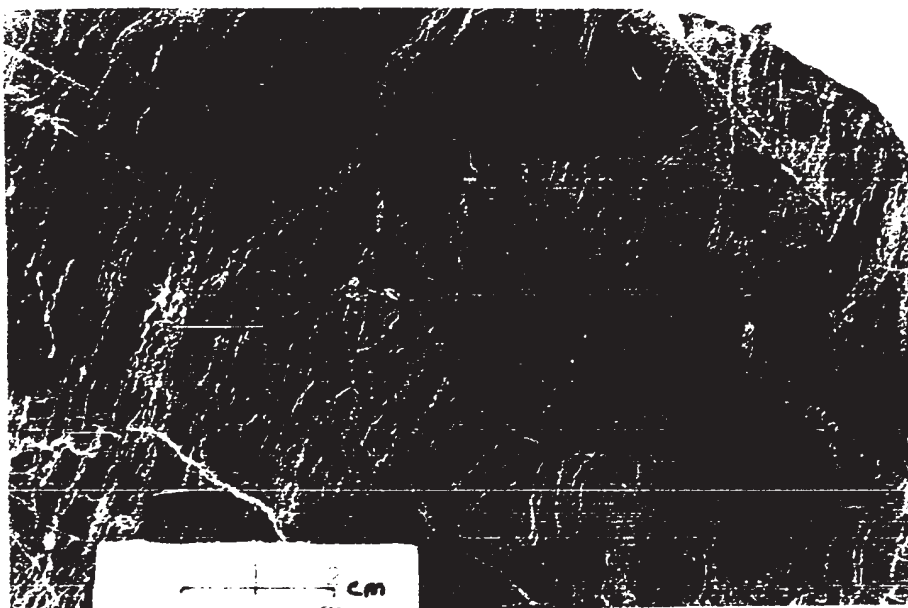


Figure 84. Chromitite in veins (light grey) grading into chromitite with "chain structure". (Hall Mine)



Figure 85. A layer (?) of chromitite with "chain structure" (dark grey). The light grey grains are serpentinized olivine. (Hall Mine)

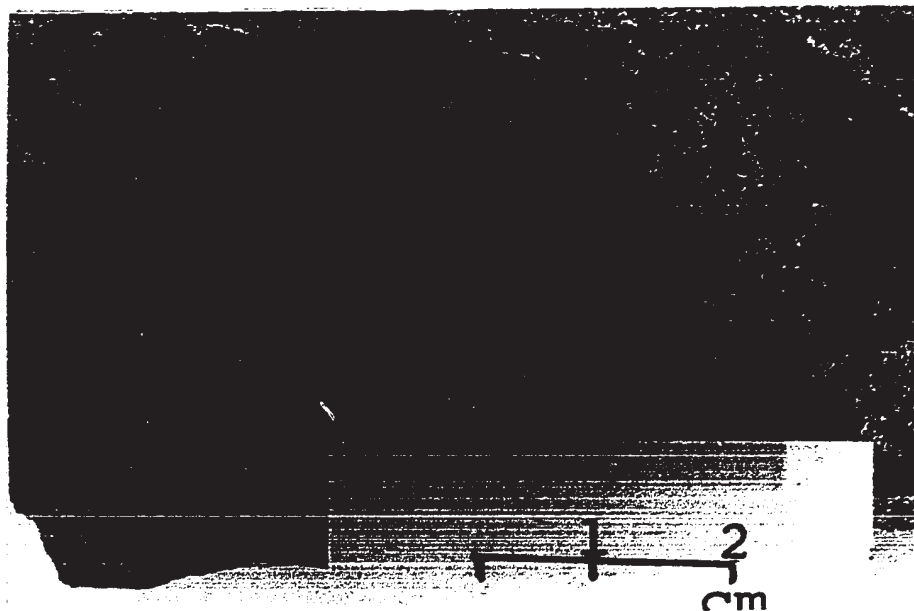


Figure 86. Chromitite with "chain structure". Chromite grains (black) surround individual olivine grains or groups of olivine grains. The figure shows the weathered surface of a sample. The dark area at the upper left corner is a broken surface. Sample No. 526 (Hall Mine)

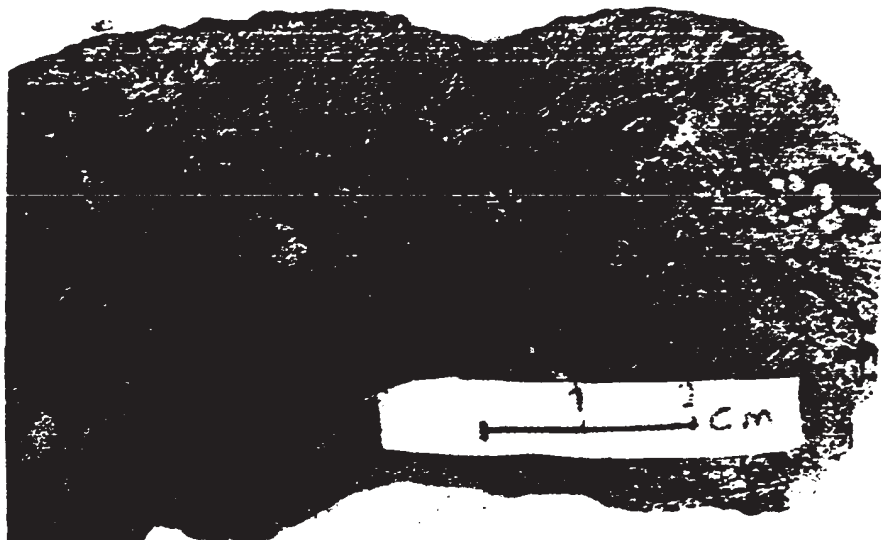


Figure 85. A layer (?) of chromitite with "chain structure" (dark grey). The light grey grains are serpentinized olivine. (Hall Mine)

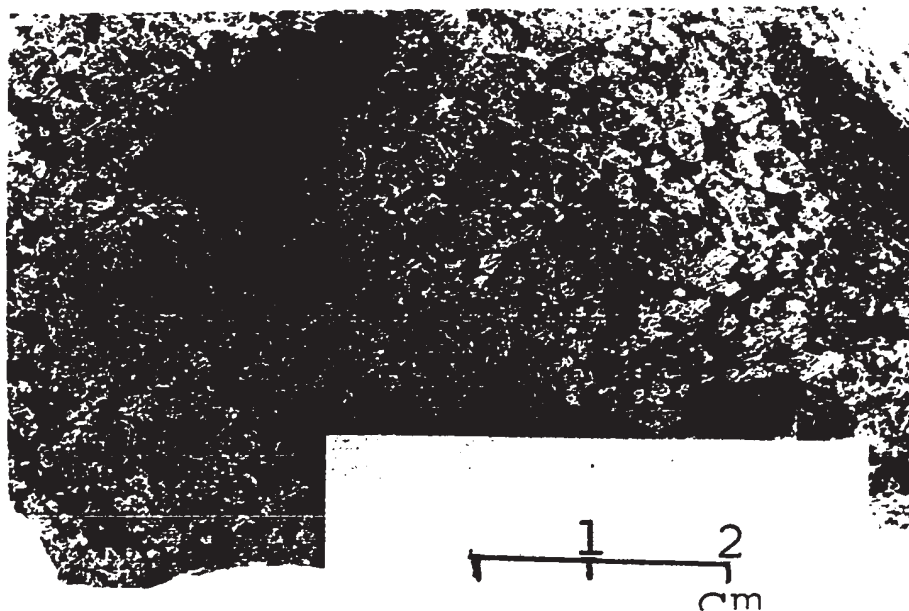


Figure 86. Chromitite with "chain structure". Chromite grains (black) surround individual olivine grains or groups of olivine grains. The figure shows the weathered surface of a sample. The dark area at the upper left corner is a broken surface. Sample No. 526 (Hall Mine)

type of structure, which he calls "chromite net" is a diagnostic product of crystal settling process in alpine-type peridotites.

VI.3. CLASSIFICATION AND DISTRIBUTION OF CHROMITE DEPOSITS

A. General statement

Based on the study of chromite workings the former chromite deposits, which are now partially or totally mined out, are classified and their distribution is discussed.

B. Classification of chromite deposits

The chromite deposits are divided into four groups: banded, lenticular deposits, lenticular deposits with schlieren, "podiform" deposits and veined deposits.

Banded, lenticular deposits

The banded, lenticular deposits consist mainly of chromitite layers with low chromite content interlayered with dunite. Massive chromitite layers and schlieren are common but not abundant and other structures are rare or absent.

As the name implies, a banded, lenticular deposit is lens-shaped. In the map-area, the visible length of the deposits of this type varies from about 10 m to 200 m. From the description of mine workings, they appear to be quite continuous down the dip, so that commonly they are disc-shaped. Along the strike, a deposit pinches out gradually or suddenly and usually another one is found at some distance. Therefore, several deposits roughly aligned parallel to their strike occur within a narrow zone (Map 3) which will be referred to as an ore zone. The Reed-Bélanger deposits (Map 3, Ore zone No. 1) and the Sterrett Mine

deposits (Appendix II) provide good examples of this type of ore zone.

The boundaries between a deposit and dunite are gradational. One passes from a deposit to the barren rock by the decrease in the number of chromitite bands and by the bands becoming thinner and less concentrated. Along the strike direction, the distance separating a deposit from the next one can be as little as a few meters or as much as 300 m. The rock within this intervening distance can be barren (i.e. containing not more than the usual amount of accessory chromite) or it can contain up to 20% chromite. The chromite content of chromitite and the width of the deposits seem to vary down the dip in a similar way to their variation along the strike.

Lenticular deposits with schlieren

Schlieren and lenses are the predominant chromitite structure in the deposits of this group. However, pods and chromitite layers are also observed. Most of the chromitite has high chromite content (65 to 90% chromite).

Some lenticular deposits of this group appear to be isolated, that is, they do not occur in ore zones. The Montreal Pit, quite a large deposit, is an example of the isolated lenticular deposit. Most of the deposits in dunite bodies surrounded by peridotite also belong to this group and are isolated. However, there are many deposits of this group which do occur in ore zones (e.g. Caribou deposits, Ore zone No. 8, Map 3).

"Podiform" deposits

This word, coined by Thayer (1964), is used here to designate chromite deposits of irregular shape. These deposits have all the charac-

teristics of the previous group, but they are not lenticular in shape. Some deposits occurring within dunite bodies in peridotite belong to this group.

Veined deposit

The essential structures of this type of deposit are chromitite veins and chromitite with "chain structure". The only known deposit of this type is the Hall Mine.

C. Distribution of chromite deposits

There are apparent relationships between the distribution of chromite deposits and the attitude of layers and the grade of ore within the deposits.

Where chromite deposits are confined to an ore zone, the strike and dip of chromitite layers, schlieren and lenses remain more or less parallel to the ore zone and concordant with the surrounding silicate rocks (e.g. Ore zone No. 1, Map 3 and the Sterrett Mine, Appendix II). In these deposits the chromite content of chromitite is usually low.

In chromite deposits which are irregularly distributed but still restricted to a small area (e.g. American Chrome Co. deposits, Appendix II), the chromitite layers, schlieren and lenses are usually massive or have high chromite content and are variable in strike and dip. The layering in surrounding silicate rocks also varies in strike and dip.

Therefore, it is postulated that the irregular distribution of chromite deposits is the result of deformation subsequent to the formation of chromitite. The study of chromite pits, published description of mine workings and the attitude of layering suggest that the distribu-

tion of chromite deposits in the third dimension is similar to their distribution at the surface (Fig. 87).

VI.4. DEFORMATION OF CHROMITITE

Anastomosing chromitite layers are thought to have been formed by deformation of chromitite layers prior to the complete solidification of the rock, since no cataclasis indicating solid state deformation of layers has been observed.

Folding occurs in the chromitite (Fig. 88) but is not common. Folding appears to predate the serpentinization, since fragile serpentine replacement textures on the axial planes of these usually tight folds are not deformed. Furthermore, serpentinite veins belonging to the late serpentinization (Chapter VII) crosscut folds.

Chromitite is commonly much faulted and sheared. The major faults can be followed in chromitite, since they are marked by fault gouges and slickenside surfaces. It would appear that most of the faulting occurred when the chromitite was solid. However, locally, chromitite layers are offset without any noticeable cataclasis (Fig. 89), and it is possible that this type of faulting occurred prior to the complete solidification of the rocks.

VI.5. PETROGRAPHY OF CHROMITITE

The grain size of chromite in chromitite increases with increasing concentration. The average grain size of chromitite with high chromite content is 2 to 3 mm compared to about 1 mm for accessory chromite in the ultramafic rocks.

The tendency of chromite to assume idiomorphic form increases with decreasing concentration. The shape of chromite grains in chromitite

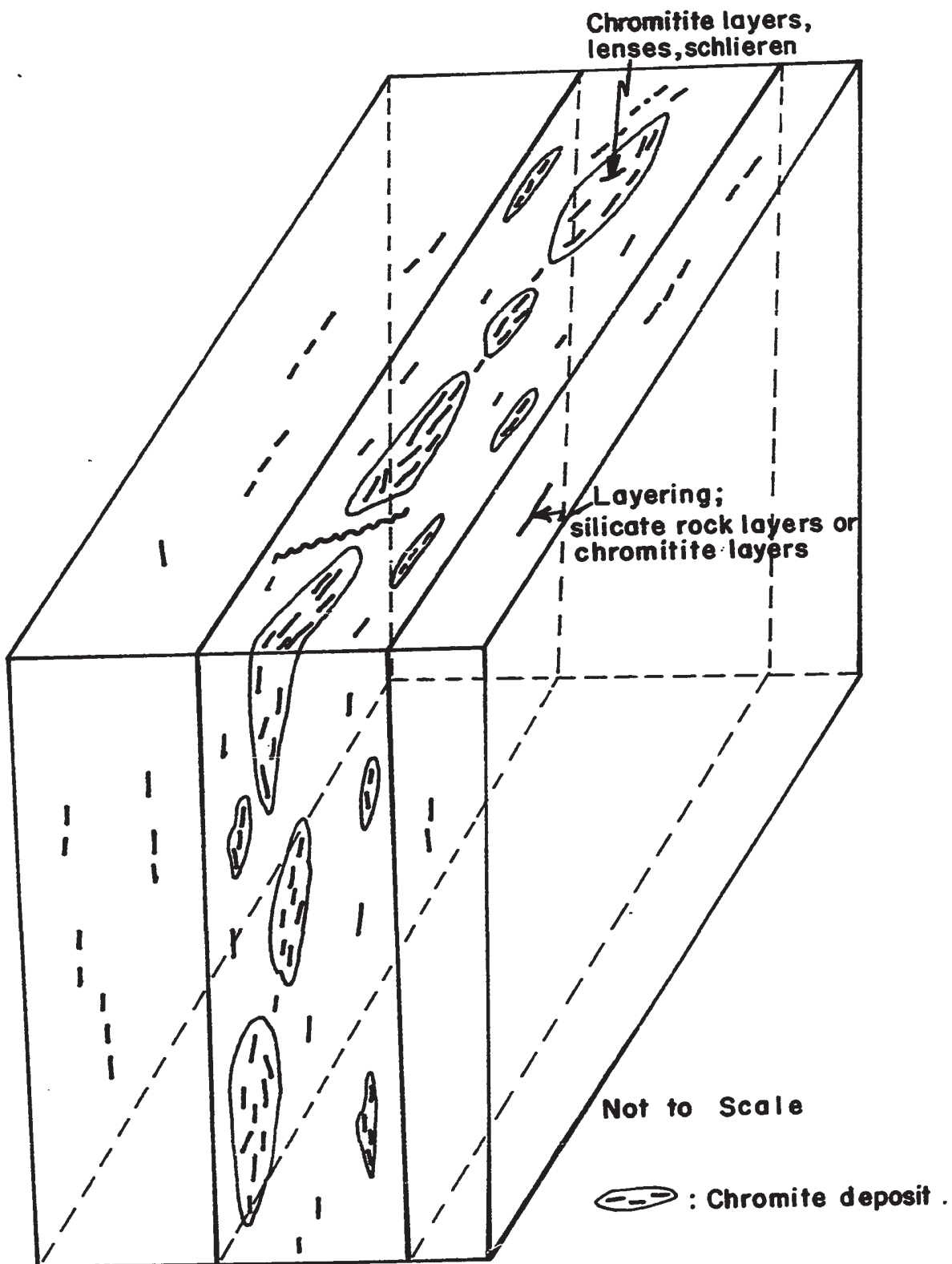


Figure 87. Vertical and plane view of a hypothetical ore zone showing the inferred (see text) distribution pattern of chromite deposits.

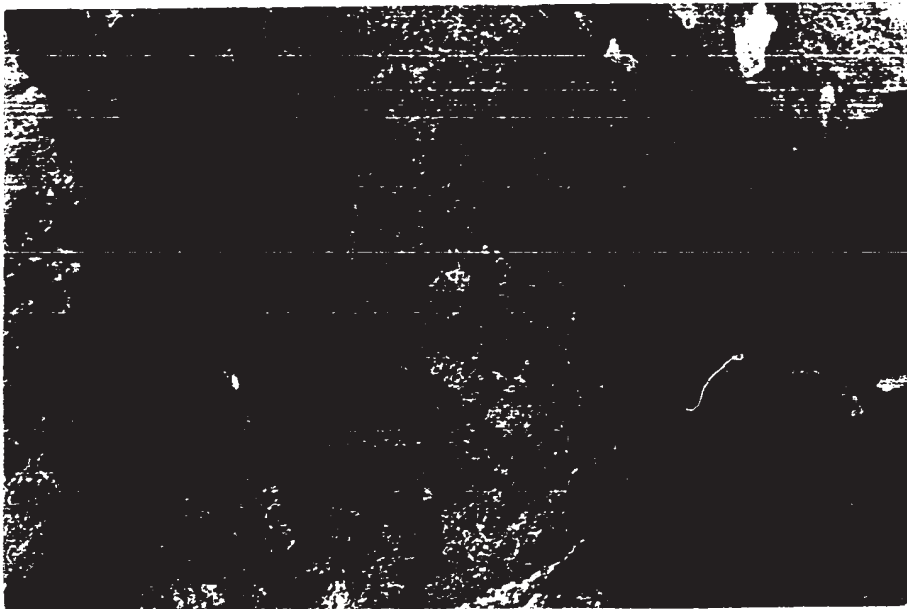


Figure 88. Folded chromitite layers.
(American Chrome Company's Pits, south of Morin Hill)

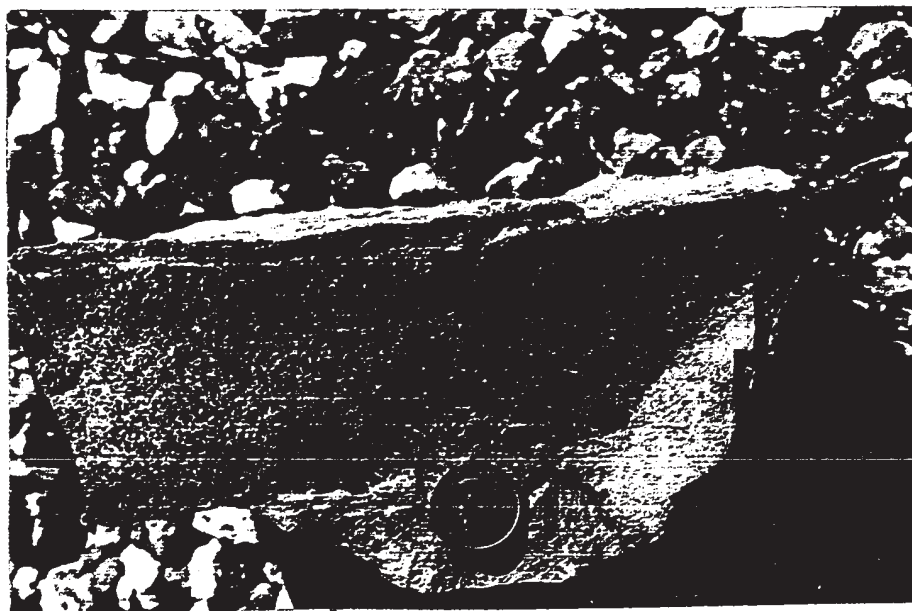


Figure 89. Faulted chromitite layer (right end of the sample).
(Same location as figure 88)

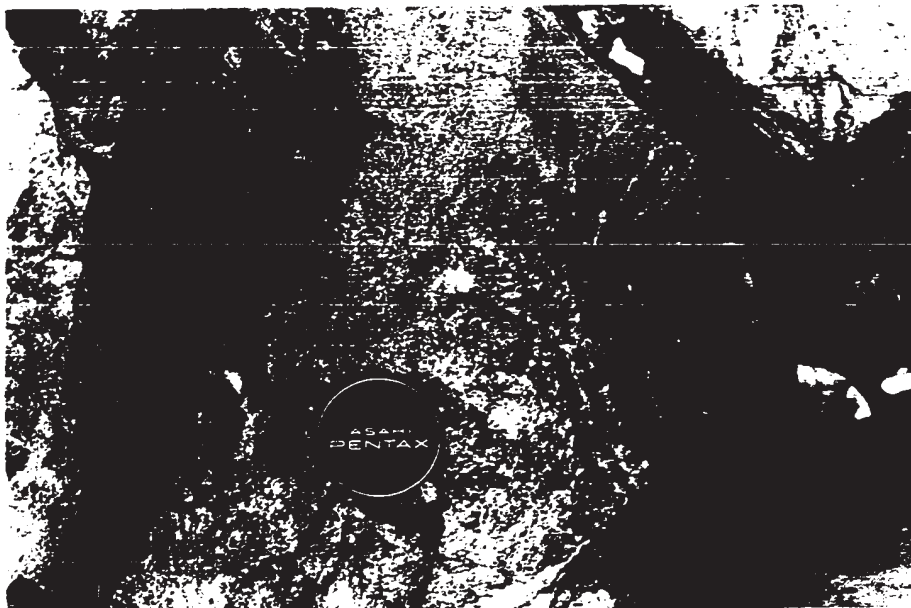


Figure 88. Folded chromitite layers.
(American Chrome Company's Pits, south of Morin Hill)

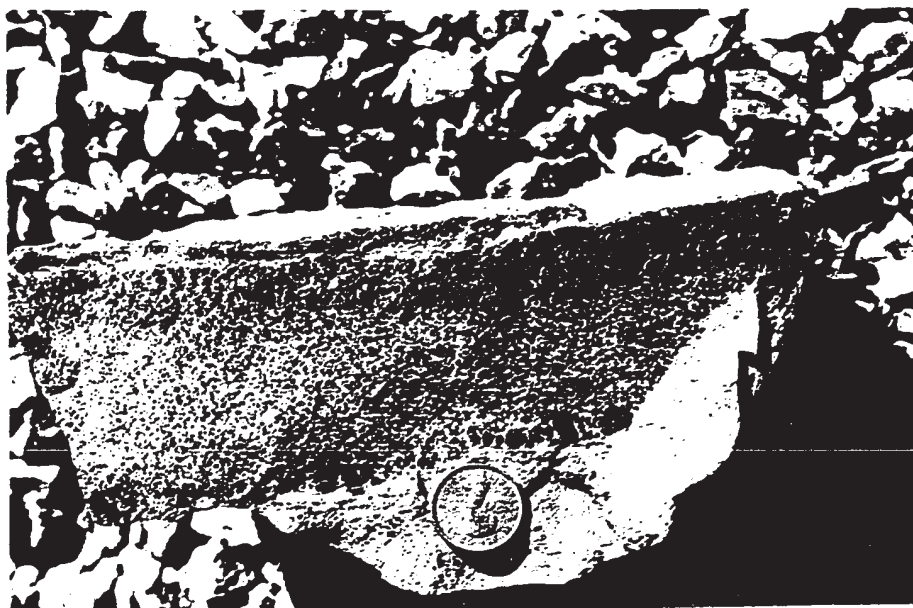


Figure 89. Faulted chromitite layer (right end of the sample).
(Same location as figure 88)

is thought to be conditioned by one or several of such factors as in situ growth and mutual interference, magmatic corrosion, possible recrystallization, secondary alteration, corrosion and fracturing.

In chromitite with "chain structure", chromite crystals surrounding olivine are in contact with each other. This is thought to be the result of in situ growth of chromite crystals. In massive chromitite the chromite crystals are densely packed and individual crystals can hardly be distinguished. This densely packed chromitite is also presumably formed by in situ growth and filling of all the interstitial space. Mutual interference between chromite crystals during growth is largely responsible for the anhedral shape of the crystals in most of the chromitite.

Chromite is commonly fractured. The amount of fracturing increases with increasing concentration of the chromite. Fracturing is mostly irregular (Figs. 90 and 91), but in some grains somewhat rectilinear fractures and en-échelon fractures have been observed. Mortar texture (Fig. 90) is very common. Fractures are usually filled with serpentine, magnetite and rarely with sulfides.

In transmitted light, an opaque variety of chromite has been observed in many chromite grains. In reflected light, there is no difference between opaque and the more common translucent chromites. The opaque chromite occurs mostly along fractures in the translucent chromite. Locally, very fine-scale mixing of the two varieties is observed. Dresser (1913, p. 76-80), in discussing the mineralogy of Quebec chromite, also distinguished these two varieties. He found the opaque chromite to be magnetic in contrast to the non-magnetic translucent chromite. His

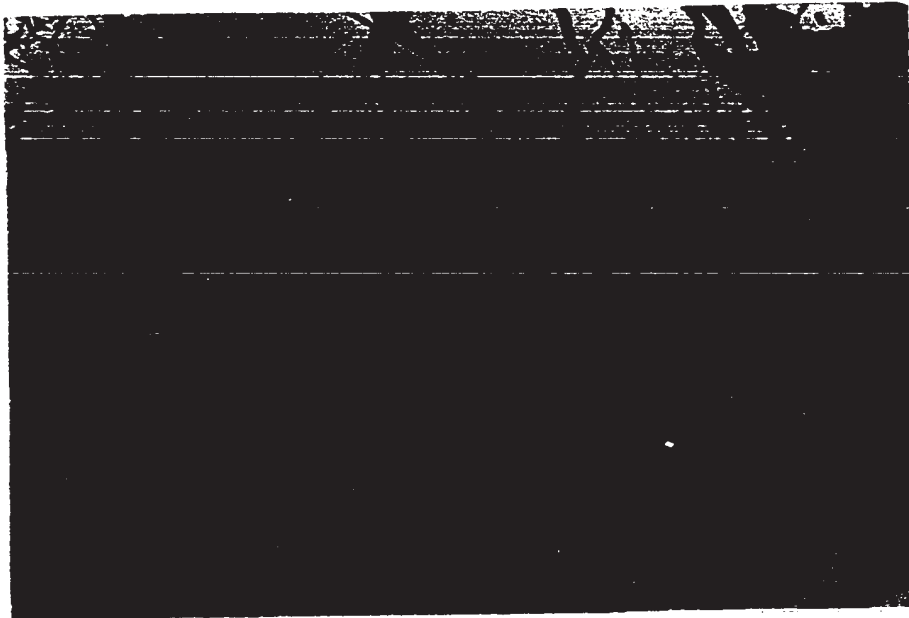


Figure 90. Photomicrograph: Mortar texture of fractured chromite (small grains) between two moderately fractured chromite grains. The fractures are filled with serpentine.
Chromitite
Reflected light, X 50

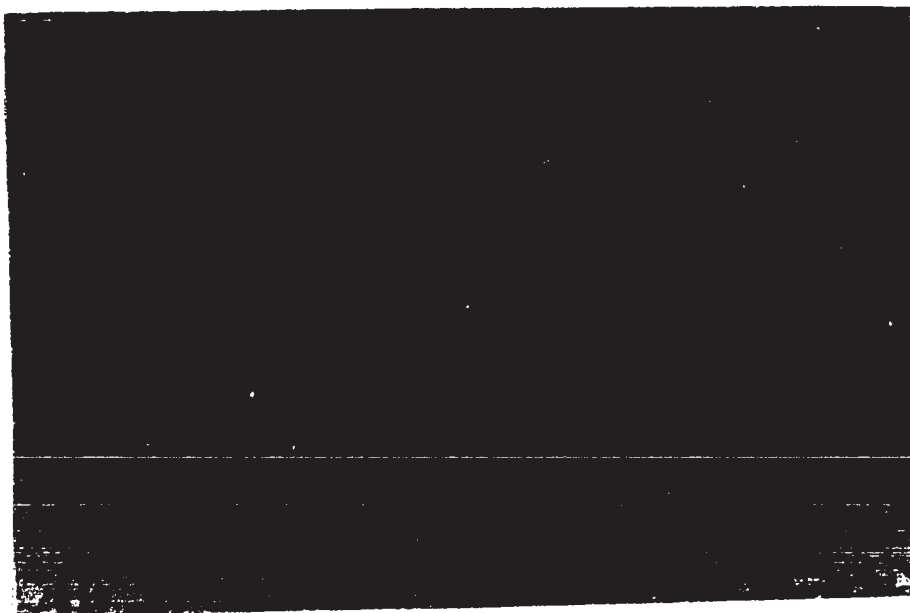


Figure 91. Photomicrograph: Irregular fracturing of chromite.
Chromitite, Sample No. 98
Reflected light, X 50

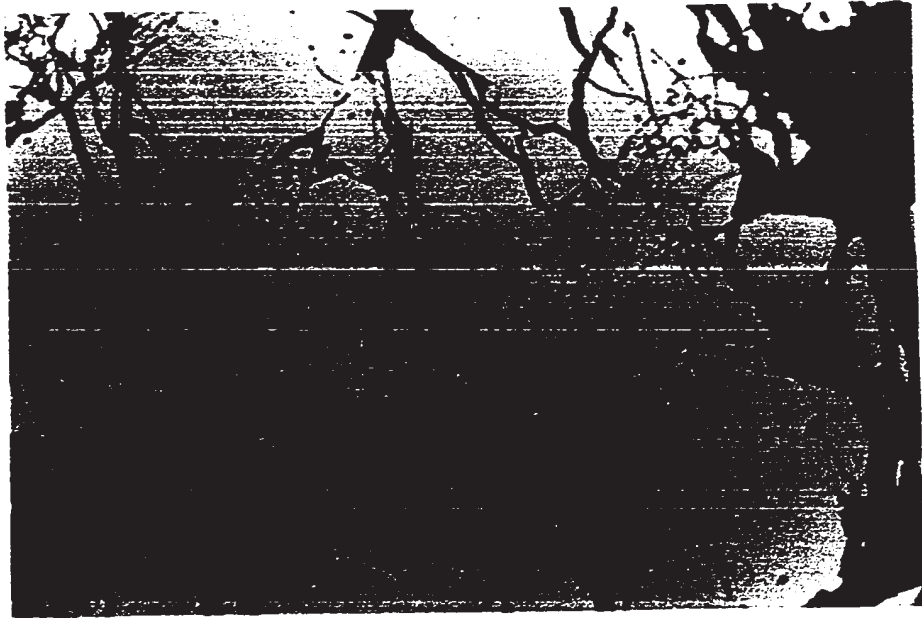


Figure 90. Photomicrograph: Mortar texture of fractured chromite (small grains) between two moderately fractured chromite grains. The fractures are filled with serpentine.
Chromitite
Reflected light, X 50



Figure 91. Photomicrograph: Irregular fracturing of chromite.
Chromitite, Sample No. 98
Reflected light, X 50

analyses showed the opaque chromite to be richer in total Fe, Ch and Al and poorer in Mg than the translucent chromite. He concluded:

"In some sections the relative position of the translucent and opaque are such as to suggest that the opaque might be an altered form of the other, but in others both appear primary. Therefore, it seems more probable that they are intergrowths ..."

Poitevin (1930) refers to opaque chromite as "oxidized chromite" and indicates the presence of picotite in the chromite ores of the map-area.

Several electron microprobe analyses and scans failed to show a consistent difference in composition between the opaque and the translucent chromite in the same grain. In the majority of cases, the opaque chromite was found to be higher in total Fe and Al and lower in Mg and Cr. However, there are several exceptions. Ferric iron values have been calculated for opaque and translucent portions of several grains. The values obtained also failed to indicate any consistent difference between the two varieties.

The opaque chromite occurs mostly with serpentine and secondary magnetite along fractures in the translucent chromite and replaces this latter from the fractures outward. Based on this texture, the opaque chromite is not a primary phase and is considered to be an oxidized form of the translucent chromite. Presumably a certain amount of ferrous iron has been oxidized to the ferric state. Oxidation most probably occurred during the serpentization.

Secondary alteration and dissolution of some chromite during the serpentization is evident. A multitude of serpentine inclusions along fractures in chromite have been observed indicating dissolution of chromite during the serpentization (see Chapter VII). Secondary magnetite commonly rims chromite grains. The replacement of chromite by secondary magnetite appears to be usually nil or negligible, but in

some instances a significant portion of the chromite has been replaced by magnetite (Fig. 92). Extensive replacement occurs at the contacts of "acidic" rocks and in serpentinite. Uvarovite replacing chromite (Fig. 93) has been observed in several localities and is very common in the chromitite from the Montreal pit.

Olivine inclusions in chromite

The chromite in chromitite commonly contains olivine inclusions. These are usually less than 0.1 mm in size and are commonly euhedral or subhedral (Figs. 94 and 95). In several instances, a single chromite crystal contains several dozen serpentized olivine inclusions. The inclusions are generally restricted to the central part of a chromite crystal which has either rounded or roughly rectangular outlines. The inclusions can be either randomly oriented or, more rarely, roughly aligned. No difference in composition has been detected between the chromite of the inclusion-rich centre and the rim. This type of inclusion-rich chromite occurs in chromitite with "chain structure" and in chromitite veins. The author can suggest only two possible explanations for this inclusion-rich chromite:

- (1) The olivine and chromite were crystallizing together and, because of the physico-chemical conditions of the magma, olivine nuclei were much more abundant than chromite nuclei. The chromite growing around the few nuclei enclosed the olivine crystals crystallizing nearby. The inclusion-free marginal zone of the chromite crystals could be due to in situ growth or to the growth of chromite at a time when no new olivine was crystallizing.

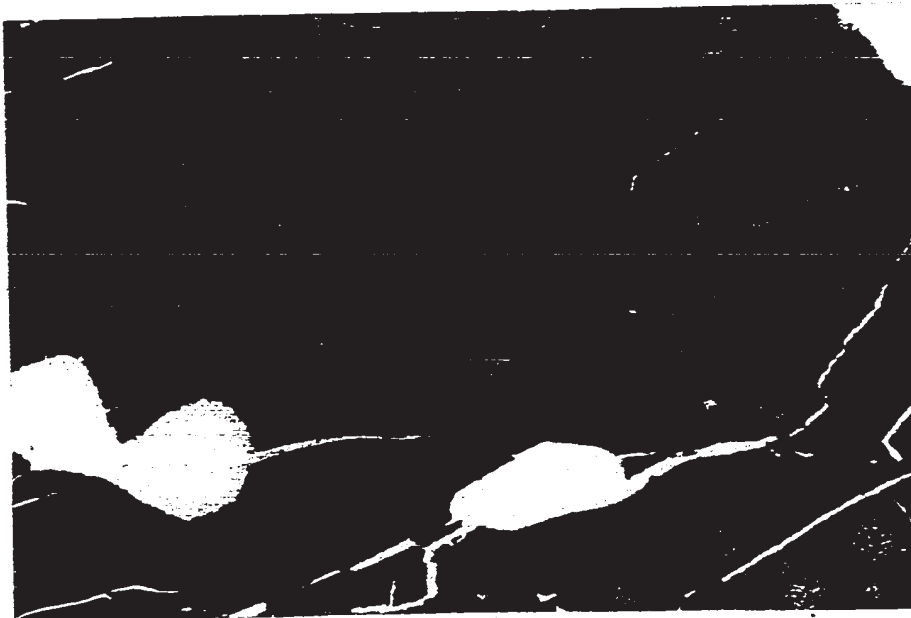


Figure 92. Photomicrograph: Magnetite (black) replacing chromite (grey). Chromitite, Sample M-4
Plane polarized light, X 40

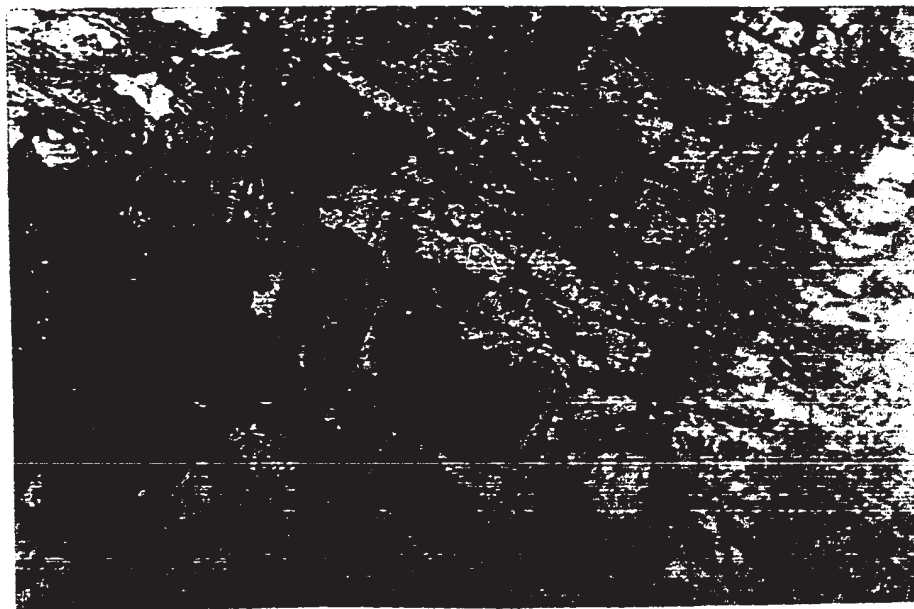


Figure 93. Photomicrograph: Corrosion and replacement of chromite (black) by uvarovite (white). Uvarovite has been observed in several localities but is not common. Chromitite, Sample No. 228-3
Plane polarized light, X 40

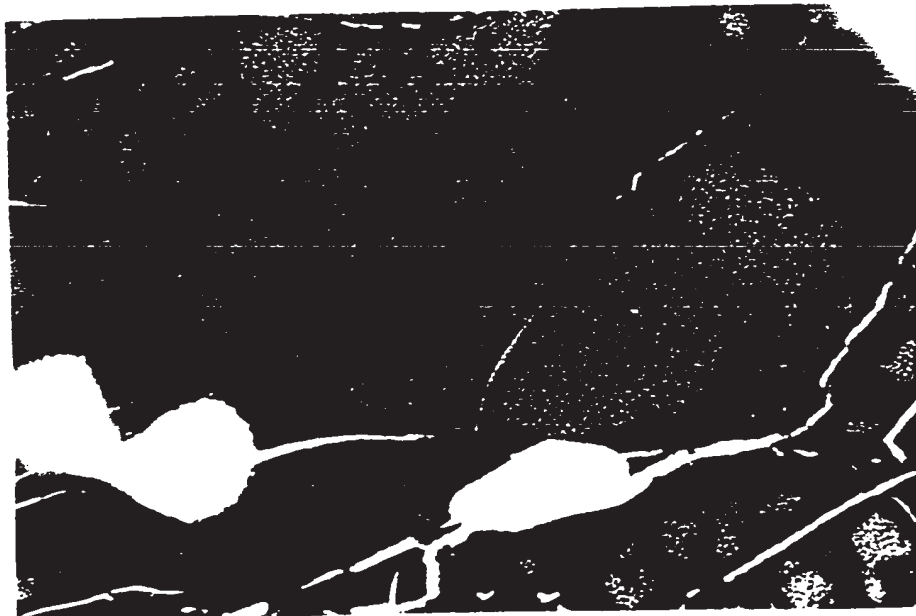


Figure 92. Photomicrograph: Magnetite (black) replacing chromite (grey). Chromitite, Sample M-4
Plane polarized light, X 40

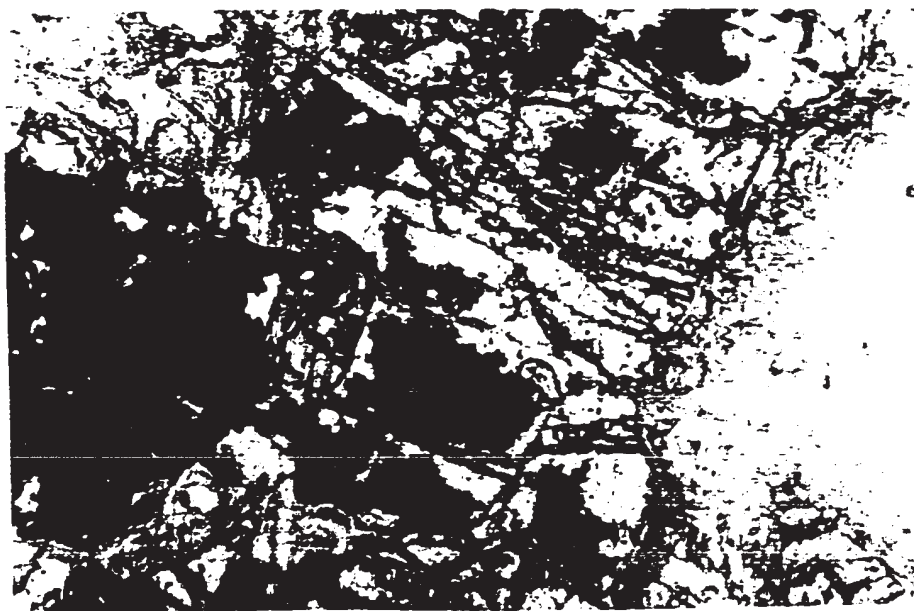


Figure 93. Photomicrograph: Corrosion and replacement of chromite (black) by uvarovite (white). Uvarovite has been observed in several localities but is not common. Chromitite, Sample No. 228-3
Plane polarized light, X 40

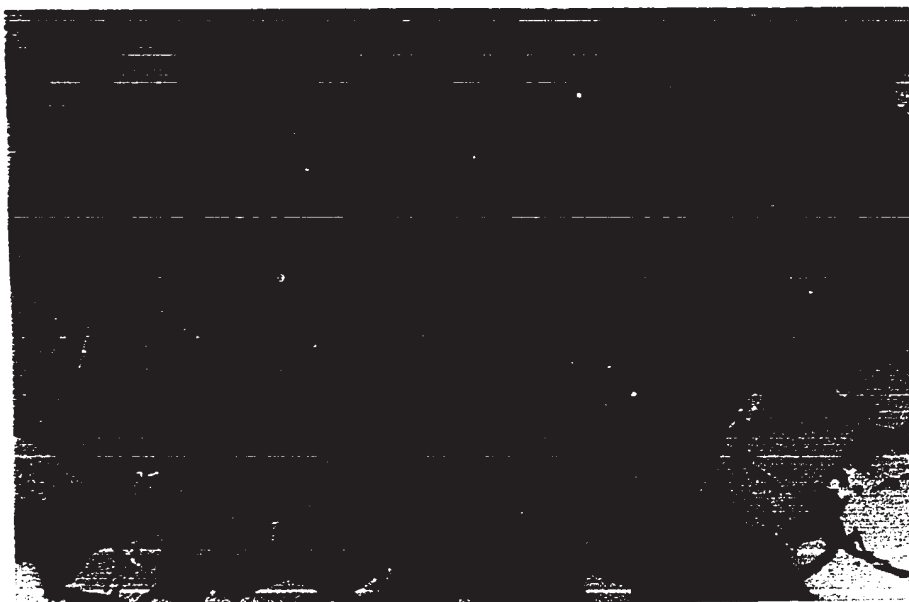


Figure 94. Photomicrograph: Olivine inclusions (grey) in chromite (white). Note the inclusion-free marginal zone and the rounded outline of the inclusion-rich central part. Chromitite. Sample No. 178
Reflected light, X 50



Figure 95. Photomicrograph: Olivine inclusions (grey) in chromite. Note the inclusion-free margin of the chromite and the rounded outline of the inclusion-rich region. The olivine inclusions are euhedral or subhedral and are serpentinized. Chromitite. Sample No. 178
Reflected light, X 150

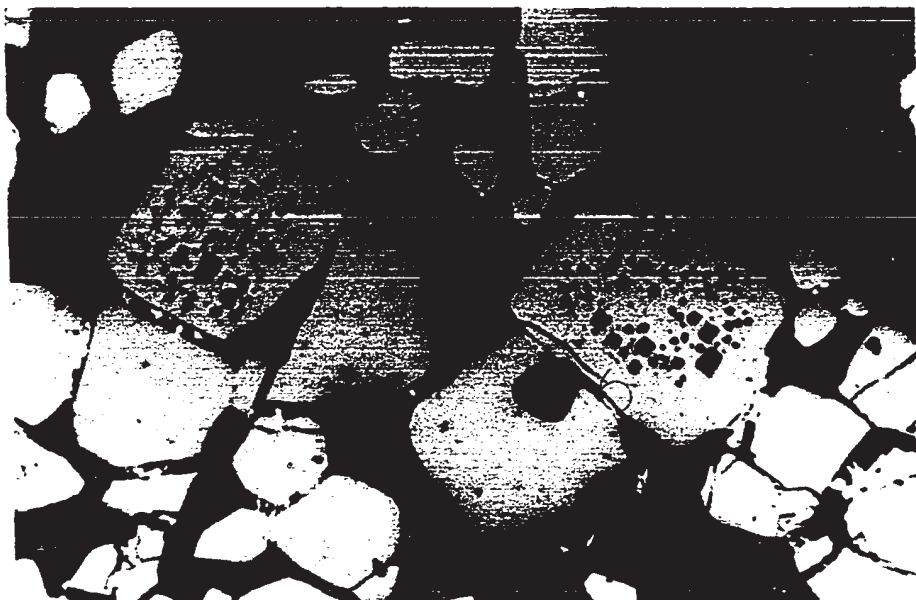


Figure 94. Photomicrograph: Olivine inclusions (grey) in chromite (white). Note the inclusion-free marginal zone and the rounded outline of the inclusion-rich central part. Chromitite. Sample No. 178
Reflected light, X 50

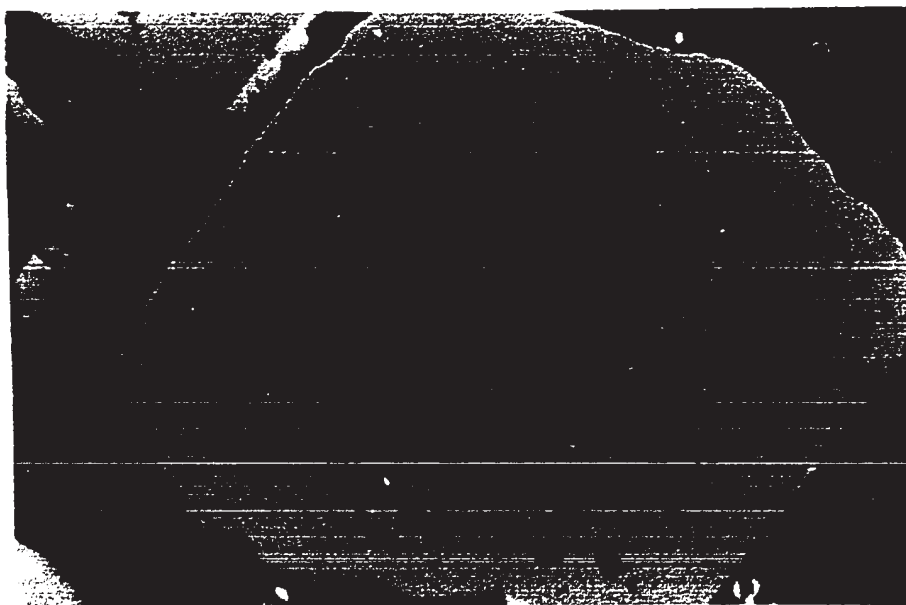


Figure 95. Photomicrograph: Olivine inclusions (grey) in chromite. Note the inclusion-free margin of the chromite and the rounded outline of the inclusion-rich region. The olivine inclusions are euhedral or subhedral and are serpentinized. Chromitite. Sample No. 178
Reflected light, X 150

- (2) The inclusion-rich central part represents an immiscible chromite-rich liquid from which olivine crystals and chromite surrounding them have crystallized upon cooling. This would explain the tendency of certain inclusions to be aligned along what might be crystallographic planes of least resistance to the growth of olivine and would also explain the rounded shape of the inclusion-rich part. The inclusion-free marginal zone could be due to in situ growth of the chromite crystal.

It is of interest that olivine inclusions surrounded by a considerable thickness of apparently unfractured chromite are always totally serpentinized. There appear to be two possible explanations:

- (1) The serpentinization is later than the formation of chromite. In the apparent absence of fractures, any migration of water and other material (Si and/or Mg depending on the process of serpentinization) must have gone on through the chromite structure. Furthermore, if this is the case, the absence of fractures also points to the lack of volume increase accompanying the serpentinization of olivine.
- (2) The olivine inclusions were already converted to serpentine at the time they were incorporated into the chromite.

The first of the above alternatives is very unlikely. In view of the tightly packed structure of chromite, transport of water and other material through it appears impossible. It is therefore proposed that the second alternative is more likely. This implies that the inclusion-rich chromite formed at low temperature ($<600^{\circ}\text{C}$) within the stability range of serpentine and that serpentine has been formed contemporan-

ously with or earlier than the chromite.

The possibility of low-temperature crystallization of olivine and chromite has been suggested by some workers. Bowen and Tuttle (1949, p. 442) demonstrated that olivine can crystallize at temperatures as low as 500°C from a mixture of powdered Mg and Si in the presence of water vapor. Further, Sampson (1929 and 1931) proposed a solution-deposited origin for chromite in conglomerates near Selukwe deposit, Southern Rhodesia, while Varma (1964) proposed a hydrothermal origin for the chromite deposits of Keonjhar district, Orissa, India. Therefore, the formation of chromite at low temperatures in a hydrous environment appears to be a possible alternative to its having been formed at an early magmatic stage.

However, several lines of evidence do not support a low-temperature origin for the chromite in the map-area. For instance, inclusion-rich chromite occurs in chromitite veins and in chromitite with "chain structure", and there is no difference in composition between these types and the chromite of other types of chromitite in the map-area. By analogy with the Stillwater Complex, chromitite with "chain structure" is probably formed by gravity settling. Furthermore, available evidence presented later (see Chapter VII) indicates that, in general, no free water was available during the crystallization of the ultramafic rocks and they have crystallized in a dry state. However, this last objection to low-temperature crystallization of chromite can be overcome in that the water need not necessarily be derived from the ultramafic mass but could be external.

To summarize, in view of the conflicting data indicated above, the

genesis of inclusion-rich chromite remains a problem. A low-temperature crystallization of inclusion-rich chromite in a hydrous environment is favoured, mainly because the present author is not aware of any other likely alternative. However, some evidence contradicts such an origin.

VI.6. CHEMISTRY

Chromitite is richer in Ti, V and Mn than the other ultramafic rocks of the map-area (Table IV, p. 48). The mean composition of chromite in 28 chromitite samples is listed in Table VIII. All chromite analyses have been done with electron microprobe analyser. The data on analytical procedure, accuracy and precision and the detail of analyses are given in Appendix III.

The chromite in chromitite shows a zoning similar to, but less well developed than, that in accessory chromite. It is usually richer in Mg (Fig. 65, p. 119.) and poorer in Fe (Fig. 64, p. 118) than the accessory chromite in the adjacent dunite. This difference in composition is most likely due to equilibration of olivine with coexisting chromite as suggested by Irvine (1966, p. 84-85). He suggested that the distribution coefficient $(\text{Mg}/\text{Fe}^{+2})_{\text{silicate}} \times (\text{Fe}^{+2}/\text{Mg})_{\text{spinel}}$ increases with falling temperature. Where chromite is a minor constituent, it will become appreciably richer in ferrous iron as the rock cools, while silicate minerals remain relatively constant in composition. When the silicate is a minor constituent, it should become appreciably more magnesian. The influence of the degree of concentration on the composition of chromite is illustrated by Figure 96 which presents the results of analyses of samples collected transverse to the well-developed layering of the Bélanger pit. The chromite in chromitite is noticeably richer in Cr and

TABLE VIII

Mean composition¹ of chromite in chromitite
Microprobe Analyses

A) Chromitite within dunite bodies in peridotite

Sample No.	Cations wt.%						
	Cr	Fe tot.	Fe ⁺²	Fe ⁺³	Mg	Al	Ti
N-8	40.84	11.83	10.88	0.95	7.70	5.91	0.06
82	40.68	16.10	15.48	0.62	6.17	7.23	0.08
86	34.71	17.86	13.21	4.65	6.32	6.43	-
90	40.20	14.95	11.93	3.02	7.26	5.29	-
92	38.87	14.60	10.79	3.81	7.87	5.84	0.10
343	40.10	12.38	11.26	1.12	7.91	6.22	0.08
350	40.61	14.50	11.25	3.25	7.49	4.81	0.04
351	38.53	12.89	11.28	1.61	7.49	6.69	0.09
364	38.37	12.88	9.02	3.86	8.77	6.41	0.06

B) Chromitite in dunite zones

Sample No.	Cations wt.%						
	Cr	Fe tot.	Fe ⁺²	Fe ⁺³	Mg	Al	Ti
G-1	37.46	11.81	7.83	3.98	9.53	7.32	0.09
M-2	34.06	12.52	9.83	2.69	8.80	10.00	0.13
M-5	33.90	14.14	10.62	3.25	8.34	9.57	0.16
6	39.40	14.89	8.00	6.89	9.64	5.29	0.11
44	39.32	12.17	9.99	2.18	8.34	6.60	0.10
45	36.88	13.96	9.93	4.03	7.82	5.77	0.07
46	40.39	10.92	9.02	1.90	8.65	6.01	0.14
98	40.68	12.33	10.09	2.24	8.17	5.16	-
104	39.90	14.46	7.52	6.94	10.11	5.56	0.09
111	38.61	15.62	12.88	2.74	6.50	5.41	0.09
114	34.11	12.76	11.36	1.40	8.14	10.32	0.07
121	38.48	13.36	9.27	4.09	8.88	6.64	0.02
180	35.92	12.99	9.46	3.53	8.88	8.47	0.07
144-1	38.54	14.56	11.54	3.02	7.63	6.55	0.14
178	39.68	16.66	12.68	3.98	6.49	4.01	0.09
178-1	40.45	16.38	12.01	4.37	7.34	4.74	0.15
179	37.78	17.41	13.71	3.70	6.55	6.34	0.17
400	38.16	17.02	12.99	4.03	6.83	5.88	0.07
515	34.98	16.60	11.00	5.60	8.13	7.74	-
518	38.41	16.38	13.13	3.25	7.70	6.00	0.11

Fe⁺² and Fe⁺³ have been calculated from total iron values.

¹ The analytical procedure, calculation of mean composition, the precision, accuracy and detail of analyses are indicated in Appendix III. Locations of samples are shown on Map 2.

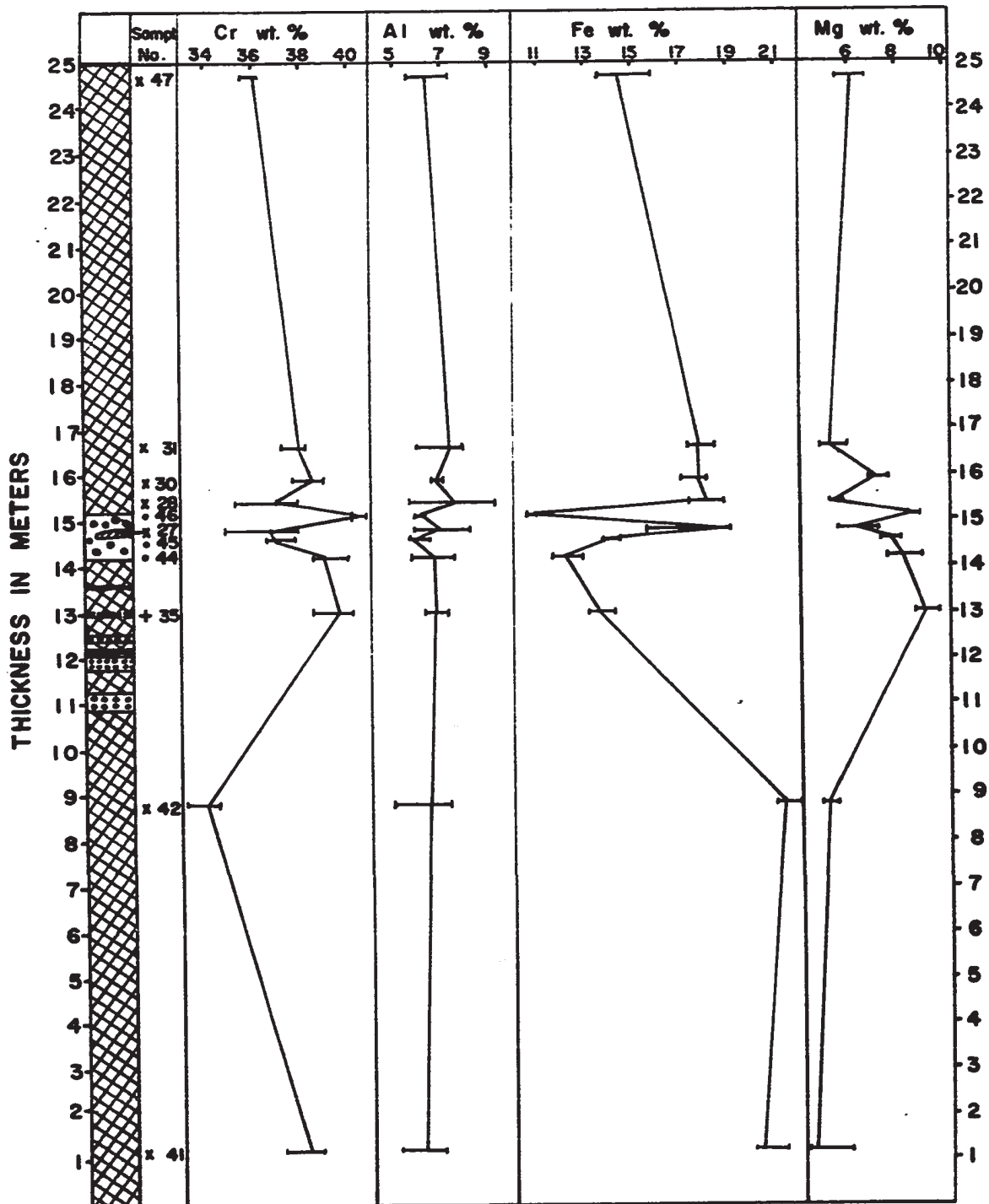


Figure 96. Composition of chromite in Bélanger pit
 Explanation

- | | |
|--|--|
| <ul style="list-style-type: none">  Dunite  Massive chromitite  Chromitite with low chromite content | <ul style="list-style-type: none"> X Accessory chromite • Massive chromitite + Chromitite with low chromite content |
|--|--|

Mg and poorer in Fe than the accessory chromite, while the Al content changes very little. No regular variation, which could be interpreted as cryptic layering, can be seen across the deposit.

Iron and Mg as well as Cr and Al content of chromite vary antipathetically (Figs. 97 and 98). There is no relation between Fe_{total} or Mg contents and the Cr content of chromite. The Cr content is highest in chromite from chromitite and lowest in some accessory chromite in peridotite (Fig. 98). The calculated ferric iron content shows considerable variation (Table VIII) even in chromite from the same deposit. Some of this spread is, however, partly due to analytical errors and perhaps to the incorrectness of the assumption that chromite is stoichiometric. However, some of the ferric iron variation is probably real. Only a very small amount of ferric iron can be accommodated in the olivine and pyroxene structures, and chromite is the only primary mineral able to accept large amounts of ferric iron. Therefore, slight variation in the ferric iron content of the magma would have been greatly magnified in the chromite.

In the Southern Dunite Zone, chromite in chromitite samples from deposits occurring near the Olivine Pyroxenite Zone (M-2, M-5, 178, 178-1, 179, 400, 515) are slightly richer in Al and/or Fe and correspondingly poorer in Mg and/or Cr (Table VIII). This is consistent with a differentiation trend from dunite to "herzolite" and "olivine" pyroxenite.

VI.7. DISCUSSION AND CONCLUSION

The texture of chromitite points to a large amount of in situ growth. The coarse grain size of chromitite in the map-area is unlike the much finer grain size of chromitite from stratiform complexes.

Comparison of composition of chromite in chromitite from the map-

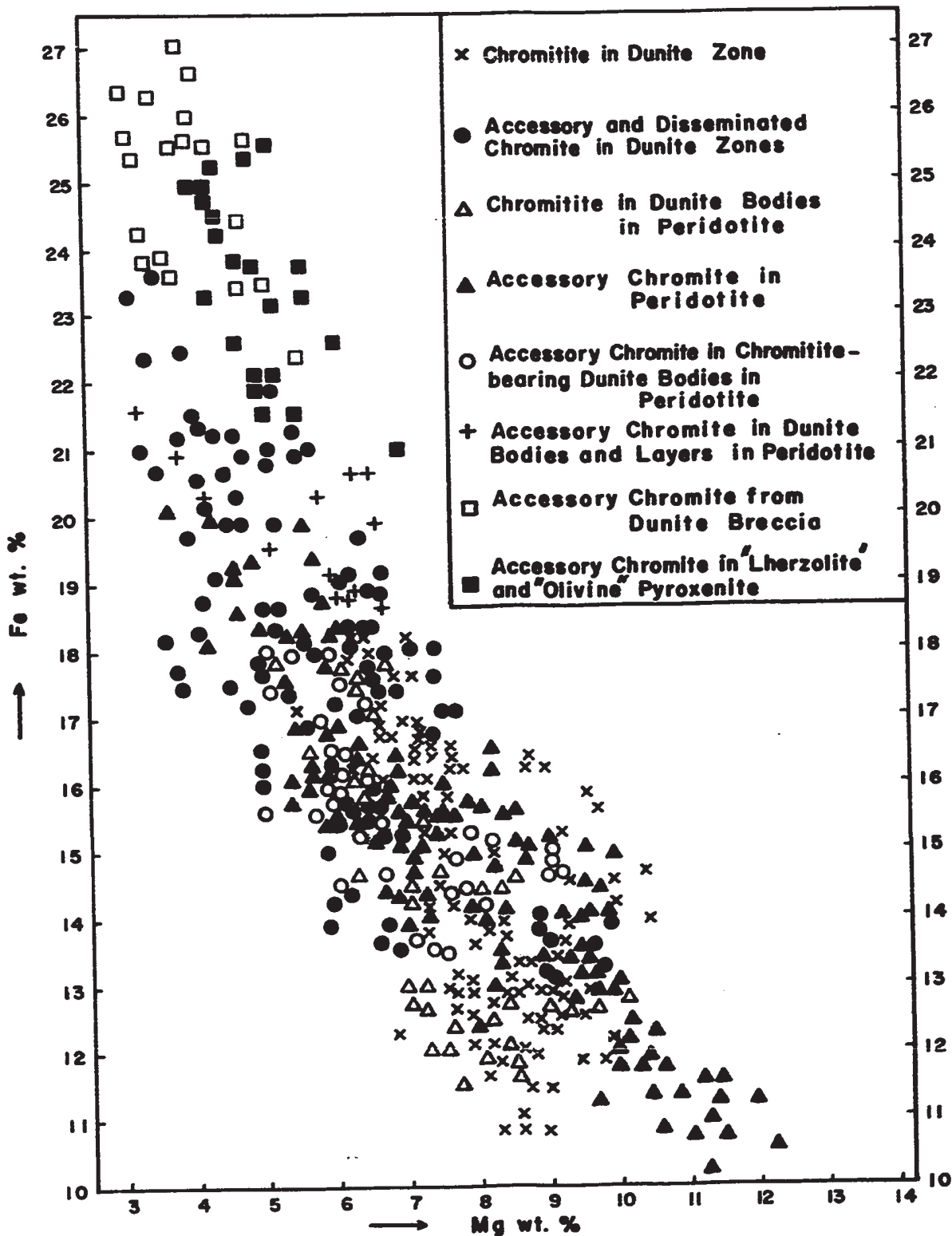


Figure 97. Total iron versus magnesium variation in chromite

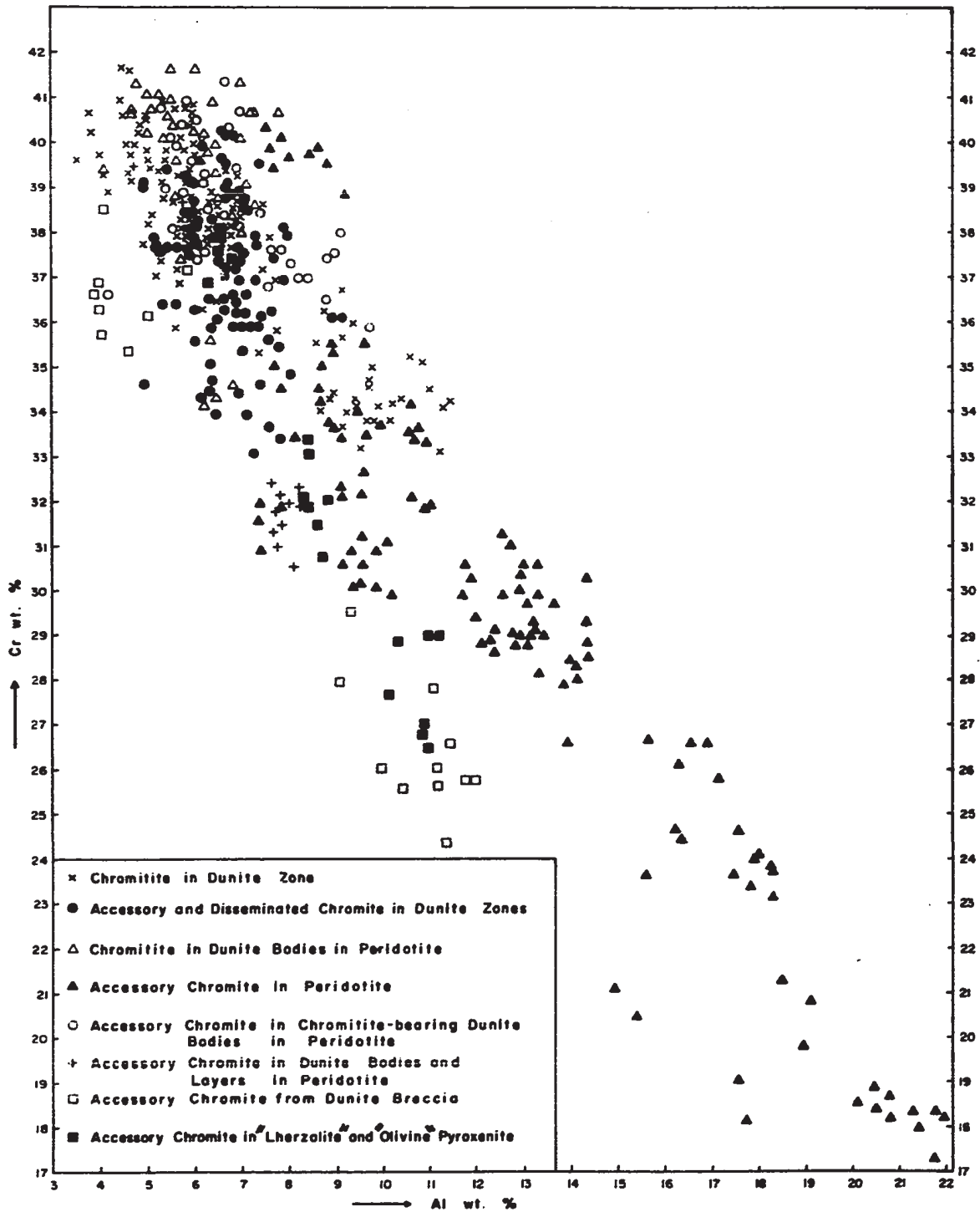


Figure 98. Chromium versus aluminum variation in chromite

area with chromitite compositions listed by Stevens (1944) and Thayer (1965) from stratiform complexes indicate that chromite from the map-area contains similar amounts of Mn and considerably less Ti than chromitite from stratiform complexes, except for some chromitite of the Great Dyke, Southern Rhodesia. The chromite from the map-area is higher in Cr and Mg and usually lower in total Fe and Fe^{+3} than that in major stratiform complexes, the Great Dyke being again an exception (Fig. 99 A and B). The Al content overlaps that in stratiform complexes. The low Fe^{+3} content of chromite is thought to indicate that chromitite in the map-area has crystallized in a relatively low oxygen fugacity environment.

In the chromite from the map-area a decrease in the Cr content is compensated mainly by an increase in the Al content rather than in the Fe content. In chromites from stratiform complexes the decreasing Cr content is compensated mainly by increasing Fe_{total} (Thayer, 1970). This difference is either due to the relatively Fe-poor nature of the magma from which chromite in the map-area has crystallized and/or to crystallization of the chromite under higher pressures than those prevailing during the formation of stratiform complexes. It is probable that pressure increase favors preferential incorporation of Al in the chromite structure at the expense of plagioclase.

In Figs. 100 and 101 the composition of chromite in chromitite from the map-area is compared with chromitite compositions from alpine-type ultramafic rocks elsewhere and from the Vourinos Complex, Greece, which, has been described as an autochthonous ophiolite complex (Maratos, 1964 and Moores, 1969). Although the Zhob Valley Complex is a high-temperature ultramafic-mafic intrusion emplaced into metasedimentary rocks, it is nevertheless an alpine-type intrusion (Bilgrami, 1963). Only

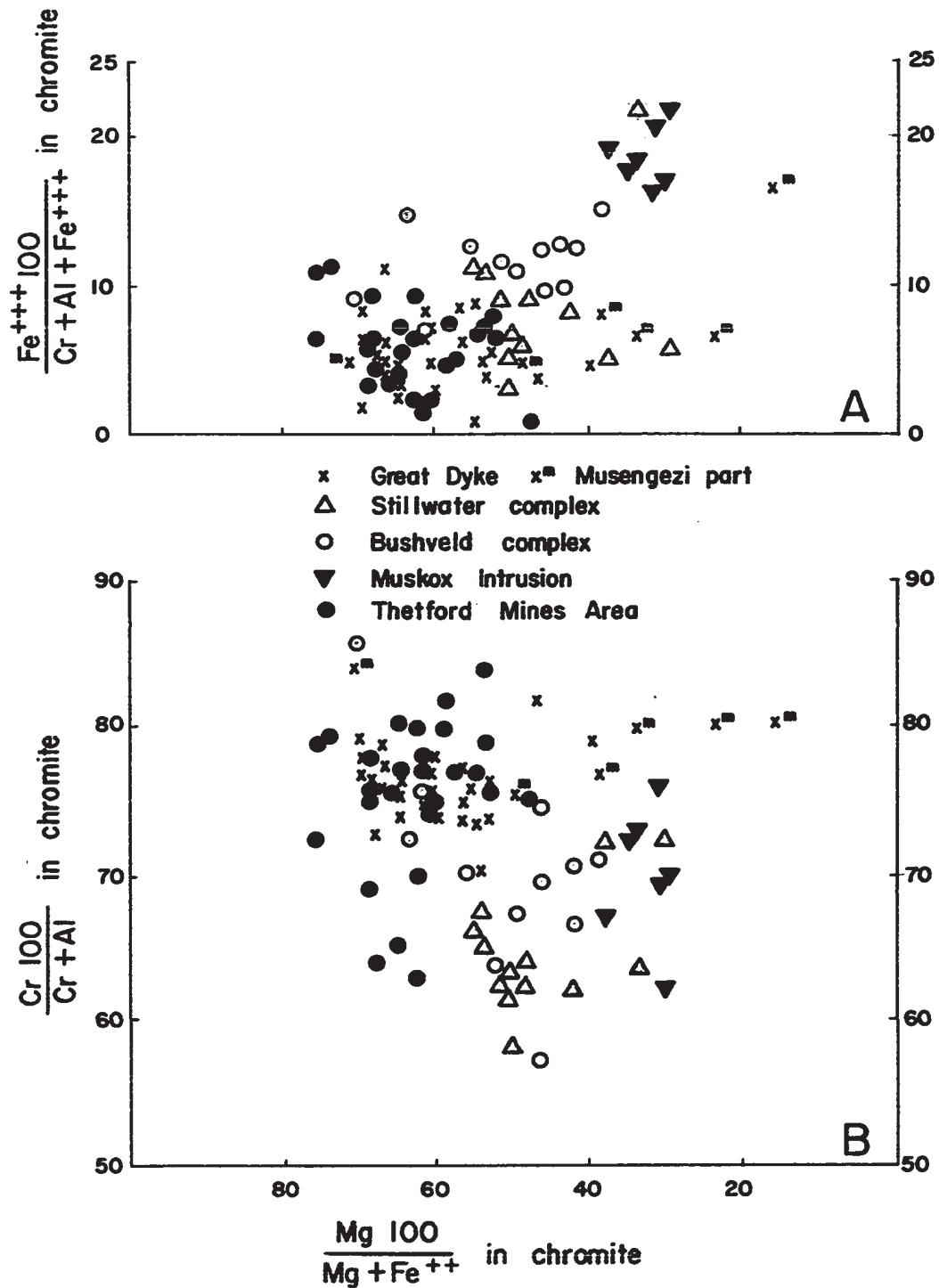


Figure 99. Plots of mean composition of chromite in chromitite from the map-area and analyses of chromite in "chromite seams" in four major stratiform complexes, the Bushveld, Great Dyke, Stillwater, and Muskox intrusions. Plots of chromite analyses of stratiform complexes have been reproduced from Irvine (1966, Fig. 5, p. 80).

- Chromitite from Grant County, Oregon (Stevens, 1944)
- * Chromitite from alpine-type ultramafic rocks of Maryland and Pennsylvania (Pearre and Heyl, 1960)
- Fethiye-Marmaris Complex, Turkey (der Kaaden, 1971)
- Zambales Complex, Philippines (Stoll, 1958)
- ▲ Bay of Islands Complex, Canada (Smith, 1958)
- △ Zhob Valley Complex, W. Pakistan (Bilgrami, 1963)
- + Chromitite in alpine-type ultramafic rocks from Eldorado, Shasta and San Luis Obispo counties, California (Stevens, 1944)
- +s Twin Sisters, Washington (Stevens, 1944)
- ▽ Camagüey district, Oriente province, Cuba (Stevens, 1944 and Thayer, 1956)
- Vourinos Complex, Greece (Zachos, 1964)
- x Ultramafic rocks of the Thetford - Disraeli Area, Quebec

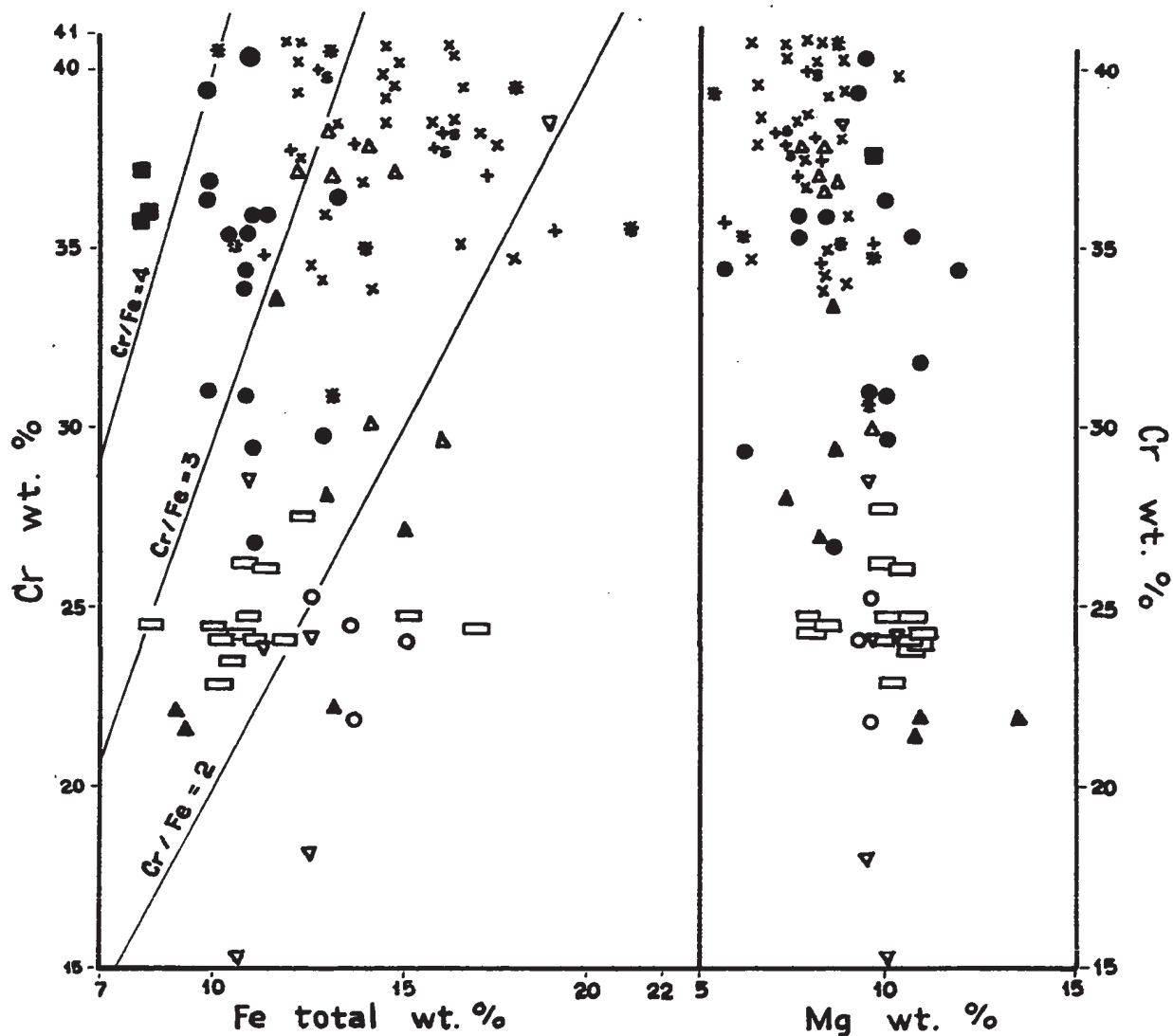


Figure 100. Plots of Cr versus Fe_{total} and Cr versus Mg in chromite of chromitite from the map-area, in chromite concentrates and massive chromitites from alpine-type ultramafic rocks elsewhere and from the Vourinos Ophiolitic Complex. The sources of the data are indicated in the legend above.

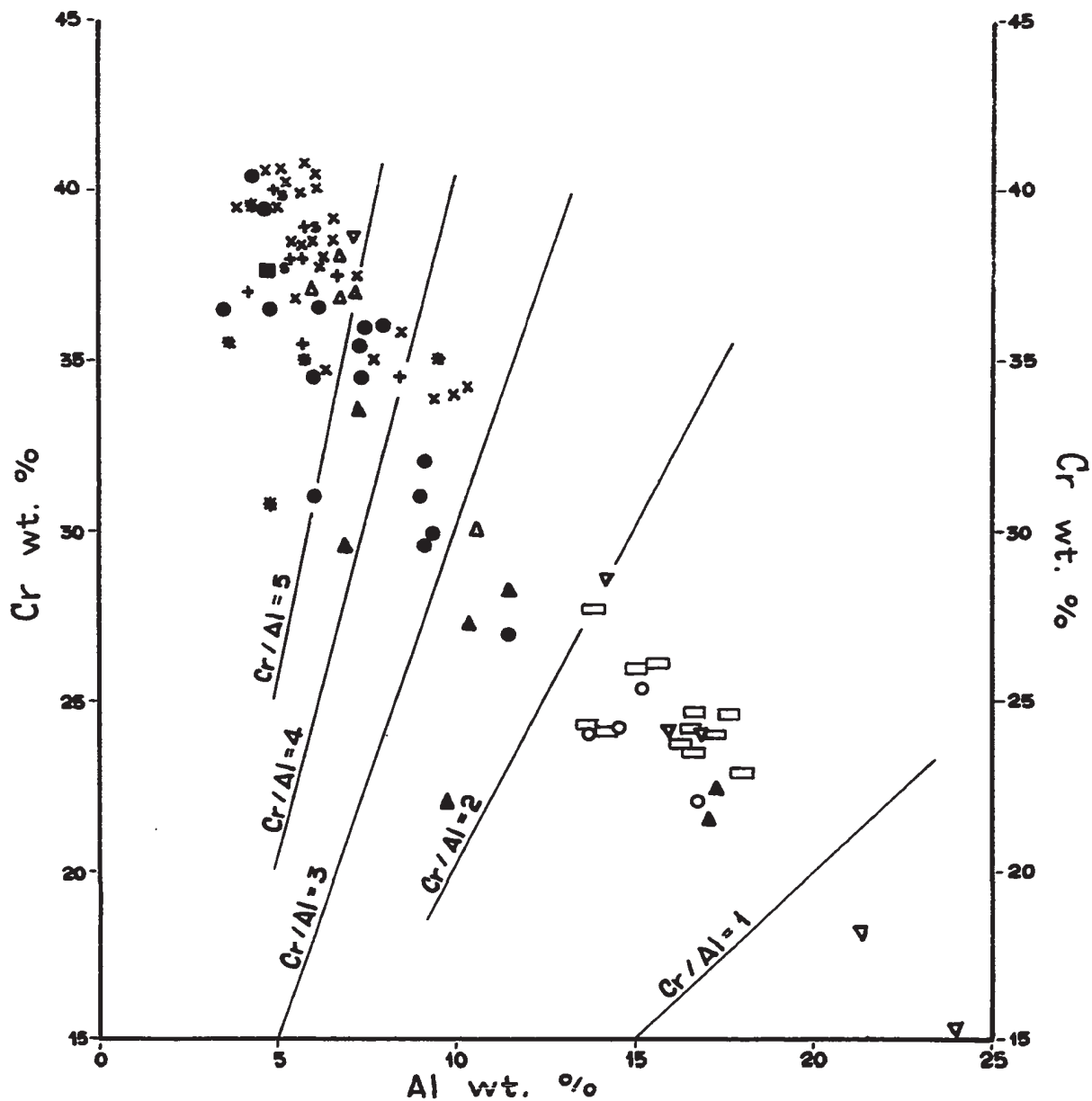


Figure 101. Chromium versus Al in chromite of chromitite from the map-area, in chromite concentrates and massive chromitites from alpine-type ultramafic rocks elsewhere and from the Vourinos Ophiolitic Complex. Same legend as for Fig. 100.

analyses of massive chromitite and "cleaned concentrates" of chromitite have been used in Figs. 100 and 101. Most of the plotted analyses contain less than 1% SiO_2 and all analyses containing more than 4% SiO_2 have been disregarded. Silica was not given in the analyses from the Vourinos Complex. In the plots of Figs. 100 and 101, the chromitite compositions have not been adjusted for Mg and Fe contained in silicate impurities present in the analysed samples.

It is notable that chromite from chromitite from any given locality and even from the same ultramafic body exhibits considerable compositional variation (Figs. 100 and 101) in contrast to olivines and orthopyroxenes which commonly do not vary much in composition (see Chapter V). Chromite in chromitite under study is similar in composition to chromites from California, from the Twin Sisters body, Washington, from the Zob Valley Complex, W. Pakistan, from the Fethiye-Marmaris Complex, Turkey, from Maryland and Pennsylvania. Analyses of chromite concentrates from the Vourinos Complex are singularly low in total Fe (Fig. 100). Whether or not this is significant is not known because of the incomplete nature of the analyses. The chromite in the chromitite from the map-area is slightly but noticeably poorer in Mg and richer in Fe, much richer in Cr and correspondingly poorer in Al than aluminous chromitites from Camagüey district, Cuba, the Zambales Complex, Philippines, the Bay of Islands Complex, Canada, and from Grant County, Oregon (Figs. 100 and 101).

The compositional difference between chromite from chromitites with high Cr content, like those of the map-area, and aluminous chromitites is consistent with the differences in their geological setting. Chromitite rich in Cr occurs in feldspar-free ultramafic rocks, whereas

aluminous chromitites from the areas mentioned above occur in, or near, feldspar-bearing rocks and ultramafic rocks grade into feldspathic rocks (e.g. gabbro, norite). For instance, in Camagüey district, the chromite deposits occur in, or close to, troctolite. Dumite grades into gabbro through troctolite and olivine gabbro, and gabbro is abundant (Thayer, 1942). In the Zambales Complex chromite deposits are in saxonite near its contact with olivine gabbro and ultramafic rocks grade into gabbroic rocks (Stoll, 1958). A similar situation is observed in the Bay of Islands Complex (Smith, 1958). In Grant County, Oregon, chromitite occurs in dumite within peridotite and this latter grades into gabbro through pyroxenite (Thayer, 1946).

The high Cr and low Al contents of the chromite in the chromitite from the map-area suggest that it has differentiated from a magma poor in Al. Furthermore, the low Al content of chromite in comparison with aluminous chromitites is consistent with the non-gradational contact relationship between the Ultramafic Suite and the Gabbroic Suite (Chapters III and IV) and it is also consistent with the separate intrusion of these two suites of rocks, as suggested earlier (Chapter IV). Further observation corroborating this latter point is that in the map-area there is no relation between the composition of chromite in chromitite and its distance from the gabbroic rocks.

CHAPTER VII

SERPENTINIZATION

VII.1. INTRODUCTION

Two types of serpentinization are distinguished. An early pervasive and quite homogeneous serpentinization that affects the whole mass of the rock and a late serpentinization which is more localised. These two types of serpentinization are best seen in the dunite and peridotite, particularly the latter. Graham (1944, p. 431) has summarized the distinction between the two types of alteration as recorded by the previous workers in this area:

" According to Harvie, not only is the degree of serpentinization uniform throughout the brown weathering core of individual blocks (joint blocks), but it is fairly constant from block to block over areas measured in hundreds of feet and thus appears to be independent of jointing. From this he concluded that the initial serpentinization of the block took place before the jointing. He found that serpentine of the core of the blocks is mesh antigorite and bastite On the other hand, the serpentine of the band of the blueish green rock adjacent to the joint plane is bladed antigorite. Cooke agrees with Harvie that there were two distinct periods of serpentinization; the first affecting the peridotite masses as a whole, the second, during which the asbestos veins were formed, more localised in the vicinity of the master joints and faults."

VII.2. PERVASIVE SERPENTINIZATION

Riordon (1952, p. 60) found that the early serpentine (pervasive type) in peridotite varies from 15 to 50% of the rock volume with an average close to 30%. Based on megascopic examination, he states (p.61)

".... There is no marked change in the degree of serpentinization in relation to the margins of the peridotite or in the vertical range of some 600 feet exposed in the higher masses of this rock type such as Caribou Mountain and Quarry Hill."

Whenever exposed, the peridotite appears to be completely serpentinized along its contact with the country rock. However, the contact is exposed only in a few localities. Therefore, whether or not the degree of serpentinization varies from the margins inward cannot be resolved with certainty.

Mode of serpentinization

The serpentinization of olivine appears to have occurred from fractures in this mineral and locally from the grain boundaries. The olivine fragments have been serpentinized in a series of rims (Fig. 102) which follow the shape of the fragment. The cores of the olivine fragments and grains have often been converted to a very fine-grained mass of serpentine which exhibits very low birefringence and a peculiar extinction (Fig. 102). At a more advanced stage of alteration, the rims disappear and only a fine-grained mass remains (Fig. 103). The former fractures, from which serpentinization began, appear now as veinlets filled with bladed serpentine. Magnetite forms a string in the middle of the veins or fractures. The alteration minerals in olivine are antigorite with a subordinate amount of brucite and magnetite. The overall appearance of a serpentinized olivine-rich rock resembles a grid (Fig. 104), referred to here as grid structure. The frequent preservation of the fragile rimmed structure of serpentinized olivine, except in serpentine, suggests that any post-serpentinization deformation has not been penetrative.

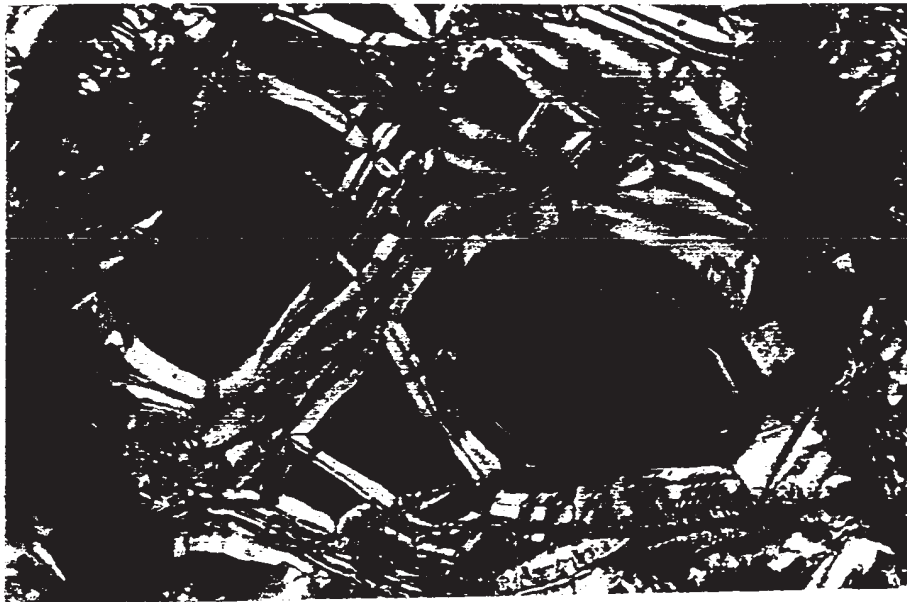


Figure 102. Photomicrograph: Detail of serpentinization of olivine. The serpentine minerals appear to be oriented perpendicular to the boundaries of the rims. Dunite, Sample No. 42
Crossed nicols, X 150

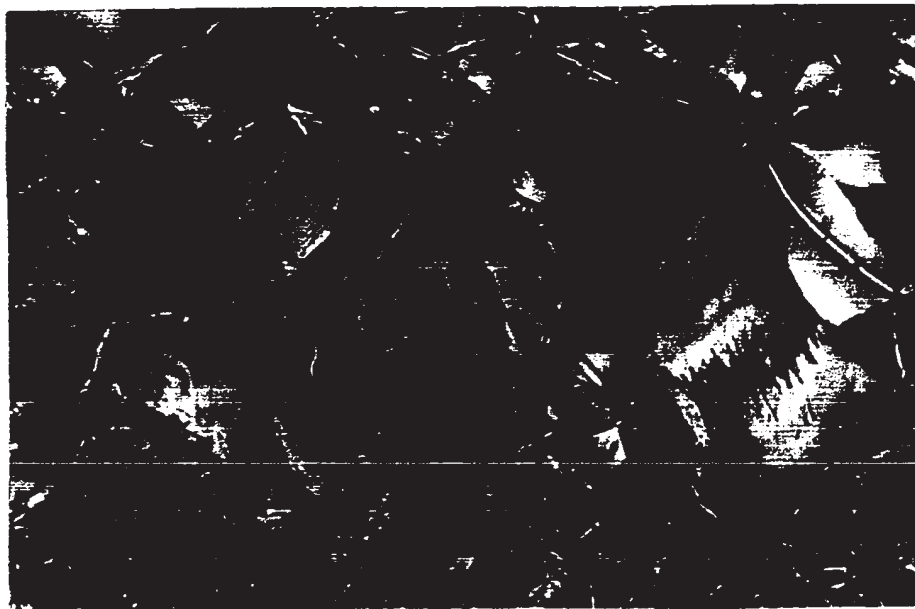


Figure 103. Photomicrograph: Completely serpentinized olivine. The areas of conical appearance are due to a peculiar extinction pattern of serpentine. Dunite, Sample No. 123
Crossed nicols, X 40

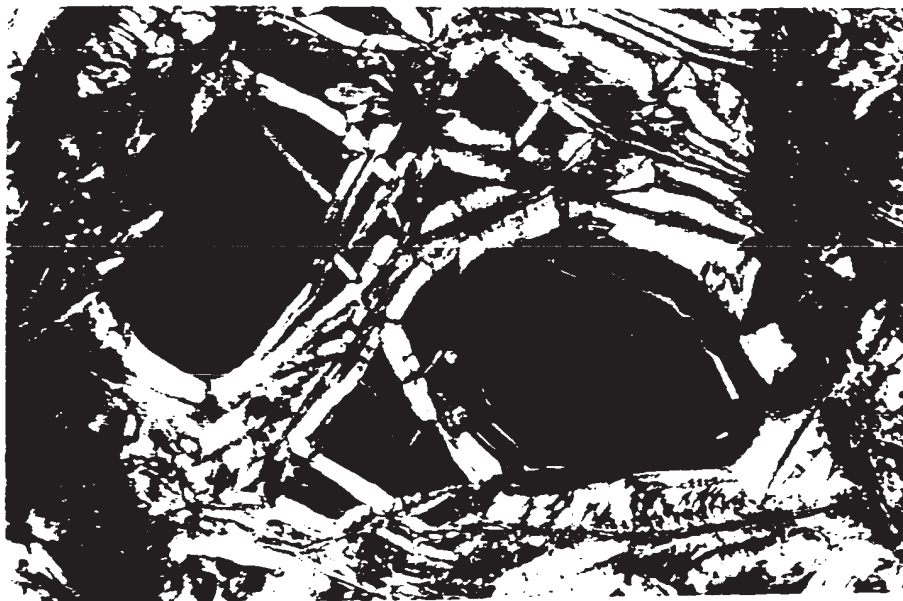


Figure 102. Photomicrograph: Detail of serpentinization of olivine. The serpentine minerals appear to be oriented perpendicular to the boundaries of the rims. Dunite, Sample No. 42
Crossed nicols, X 150

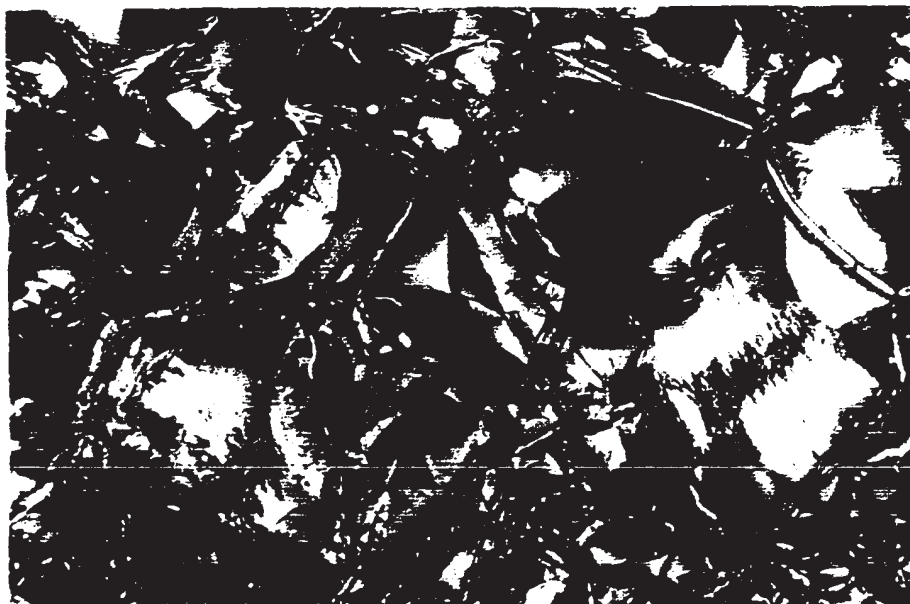


Figure 103. Photomicrograph: Completely serpentinized olivine. The areas of conical appearance are due to a peculiar extinction pattern of serpentine. Dunite, Sample No. 123
Crossed nicols, X 40



Figure 104. Photomicrograph: The grid structure of serpentinized dunite. The serpentinization yielding this grid structure was an impervious and early serpentinization. The narrow serpentine veins are somewhat later, since they crosscut the grid structure. Note that the grid structure is not disturbed by deformation. Dunite, Sample No. 42 Crossed nicols, X 40

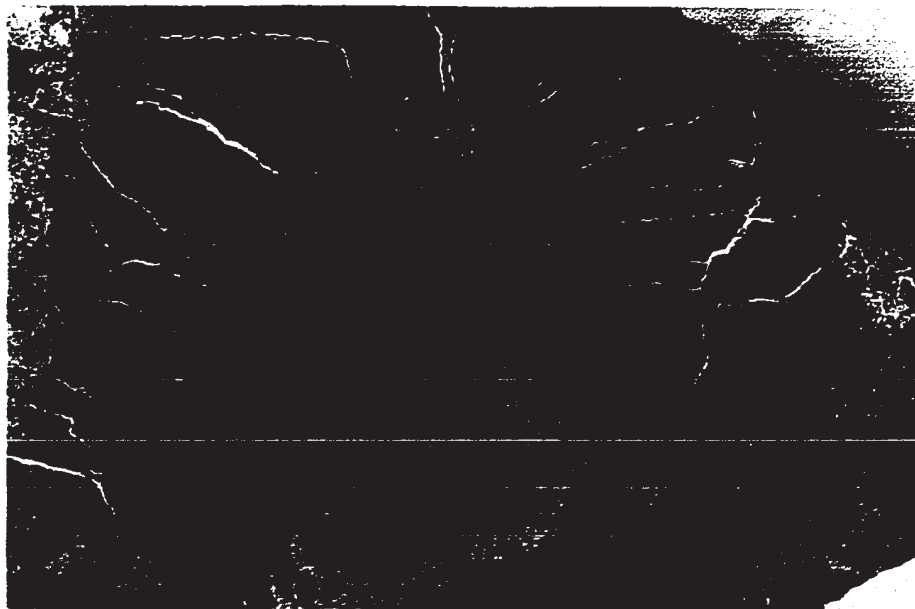


Figure 105. Radial fracture system in massive chromitite (dark grey) surrounding serpentinized dunite. (From the tailing of the Hall Mine)



Figure 104. Photomicrograph: The grid structure of serpentinized dunite. The serpentinization yielding this grid structure was an impervious and early serpentinization. The narrow serpentine veins are somewhat later, since they crosscut the grid structure. Note that the grid structure is not disturbed by deformation. Dunite, Sample No. 42
Crossed nicols, X 40

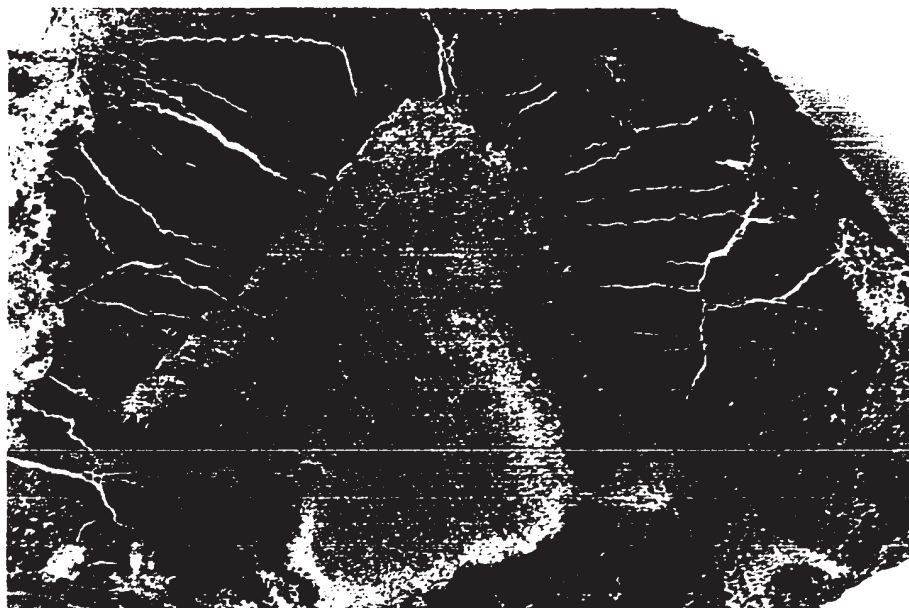


Figure 105. Radial fracture system in massive chromitite (dark grey) surrounding serpentinized dunite.
(From the tailing of the Hall Mine)

The serpentinization of orthopyroxene proceeds mainly along the cleavage. Orthopyroxene often alters to coarser serpentine than that resulting from the alteration of olivine. Serpentinized orthopyroxene often preserves straight and simultaneous extinction and rims are absent.

VII.3. LATE SERPENTINIZATION

This type of serpentinization occurs along joints and faults and over broad zones. Asbestos mineralization is related to this stage of serpentinization. It is believed that the late serpentinization does not have any bearing on the genesis of the ultramafic rocks. Therefore, it is not described further.

VII.4. THE SERPENTINIZATION PROCESSES

A considerable amount of literature is available on the serpentinization of ultramafic rocks. Two principal models have been proposed, the first that serpentine minerals crystallize from a magma, the second that serpentine minerals result from the alteration of solid ultramafic rocks. Both of these models are discussed below.

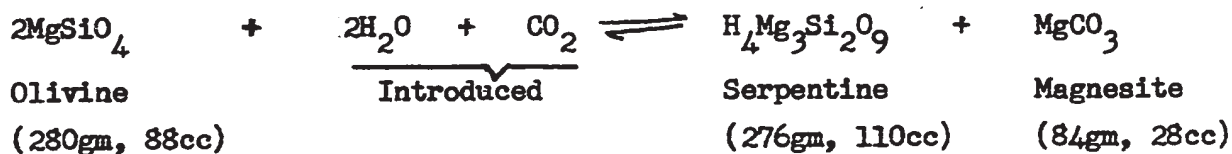
Hess (1933, p. 652) proposed that the parent magma of the peridotite and serpentinite is a highly aqueous, low-temperature ultramafic liquid approaching serpentine in composition. He suggested that such a magma could be generated by the differential fusion of a peridotite mantle under local impact of a very greatly thickened segment of the overlying granitic crust where this is folded downward at the beginning of orogeny. According to Hess, serpentine could crystallize directly from such a magma in addition to the serpentine produced by the reaction of the liquid with olivine and pyroxene that

forms. Turner (1948, p. 131) has pointed out the difficulties of reconciling this hypothesis with the prevalent structure of ultramafic rocks. He suggested that the allotriomorphic, equigranular texture of the interlocking olivine crystals, the general lack of interstitial serpentine, the undulose extinction of olivine and enstatite crystals, and the serpentinization from fractures outward are all features that point to an originally solid state prior to serpentinization.

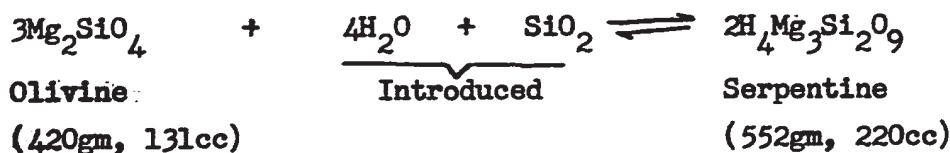
Bowen and Tuttle (1949) have investigated experimentally the system $MgO-SiO_2-H_2O$ and found no liquid phase in this system, neither at temperatures up to $9000^{\circ}C$ and pressures as high as $30,000\text{ lb/in}^2$ nor at $10000^{\circ}C$ and pressures up to $15,000\text{ lb/in}^2$. They therefore concluded that a low-temperature ultramafic magma as postulated by Hess does not exist under crustal conditions.

The second model proposes that serpentine is not a primary mineral but results from metasomatism of solid ultramafic rocks by solutions from external sources. However, serpentinization according to this model poses considerable problems. The decrease of density from about 3.2 to 2.6 gm/cc and the addition of water during the process leave three alternatives (Thayer, 1966). (1) An increase in volume by 35 to 40%, (2) the removal of about 30% of the original material in solution, (3) the combination of 1 and 2.

Serpentinization by the addition of silica, water and carbon dioxide without removal of magnesia would cause considerable volume increase as illustrated by the following two equations (Turner and Verhoogen, 1960, p. 318). (n.b. Part of the iron in olivine will be converted to magnetite during serpentinization):



and

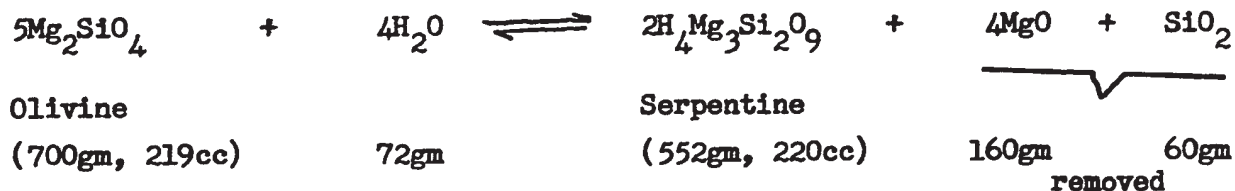


The first reaction implies almost doubling the volume, whereas the second involves a volume increase of more than 65%. Turner and Verhoogen (1960, p. 318) state:

"The microscopic fabric and field relations of undeformed serpentinites show clearly, however, that serpentization is commonly accompanied by little or no increase in volume. Equations such as these just cited cannot therefore represent truly the course of serpentization of dunite."

Thayer (1966) and several other workers hold a similar view.

On the other hand, constant volume serpentization requires the removal of great quantities of MgO and SiO₂. The equation approximating the process proposed by Turner and Verhoogen (1960, p. 319) is:



The authors state (p. 319):

"Great quantities of water would therefore have to be available. Thus, if 700gm of olivine were converted to serpentine through the chemical action of an equal weight of water, 72gm of water would remain as serpentine and the remaining 628 would have to remove 160gm MgO and 60gm SiO₂ from the system. Moreover, if solutions so rich in magnesia and silica were continuously expelled from the ultramafic mass at a temperature of 200 or 300°C, noteworthy magnesia metasomatism of the adjoining rocks

would be expected. Such effects are seldom conspicuous, though a number of instances of regional silification of serpentine belts have been recorded."

This quotation summarizes also the view of those workers (Hess and Otalora, 1964, Green, 1964 and others) who object to constant volume serpentinization on the grounds that the composition of the rock remains constant during serpentinization except for hydration, indicating no movement of material except water. They also question the source of the enormous quantity of water required. Thayer (1966) finds these objections invalid and shows that the composition of ultramafic rocks varies considerably during serpentinization, pointing to the high mobility of magnesia, silica and iron. The water can be juvenile water from acid plutons or connate water from intruded sediments. Thayer thinks that the great quantities of water necessary for constant volume serpentinization do not constitute a valid objection to such a process. He states (1966, p. 686):

"Volume for volume replacement of olivine and pyroxene by serpentine or other minerals requires movement of large quantities of water or other solvents in an open system, but this concept is fundamental in genesis of many kinds of ore deposits. Refusal to apply the same concept to serpentinization, even though it involves unsolved problems, seems inconsistent."

Taylor (1967) found that O^{18} values of serpentinized and un-serpentinized peridotites are similar and show very small spread. He therefore suggested that, except under special conditions, meteoric water is to be eliminated as a possible source of water in the process of serpentinization.

VII.5. SERPENTINIZATION OF ULTRAMAFIC ROCKS IN THE MAP-AREA

The present observations, similar to those of Turner (1948) quoted on p. 178, on the texture of the ultramafic rocks indicate that serpentine is not a primary mineral. Thus, serpentinization resulted from metasomatism of solidified ultramafic rocks by solutions from external sources. It is very likely that the original magma was dry or did not reach the saturation point so as to liberate water since, presumably, this would have caused the crystallization of primary hydrous minerals, especially amphiboles, and no primary hydrous mineral has been observed in the ultramafic rocks. The serpentinization, then, was accompanied by volume increase and/or by addition and subtraction of material, according to the second model of serpentinization discussed earlier.

In the ultramafic rocks of the map-area, evidence indicating volume increase is present (Figs. 105 and 106) but not abundant. The volume increase does not seem to have been sufficient in amount to account by itself for the degree of serpentinization. If serpentinization was accompanied by volume increase only, this latter would have been about 15% for peridotite and about 80% for dunite. Such a volume increase would have caused considerable deformation of the serpentinization textures and movement of un-serpentinized fragments by pushing them apart. These conditions have not been observed.

Evidence indicating the mobility of elements is plentiful. For instance, thick secondary magnetite rims are observed around chromite grains, pointing to the mobility of iron. Serpentine alone, or magnetite accompanied by small serpentine grains, fill fractures in chromite and a multitude of serpentine inclusions are formed along the



Figure 106. Photomicrograph: Radial fractures in chromite around a serpentinized olivine island (right of the centre). Such features are rare. Chromitite
Reflected light, X 50

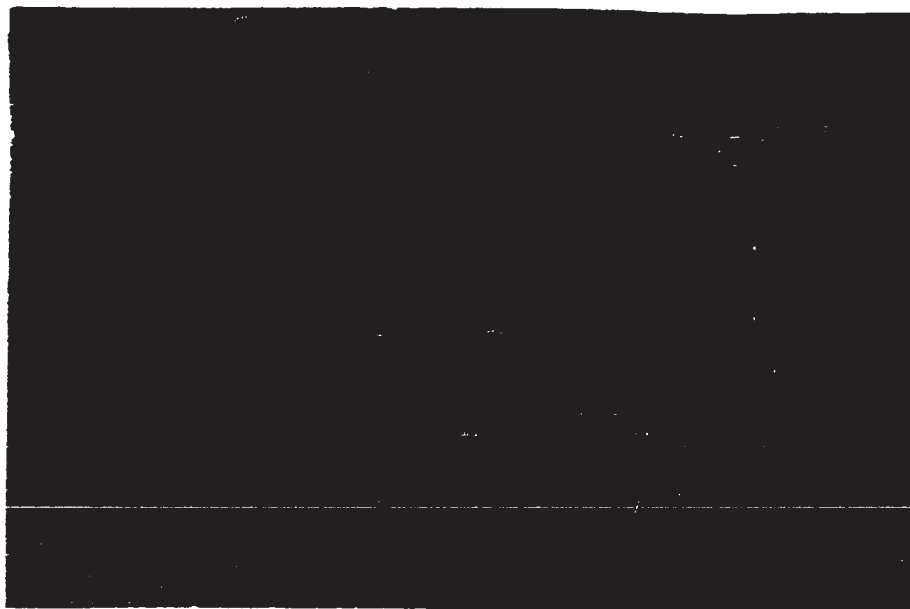


Figure 107. Photomicrograph: Alteration of chromite by serpentinization. Note the mixture of serpentine (dark grey) and magnetite along still observable (left side of the figure) or former fractures (centre of the figure).
Chromitite, Sample M-1
Reflected light, X 50

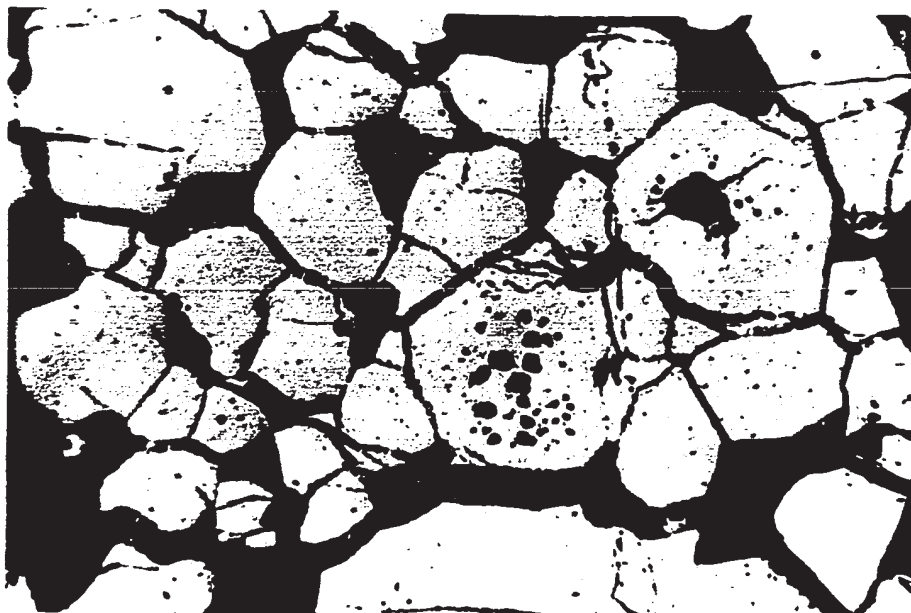


Figure 106. Photomicrograph: Radial fractures in chromite around a serpentinized olivine island (right of the centre). Such features are rare. Chromitite
Reflected light, X 50



Figure 107. Photomicrograph: Alteration of chromite by serpentinization. Note the mixture of serpentine (dark grey) and magnetite along still observable (left side of the figure) or former fractures (centre of the figure).
Chromitite, Sample M-1
Reflected light, X 50

fractures (Fig. 107). These features point to the partial dissolution of chromite and the formation of serpentine, with or without magnetite, in its place. Furthermore, they indicate that serpentinization is not solely a static alteration, but serpentine can form where no silicate mineral existed previously, thus pointing to the mobility of magnesia and silica. The appearance of hypersthene (6.595%) in the norm of a completely serpentinized dunite sample (sample K-12, Table IX) from Bélanger pit suggests that the Si/Mg ratio in dunite did increase during serpentinization. However, the increase in Si relative to Mg is too small to account for the complete serpentinization if this latter were a constant volume process.

To summarize, it can be concluded that volume increase, as well as mobilisation of material with possible subsequent removal, seem to have occurred during serpentinization. The removal of material must have been a major factor, since volume increase appears to have been small.

It has been stated (see Chapter II) that the ultramafic rocks have been emplaced along a zone of weakness, possibly a major fracture zone. This latter might also have been a passage for aqueous solutions, juvenile, conate and/or meteoric in origin which could have serpentinized the ultramafic rocks. The material removed from the ultramafic rocks, by the serpentinizing solutions, perhaps went partially into the country rock causing metasomatism, but possibly most of it continued its ascent along the zone of weakness to end up at the bottom of the sea as hot springs or as volcanic gas and vapor. It is also quite conceivable that, because of its deficiency in water, the ultramafic rock attracted conate water from the adjacent sedimentary rocks, in which case its margins should have been more serpentinized than its interior.

This highly serpentized marginal zone could perhaps have acted as a friction collar during the intrusion of the ultramafic body and has gradually been left behind. A similar process of emplacement has been proposed by Burch (1968) for the ultramafic body of Burro Mountain, California.

The pervasive serpentization of the ultramafic rock continued until completion and/or until the end of the circulation of solutions in the zone of weakness. It is, however, to be stressed that during the pervasive serpentization the ultramafic mass was perhaps not static but continued its movement.

The model of pervasive serpentization postulated above is consistent with the field observations and satisfies most of the objections to the available models discussed previously.

CHAPTER VIII

GENESIS OF ULTRAMAFIC ROCKS AND ASSOCIATED CHROMITITE

VIII.1. INTRODUCTION

The textural, structural and chemical characteristics and the geological setting of the ultramafic rocks, which were described in the previous chapters, are those of alpine-type ultramafic rocks. Thayer (1960) refined the definition of the term "alpine-type" and proposed (1967) six essential characteristics which an alpine-type complex should ideally have. These are:

- 1) Close areal association of ultramafic, gabbroic, dioritic and granophyric rocks.
- 2) Predominance of highly magnesian olivine over pyroxene in ultramafic parts of the complexes.
- 3) Podiform chromite deposits.
- 4) Flow layering and related structures and textures characteristic of high-grade metamorphic rocks.
- 5) Complicated structural relations between gabbroic and ultramafic rocks, such as intertonguing of major units along flow layering; intrusive relations between various facies, etc.
- 6) Distribution of soda-rich dioritic and granophyric rocks within or near gabbroic rocks, commonly hybrid and accompanied

by much albitization and brecciation.

The intrusive complex under study exhibits the first five of the six characteristics enumerated above. Whether or not the sixth characteristic is also present is not known; data are lacking on the chemistry and petrology of silicic rocks (e.g. quartz diorites) in the Gabbroic Suite.

The following section deals with the possible origin and mode of emplacement of the ultramafic rocks, including chromitite, in the map-area. This is followed by a discussion of other genetic concepts. In the last section of the chapter the general problem of ultramafic rocks in orogenic belts, zoned ultramafic complexes (Alaskan-type) excluded, is considered briefly.

VIII.2. FORMATION OF ULTRAMAFIC ROCKS

A. Differentiation process

The observed interlayering of different ultramafic rock types makes the conclusion inescapable that these rocks have differentiated from some parent material. Chromitite with "chain structure" and nodular chromitite, which are present in the map-area, are presumably fairly diagnostic features of magmatic differentiation. Similarly, the abundance of inclusions (e.g. olivine inclusions in chromite, olivine and chromite inclusions in pyroxene), diopside exsolution lamellae in orthopyroxene, in situ growth and magmatic corrosion are all features suggestive of magmatic origin.

Metamorphic differentiation has not been disregarded as a possible alternative. However, it appears unlikely that metamorphism could be the primary cause of differentiation. It would be difficult to explain

how metamorphic differentiation of a homogeneous rock could lead to the concentration of chromitite into regular zones which occur only in dunite. Also, the extensive ultramafic rock units, such as the dunite zones and the Olivine Pyroxenite Zone, could not have been formed by metamorphic differentiation. Furthermore, the lack of correlation in thickness or abundance of interlayered ultramafic bands of different composition argues against their having been formed by metamorphic differentiation.

B. Nature of the original magma and place of differentiation

There appear to be two genetic models which are compatible with the available data.

Model 1: The ultramafic rocks have differentiated by fractionation and gravity settling from an ultrabasic magma generated from the mantle and the Gabbroic Suite is genetically related to the Ultramafic Suite. The mantle material from which these two suites of rocks have been derived perhaps had the composition of O'Hara's (1967b) "Four phase lherzolite" or that of Ringwood's (1964) "Pyrolite". This starting material began to melt either due to a temperature gradient produced by convection currents (Turner and Verhoogen, 1960, p. 445) or by the heat of impact on the mantle of a downwarping geosynclinal mass (Hess, 1938). Melting could have been aided by a sudden pressure decrease due to deep faulting. Gabbroic rocks probably represent the first partial melt. As the temperature continued to rise more and more pyroxene,

olivine and feldspar melted to yield a largely liquid ultrabasic magma from which the ultramafic and perhaps some gabbroic rocks have differentiated by fractional crystallization and gravity settling. Differentiation proceeded very slowly and probably occurred in the upper mantle or lower crust.

Model 2: The Ultramafic and Gabbroic Suites of rocks have differentiated from a large volume of basic magma. The non-ultramafic residual liquids have been removed, perhaps to form mainly volcanic rocks and a smaller volume of gabbroic rocks. The ultramafic cumulates have later been emplaced in their present location.

The lack of significant variation in the composition of silicate minerals within any rock type suggests that fractionation between the magma and the solid was not very significant during the differentiation of the ultramafic rocks. This suggests that the magma was either ultrabasic in composition or, if basaltic, large in volume.

The available data do not permit clear discrimination between the two genetic models summarized above. However, it appears more likely that the ultramafic rocks have differentiated from an ultrabasic magma. This conclusion is based on the following observed differences between the rocks under study and those known to have differentiated from a basaltic magma.

- a) In the map-area, as elsewhere in alpine-type ultramafic belts, the apparent proportion of gabbro and pyroxenite to olivine-rich rocks (dunite, peridotite) is much smaller than in basaltic differentiates.
- b) Intermediate to acidic rocks, which should have been formed in large

volumes in a sequence of differentiation from basalt, are virtually lacking in the map-area.

c) The Mg/Fe ratio in olivine and pyroxene is higher in the same minerals of equivalent rocks in basaltic differentiates (the Great Dyke, Rhodesia is a notable exception where olivine of Fo_{94} occurs, Jackson, 1967).

d) Chromitite occurs only in dunite. In fact, from the published accounts of alpine-type peridotite elsewhere, chromitite does not occur in pyroxene-bearing rocks; dunite and troctolite are the only host rocks (Thayer, 1960). In basaltic differentiates chromitite may occur in pyroxene-bearing rocks (Thayer, 1960, Jackson, 1967).

e) Nodular chromitite is common in the map-area but has not been reported from basaltic differentiates (Thayer, 1960).

f) In the ultramafic rocks of the map-area the Mg/Fe ratio is lower in olivine than in coexisting orthopyroxene. In basaltic differentiates this ratio in olivine is equal to or higher than that in orthopyroxene (see p. 92 and O'Hara, 1967a, p. 11).

g) Chromite in chromitite from the map-area is poorer in Fe and Ti, richer in Cr and Mg than chromite in chromitite in most described basaltic differentiates.

h) Although the data presented here and those which have been published are scanty, it appears that the gabbro in the map-area is poorer in Fe, Ti and P, richer in Mg, Ni and Cr than the gabbros believed to have differentiated from a basic magma.

This postulated ultrabasic parent magma appears to have been poor in Fe, Al and Ti, rich in Mg, Cr and relatively rich in Ca. Its exact composition cannot be determined, for it is not known whether or not

the ultramafic rocks represent all the differentiation products of this magma in their approximate original proportions. If the ultramafic rocks were assumed to represent all the differentiates and if the abundance of ultramafic rocks were somewhat proportional to their outcrop area, then an ultrabasic magma containing 55 to 60% normative Fo might perhaps be considered an appropriate approximation of the parent magma. The synthetic systems diopside-anorthite-forsterite (Osborn and Tait, 1952, op. cit. in Wyllie, 1960) and CaO-MgO-SiO₂-FeO (Rieker, 1952, op. cit. in Wyllie, 1960) suggest that such a magma would be entirely liquid at about 1600°C.

On the basis of experimental data on the system CaO-MgO-SiO₂-FeO, Wyllie (1960) has suggested that for a small drop in temperature large amounts of olivine would crystallize from a Fo-rich picritic magma. Furthermore, during the differentiation the composition of olivine would change only slightly for large variations in the composition of the liquid (Wyllie, 1960, p. 465). Therefore, the fact that olivine in the peridotite and dunite of the map-area exhibits little compositional variation appears to be consistent with an ultrabasic parent magma.

If one assumes that the mafic and ultramafic rocks of the map-area are fractions of the same original material, this latter would have had a composition comparable to Ringwood's (1964) "Pyrolite". That the gabbroic and ultramafic rocks are probably related is supported by the fact that gabbroic rocks rich in Mg, poor in Ti, P and Fe like those in the map-area accompany alpine-type ultramafic rocks throughout the world (Thayer, 1961, 1967 and 1970). Furthermore, a genetic relationship between gabbroic and ultramafic rocks has been satisfactorily demonstrated in some localities (Smith, 1958, Thayer, 1942 and 1967).

The gabbro in the map-area appears to be similar in occurrence to the gabbros in alpine-type ultramafic belts elsewhere.

Hence the genetic model favoured here requires that the gabbroic rocks represent an early fractional melt of the original material and that the ultramafic rocks have probably differentiated after the bulk of the gabbroic material had left the system. Field observations indicate a separate intrusion of the gabbro. The low Al content of pyroxenes and of chromite in chromitite and the lack of feldspar-bearing ultramafic rocks suggest that the ultramafic rocks have differentiated from a magma low in Al, hence probably with very little gabbroic component. By way of contrast it is worth noting that in the ultramafic belt of the Camaguey district, Cuba (Thayer, 1946), in the Zambales Complex, Philippines (Stoll, 1958) and in the Bay of Islands Complex, Canada (Smith, 1958) there is a very close association of gabbro and ultramafic rocks with the presence of transitional rock types and the chromite in chromitite is highly aluminous.

It has been speculated (de Roever, 1957) that differentiation of alpine-type ultramafic rocks could have occurred during the consolidation of the Earth, hence magmatic layering and textures observed in ultramafic rocks might be inherited from the mantle. In the absence of more detailed knowledge of the mantle this speculation cannot be discussed adequately. However, even if the above speculation were true this would only push back in time the problem of differentiation of the ultramafic rocks and of the nature of their parent material.

The ultimate relationship between the phaneritic rocks and the volcanic rocks in the map-area is not known. It may well be that the volcanic rocks formed by partial melting of the same portion of the

mantle as the phaneritic rocks.

For the following reasons, it is concluded that the ultramafic rocks did not differentiate at their present place.

- a) There is no autochthonous contact metamorphism in the country rock and no observable chilled margin in the ultramafic rocks. This suggests "cold" intrusion.
- b) The ultramafic rocks do not form a continuous in situ differentiation series in their distribution (see Chapter III).
- c) The igneous layering is vertical or steeply dipping and discordant to the schistosity and bedding in the country rock. Also, the layering is locally discordant to the boundaries between the major ultramafic rock units.

The grain size and textural and chemical characteristics of the ultramafic rocks indicate slow cooling, hence perhaps deep-seated differentiation. Mineral chemistry suggests crystallization at high pressure. Furthermore, hundreds of apparently contemporaneous ultramafic intrusions occur in the Appalachian Serpentine Belt and a wedge of the mantle is inferred to underly the area (see Chapter III). Therefore, the source from which these bodies have originated is not a point source but must underlie a considerable area. It is therefore suggested that the ultramafic rocks originated in the upper mantle and either differentiated there or deep in the crust. Subsequently, they were emplaced in their present location.

VIII.3. FORMATION OF CHROMITITE

It has been concluded that the ultramafic rocks have been formed by fractional crystallization and gravity settling from a magma. This

conclusion can also be extended to the chromitite.

During the differentiation the availability of Cr rather than that of Al, Fe and Mg seems to have been the controlling factor in the amount of chromite crystallization. The crystallization of pyroxenes, which contain about 0.15 to 0.20% Cr, appears to have hindered the crystallization of chromite, since chromitite is absent in the pyroxene-bearing rocks.

Assuming that chromitite layers in dunite accumulated by crystal settling the interlayering could result either from the action of convection currents as discussed by Wager and Deer (1939) or from varying rates of crystal settling (Jackson, 1961) or from a combination of both. In the rocks under study the grain size of olivine in dunite and chromite in chromitite are comparable. Therefore, crystal settling alone cannot account for the banding; either the chromite and olivine must have crystallized periodically and at different times and/or places in the magma chamber or one or the other of the phases must have been introduced from outside the immediate area of the accumulation.

The formation of chromitite by gravity settling would imply that the original ore-bearing horizons were extensive and formed regular layers providing that the original magmatic layering was flat-lying or with small slope. However, in the map-area the chromitite layers are discontinuous and commonly they vary rapidly in thickness (see Chapter VI). Borchert (1964) made a similar observation and claimed that regular layers are formed by crystal settling on a flat-lying magma floor, while lenses and irregular layers are formed on a steeply inclined floor (Fig. 108). Local irregularities on the floor can cause local

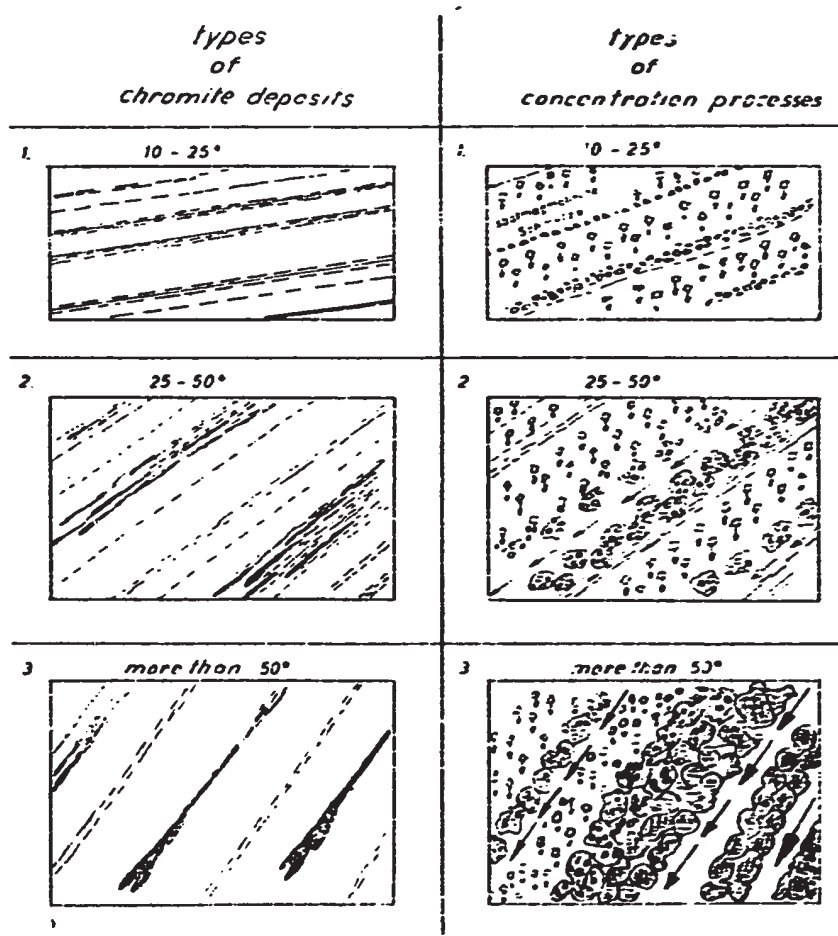


Figure 108. Types of chromitite structures in relation to the inclination of the primary magmatic layering.
(From Borchert, 1964)

concentration of chromite, hence isolated chromite deposits and very thick chromitite lenses. However, all these structures can also be explained by deformation, during and after the differentiation, superimposed on the original magmatic features.

VIII.4. EMPLACEMENT AND RE-EMPLACEMENT OF THE ULTRAMAFIC ROCKS

It has already been postulated that the ultramafic rocks did not differentiate in their present location. It is envisaged that their emplacement took place in two stages. In the first stage the rocks flowed likely as a crystal mush or possibly by plastic flow; this may have occurred soon after differentiation. In the second stage of emplacement the ultramafic rocks moved as solid blocks; serpentinization began before this movement and presumably continued during and after the emplacement.

A. First stage: Flow

The attitude of layering and the preferred, linear orientation of chromitite nodules and lenses in the ultramafic rocks under study have been described earlier (see Chapters III and VI). Similar layering in alpine-type peridotites elsewhere has been interpreted as flow layering brought about by the flow of ultramafic material either as a crystal mush (Thayer, 1963 and 1964) or as a plastic solid accompanied by recrystallization (Green, 1967; Lappin, 1967; Ragan, 1967). Some layers have presumably formed during flow, while others are remnant magmatic layers (Thayer, 1963). "Pull-apart" texture in chromitite and the preferred orientation of chromitite nodules and lenses have also been interpreted by Thayer as diagnostic flow features.

As recognizable recrystallization textures are rare in the ultramafic rocks, flow in the form of a crystal mush seems more plausible than plastic flow. Furthermore, orthopyroxenite, pyroxenite and ultrabasic dykes do not seem to have been deformed. This is most readily explained if such dykes represent the final injection to residual liquid present during the crystal mush flow.

The extent of this postulated crystal mush flow has not been determined. However, high-temperature contact metamorphism of the Caldwell metagreywackes suggests that at least some ultramafic rocks were at high temperatures, hence perhaps as a crystal mush, when they reached the upper crust.

The intrusion of dunite and chromitite dykes and the fragmentation of formerly more extensive layers in the ultramafic rocks are thought to have occurred during flowage. Chromitite layers are commonly more discontinuous and more variable in strike and dip than silicate rock layers perhaps reflecting more competent behavior. It is likely that chromitite solidified earlier than the enclosing silicate rocks and hence deformed by fragmentation.

It is suggested, for the following reasons, that the ultramafic rocks did not reach their present place by flowage.

- 1) Emplacement of ultramafic crystal mush should perhaps have caused contact metamorphism similar to those of high-temperature peridotite intrusions. With the possible exception of the Belmina Ridge peridotite, this is not observed in the map-area.
- 2) As discussed above, plastic flow by recrystallization does not appear to be very likely. Even if the ultramafic rocks were

assumed to be emplaced by plastic flowage in the solid state, this would still require high temperatures of intrusion (see Chapter V).

- 3) The noticeable parallelism of layers in the ultramafic rocks suggests that the presumed flow was laminar in character. Emplacement of ultramafic rocks by laminar flow would require concordance of layering with footwall and hanging wall of the intrusion, at least close to the contacts. Except for the Belmina Ridge peridotite body, this has not been observed in the map-area.
- 4) No penetrative deformation (e.g. recrystallization, cataclasis of minerals) occurred within the stability range of serpentine ($< 600^{\circ} \text{C}$). Hence a truly "cold" intrusion by flow is very unlikely.

B. Second stage: Re-emplacment

It is suggested, for the reasons listed above, that the ultramafic rocks solidified at depth and have subsequently been re-emplaced as solidified masses. The process of re-emplacment of the ultramafic rocks is speculative. One or both of the following processes might have been responsible for the final emplacement:

- 1) The ultramafic rocks ascended along a deep fracture zone and the moving force was the lithostatic pressure.
- 2) During orogenic movements tectonic stress forced the ultramafic rocks to move, the serpentized margin acting as a low-friction skin. The decreased strength of the serpentized margin might be due to two processes (Raleigh, 1967).

- (a) Dehydration of serpentine by heating above its stability range.
- (b) The intrusion of the ultramafic body, which was hotter than the adjacent sedimentary rocks, caused heating of interstitial water in the sediments resulting in tremendous increase in the pore pressure around the margin of the body.

Raleigh (1967) states:

"The marginal envelope of sediment and serpentizing peridotite into which the water has penetrated under pressure will then be weakened in relation to the cooler surrounding sedimentary rock and, given the appropriate tectonic stress gradient, solid emplacement should be possible."

Whatever the process of re-emplacment, the contacts between ultramafic rocks and country rock are, therefore, essentially intrusive faults.

VIII.5. OPHIOLITE HYPOTHESIS

Ophiolites are considered to be stratigraphic units composed ideally of the sequence peridotite, gabbro, "sheeted" diabase, pillow lavas and associated chert, in that ascending stratigraphic order (Church and Stevens, 1971). Gabbro and "sheeted" diabase may not always be present. The igneous rocks forming a given ophiolite complex are commonly assumed to be consanguineous. The contacts between phaneritic rocks and volcanic rocks are never gradational (Steinmann, 1927) or not convincingly so (Vuagnat, 1963), although some possible exceptions have been described (Moore, 1969, Upadhyay et al. 1971). Ophiolites where the characteristic stratigraphic succession can be observed unequivocally are admittedly rare (Vuagnat, 1963). However, well developed examples have been described from Newfoundland (Church and

Stevens, 1971), from Oman (Reinhardt, 1969), from Papua (Davies, 1968) and from Greece (Moore, 1969).

It has been suggested (Lamarche, 1971, in press) that all the igneous rocks in the map-area are part of a large ophiolite complex extending from north of Thetford Mines to the northwest, to Ham Mountain some 60 km. to the southwest. In the map-area the igneous complex exhibits three essential rock groups of ophiolites; namely ultramafic, gabbroic and volcanic rocks. However, the phaneritic rocks do not seem to be stratigraphically located; discordant and intrusive character is observable for some of them. Nevertheless, available data do not allow ruling out completely the possibility of the igneous complex being an ophiolite but suggest that this possibility is unlikely. Three genetic models for the formation of ophiolites are discussed below and tested in the map-area.

Lamarche (1971, in press) believes that the ophiolitic complex, which includes the igneous rocks of the map-area, formed as a giant submarine extrusion, peridotitic in composition, and differentiated under a self-formed roof of spilitic mafic volcanic rocks during the lower Ordovician epoch. Intrusive ultramafic rocks are interpreted either as feeders to the ophiolite or sill-like intrusions. Ultramafic offshoots from the presumed extrusive bodies are minor intrusions which occurred during the cooling of the flow. Stratigraphic discordances of the extrusive masses are attributed to faulting, subsequent to extrusion.

Lamarche's model, summarized above, answers some of the objections to similar models calling for in situ differentiation of alpine-type peridotites from giant extrusions of basaltic magma (Aubouin, 1959,

Brunn, 1956, Dubertret, 1953 and others). It also explains the fact that the ultramafic rocks are "underlain" by volcanic rocks and accounts for the observable intrusive nature of some phaneritic rock bodies. Nevertheless, the present author cannot subscribe to this model for the following reasons:

- 1) Field evidence indicates separate intrusion of gabbroic magma and ultramafic rocks.
- 2) The textural and chemical data point to a history of slow cooling in a low oxygen fugacity and perhaps relatively high-pressure environment for the ultramafic rocks. Hence these latter are inferred to have differentiated at depth.
- 3) Even allowing for faulting, the distribution of rock types and layering cannot be accounted for by in situ differentiation, particularly where this requires general conformity, over wide areas, to metasedimentary and metavolcanic contacts.
- 4) If the igneous rocks in the map-area are considered to have differentiated from one flow, the latter would have had to have a thickness of 10 km or more. If the rocks formed through differentiation of a multitude of flows of more common thickness (approximately 30 m each), a more cyclical distribution of rock types should be present. Furthermore, inevitably some sedimentary interlayering should separate the ultrabasic flows. Such features are not observed in the map-area.
- 5) No chilled margin was observed in the ultramafic rocks, such a margin should be present if a peridotitic lava, which by its nature would be very hot, was extruded.
- 6) The model does not explain the fact that the Ultramafic Suite

consists of two distinct and unmixed rock assemblages, namely the Northern Assemblage and the Southern Assemblage (see Chapter III).

According to Maxwell (1970, in press) the ophiolite of the Alps formed by partial melting of the mantle peridotite. This author states:

"... mantle peridotite rose as a plastic mass, probably facilitated by partial melting and formation of intergranular liquid. The intergranular melt might be expected to coalesce and rise faster than the ultramafic mass, perhaps breaking out on the sea floor as shield volcanoes. the ultramafic part of the column locally reached the level of the sea bottom and flowed plastically beneath the carapace of diabase and lavas, Gabbroic differentiates formed pegmatitic masses and great sill-like lenses between the ultramafic rocks and already solid overlying diabase."

A similar process of formation has been proposed by Moores (1969) for the Vourinos ophiolitic complex, Greece. The Vourinos complex consists of a basal ultramafic zone and an upper basic zone. This latter includes, in ascending stratigraphic order, pyroxenite, gabbro, quartz diorite and basic lavas. The ultramafic zone "grades" into the mafic zone and mafic phanerites are in "gradational" contact with overlying lavas. Moores does not state whether the mafic zone represents a differentiated flow or sill-like intrusions of mafic phanerites beneath the lavas. The ultramafic zone was emplaced as a "nearly solid" mass and "spread out" beneath the mafic zone. Layers of gabbro and pyroxenite in the ultramafic zone and some dunite-peridotite interlayering are interpreted as flow layering, while others might presumably be magmatic layers inherited from a differentiation in the mantle (Moores, 1969). Moores suggests that all igneous rocks of the complex are consanguineous and formed by differential melting of mantle peridotite.

The genetic concept proposed by the present author, and discussed earlier, has some similarities with Moores's and Maxwell's models, summarized above, but differs in two main points from them. Firstly, the consanguinity of all the igneous rocks in the map-area is not assumed. Secondly, the ultramafic rocks under study are thought to have been solidified "cold" masses at the time of their final emplacement and concordant intrusion of the ultramafic rocks is not consistent with the available field evidence.

With a few possible exceptions (Moores, 1969, Upadhyay et al., 1971) the consanguinity of phanerites with aphanitic volcanic rocks is hypothetical in ophiolites. In the map-area, data are not sufficient to refute or confirm the consanguinity of the two rock groups, but sufficient to suggest that if they are related they may only be so through a process of differentiation prior to their emplacement (see Chapter IV).

As discussed previously, the emplacement of ultramafic rocks to their present location as a crystal mush appears unlikely. Furthermore, the spreading out of unconsolidated ultramafic material beneath the extrusive rocks or their concordant intrusion requires concordance of flow layering to the footwall and hanging wall of the intrusion, hence to stratification. Similarly, the contacts between major phaneritic rock units might also be expected to be concordant with stratification in the overlying country rock and with the presumed footwall. Except for the Belmina Ridge peridotite, such features are not observed in the map-area.

As suggested earlier (Chapter II), it is possible that solidified ultramafic masses might have emplaced partly along the surface of discontinuity between the Caldwell Formation and the overlying volcanic

and sedimentary rocks. However, perfectly concordant intrusion of large solidified masses is quite unlikely. It is therefore suggested that the igneous complex in the map-area does not constitute an ophiolite.

Other concepts on the genesis of ultramafic-mafic rock associations of orogenic belts appear unlikely for the map-area and their discussion is omitted here.

VIII.6. GENERAL PROBLEM OF ALPINE-TYPE ULTRAMAFIC ROCKS

Considerable controversy exists concerning the origin of alpine-type ultramafic rocks. A survey of the literature suggests that the controversy centers around three main points; namely the nature of their parent material, their relationship with coexisting mafic to acidic phaneritic and aphanitic rocks and the mode of emplacement of ultramafic rocks.

Many workers (e.g. Borchert, 1964; Challis, 1965 and 1969; Osborn, 1969, etc.) believe that ultramafic rocks are consanguineous with all spatially associated igneous rocks and are differentiated from basaltic magma. Borchert (1964) considers alpine-type complexes as greatly deformed stratiform intrusions. Some other authors (e.g. Hess, 1955; Noble and Taylor, 1960; den Tex, 1969) separate the ultramafic rocks from all other coexisting igneous rocks. Thayer (1969b and 1970) and der Kaaden (1971) reject any relation between ultramafic rocks and volcanic rocks, but Thayer maintains that ultramafic rocks are genetically related to adjacent gabbroic rocks and granophyres. Thayer (1960) considers alpine-type complexes as a distinct igneous group unrelated to stratiform intrusions.

While some workers (e.g. de Roever, 1957; Rost, 1959; den Tex, 1969) believe in the emplacement of entirely solidified ultramafic rocks,

others suggest intrusion (e.g. Maxwell, 1970, in press; Moores, 1969; Stoll, 1958; Thayer, 1963 and 1967) or even extrusion (Bailey and McCallien, 1953; Rittman, 1960, op. cit. in Vuagnat, 1963) of ultramafic material as a crystal mush. Hess (1955), Lamarche (1971, in press), Noble and Taylor (1960), Wijkerslooth (1954) and others believe that the ultramafic rocks represent intrusion or extrusion (Lamarche, 1971, in press) of ultramafic magma. A metasomatic origin for alpine-type ultramafic rocks has been proposed (e.g. Avias, 1949; Sorensen, 1967) but appears to be too unlikely as a general concept, although small ultramafic lenses might have formed by metasomatism (Vuagnat, 1963).

Some ophiolite complexes have been described (e.g. Church and Stevens, 1971; Davies, 1968; Reinhardt, 1969) as overthrust oceanic crust (mafic rocks) and mantle (ultramafic rocks), although opinions seem to differ somewhat as to the mode of formation of rock assemblages prior to thrusting.

Alpine-type ultramafic rocks exhibit relict magmatic textures and structures. Relict graded bedding and other evidences of gravity fractionation appear to be common in alpine-type chromitites (Thayer, 1969b). Gravity stratification and chromitite nodules indicate that ultramafic rocks differentiated from a largely liquid magma. Therefore, most alpine-type peridotites and dunites do not appear to be "refractory residues" from partial melting of mantle peridotite but cumulates from a magma. Alpine-type ultramafic rocks perhaps represent or approach ideal "adcumulates" as defined by Wager and Wadsworth (1960). Common homogeneity of minerals, virtual absence of interstitial phases, coarse grain size, considerable thickness of chromitite masses in some alpine-type ultramafic masses suggest that these

rocks have differentiated slowly.

The chromitite masses in alpine-type ultramafic rocks have been formed most likely, in the main, by fractional crystallization and gravity settling. Separation of an immiscible chromite-rich liquid might have played a very important role in the formation of chromite deposits, although most students of chromite deposits seem to disregard totally this possibility. The discontinuous nature of chromitite masses is likely due to deformation subsequent to differentiation, as suggested for the map-area.

In view of consistent petrological and structural differences between alpine-type and stratiform complexes (Thayer, 1960), it appears that these two groups are genetically different. It is probable that most alpine-type ultramafic rocks differentiated either from an ultrabasic magma, as suggested earlier for the ultramafic rocks under study, or from a basic magma which has differentiated under conditions unlike those under which stratiform complexes have been formed (Thayer, 1969b). Nevertheless, the possibility of some alpine-type ultramafic rocks being reentruded cumulates from shallow basic intrusions (Challis, 1965, Osborn, 1969) cannot perhaps be discounted entirely. In this respect Moores (1969) notes that the stratiform complex of the Great Dyke exhibits gradation from very magnesian minerals, like those in alpine-type peridotites, to more iron-rich minerals like those in other basic complexes and suggests that Thayer's (1960) sharp line of division between stratiform and alpine-type complexes is perhaps not entirely justified.

The common areal association of alpine-type ultramafic rocks with volcanic rocks is unlikely to be fortuitous, contrary to the opinion

of some workers (e.g. Hess, 1955; der Kaaden, 1971, etc.). However, the areal association alone cannot constitute evidence for the consanguinity of the two groups of rocks as was implied by some authors (e.g. Challis, 1965; Osborn, 1969). Structural factors and general contemporaneity of intrusive and extrusive activity, suggested earlier for the map-area, might also explain the areal association of ultramafic rocks with volcanic rocks. Furthermore, it is to be noted that most alpine-type peridotites presumably crystallized at depths less than 25 to 30 km. (Kushiro and Yoder, 1966, op. cit. in Thayer, 1969b; O'Hara, 1967b), whereas basaltic magma is believed to be generated at depths of not less than 50 km. (Green and Ringwood, 1963, Yoder and Tilley, 1962, op. cit. in Thayer, 1969b).

It appears likely that, as groups, high-temperature peridotite intrusions, ultramafic portions of ophiolite complexes and "cold" intruded alpine-type ultramafic rocks differ essentially in their history of emplacement. It is probable that high-temperature peridotite intrusions are deeper intrusive equivalent of ultramafic rocks in ophiolites (Moore, 1969) and of "cold" intruded alpine-type peridotites. They may also be intrusions which did not undergo a re-emplacment process subsequent to their solidification in contrast to "cold" intrusions which might have been re-emplaced. Similarly, the ultramafic portion of ophiolites might be extruded or concordant intrusive equivalents of discordant ultramafic rocks. Several ophiolite complexes have been described as overthrust oceanic crust and mantle (e.g. Church and Stevens, 1971; Davies, 1968; Reinhardt, 1969). It is at least probable that some alpine-type ultramafic masses which do not exhibit ophiolite stratigraphy (der Kaaden, 1971) may also be tectonic slices

of the mantle. Except for stratigraphic occurrence of ophiolitic ultramafic rocks nothing seems to distinguish them, as a group, from "intrusive" alpine-type ultramafic rocks or from those which do not occur in ophiolites.

REFERENCES

- Adams, F.D., (1883), Notes on the microscopic structures of some rocks of the Quebec Group: Geol. Survey, Canada, Rept. Prog. 1880-1881-1882, pt. A, pp. 8-23.
- Aubouin, J., (1959), Contribution à l'étude géologique de la Grèce septentrionale: Les confins de l'Épire et de la Thessalie: Ann. Geol. Pays helléniques, v. 10, pp. 1-483.
- Avias, T., (1949), Note préliminaire et interprétations nouvelles concernant les peridotites et serpentinites de Nouvelle Calédonie (secteur central): Bull. Soc. Geol. France, 5^{eme} ser., v. 19, pp. 439-451.
- Bailey, E.B., and McCallien, W.J., (1953), Serpentine lavas, the Ankara mélange and the Anatolian thrust: Trans. Royal Soc. Edinburgh, v. 62, pp. 403-442.
- Barth, T.F.W., (1962), Theoretical Petrology: Wiley, New York, N.Y.
- Bartholomé, P., (1961), Coexisting pyroxenes in igneous and metamorphic rocks: Geol. Mag., v. 98, pp. 346-348.
- _____ (1962), Iron-magnesium ratio in associated pyroxenes and olivines: Geol. Soc. America, Buddington Volume, pp. 1-20.
- Bilgrami, S.A., (1963), Further data on the chemical composition of Zhob Valley chromites: Am. Min., v. 48, pp. 573-587.
- Borchert, H., (1964), Principles of genesis and enrichment of chromite ore deposits. In R. Woodtli (Ed.), Methods of prospection for chromite: O.E.C.D., Paris, pp. 175-202.
- Bowen, N.L., and Tuttle, O.F., (1949), The system $MgO-SiO_2-H_2O$: Geol. Soc. America Bull., v. 60, pp. 439-460.
- Boyd, F.R., (1966), Short course lecture notes on chain silicates (unpublished): American Geol. Institute, Washington, D.C.
- Boyd, F.R., and Schairer, J.F., (1964), The system $MgSiO_3-CaMgSi_2O_6$: Jour. Petrology, v. 5, pp. 275-309.

- Brunn, I.H., (1956), Contribution à l'étude géologique du Pinde septentrional et d'une partie de la Macédoine occidentale: Ann. Geol. Pays helléniques, No. 7.
- Burch, H.S., (1968), Tectonic emplacement of the Burro Mountain ultramafic body, Santa Lucia Range, Calif.: Geol. Soc. America Bull. v. 79, pp. 527-544.
- Challis, G.A., (1965), The origin of New Zealand ultramafic intrusions: Jour. Petrology, v. 6, pp. 322-364.
- _____ (1967), X-Ray study of deformation lamellae in olivine of ultramafic rocks: Min. Mag., v. 36, pp. 195-203.
- _____ (1969), Discussion on the paper "The origin of ultramafic and ultrabasic rocks", by Wyllie, P.J.: Tectonophysics, v. 7, pp. 495-506.
- Church, W.R., and Stevens, R.K., (1971), Early Paleozoic ophiolitic complexes of the Newfoundland Appalachians as mantle-oceanic crust sequences: Jour. Geophys. Res., v. 76, pp. 1460-1466.
- Cooke, H.C., (1937), Thetford, Disraeli and eastern half of Warwick map-areas, Quebec: Geol. Survey, Canada, Mem. 211.
- Davies, H.L., (1968), Papuan ultramafic belt: 23rd Internat. Geol. Congr. Rept., Prague, pt. 1-2, pp. 209-220.
- Deer, W.A., Howie, R.A., and Zussman, J., (1963), Rock forming minerals. Fourth edition, Longmans, London, England.
- Denis, B.T., (1932), The chromite deposits of the Eastern Townships of the Province of Quebec: Que. Bur. Mines, Ann. Rept. pt. D, (1931).
- Dresser, J.A., (1913), Serpentine and associated rocks, southern Quebec: Geol. Survey, Canada, Mem. 22.
- Dubertret, L., (1953), Géologie des roches vertes du Nord-Ouest de la Syrie et de Hatay (Turquie): Mus. Nat. Hist. Nat. Notes et Mem. Moyen-Orient, v. 6.
- Enos, P., (1965), Anatomy of flysch, Middle Ordovician, chloridorme formation, northern Gaspé peninsula: Dissert. Abs., v. 26, p. 2133.
- Faessler, C., (1962), Analyses of rocks of the Province of Quebec: Quebec Dept. Nat. Resources.
- Graham, R.P.D., (1944), Serpentine Belt, Eastern Townships. In J.A. Dresser and T.C. Denis, Geology of Quebec: Que. Dept. Mines, Geol. Rept. 20, II, pp. 413-447.

- Green, D.H., (1964), The petrogenesis of the high-temperature peridotite intrusion in the Lizard area, Cornwall: Jour. Petrology, v. 5, pp. 134-188.
- _____ (1967), High-temperature peridotite intrusions. In P.J. Wyllie (Ed.), Ultramafic and related rocks, pp. 212-221: Wiley, New York, N.Y.
- Harvie, R., (1923), Thetford map-area: Geol. Survey, Canada, Unpub. Rept.
- Hess, H.H., (1933), The problem of serpentinization and the origin of certain chrysotile asbestos, talc and soapstone deposits: Econ. Geology, v. 28, pp. 634-657.
- _____ (1938), A primary peridotite magma: Am. Jour. Science, v. 35, pp. 321-344.
- _____ (1955), Serpentine, orogeny, epeirogeny: In A. Poldervaart (Ed.), Crust of the Earth: Geol. Soc. America, Special Paper 62, pp. 391-407.
- _____ (1960), Stillwater igneous complex, Montana; a quantitative mineralogical study: Geol. Soc. America, Mem. 80, 230 pages.
- Hess, H.H., and Otalora, G., (1964), Mineralogical and chemical composition of the Mayaguez serpentine cores, in a study of serpentine, the AMSOC core hole near Mayagüez, Puerto Rico: Nat. Acad. Science, Nat. Res. Council Pub. 1188, pp. 152-168.
- Innes, M.J., and Argun-Weston, A., (1967), Gravity measurements in Appalachia and their structural implications. In T.H.C. Clark (Ed.), Appalachian tectonics: Univ. Toronto Press.
- Irvine, T.N., (1965), Chromian spinel as a petrogenetic indicator: Can. Jour. Earth Sci., v. 2, pp. 648-671.
- _____ (1966), Chromian spinel as a petrogenetic indicator: Can. Jour. Earth Sci., v. 4, pp. 71-103.
- Irvine, T.N., and Smith, C.H., (1967), The ultramafic rocks of the Muskox intrusion, Northwest Territories, Canada. In P.J. Wyllie (Ed.), Ultramafic and related rocks, pp. 38-49: Wiley, New York, N.Y.
- Jackson, E.D., (1961), Primary textures and mineral associations in the ultramafic zone of the Stillwater Complex, Montana: U.S. Geol. Survey Prof. Paper 358.
- _____ (1967), Ultramafic cumulates in the Stillwater, Great Dyke and Bushveld intrusions. In P.J. Wyllie (Ed.), Ultramafic and related rocks, pp. 20-38: Wiley, New York, N.Y.

- Kaaden, G., van der, (1971), Chromite-bearing ultramafic and related gabbroic rocks and their relationship to "ophiolitic" extrusive basic rocks and diabases in Turkey: Geol. Soc. South Africa, Special publication 1, pp. 511-531.
- Keith, M.L., (1954), Phase equilibria in the system $MgO-Cr_2O_3-SiO_2$: Jour. Am. Ceram. Soc., v. 37, pp. 490-496.
- Knox, T.K., (1917), Southwestern part of the Thetford-Black Lake mining district: Geol. Survey, Canada, Summary Rept., pp. 229-245.
- Lamarche, R.Y., (1971), Ophiolites of southern Quebec: In the Publications of the Earth Physics Branch, Department of Energy, Mines and Resources, Ottawa: In press.
- Lappin, M.A., (1967), Structural and petrofabric studies of the dunites of Almklovdaalen, Nordfjord, Norway. In P.J. Wyllie (Ed.), Ultramafic and related rocks, pp. 183-190: Wiley, New York, N.Y.
- Leech, G.G., Lowden, J.A., Stockwell, G.H., and Wanless, R.K., (1963), Age determinations and geological studies: Geol. Survey, Canada, Paper 63-17.
- Lipman, P.W., (1964), Structure and origin of an ultramafic pluton in the Klamath Mountains, Calif.: Am. Jour. Sci., v. 262, pp. 199-222.
- Logan, W.E., (1863), Geology of Canada: Geol. Survey, Canada.
- MacGregor, I.D., (1961), Geology, petrology, geochemistry of the Mount Albert and associated ultramafic bodies of central Gaspé, Quebec: M.Sc. Thesis, 288 pages. Queen's University, Kingston, Canada.
- _____ (1967), Mineralogy and model mantle composition. In P.J. Wyllie (Ed.), Ultramafic and related rocks, pp. 382-393: Wiley, New York, N.Y.
- MacRae, N.D., (1969), Ultramafic intrusions of the Abitibi area, Ontario: Can. Jour. Earth Sci., v. 6, pp. 281-303.
- Manson, V., (1967), Geochemistry of basaltic rocks: Major elements. In H.H. Hess and A. Poldervaart (Eds.), Basalts, pp. 215-271: Interscience Publishers, New York, N.Y.
- Maratos, G., (1964), Les roches ultrabasiques et basiques de la Grèce: In R. Woodtli (Ed.), Methods of prospection for chromite: O.E.C.D., Paris, pp. 27-42.
- Marleau, R.A., (1968), Woburn-East Megantic-Armstrong area, Frontenac and Beauce Counties, Quebec: Quebec Dept. Nat. Resources, Geol. Rept. 131, 55 pages.

- Maxwell, J.C., (1970), The Mediterranean ophiolites and continental drift: To be published in H. Johnson (Ed.), The megatectonics of continents and oceans: Rutgers University Press.
- Miller, R., III, (1953), The Webster-Addie ultramafic ring, Jackson County, North Carolina, and secondary alteration of its chromite: *Am. Mineralogist*, v. 38, pp. 1134-1147.
- Moore, E.M., (1969), Petrology and structure of the Vourinos ophiolitic complex of northern Greece: *Geol. Soc. America, Special Paper No. 118*, 71 pages.
- Noble, J.A., and Taylor, H.P., (1960), Correlation of the ultramafic complexes of southeastern Alaska with those of the other parts of North America and the world: 21st Internat. Geol. Cong. Rept., Copenhagen, pt. XVII, pp. 176-197.
- O'Hara, M.J., (1963), Distribution of iron between coexisting olivines and calcium-poor pyroxenes in peridotites, gabbros and other magnesian environments: *Amer. Jour. Sci.*, v. 261, pp. 32-46.
- _____ (1967a), Mineral facies in ultrabasic rocks.
In P.J. Wyllie (Ed.), *Ultramafic and related rocks*, pp. 7-18: Wiley, New York, N.Y.
- _____ (1967b), Mineral paragenesis in ultramafic rocks.
In P.J. Wyllie (Ed.), *Ultramafic and related rocks*, pp. 393-403: Wiley, New York, N.Y.
- Olsen, E.J., (1961), High-temperature acid rocks associated with serpentine in eastern Quebec: *Am. Jour. Sci.*, v. 259, pp. 329-347.
- Osborn, E.F., (1969), The complementariness of orogenic andesite and alpine peridotite: *Geoch. Cosmochemica Acta*, v. 33, pp. 307-324.
- Pearre, C.N., and Heyl, A.V., Jr., (1960), Chromite and other mineral deposits in serpentine rocks of the Piedmont Upland, Maryland, Pennsylvania and Delaware: *U.S. Geol. Sur. Bull.* 1082-K.
- Poitevin, E., (1930), Chemical and mineralogical studies of some Quebec chromites: *Geol. Survey, Canada, Ann. Rept.*, Part D.
- Poole, W.H., (1967), Tectonic evolution of Appalachian region of Canada, *Geol. Ass. of Canada, Special Paper No. 4*, pp. 9-52.
- Ragan, D.M., (1967), The Twin Sisters dunite, Washington.
In P.J. Wyllie (Ed.), *Ultramafic and related rocks*, pp. 160-166: Wiley, New York, N.Y.
- Raleigh, C.B., (1967), Experimental deformation of ultramafic rocks and minerals. In P.J. Wyllie (Ed.), *Ultramafic and related rocks*, pp. 191-200: Wiley, New York, N.Y.

- Reinhardt, B.M., (1969), On the genesis and emplacement of ophiolites in the Oman Mountains geosyncline: Schweiz. Mineral. Petrogr. Mitt., v. 49, pp. 1-30.
- Ringwood, A.E., (1964), Mineralogy of the mantle. In P.M. Hurley (Ed.), Advances in earth sciences, pp. 357-399: M.I.T. Press.
- Riordon, P.H., (1952), Geology of the Thetford-Black Lake district of Quebec: Ph.D. Thesis, McGill University, Montreal, Canada.
- Roever, W.P., de, (1957), Sind die alpinotypen Peridotitmassen vielleicht tektonisch verfrachtete Bruchstücke der Peridotit-schale?: Geol. Rundschau, v. 46, pp. 137-147.
- Rost, F., (1959), Probleme ultrabasischer Gesteine und ihrer Lagerstätten: Freiburger Forschungshefte, v. 58, pp. 28-64.
- Rucklidge, J., (1967), Specification of a computer program for processing electron microprobe analytical data: Dept. of Geology, Univ. of Toronto, Canada.
- Sampson, E., (1929), May chromite crystallize late?: Econ. Geology, v. 24, pp. 632-649.
- _____ (1931), Varieties of chromite deposits: Econ. Geology, v. 26, pp. 833-839.
- Shams, F.A., (1964), Structures in chromite-bearing serpentinite Hindubagh, Zhob Valley, W. Pakistan: Econ. Geology, v. 59, pp. 1343-1347.
- Smith, C.H., (1958), Bay of Islands igneous complex, western Newfoundland: Geol. Survey, Canada, Mem. 290.
- _____ (1962), Ultramafic intrusions in Canada and their significance to Upper Mantle studies: Canadian Geophys. Bull., v. 14, pp. 151-169.
- Sørensen, H., (1967), Metamorphic and metasomatic processes in the formation of ultramafic rocks: In P.J. Wyllie (Ed.), Ultramafic and related rocks, pp. 204-212: Wiley, New York, N.Y.
- Steinmann, G., (1927), Die ophiolitischen Zonen in den Mediterranen Kettengebirgen: 14th Int. Geol. Congress Rept., Madrid, pt. 2, pp. 637-668.
- Stevens, E.R., (1944), Composition of some chromites of the Western Hemisphere: Am. Mineral., v. 29, pp. 1-34.
- Stockwell, C.H., (1944), Chromite deposits of the Eastern Townships, Quebec: Can. Min. Met. Bull., No. 382, pp. 71-86.

- Stoll, W.C., (1958), Geology and petrology of Masinloc chromite deposit, Zambales Complex, Luzon, Philippine Islands: Geol. Soc. America Bull., v. 69, pp. 419-448.
- Taylor, H.P., (1967), Stable isotope studies in ultramafic rocks and meteorites. In P.J. Wyllie (Ed.), Ultramafic and related rocks, pp. 362-375: Wiley, New York, N.Y.
- Tex, E., den, (1969), Origin of ultramafic rocks, their tectonic setting and history; a contribution to the discussion of the paper "The origin of ultramafic and ultrabasic rocks," by P.J. Wyllie: Tectonophysics, v. 7, pp. 457-487.
- Thayer, T.P., (1942), Chrome resources of Cuba: U.S. Geol. Survey Bull. 935-A, pp. 1-74.
- _____ (1946), Preliminary chemical correlation of chromite with the containing rocks: Econ. Geology, v. 41, pp. 202-217.
- _____ (1956); Mineralogy and geology of chromium: In M.J. Udy (Ed.), Chromium: chemistry of chromium and its compounds: Am. Chem. Soc. Mon. 132, pp. 14-52.
- _____ (1960), Some critical differences between alpine-type and stratiform peridotite-gabbro complexes: 21st Intern. Geol. Cong. Copenhagen, 1960, pt. XIII, pp. 247-259.
- _____ (1963), Flow layering in alpine peridotite-gabbro complexes: Mineralog. Soc. America, Special Paper 1, pp. 55-61.
- _____ (1964), Geologic features of podiform chromite deposits. In R. Woodtli (Ed.), Methods of prospection for chromite: O.E.C.D., Paris, pp. 135-148.
- _____ (1966), Serpentinization considered as a constant volume metasomatic process: Am. Mineral., v. 51, pp. 655-709.
- _____ (1967), Chemical and structural relations of ultramafic and feldspathic rocks in alpine intrusive complexes. In P.J. Wyllie (Ed.), Ultramafic and related rocks, pp. 222-239: Wiley, New York, N.Y.
- _____ (1969a), Gravity differentiation and magmatic reemplacment of podiform chromite deposits. In H.D.B. Wilson (Ed.), Symposium on magmatic ore deposits: Econ. Geology, Mon. 4.
- _____ (1969b), Alpine-type sensu strictu (ophiolitic) peridotites: Refractory residue from partial melting or igneous sediments? A contribution to the discussion of the Paper "The origin of ultramafic and ultrabasic rocks" by P.J. Wyllie: Tectonophysics, v. 7, pp. 511-515.
- _____ (1970), Chromite segregations as petrogenetic indicators. Geol. Soc. South Africa, Special publication 1, pp. 380-390.

- Turner, F.J., (1948), Mineralogical and structural evolution of the metamorphic rocks: Geol. Soc. America, Mem. 30.
- Turner, F.J., and Verhoogen, J., (1960), Igneous and metamorphic petrology (2nd edition): McGraw-Hill, New York, N.Y.
- Upadhyay, H.D., Dewey, J.F., and Neale, E.R.W., (1971), The Betts Cove Ophiolite Complex, Newfoundland: Appalachian Oceanic Crust and Mantle: Geol. Ass. Canada, Proceedings, v. 24, pp.27-34.
- Varma, O.P., (1964), Chromite deposits of the Keonjhar district, Orissa (India): Econ. Geology, v. 59, pp. 799-825.
- Vuagnat, M., (1963), Remarques sur la trilogie serpentinites-gabbros-diabases dans le bassin de la Mediterranée occidentale: Geol. Rdsch., v. 53, pp. 336-358.
- Wager, L.R., and Deer, W.A., (1939), The petrology of the Skaergaard intrusion, Kangerdlugssuaq, East Greenland: Meddelelser Om Grønland, v. 105, No. 4.
- Wager, L.R., and Wadsworth, W.J., (1960), Types of igneous cumulates: J. Petrol., v. 1, pp. 73-85.
- Wijkerslooth, P., de, (1954), Einiges über die Entstehung von Chromitkonzentrationen und Chromerzlagerstätten an Hand von neuen Beobachtungen in Anatolien: Neues Jhrb. Mineral. Abhandlung, v. 91, pp. 190-200.
- Williamson, J.T., (1933), The origin and occurrence of the chromite deposits of the Eastern Townships, Quebec: Ph.D. Thesis, McGill University, Montreal, Canada.
- Wyllie, P.J., (1960), The system CaO-MgO-FeO-SiO_2 and its bearing on the origin of ultrabasic and basic rocks. Mineral. Mag., v. 32, pp. 459-470.
- Zachos, K., (1964), Mineralization of the Greek serpentine: In R. Woodtli (Ed.), Methods of prospection for chromite: O.E.C.D., Paris, pp. 49-58.

APPENDIX I

Description and location of samples analysed for major elements (Table III) and minor elements (Table IV). Except sample K-1 (outside Map 2), the locations of all samples are indicated on Map 2.

K-5 : Amphibolite. 1 km ESE of Chalet Hill.

K-13: Diabase. From diabase dykes, SW face of Bengel Hill.

Gabbroic Suite

K-2 : Microgabbro xenolith in gabbro, on the river bed, 1 km. ESE of Chalet Hill.

K-3 : Medium-grained melanogabbro. Same location as K-2.

K-4 : Coarse-grained melanogabbro. Same location as K-2.

K-6 : Coarse melagabbro. $1\frac{1}{2}$ km SSW of Bengel Hill. In the field, no feldspar was identified in this sample. However, chemical analysis indicates high Al_2O_3 content from which the presence of feldspar is inferred.

K-7 : Coarsely granular gabbro. $1\frac{1}{2}$ km SSW of Bengel Hill.

K-8 : Gabbro. Same location as K-7.

K-20: Gabbro. West slope of Nadeau Hill.

Ultramafic Suite

K-10: Discordant pyroxenite cementing dunite breccia. WSW edge of Nadeau Hill.

K-9 : "Olivine" pyroxenite. SSW part of Bengel Hill.

K-16: Peridotite. Top of Caribou Mountain

K-22: Peridotite. Quarry Hill.

K-23: Peridotite. Quarry Hill.

K-30: Peridotite. On Highway 1, beside Lake Asbestos Mine

K-31: Peridotite. 1 km. NW of Murphy Hill.

K-32: Peridotite. King Mountains.

- K-33: Peridotite. NW part of Murphy Hill.
- K-17: Orthopyroxenite. Caribou Mountain.
- K-11: Serpentinized dunite. From a block in dunite breccia. WSW edge of Nadeau Hill.
- K-12: Serpentinized dunite. $\frac{1}{2}$ km W of Caribou Lake.
- K-24: Dunite, largely serpentinized. W slope of Quarry Hill.
- K-25: Serpentinized dunite. From the tailing of the Huard Mine. 900 m NW of Little Lake St. Francis.
- K-26: Serpentinized dunite. 800 m N of Little Lake St. Francis.
- K-27: Serpentinized dunite. From the tailing of a chromite pit. 1 km N of Little Lake St. Francis.
- K-1 : Serpentinite. From a serpentinite body, 4 km NW of Black Lake (Outside Map 2, see Map 1).
- K-28: Massive chromitite. From chromite workings on the S slope of Quarry Hill.
- K-29: Chromitite. From chromite workings, 500 m NW of Caribou Lake.

APPENDIX II

CHROMITE DEPOSITS

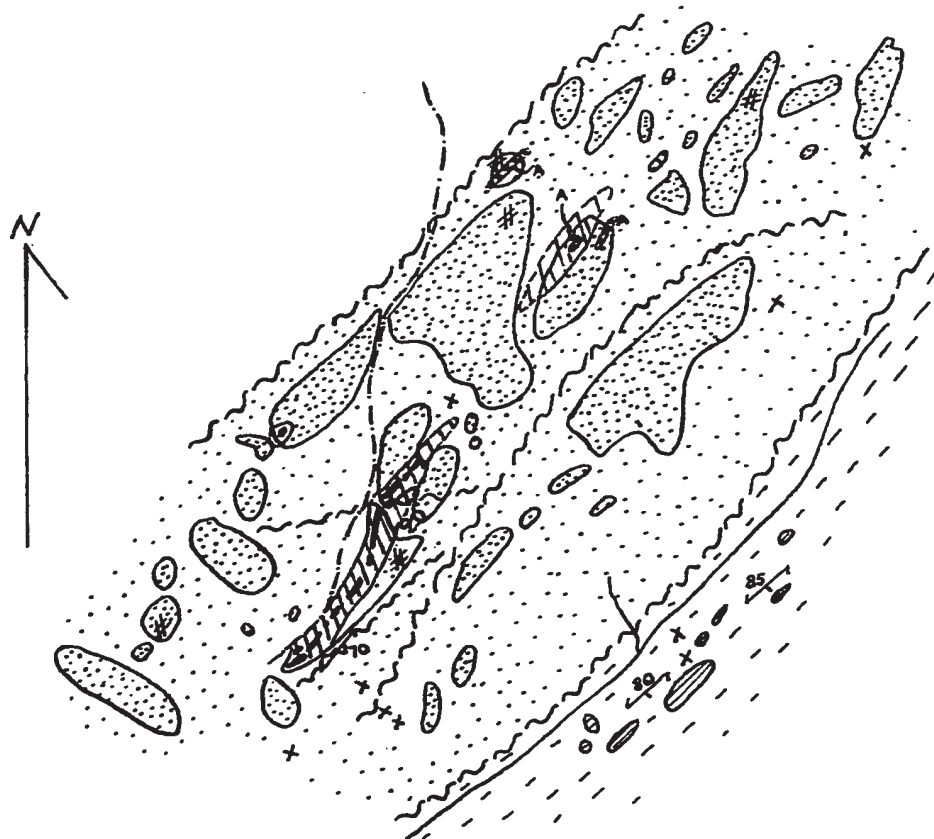
The Sterret Mine, in Cleveland Township, some 100 km. southwest of the map-area, is described below to serve as an example of ore zone. American Chrome Company's deposits typify irregularly distributed chromite deposits.

The Sterrett Mine

The Sterrett Mine is located 6 km. southeast of St. Cyr station on the Quebec Central Railway (St. Cyr is 9.5 km east-northeast of Richmond, in Cleveland Township, southern Quebec). It occurs in a narrow dunite lens which appears to be surrounded by peridotite (Fig. 109). The ultramafic rocks apparently form a southwest-northeast oriented "sill", 19 km. long and less than 1.6 km thick. The dunite is moderately schistose and the peridotite is usually rather poor in pyroxene. Graphitic slates to the east are similar to the grey slates of the St. Daniel Formation in the Thetford Mines district. The distribution of the open pits is shown in Fig. 110. The ore zone is 650 m. long, very narrow and has a vertical dip. According to a section given by Stockwell (1944, p. 76) the ore zone is cut by numerous, approximately east-west faults and three "acidic" dykes. The chromite occurs as chromitite layers with low chromite content. Apparently some massive schlieren, lenses and a few pods of chromitite were also present. The Sterrett Mine was opened in 1916 and was worked in 1917-18, producing nearly 16,000 tons of ore. The major part of the ore

STERRETT MINE

St. Cyr, Cleveland Tp., Richmond County, P. Q.



Scale: 1:15,340 approx.
 1 mile = 4 inches approx.

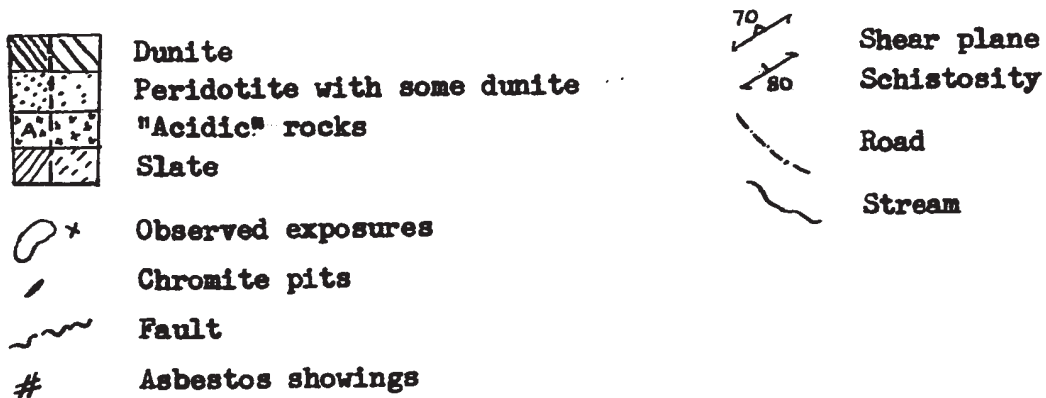


Figure 109. Geological plan of the area around the Sterrett Mine

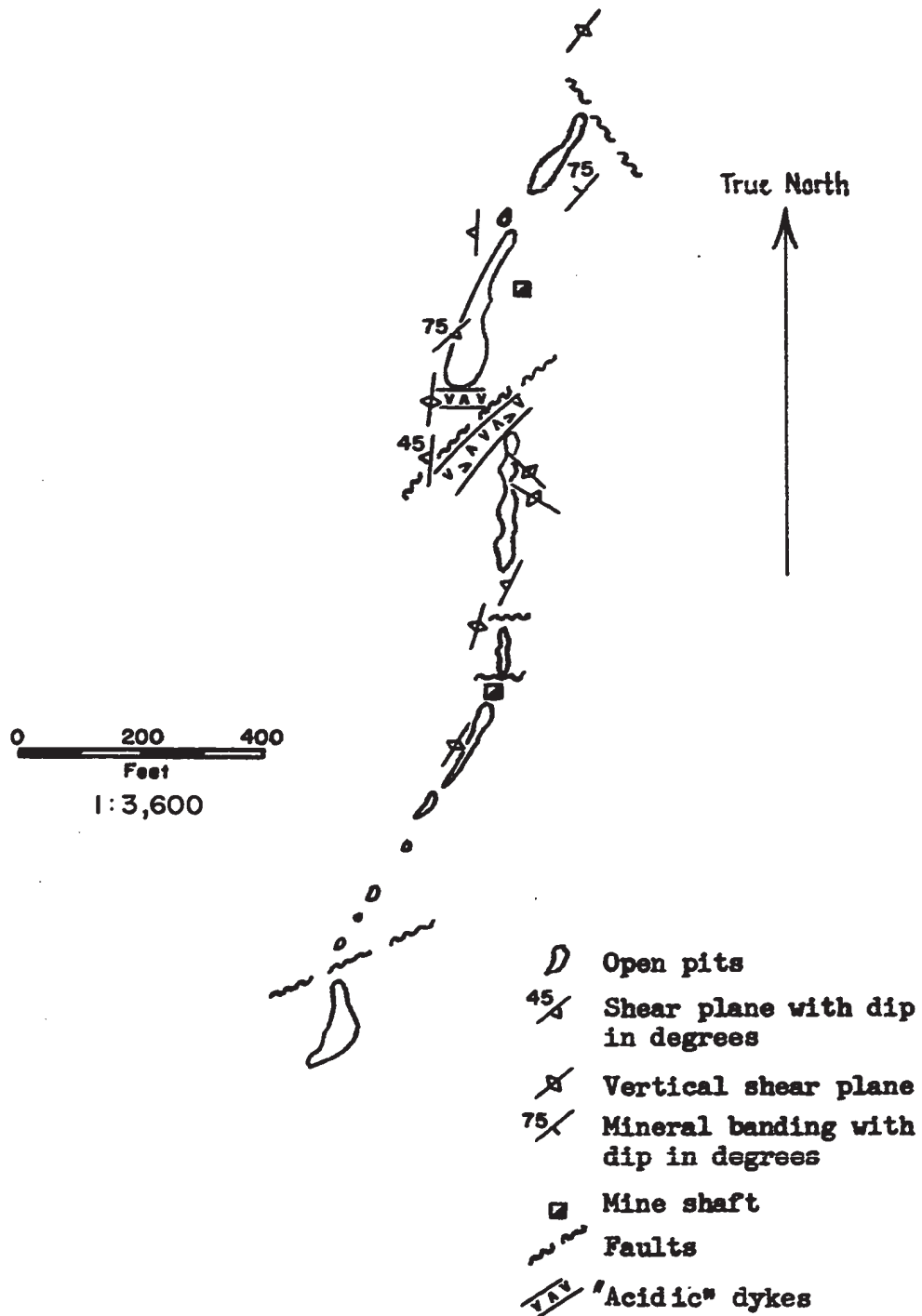


Figure 110. Distribution of open pits in Sterrett Mine
 Source of information:
 Denis (1932, p. 97)
 Stockwell (1944)
 Company Report; Union Carbide Exploration (Canada)
 Ltd.

was extracted from underground operations with drifts at 109 feet and 184 feet levels. During World War II the underground operations extended down to 280 feet level and an unrecorded quantity of ore was extracted.

American Chrome Company's Deposits

These deposits are situated 800 m to the south of Morin Hill. The distribution of the open pits is shown in Fig. 111. The chromitite occurs, in the main, as schlieren and short, irregular bands and lenses usually high in chromite content. The strike of the chromitite bands is irregular and commonly not parallel to the elongation of the pits. In the tailings from these deposits nodular chromitite and tightly folded chromitite bands have been observed.

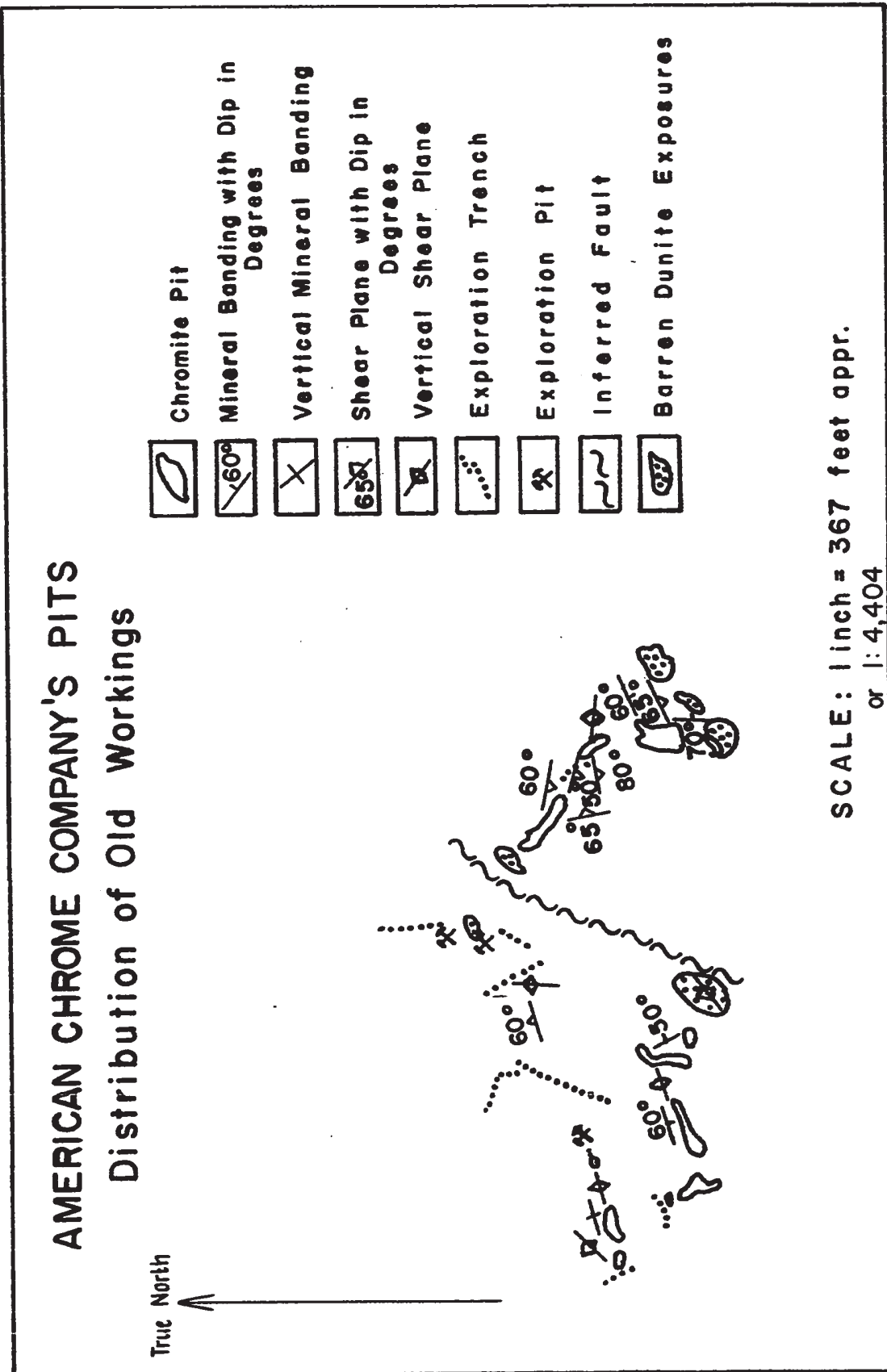


Figure 111.

APPENDIX III

CHEMICAL ANALYSES

A. Whole rock analyses

The chemical analyses of seven samples are listed in Table III. Norm calculations, according to the method by Barth (1962), are listed in Table IX. The presence of normative wollastonite in the samples K-6 and K-7 is due to excess silica in their norms. The excess silica is probably the result of low Na and K contents of the two samples so that little Si is used to make albite and orthoclase.

B. Whole rock trace element analyses

The whole rock trace element analyses are listed in Table IV. No precision and accuracy tests have been done for these analyses. Analyses of Cu, Co and Ti are semi-quantitative and errors up to $\pm 30\%$ can be expected. Vanadium, Cr, Ni and Mn analyses are quantitative and errors are expected to be less than $\pm 5\%$.

Serpentinization is postulated to have involved extensive movement of material (see Chapter VII) and hence some variation in trace element content of the rocks is likely to have occurred. Nickel released by serpentinization of olivine occurs as haezlewoodite, awaruite and as a nickel-iron alloy, randomly distributed in the rocks. It is possible that variation in Ni content of the ultramafic rocks is partly due to serpentinization.

TABLE IX

Molecular Norm Calculations¹ (in Mole. weight percent)

Ser.D.: serpentinitized dunite, Ol.Py.: "olivine" pyroxenite, Orp.: orthopyroxenite, Py.: pyroxenite.

Mineral	----- Gabbroic Suite -----			----- Ultramafic Suite -----			
	25-17* Gabbro	K-6 Melagabbro	K-7 Gabbro	K-10 Py.	K-2 Ol.Py.	K-17 Orp.	K-12 Ser.D.
Albite	23.773	1.577	2.135	0.645	0.558	0.172	-
Anorthite	31.038	13.788	29.512	4.262	2.997	4.336	-
Apatite	0.554	-	-	-	-	-	-
Acmite	-	-	-	-	-	-	0.076
Calcite	-	0.157	0.105	0.234	0.402	0.243	1.091
Diopside	17.438	-	-	26.998	23.924	1.721	-
Hypersthene	10.433	62.013	50.348	57.906	37.702	71.472	6.595
Ilmenite	2.270	0.043	0.043	0.057	0.043	0.027	0.337
Forsterite	5.286	-	-	4.633	27.899	18.996	86.499
Fayalite	2.228	-	-	0.399	1.637	1.077	2.418
Magnetite	2.768	1.242	1.405	4.516	4.592	1.816	3.240
Orthoclase	4.211	0.183	0.244	0.242	0.122	0.113	0.187
Pyrite	-	0.027	0.027	0.107	0.054	0.025	0.055
Wollastonite	-	14.244	14.333	-	-	-	-
Quartz	-	6.725	1.849	-	-	-	-

¹ Calculated according to the method by Barth (1962)

* Gabbro: Munro Lake Sill (Differentiated basic sill), Lake Abitibi area, Ont., MacRae, 1969, p. 303.

** Average of 127 "superior" analyses of gabbro, collected from literature. Manson, 1967, p. 227.

These two gabbro analyses from literature are included here for comparison with the present gabbro analyses.

C. Mineral analyses

Analytical procedure

The constituent minerals of the rocks have been analysed with an electron microprobe analyser (Model 400, Material Analyses Co.). The potential used was 15 Kv. and the count time was 10 seconds. A sample current of approximately 0.01 microampere was used for the silicate minerals, the sample current for chromite was 0.012-0.014 microampere. The data was standardized using chemically analysed natural minerals approximating the composition of the unknown materials. The microprobe data were reduced using a computer program by Rucklidge (1967).

Presentation of the data

The locations of all the analysed samples are indicated on Map 2. Analyses for all the analysed points are listed in Table XI. In the numbering of analyses (e.g. 92 2B), the first number (92) is the sample number, the second (2) is the number of a grain in that sample and a letter (B) designates the analysed point in the grain. When there is only one analysis for a given grain, there is no letter (e.g. 82 1).

The mean composition of the minerals in each sample has been presented as tables in the text. Except for olivine, the arithmetic mean of all the analyses in a given sample has been taken as the composition of the mineral in that sample. For olivine, the mean value for each analysed grain has been calculated and the mean composition of all the analysed grains in a sample is given as the composition of olivine in that sample. This different treatment was made to obtain a finer average for olivine, since compositional variations are very small for this mineral.

TABLE X

Precision and accuracy of mineral analyses

A. Precision: Standard deviation in percent of the mean value
(to the nearest whole number)

Element	Mineral		
	<u>Chromite</u>	<u>Olivine</u>	<u>Orthopyroxene</u>
Cr	2	28	25
Fe _{total}	4	3	2
Mg	3	3	2
Al	4	-	15
Ti	10	-	-
Si	-	4	5
Ca	-	-	15
Ni	-	15	-

B. Accuracy: Highest deviation in cation weight percent (should read \pm)

Cr	2.4	-	0.25
Fe _{total}	2.7	0.8	1.1
Mg	1.2	1.9	1.6
Al	1.5	-	0.40
Ti	0.30	-	-
Si	-	2.1	2.8
Ca	-	-	0.40
Ni	-	0.15	-

C. Accuracy: Mean deviation of analysed values from their true values
in cation weight percent (should read \pm)

Cr	1.3	-	0.1
Fe _{total}	1.1	0.4	0.4
Mg	0.6	0.9	0.8
Al	0.5	-	0.25
Ti	0.1	-	-
Si	-	1.3	1.5
Ca	-	-	0.15
Ni	-	0.08	-

Precision and accuracy

Precision and accuracy tests have been done for chromite (24 test analyses), olivine (17 test analyses) and orthopyroxene (14 test analyses).

In estimating precision and accuracy, test samples are assumed to be homogeneous. Furthermore, obviously inaccurate analyses (e.g. where total oxides were greater than 108) have been eliminated (the same has been done for analyses of samples).

Precision is given (Table X, A) as standard deviation in percent of the mean value of the element in the test analyses.

To estimate accuracy, test samples of known composition were analysed. For any given element the highest deviations (errors) above and below its true value have been averaged (thus average of two values for each element) and are listed in Table X, B. It is hoped that this will convey a better idea about the errors to be expected in analyses listed in Table XI. In Table X, C, mean deviations (standard errors) are listed as cation weight percent. These latter values probably reflect better the errors in the mean composition of minerals listed in Tables V to VIII in the text.

TABLE XI
MICROPROBE ANALYSES OF MINERALS

A) CHROMITE ANALYSES

Cations wt.%

Accessory chromite in "olivine" pyroxenite (K-9, 189) and "herzolite" (154, 391)

Sample No.	Cr	Fe	Mg	Al	Ti
K-9 1A	26.94	23.30	5.51	10.88	0.22
1B	26.75	23.78	5.48	10.79	0.24
2A	29.02	22.64	5.95	11.16	0.13
2B	29.05	19.47	6.00	10.99	0.26
189 1A	30.74	24.82	4.19	8.73	0.14
1B	26.43	25.55	5.02	10.98	0.16
2	30.99	23.72	4.80	8.91	0.13
3	27.68	25.35	4.75	10.15	0.12
4	30.86	23.82	4.60	9.34	0.13
5	28.88	24.28	4.29	10.29	0.11
6	29.98	24.79	4.25	9.43	0.11
154 1A	36.87	22.01	4.86	6.33	0.08
2A	37.37	21.55	5.40	6.56	0.05
2B	37.56	22.12	5.10	6.59	0.05
3	37.87	22.61	4.56	6.52	-
4	37.23	23.30	4.15	6.27	0.07
6A	37.46	21.53	5.01	6.73	0.05
6B	37.30	22.13	4.81	6.69	0.08
391 1A	33.06	21.04	6.84	8.44	0.13
1B	33.38	17.82	6.02	8.49	0.10
2A	32.00	23.18	5.02	8.80	0.09
3	31.40	24.92	3.99	8.62	0.11
4	31.88	25.18	4.23	8.34	0.10
5	32.10	24.89	4.09	8.31	0.12

Accessory chromite in peridotite and olivine orthopyroxenite (K-57)

A		18.20	11.34	10.79	21.97	0.14
B	1A	23.72	12.03	9.82	17.50	0.01
	1B	23.71	12.18	9.95	18.31	0.01
	2A	24.05	11.78	9.97	18.07	0.04
	2B	23.81	12.70	9.48	18.30	-
	2C	23.35	11.75	10.26	17.93	0.01
C	1	29.97	12.49	8.97	13.31	0.03
	2A	31.02	13.03	8.71	12.74	0.03
	2B	30.32	12.96	8.22	11.84	0.03
D	1A	18.35	10.32	11.60	21.30	0.04
	1B	17.27	10.20	11.25	21.74	0.04
	2A	18.89	10.78	11.03	24.04	0.08
	2B	19.83	10.58	12.21	18.92	0.10
	2C	18.56	11.01	11.31	20.12	0.08

Accessory chromite in peridotite and olivine orthopyroxenite

Sample No.	Cr	Fe	Mg	Al	Ti
E 1	18.31	11.26	10.69	20.52	0.04
2	18.35	11.56	11.22	21.75	0.03
3	18.68	11.31	10.61	20.17	-
4	18.11	11.20	11.38	20.81	-
5A	21.26	11.31	10.44	18.50	-
5B	24.20	11.54	10.46	19.12	-
F 1	26.12	13.22	9.38	16.37	-
2A	26.57	13.36	9.53	16.62	0.04
2B	26.18	12.97	9.59	16.94	0.03
2C	24.60	13.08	9.94	17.62	0.03
3A	16.68	13.17	9.67	15.68	0.02
3B	25.73	13.99	9.37	17.18	0.04
G 1A	33.59	14.40	6.74	10.56	0.06
1B	33.45	14.67	7.02	10.64	-
2A	34.15	13.91	6.98	10.55	0.04
2B	33.66	14.35	7.19	10.72	-
H 2	24.45	12.32	10.47	16.34	0.06
3A	24.71	12.49	10.10	16.25	0.05
3B	23.73	12.94	9.94	15.67	0.03
I 1A	28.96	13.48	8.57	12.45	0.05
1B	28.94	13.42	8.56	13.14	0.04
2A	29.27	13.81	9.27	13.25	0.06
2B	29.55	13.41	9.29	13.41	0.05
2C	28.78	14.18	9.79	14.37	0.07
3A	28.99	13.55	9.42	13.01	0.05
3B	28.81	12.44	7.92	12.91	-
K-57 1A	30.05	15.03	9.85	12.95	0.01
1B	30.35	15.10	8.68	13.02	0.03
1C	29.85	15.44	5.82	12.59	-
1D	30.66	15.22	8.51	13.10	0.02
2A	29.64	15.48	7.64	13.18	0.04
2B	29.15	15.47	7.02	13.34	-
2C	28.41	16.04	6.71	14.31	0.02
K-58 1	39.94	17.76	5.73	7.63	0.08
2A	40.39	16.89	5.38	7.50	0.10
2B	40.17	15.49	6.03	7.86	0.09
3	39.22	15.88	6.25	8.03	0.10
4A	39.40	18.36	4.95	7.70	0.09
4B	40.14	17.61	5.26	7.91	0.12
48 1	30.65	14.54	9.49	13.35	0.09
2	31.30	14.11	9.52	12.54	0.09
56 1A	35.48	17.77	5.90	9.61	-
1B	35.36	18.24	5.90	8.97	-
1C	35.05	18.29	5.50	8.69	-
1D	35.54	18.31	5.99	8.90	-
58 1A	31.93	18.57	4.62	7.42	0.02
1B	31.84	19.36	4.79	7.83	0.03
2A	31.53	19.29	4.56	7.36	0.04
2B	30.88	20.10	3.58	7.41	0.03
65 1A	33.67	15.36	7.41	8.85	-
1B	32.07	15.02	7.66	9.15	0.06

Accessory chromite in peridotite and olivine orthopyroxenite (Cont.)

Sample No.	Cr	Fe	Mg	Al	Ti
65 1C	29.91	19.38	5.67	10.21	0.03
1D	30.10	17.47	6.23	9.79	0.05
1E	33.41	15.15	6.85	8.16	0.01
2A	30.58	16.40	6.79	9.15	0.03
2B	30.15	16.58	6.24	9.33	0.03
2C	30.21	20.02	4.19	9.44	0.01
3A	31.04	16.18	5.63	10.08	0.07
3B	30.94	18.19	4.19	9.35	0.03
3C	30.54	19.18	4.51	9.10	0.07
72 1A	32.08	15.66	8.31	10.52	0.10
1B	33.73	15.68	7.08	9.86	0.11
1C	30.80	15.75	7.85	9.85	0.08
2A	30.53	15.26	7.38	9.56	0.14
2B	33.60	15.45	6.30	9.05	0.13
87 2	28.58	15.18	9.05	14.33	0.11
3	29.71	15.43	7.55	13.69	0.11
4	30.38	15.60	8.24	14.34	0.11
218 1A	39.93	14.99	7.12	8.62	0.04
1B	39.50	14.35	6.86	8.80	0.06
2A	39.78	15.34	7.26	8.44	0.05
2B	39.54	14.81	7.02	6.13	0.06
2C	37.88	15.45	7.20	9.22	0.06
221 1	29.14	17.06	6.53	13.25	0.19
2	28.55	16.37	6.89	13.62	0.22
3	27.91	16.58	8.15	13.89	0.20
4	28.01	15.70	8.00	14.16	0.21
5	28.35	16.20	8.16	14.15	0.18
225 1A	26.51	13.36	8.84	14.20	-
1B	28.79	14.11	8.00	12.14	-
2A	28.71	13.34	8.88	13.19	-
2B	29.22	14.01	8.32	12.44	-
3A	28.14	14.01	7.24	13.29	-
3B	19.87	14.24	7.90	11.66	-
4	28.60	16.07	7.52	12.33	-
5A	29.40	14.83	8.25	11.97	-
5B	28.84	14.92	8.60	12.28	-
258 1A	34.21	15.54	6.83	8.70	0.01
1B	33.30	16.80	5.84	9.19	0.02
1C	33.47	15.89	6.67	9.65	0.01
2A	32.66	15.73	5.34	9.53	-
2B	32.19	15.41	6.19	9.58	0.01
3A	33.31	16.16	6.91	10.59	-
3B	31.82	16.28	5.71	10.97	0.01
4	31.81	16.85	5.95	10.86	0.02
366 1A	23.13	12.06	9.88	18.29	0.03
1B	23.12	11.75	10.60	18.31	0.04
1C	23.97	8.28	10.35	17.91	0.05
476 1A	21.10	14.11	9.22	14.98	0.03
1B	20.47	15.16	9.49	15.16	0.02
2A	18.15	11.27	9.65	17.73	0.02
2B	19.05	11.84	10.41	17.54	0.08

Accessory chromite in peridotite and olivine orthopyroxenite (Cont.)

Sample No.	Cr	Fe	Mg	Al	Ti
554 1	35.01	18.23	5.44	8.61	0.17
2A	34.49	19.90	5.50	7.85	0.14
2B	35.86	18.73	5.78	7.71	0.05

Accessory chromite in chromitite-bearing dunite bodies in peridotite

N-6 1	37.61	14.72	8.94	7.67	0.05
2	37.13	14.76	7.60	6.99	0.03
3	37.76	14.36	7.96	7.64	0.04
4	37.28	15.49	6.57	6.11	0.06
5	39.24	14.33	7.66	6.24	0.05
228 1A	37.02	17.99	5.88	8.24	0.10
1B	37.48	17.23	6.35	8.99	0.09
1C	35.91	17.55	6.07	9.75	0.08
2A	37.02	16.00	6.39	8.81	0.11
2B	37.99	16.15	6.08	9.05	0.09
3A	37.63	15.90	6.10	7.86	0.10
3B	36.96	16.48	6.13	8.40	0.13
4A	37.48	13.87	7.08	7.10	0.09
4B	37.28	13.68	7.12	8.04	0.08
4C	39.48	13.67	7.09	6.88	0.09
5A	38.48	13.56	7.32	7.42	0.09
5B	38.47	13.02	7.55	8.86	0.09
364 5A	37.52	15.08	9.05	6.34	0.07
5B	36.57	18.35	9.27	4.16	0.07
6A	38.18	15.10	8.20	6.94	0.09
6B	38.83	14.31	7.81	6.65	0.07
369 1	39.91	17.41	5.07	5.68	0.06
2A	40.27	15.56	5.74	6.65	0.07
2B	39.62	17.88	5.93	6.02	0.08
3	39.88	16.53	5.94	5.74	0.08
4	40.70	15.77	5.94	7.04	0.08
5A	41.33	15.35	6.30	6.68	0.07
5B	40.50	16.92	5.75	6.09	0.07
6A	40.88	16.05	5.85	5.83	0.06
6B	40.35	18.04	5.32	5.77	0.09
7	40.74	16.53	6.01	5.37	0.07

Accessory chromite in dunite layer (57) and dunite body (236) in peridotite

57 1A	32.32	18.83	6.01	8.23	0.19
1B	31.38	19.51	5.05	7.70	0.19
2A	31.92	18.93	6.28	8.31	0.23
2B	31.00	20.64	6.29	7.74	0.22
3A	32.46	18.59	6.62	7.64	0.20
3B	31.79	19.13	5.83	7.77	0.23
4A	32.15	18.80	6.16	7.81	0.20
4B	31.49	20.30	5.73	7.85	0.20
5	32.45	19.92	6.54	7.97	0.25
6	30.54	20.68	6.39	8.14	0.25

Accessory chromite in dunite layer (57) and dunite body (236) in peridotite (Cont.)

Sample No.	Cr	Fe	Mg	Al	Ti
236 1A	39.39	17.38	4.08	4.75	0.06
1B	38.57	21.81	3.19	5.76	0.05
2	38.97	20.27	4.13	6.06	0.06

Accessory chromite in dunite from the Olivine Pyroxenite Zone

138 1A	36.27	23.82	3.52	4.06	0.08
1B	35.31	26.50	3.31	4.60	0.10
2A	36.63	24.24	3.20	3.96	0.11
2B	36.84	25.32	3.17	4.07	0.10
3	35.73	25.69	3.06	4.08	0.11
4A	37.16	23.76	3.28	5.77	0.10
4B	38.48	23.62	3.63	4.11	0.11
4C	36.13	26.34	2.94	5.07	0.12
161 1A	27.95	23.26	7.20	9.07	0.18
1B	25.56	27.02	3.75	10.41	0.19
1C	26.00	25.62	4.69	10.07	0.18
2	25.98	26.64	3.99	11.13	0.19
3A	26.58	24.43	4.57	11.41	0.19
3B	25.74	25.95	3.89	12.08	0.22
4	25.75	25.50	4.14	11.77	0.18
5A	27.83	23.51	4.97	11.08	0.17
5B	24.36	25.56	3.65	11.36	0.19
6	27.04	23.63	4.54	10.91	0.17
7A	29.51	22.39	5.43	9.29	0.11
7B	25.96	25.65	3.92	11.18	0.22

Accessory and disseminated chromite in dunite from dunite zones

K-611	38.73	21.51	3.97	6.06	0.08
2	37.46	23.67	3.43	5.95	0.08
3A	39.23	21.29	4.06	5.91	0.08
3B	38.53	21.26	4.27	5.84	0.09
4	38.68	23.32	3.14	5.50	0.08
27 1A	36.07	16.77	7.34	6.51	0.13
1B	36.48	17.66	6.49	6.40	0.14
2A	36.11	15.54	6.25	7.41	0.14
2B	36.30	18.84	5.66	6.92	0.14
3	36.32	19.72	6.33	6.60	0.13
4A	35.90	18.94	6.34	7.20	0.13
4B	36.76	19.14	6.30	7.01	0.13
5A	37.01	18.81	5.69	7.88	0.14
5B	34.83	19.22	6.67	8.11	0.14
5C	37.78	19.14	6.16	5.79	0.14
28 1A	37.85	17.45	6.80	6.42	0.16
1B	37.64	17.40	6.17	7.38	0.14
2A	36.59	18.06	6.43	7.17	0.16
2B	36.07	18.38	6.10	9.11	0.16
3	17.37	17.75	6.49	6.18	0.16
4A	36.65	18.11	6.20	8.48	0.16

Accessory and disseminated chromite in dunite from dunite zones (Cont.)

Sample No.	Cr	Fe	Mg	Al	Ti
28 4B	36.17	18.36	6.30	8.80	0.11
7A	36.25	18.41	6.44	7.69	0.17
7B	35.25	18.62	6.62	7.78	0.14
7C	37.89	18.80	6.59	7.27	0.15
8	37.58	17.33	6.66	5.44	0.14
30 1	37.95	17.95	7.04	6.52	0.10
2	37.66	18.12	6.64	6.88	0.11
3	38.89	17.09	7.68	6.95	0.10
4	38.44	18.11	7.39	6.72	0.12
5	38.91	17.04	7.53	6.72	0.10
7	39.03	17.58	7.36	6.64	0.11
31 1A	39.21	17.68	4.97	5.95	0.09
1B	38.59	18.32	5.14	7.04	0.13
2A	37.96	17.79	4.84	7.56	0.11
2B	37.44	21.04	3.22	6.98	0.14
2C	38.05	17.77	6.07	7.84	0.10
3A	37.35	17.19	4.77	7.69	0.10
3B	35.62	17.61	5.49	7.77	0.10
35 1A	40.18	13.88	9.88	6.92	0.14
1B	39.87	13.48	9.57	6.69	0.15
1C	38.87	14.07	8.86	6.74	0.15
3	39.45	13.26	9.78	6.66	0.11
4A	40.18	13.10	9.10	6.57	0.11
4B	39.75	13.71	8.95	6.68	0.12
6A	39.62	13.33	8.94	6.63	0.10
6B	38.52	13.86	8.84	7.16	0.12
6C	39.93	13.27	8.98	6.22	0.12
41 1A	37.72	20.17	4.13	6.18	0.11
1B	37.16	21.25	4.53	5.69	0.10
1C	37.40	20.72	4.40	6.91	0.10
2A	38.94	20.33	5.06	6.87	0.10
2B	37.22	20.87	4.70	6.85	0.14
3A	39.45	19.74	3.93	5.34	0.11
3B	39.73	19.94	5.17	5.01	0.11
3C	38.70	20.54	4.01	5.60	0.13
4A	39.10	19.90	4.62	6.05	0.09
4B	38.16	20.32	4.58	6.50	0.14
5	37.87	20.69	3.46	5.92	0.13
42 1	34.57	21.00	5.65	6.42	0.15
2B	34.29	21.05	5.06	6.20	0.12
2C	33.10	23.77	4.92	7.25	0.14
3	34.59	21.29	5.40	4.95	0.15
4	33.96	21.98	5.07	7.11	0.14
5A	34.40	20.97	5.44	6.31	0.15
5B	33.84	21.48	5.38	6.44	0.16
47 1A	35.94	13.84	5.82	7.25	0.07
1B	36.57	14.26	5.98	6.79	0.08
1C	35.65	14.33	6.23	6.07	0.09
3A	36.43	13.65	6.79	5.65	0.09
3B	35.89	13.59	6.84	7.15	0.11

Accessory and disseminated chromite in dumite from dumite zones (Cont.)

Sample No.	Cr	Fe	Mg	Al	Ti
47 3C	36.41	13.91	6.73	5.46	0.08
4A	35.87	15.34	5.98	6.34	0.09
4B	36.27	15.90	5.46	6.02	0.12
5	35.88	14.96	5.85	6.95	0.13
61 1A	38.90	17.73	3.74	4.94	0.07
1B	37.55	19.09	4.32	5.29	0.04
2A	39.08	17.45	3.79	4.93	0.05
2B	37.87	18.29	4.05	5.24	0.06
3A	38.62	16.00	4.91	5.85	0.06
3B	38.93	16.26	4.88	6.05	0.06
4	38.17	18.17	3.57	5.96	0.11
5	37.68	16.84	3.88	5.69	-
116 1A	36.20	16.23	5.69	7.12	0.06
1B	34.38	22.38	3.29	6.84	0.05
1C	35.41	21.19	3.71	7.06	0.07
1D	33.35	22.51	3.82	7.88	0.08
2A	36.49	17.04	6.32	6.63	0.07
2B	34.66	18.11	6.19	7.45	0.06
3A	36.25	16.48	4.93	6.82	0.08
3B	35.15	18.76	4.18	6.43	0.07
380 1A	37.14	17.67	5.99	6.63	0.11
1B	38.14	17.40	5.26	6.15	0.09
1C	37.47	17.64	5.96	7.00	0.09
2B	37.73	18.17	5.50	5.22	0.09
2C	37.59	18.63	5.21	5.82	0.08
3	38.43	18.09	5.46	5.89	0.09
4A	38.64	17.25	5.97	6.67	0.23
4B	38.15	16.89	5.54	6.60	0.09
5A	38.39	17.98	5.72	6.47	0.12
5B	36.89	18.66	4.92	7.28	0.11
6A	38.63	15.90	6.90	6.01	0.06
6B	38.76	15.60	6.70	7.00	0.08
7A	38.92	15.83	6.51	6.63	0.09
7B	39.55	15.21	6.83	7.41	0.10
8A	39.15	16.34	5.87	6.07	0.09
8B	39.33	15.99	6.50	6.15	0.10

Chromitite within dumite bodies in peridotite

N-8 1A	41.64	12.04	7.28	5.48	0.05
1B	40.80	11.97	7.79	5.81	0.06
2A	40.69	11.65	8.55	5.44	0.08
2B	40.80	11.49	7.71	6.38	0.11
3	40.29	13.01	7.17	6.44	0.04
82 1	40.11	16.23	6.44	6.95	0.08
2	41.31	15.79	6.44	6.94	0.09
3	40.72	16.44	5.67	7.16	0.06
4A	40.68	16.16	6.21	7.27	0.09
4B	40.60	15.86	6.09	7.83	0.07

Chromitite within dunite bodies in peridotite (Cont.)

Sample No.	Cr	Fe	Mg	Al	Ti
86 1A	34.38	18.21	6.38	6.40	-
1B	34.14	17.73	6.29	6.21	-
2A	35.69	17.77	6.58	6.32	0.04
2B	34.64	17.74	6.05	6.80	0.01
90 1A	40.58	14.68	7.41	4.56	-
1B	40.22	14.66	6.26	4.91	-
2A	40.82	14.44	8.22	5.43	-
2B	40.05	14.39	8.04	5.37	-
3A	39.56	16.18	6.18	5.67	-
3B	39.99	15.36	7.45	5.79	-
92 2	38.96	12.62	9.28	5.99	0.11
3A	38.03	14.68	6.67	5.56	0.09
3B	38.52	14.49	6.07	6.37	0.08
4A	39.97	15.33	7.72	5.53	0.09
4B	38.58	15.64	7.13	5.79	0.11
5A	38.94	15.65	9.21	5.49	0.13
5B	39.12	14.78	9.02	6.16	0.11
343 1A	40.37	12.96	7.05	5.63	0.03
1B	39.89	12.16	8.21	6.45	-
2A	39.75	12.47	8.12	6.27	0.05
2B	39.76	11.84	8.49	6.77	0.02
3A	40.18	11.92	8.15	6.20	0.06
3B	41.65	12.66	7.22	6.02	0.05
350 1A	41.31	14.45	7.15	4.73	0.03
1B	40.97	14.65	7.33	5.26	0.07
2A	40.74	14.28	7.03	5.11	0.05
2B	39.43	14.61	8.46	4.13	0.02
351 1	38.52	12.74	7.01	7.34	0.08
2A	38.84	13.07	7.84	5.82	0.09
2B	38.05	12.83	7.58	7.09	0.12
3	38.72	12.92	7.54	6.51	0.08
364 1A	39.29	12.78	10.17	6.42	0.06
1B	38.41	13.32	8.74	6.71	0.05
1C	38.76	12.73	8.38	5.57	0.05
1D	38.84	12.91	9.16	6.82	0.06
2	39.02	12.67	9.01	7.07	0.04
3	38.46	12.61	9.54	6.97	0.08
4A	37.43	12.37	7.65	5.84	0.09
4B	36.72	13.66	7.56	5.87	0.06

Chromite in chromitite from dunite zones

G-1 1A	37.32	11.89	9.76	6.91	0.10
1B	37.19	12.13	9.85	7.44	0.09
2	37.86	11.43	8.98	7.61	0.19
M-2 1A	34.31	12.59	8.81	10.39	0.14
1B	34.71	12.59	7.65	9.69	0.12
1C	34.33	12.84	8.54	8.93	0.15
1D	34.23	13.01	8.71	10.23	0.15
1E	33.86	12.89	9.15	9.86	0.11
2A	33.72	12.37	9.02	9.67	0.14

Chromite in chromitite from dunite zones (Cont.)

Sample No.	Cr	Fe	Mg	Al	Ti
M-2 2B	33.14	11.91	9.38	11.25	0.10
3	34.15	12.33	8.80	9.89	0.15
4A	33.71	12.57	9.44	9.12	0.12
4B	34.51	12.06	8.52	11.01	0.13
M-5 1A	33.82	13.93	9.30	10.14	0.16
1B	34.31	13.71	8.37	9.45	0.16
2A	34.20	13.86	8.11	9.48	0.13
2B	33.97	14.03	7.83	9.26	0.18
3	33.19	13.83	8.10	9.53	0.14
6 1B	39.39	14.02	10.40	5.28	0.11
1C	39.26	14.61	9.27	5.70	0.11
2A	39.07	15.23	9.10	5.33	0.12
2B	39.58	15.87	9.54	5.35	0.12
3	39.45	14.56	9.83	5.10	0.10
4	39.65	15.65	9.70	5.00	0.10
44 1A	39.25	12.14	8.44	6.96	0.12
1B	38.95	11.94	8.68	6.33	0.10
2A	38.51	11.63	8.13	7.00	0.10
2B	38.58	12.84	7.66	7.52	0.13
3	39.66	12.31	8.93	6.08	0.08
4	39.97	12.12	8.21	5.69	0.09
45 1A	36.46	14.50	7.33	6.41	0.04
1B	37.38	13.84	7.24	5.32	0.07
2A	37.81	13.78	8.30	5.86	0.07
2B	35.88	13.63	7.93	5.58	0.06
3	36.88	14.06	8.28	5.69	0.09
46 1	40.75	11.02	8.62	5.96	0.12
2	40.51	11.40	8.69	5.91	0.14
3	40.05	10.85	8.29	6.19	0.14
4	40.02	10.86	8.97	6.04	0.13
5	40.64	10.44	8.56	5.96	0.16
98 1A	40.34	12.12	7.89	5.88	-
1B	40.73	11.85	8.32	5.55	-
2	40.75	12.85	8.29	5.89	0.04
3	40.90	12.51	8.17	5.28	-
104 2A	39.83	14.23	9.88	5.36	0.08
2B	39.97	14.72	10.34	5.76	0.09
111 1A	38.66	15.47	6.47	5.58	0.07
1B	39.20	15.63	6.03	4.68	0.07
1C	38.31	15.85	6.40	5.17	0.08
2A	38.99	15.60	6.47	6.05	0.08
2B	38.46	15.14	6.42	6.04	0.10
3	39.36	15.35	6.74	5.88	0.09
4A	37.75	15.57	6.65	4.94	0.10
4B	38.31	15.95	6.73	5.15	0.11
4C	38.23	15.81	6.60	5.03	0.10
5	37.82	15.80	6.48	5.62	0.10
114 1A	36.03	12.23	6.76	9.38	0.04
1B	34.99	12.87	7.87	9.91	0.04
2A	34.18	12.95	9.06	9.49	0.07
2B	35.12	12.57	7.92	10.82	0.07

Chromite in chromitite from dunite zones (Cont.)

Sample No.	Cr	Fe	Mg	Al	Ti
114 3A	34.60	13.16	7.67	9.69	0.05
3B	35.26	12.92	8.06	10.58	0.07
4A	34.11	12.52	8.68	11.30	0.05
4B	34.26	12.84	9.12	11.42	0.07
121 1	38.11	13.38	9.16	7.00	0.06
2A	39.34	13.43	9.13	6.66	0.02
2B	38.29	13.19	8.35	5.85	0.02
3A	38.24	13.64	9.08	6.92	0.02
3B	38.45	13.13	8.42	6.75	0.12
144-1 1A	38.70	13.36	7.25	6.88	0.13
1B	38.56	14.20	7.23	6.40	0.13
2A	38.77	14.98	8.17	5.92	0.10
2B	38.63	14.16	7.60	6.34	0.15
3A	38.15	13.90	8.05	6.79	0.16
3B	38.41	14.78	7.47	6.94	0.15
178 1A	40.64	16.66	6.75	3.79	0.09
1B	39.31	16.20	6.73	4.63	0.08
2	39.68	16.24	6.53	3.58	0.12
3A	39.72	17.01	6.90	4.00	0.09
3B	40.22	16.36	6.45	3.84	0.06
4A	39.32	17.00	6.65	4.12	0.09
4B	38.84	17.18	5.43	4.14	0.18
178-1 2A	36.96	16.79	7.21	4.73	0.14
2B	40.15	16.52	7.14	4.87	0.11
2C	39.72	16.40	7.35	4.74	0.14
2D	39.97	16.56	7.32	4.63	0.13
3A	40.96	16.17	7.03	4.46	0.12
3B	41.65	16.15	7.19	4.47	0.13
3C	40.44	16.53	7.32	4.92	0.15
4A	41.60	16.35	7.65	4.53	0.12
4B	40.34	15.81	7.55	4.89	0.14
4C	40.58	16.54	7.01	4.51	0.15
5B	40.33	16.49	7.34	4.81	0.15
5C	39.72	16.28	7.77	5.07	0.14
6	40.44	16.30	7.59	5.01	0.15
179 1	37.96	16.25	7.62	6.72	0.17
2A	38.35	18.29	6.38	5.95	0.17
2B	36.27	18.25	6.22	6.13	0.12
2C	37.70	18.24	6.28	5.90	0.22
3A	37.77	17.23	6.61	6.58	0.15
3C	38.60	16.23	6.21	6.75	0.19
180 1A	35.55	12.88	8.85	8.63	0.07
1B	35.84	13.35	8.66	7.78	0.08
2A	34.45	12.97	9.23	8.19	0.04
2B	36.28	12.92	9.48	8.75	0.05
3	36.94	12.58	9.07	6.64	0.06
4A	35.58	13.35	8.72	9.16	0.06
4B	36.79	12.88	8.15	9.14	0.08
400 1A	37.88	16.71	6.67	6.28	0.07
1B	39.13	15.88	7.20	5.86	0.06

Chromite in chromitite from dunite zones (Cont.)

<u>Sample No.</u>	<u>Cr</u>	<u>Fe</u>	<u>Mg</u>	<u>Al</u>	<u>Ti</u>
400 2A	38.15	16.43	7.06	6.14	0.06
2B	37.14	17.92	6.18	5.61	0.14
3A	38.08	16.39	7.62	6.19	0.05
3B	37.86	18.26	5.97	5.87	-
4A	38.76	16.92	7.15	5.29	0.08
4B	38.30	17.67	6.79	5.74	0.11
515 1A	31.50	16.29	8.65	10.34	0.05
1B	34.45	16.32	8.97	8.96	0.03
2A	34.13	15.03	8.96	6.66	0.12
2B	35.37	16.21	8.67	7.30	0.16
3A	37.38	17.98	6.46	5.96	0.18
3B	37.05	17.70	7.07	5.23	0.10
518 1A	38.10	16.71	7.15	5.72	0.11
1B	37.76	15.26	6.57	6.27	0.10
2A	38.25	17.00	6.56	5.94	0.11
2B	39.63	16.78	6.60	6.00	0.08
2C	38.31	16.16	6.63	6.05	0.11

B) OLIVINE ANALYSES

Cations wt.%

Olivine in peridotite and olivine orthopyroxenite (K-57)

Sample No.	Mg	Fe	Ni	Si
A 11	28.39	7.26	0.30	18.74
2	31.56	7.02	0.40	18.60
C 1	27.71	7.34	0.23	18.88
2	28.32	7.32	0.29	18.96
D 1	29.22	7.65	0.47	18.66
2	27.18	7.26	0.35	19.52
3	30.77	7.32	0.55	19.04
E 1	28.32	7.47	0.27	18.20
2	29.87	7.24	0.27	18.45
3	28.20	7.24	0.24	18.68
G 1	26.49	7.73	0.34	18.77
2A	26.93	7.46	0.33	18.55
2B	27.53	7.66	0.33	18.55
3	27.30	7.53	0.24	18.98
I 1	27.67	7.45	0.26	19.60
K-57 1	29.61	7.54	0.32	18.61
2A	30.92	7.55	0.35	18.52
2B	29.36	7.49	0.29	18.69
2C	29.44	7.51	0.28	18.48
K-58 1A	29.35	7.94	0.35	19.73
1B	29.35	7.70	0.26	18.94
1C	28.91	7.67	0.24	18.98
1D	29.37	7.78	0.25	19.51
2A	28.88	7.77	0.36	18.41
2B	29.50	7.89	0.26	18.07
3A	29.93	8.07	0.30	18.22
3B	30.11	7.83	0.33	18.66
48 1	28.15	7.60	0.51	18.87
2A	29.82	6.97	0.27	18.64
2B	30.04	6.81	0.38	18.54
3A	29.54	6.70	0.28	19.05
3B	30.93	7.03	0.30	18.86
3C	29.36	6.95	0.36	19.14
4	30.88	7.06	0.35	18.99
56 1	30.01	7.43	0.25	19.37
2	29.89	7.18	0.24	19.60
3A	29.34	7.51	0.27	18.94
3B	29.57	7.04	0.25	18.82
4	29.64	7.31	0.18	18.90
65 1A	30.50	7.41	-	18.95
1B	29.43	7.22	-	18.29
1C	28.89	6.88	-	18.69

Olivine in peridotite and olivine orthopyroxenite (Cont.)

Sample No.	Mg	Fe	Ni	Si	
65	2A	29.11	7.06	-	19.27
	2B	29.31	7.06	-	19.02
	3	29.86	7.19	-	18.81
	4A	29.83	6.96	-	19.14
	4B	29.49	6.79	-	18.57
72	1B	30.83	7.19	-	18.67
	1C	29.94	7.45	-	18.48
	1D	30.05	7.46	-	18.26
	1E	31.13	7.42	-	18.68
	2A	30.85	7.44	-	18.39
	2B	30.63	7.87	-	18.66
87	1	30.22	7.66	-	18.91
	2	29.54	6.68	-	18.71
	3	29.64	7.51	-	18.28
218	1A	29.94	7.11	0.22	17.18
	1C	29.80	7.09	0.27	17.82
	2A	29.91	6.78	0.28	17.73
	2B	29.97	7.19	0.27	17.51
	3A	30.50	7.01	0.25	18.42
	3B	30.20	7.10	0.24	18.57
221	3	29.23	6.88	-	18.92
	4	29.26	6.38	-	18.92
	5	29.13	6.95	-	18.73
225	1	29.77	7.18	-	18.39
	2	30.65	7.28	-	18.41
	3	29.06	7.46	-	18.73
	4	31.26	7.23	-	18.06
	5A	30.19	7.19	-	18.93
	5B	31.79	7.62	-	17.92
	6	30.72	6.94	-	18.13
258	1	28.69	6.58	-	19.35
	2A	29.41	7.17	-	18.75
	2B	29.32	7.23	-	18.63
	2C	29.21	7.37	-	18.84
	3	29.88	7.57	-	18.74
	4	28.07	7.76	-	19.30
	5A	29.57	7.87	-	18.15
	5B	29.06	6.62	-	19.61
366		29.13	7.48	0.27	19.06
476	1A	29.31	7.19	-	19.18
	1B	29.52	7.64	-	18.60
	2A	30.22	7.92	-	18.19
	2B	29.88	7.60	-	18.54
	3A	30.25	7.71	-	18.55
	3B	30.29	7.49	-	19.16
554	1	30.16	6.29	-	19.58
	2A	30.51	7.79	-	18.94
	2B	30.10	7.65	-	18.68
	3	30.65	7.66	-	19.01

Olivine in dunite (all the samples are from chromitite-bearing dunite bodies in peridotite)

Sample No.	Mg	Fe	Ni	Si	Ca	
82	1	30.76	5.58	0.28	18.71	-
	2	30.06	5.91	0.39	19.04	-
	3	30.40	5.62	0.27	19.10	-
	4	31.44	5.12	0.25	19.52	-
92	1A	32.03	4.77	0.27	19.14	0.35
	1B	31.88	4.61	0.22	19.91	0.42
	1C	30.61	4.99	0.22	19.43	0.33
	1D	31.21	4.93	0.17	19.17	0.35
	2A	31.57	4.83	0.22	19.24	0.26
	2B	30.69	4.70	0.23	18.93	0.34
	2C	29.50	5.14	0.29	19.02	0.28
	3A	31.92	4.93	0.29	19.26	0.29
	3B	31.59	4.74	0.21	18.86	0.44
	3C	30.50	4.95	0.25	19.37	0.46
228	1	30.54	5.76	0.38	19.09	-
	2A	31.07	5.87	0.27	19.50	-
	2B	29.68	5.33	0.30	19.55	-
	3A	32.02	5.42	0.27	18.48	-
	3B	31.76	5.67	0.23	19.79	-
236		29.24	6.91	0.22	19.32	-
364	1	31.17	4.53	0.26	19.22	0.20
	2	30.42	4.43	0.35	18.97	0.29
	3A	30.02	5.63	0.21	19.01	0.31
	3B	29.72	5.66	0.21	19.00	0.18
	4	30.02	5.76	0.16	18.93	0.23
	5A	30.47	5.49	0.18	19.16	0.37
	5B	30.54	5.91	0.18	19.19	0.33
369	1	31.30	5.68	0.33	19.15	-
	2	31.56	5.82	0.34	19.17	-
	3	30.14	5.99	0.35	19.35	-

C) ORTHOPYROXENE ANALYSES

Cations wt.%

Orthopyroxene in peridotite and olivine orthopyroxenite (K-57)

Sample No.	Mg	Fe	Si	Al	Cr	Ca	Ni		
A	1A	20.35	3.84	26.89	1.03	0.19	0.18	0.11	
	1C	21.20	3.68	27.31	0.95	0.16	0.20	0.07	
	1D	21.94	3.83	26.43	0.91	0.17	0.21	0.02	
	2A	20.81	3.96	26.59	0.92	0.15	0.20	0.01	
	2B	21.52	3.81	26.36	1.04	0.17	0.19	0.01	
	3A	19.69	3.54	26.94	1.02	0.15	0.13	0.00	
	3B	20.95	3.78	26.11	1.03	0.15	0.32	0.03	
C	1A	21.31	3.86	26.84	0.69	0.22	0.44	-	
	1B	21.51	3.83	27.45	0.69	0.18	0.32	-	
	1C	21.92	3.83	27.13	0.70	0.17	0.97	-	
D	1A	21.05	3.74	26.52	1.15	0.15	0.39	0.08	
	1C	21.27	3.97	26.91	0.69	0.06	0.40	0.07	
	2A	21.08	3.83	27.26	0.95	0.15	0.33	0.03	
	2B	20.60	3.97	27.29	0.95	0.13	0.20	-	
	3A	20.10	3.96	27.09	1.00	0.14	0.25	0.04	
	3B	21.32	4.03	26.76	0.90	0.11	0.20	0.07	
E	1A	20.35	3.97	26.90	1.08	0.18	0.33	-	
	1B	20.86	3.84	26.99	1.15	0.21	0.33	-	
	2A	21.08	3.76	27.74	0.81	0.08	0.28	-	
	2B	21.57	3.89	27.08	0.97	0.19	0.52	-	
G	1A	22.07	3.56	27.42	0.57	0.12	0.17	-	
	1B	22.34	3.46	28.13	0.46	0.10	0.19	-	
I	1A	22.74	3.90	27.74	0.43	-	-	-	
	1C	21.04	3.84	27.61	0.52	-	-	-	
	1E	21.10	3.84	27.57	0.55	-	-	-	
K-57	1A	21.92	3.80	26.68	0.71	0.18	0.51	-	
	1B	22.13	3.84	27.06	0.41	-	-	-	
	2A	20.99	4.00	26.94	0.71	0.21	0.60	-	
	2B	21.28	4.13	27.17	0.65	0.18	0.60	-	
	48	1A	20.23	3.65	27.38	0.54	0.16	0.45	0.08
48	1B	21.71	3.51	26.87	0.61	0.11	0.42	0.07	
	2A	20.22	3.64	27.80	0.54	0.16	0.45	0.10	
	2B	19.51	3.70	27.32	0.55	0.19	0.42	0.08	
	3A	22.14	3.82	27.61	0.53	0.16	0.39	0.13	
	3B	22.10	3.91	27.55	0.57	0.13	0.38	0.16	
	56	1A	22.36	4.08	-	0.54	0.16	0.38	0.07
	1B	22.96	3.90	-	0.55	0.15	0.23	0.07	
56	1C	22.79	3.95	-	0.52	0.16	0.44	0.08	
	1D	23.09	4.01	-	0.67	0.15	0.67	0.14	
	1E	22.91	4.02	-	0.52	0.13	0.39	0.15	
	65	1B	21.09	4.07	27.40	0.45	0.11	0.46	-
	1C	21.52	3.82	26.80	0.39	0.12	0.45	-	

Orthopyroxene in peridotite and olivine orthopyroxenite (Cont.)

Sample No.	Mg	Fe	Si	Al	Cr	Ca	Ni
65 2A	21.90	3.88	27.79	0.44	0.15	0.31	-
2B	20.55	4.08	26.94	0.49	0.18	0.45	-
2C	20.99	3.74	27.60	0.56	0.12	0.64	-
87 1A	17.07	3.91	28.70	0.62	0.22	0.42	-
1B	19.92	4.03	28.80	0.61	0.20	0.42	-
2A	20.40	4.05	28.83	0.55	0.17	0.29	-
2B	21.18	3.58	27.61	0.65	0.16	0.50	-
218 1A	21.07	3.87	27.80	0.33	0.15	0.29	-
1B	21.45	3.67	26.23	0.36	0.13	0.46	-
2	21.40	3.66	27.37	0.41	0.17	0.38	-
3	21.33	3.75	26.69	0.44	0.18	0.34	-
221 1	20.81	4.81	27.51	0.86	0.36	0.76	-
2	20.88	4.55	26.68	0.83	0.30	0.90	-
3	21.74	4.94	25.47	0.71	0.30	0.49	-
4	20.12	4.47	27.29	0.91	0.35	0.67	-
5	20.39	4.63	26.50	0.88	0.33	0.53	-
225	19.85	4.35	28.00	0.66	0.17	0.59	-
258 1A	18.14	3.83	28.05	0.51	0.21	0.30	-
1B	18.10	3.84	28.15	0.46	0.18	0.34	-
3B	20.79	4.33	28.45	0.50	0.15	0.62	-
3C	20.25	4.40	27.11	0.49	0.18	0.39	-
366 1A	18.61	3.88	28.01	0.81	-	-	-
1B	19.27	3.76	27.08	1.07	-	-	-
1C	20.65	4.24	26.89	0.91	-	-	-
476 1A	20.61	3.33	28.11	1.15	0.14	0.19	-
1B	20.83	4.25	27.24	1.04	0.11	0.23	-
2A	20.24	4.13	27.27	1.06	0.16	0.28	-
2B	21.42	4.12	27.05	1.23	0.13	0.27	-

Orthopyroxene in orthopyroxenite layer (K-58) and orthopyroxenite vein (554)

K-58 1A	20.93	4.40	26.31	0.27	0.03	0.47	-
1B	21.24	4.33	27.02	0.23	0.05	0.53	-
1C	21.24	4.34	27.10	0.25	0.06	0.88	-
2A	21.05	5.04	27.24	0.31	0.06	0.56	-
2C	21.26	4.80	26.74	0.31	0.03	0.59	-
554 1A	21.98	4.94	26.98	0.58	0.51	0.60	-
1B	21.43	4.77	26.45	0.57	0.59	0.86	-
3A	21.58	5.74	25.44	0.42	0.42	0.44	-
3B	21.25	4.78	25.44	0.64	0.41	0.54	-
4A	20.82	5.23	25.33	0.42	0.19	0.68	-
4B	20.93	5.16	25.87	0.53	0.19	0.50	-
5	19.35	8.86	26.54	0.51	0.20	-	-

Orthopyroxene in pyroxenite

<u>Sample No.</u>	<u>Mg</u>	<u>Fe</u>	<u>Si</u>	<u>Al</u>	<u>Cr</u>	<u>Ca</u>	<u>Ni</u>
142 1A	20.57	9.59	-	0.62	0.07	0.72	-
1B	19.67	9.71	-	0.66	0.07	0.65	0.02
1C	19.93	9.40	-	0.56	0.07	0.80	-
1D	19.98	9.27	-	0.63	0.06	0.63	0.02
1F	19.58	9.29	-	0.61	0.04	0.61	0.07
2A	19.90	9.13	-	0.57	0.06	0.83	0.06
2B	19.29	9.33	-	0.69	0.07	0.47	0.04
3A	20.03	9.33	-	0.63	0.06	0.63	0.02
3B	20.34	9.00	-	0.61	0.03	0.61	0.02

D) CLINOPYROXENE ANALYSES

Pyroxenite: 39, 142, 444; "Lherzolite": 154; "Olivine" pyroxenite: K-9, 189; Peridotite: 221; Orthopyroxenite (layer): K-58.

Cations wt.%

Sample No.	Mg	Fe	Si	Al	Cr	Ca	Ni	
39	1A	11.43	4.52	-	1.08	0.27	15.58	0.05
	EB	11.25	4.68	-	1.12	0.30	14.58	0.06
	2A	11.92	4.80	-	1.12	0.32	14.82	0.02
	2B	11.62	4.69	-	1.12	0.29	14.55	0.10
	3	10.82	4.79	-	1.24	0.35	12.91	0.06
	4A	11.05	4.35	-	1.20	0.29	14.58	0.13
	4B	11.26	4.60	-	1.03	0.25	14.06	0.06
	5	11.42	4.48	-	1.13	0.27	15.65	0.08
	6	11.01	4.67	-	1.26	0.32	14.91	0.08
	142	1	11.20	5.10	-	1.10	0.28	14.21
2A		11.30	4.95	-	1.11	0.28	14.32	0.03
2B		10.99	4.95	-	0.79	0.11	14.96	0.04
3		11.11	5.83	-	1.39	0.26	14.55	0.05
4		12.12	5.58	-	1.17	0.28	14.64	0.04
5		11.26	5.04	-	1.31	0.26	15.61	0.03
444	1B	11.19	4.67	-	1.24	0.28	14.67	0.07
	1C	11.57	4.63	-	1.19	0.27	14.40	0.07
	2	11.66	5.20	-	1.15	0.24	14.25	0.11
	3	11.91	5.11	-	1.35	0.26	13.90	0.07
154	4	11.58	5.22	-	0.69	0.20	14.92	0.03
	1A	11.95	4.12	25.31	1.00	-	13.18	-
	1B	12.12	4.29	25.31	0.92	-	12.11	-
	1C	12.40	4.62	24.70	0.93	-	11.96	-
K-9	1A	10.63	3.86	23.21	1.25	0.14	16.21	-
	1B	10.52	3.77	24.63	1.21	0.15	15.70	-
	2A	10.76	3.72	25.18	1.26	0.24	16.01	-
	2B	10.42	4.24	24.18	1.18	0.31	16.17	-
189	1A	11.23	2.59	25.23	0.75	-	15.60	-
	1B	11.78	2.95	24.96	0.78	-	14.30	-
	2	11.07	2.80	25.03	0.64	-	15.20	-
	3	11.76	2.95	23.99	0.82	-	14.90	-
	4	11.43	2.77	24.41	0.77	-	16.44	-
	5	11.63	3.40	25.49	0.79	-	15.75	-
	6A	11.01	2.83	25.73	0.61	-	15.59	-
	6B	11.39	3.19	24.72	0.74	-	15.48	-
221	1	9.89	1.55	24.70	0.75	0.24	20.09	-
	2	10.02	1.25	23.81	1.16	0.29	18.11	-
	3	10.43	1.69	25.26	0.94	0.08	18.03	-
K-58	1A	11.02	2.10	25.40	0.46	0.18	17.10	-
	1B	10.88	2.11	25.29	0.59	0.13	18.40	-

TABLE XII

Equilibrium constant $K_T = (Fe^{++}/Mg)_{ol} (Mg/Fe^{++})^2_{opx}$ for the olivine-orthopyroxene pair in peridotite samples.

Sample No.	K	Sample No.	K
A	17.44	65	16.47
C	19.07	87	15.30
D	16.90	218	17.76
E	17.40	221	10.62
G*	25.6	225	11.56
I	17.84	258	13.09
K-58	11.72	366	14.46
48	17.94	476	15.94
56	18.96		

* Excluded from the plot because of its singularly high value.

TABLE XIII

Compositions of clinopyroxenes from "Iherzolite" (154), "olivine" pyroxenite (K-9, 189) recalculated according to the convention used by O'Hara (1967b), and parameters α and β . Compositions of clinopyroxenes in cation wt. % are given in Table XI D.

Sample No.	K-9 1	K-9 2	189 1	189 2	189 3	189 4	189 5	189 6	154
CaSiO ₃	46.2	46.5	43.5	44	43.3	47.5	45.5	43.5	37.8
MgSiO ₃	52.8	53.2	54.4	49.8	55.6	54	56.2	53.6	61
Al ₂ O ₃	2.58	2.65	1.44	1.21	1.56	1.45	1.49	1.79	1.79
α	43.6	46.9	44.5	46.8	44	46.4	44	44.5	37.8
β	2.50	2.53	1.47	1.26	1.55	1.40	1.31	1.31	1.80

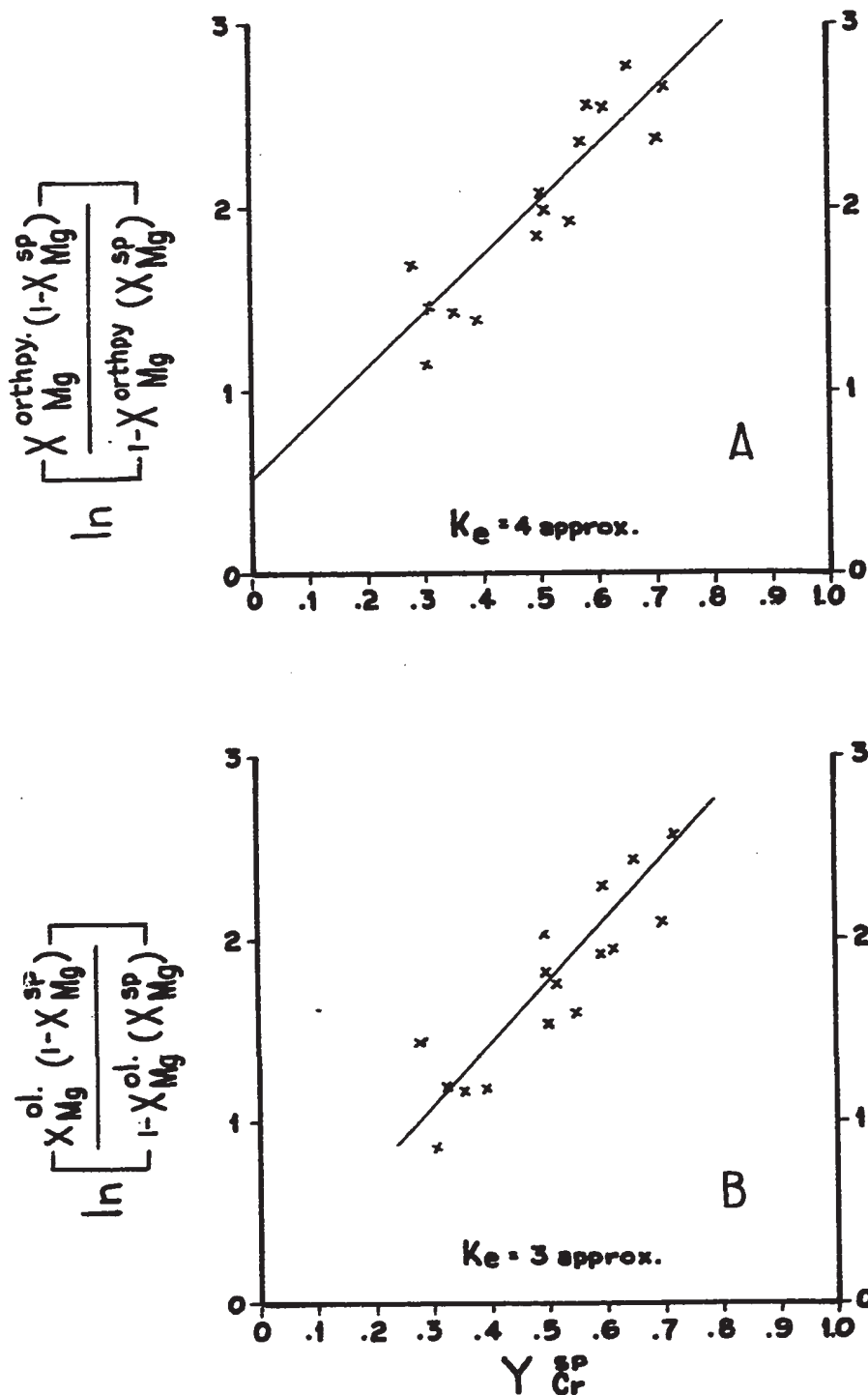
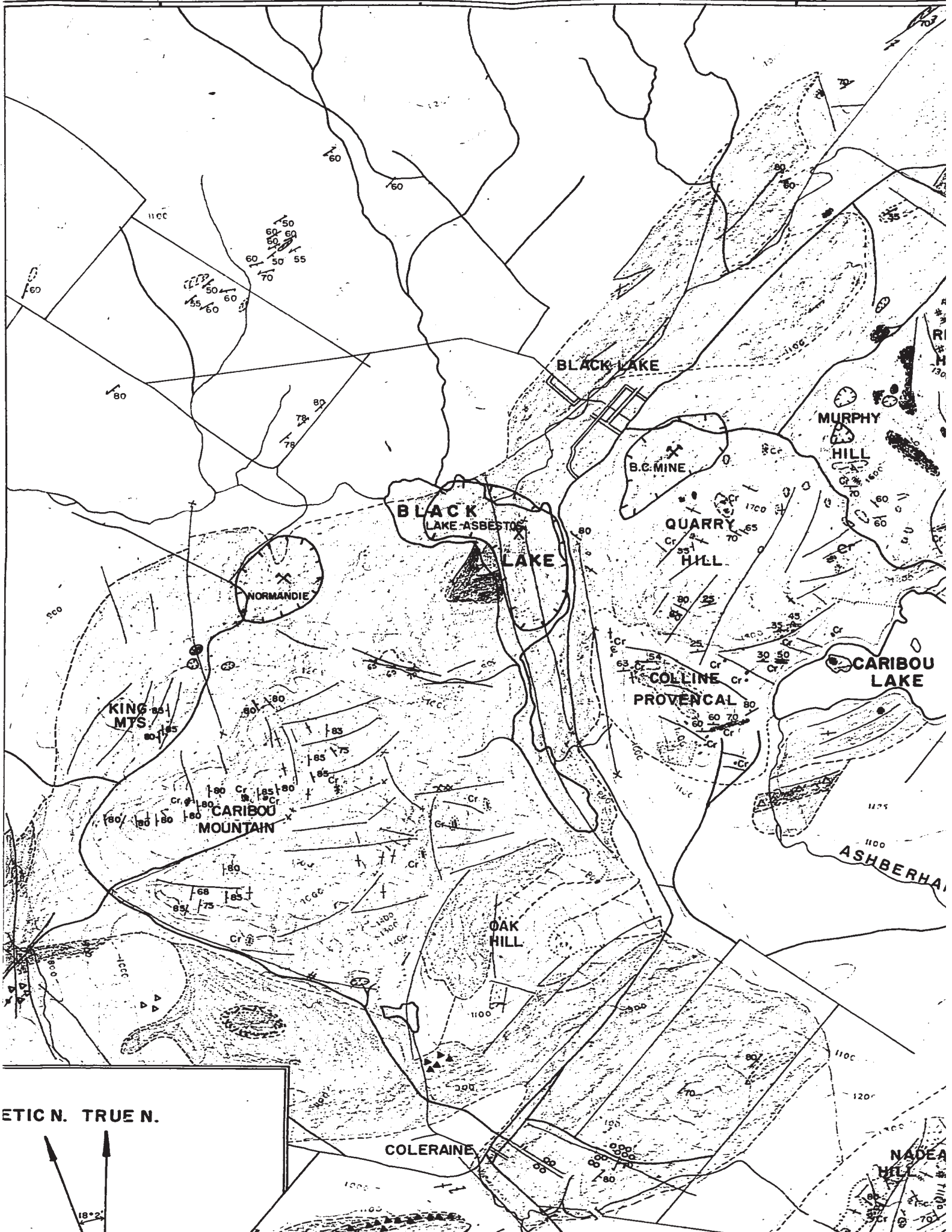


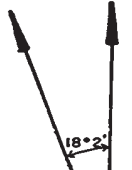
Figure 112. Plots of Mg-Fe distribution coefficients against Y_{Cr}^{SP} (where $Y_{Cr}^{SP} + Y_{Al}^{SP} + Y_{Fe}^{SP} = 1$) for coexisting orthopyroxene and chromite (A), and olivine and chromite (B). All analyses are from peridotite. Lines in both figures have been visually fitted to the distribution of points. The slope of both lines is theoretically equal to K_e (see text p. 90) (After Irvine, 1965).

71°25'

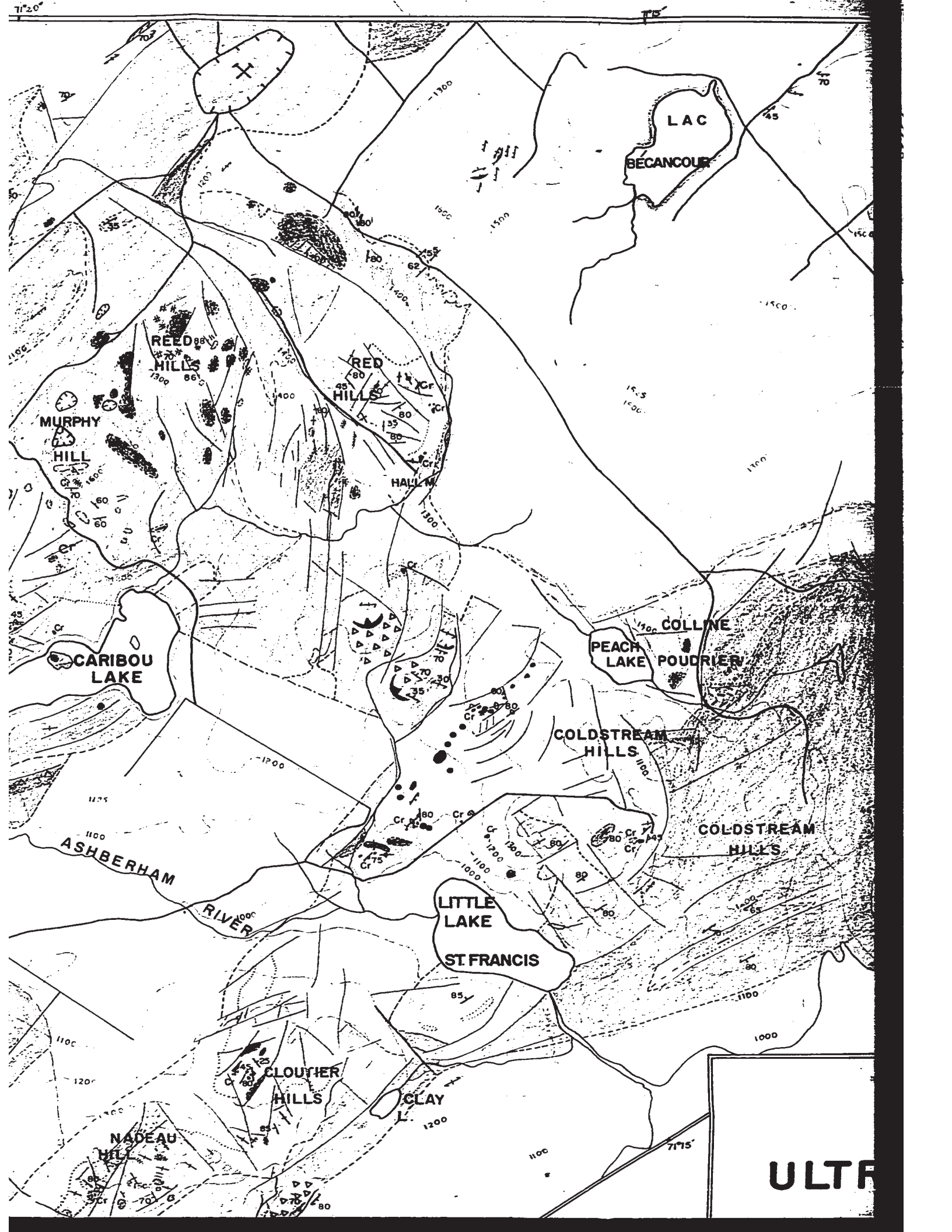
71°20'



ETIC N. TRUEN N.



NADEA HILL



LAC
BECANCOLE

REED
HILLS

RED
HILLS

MURPHY
HILL

CARIBOU
LAKE

COLLINE
PEACH
LAKE
POUDRIER

COLDSTREAM
HILLS

COLDSTREAM
HILLS

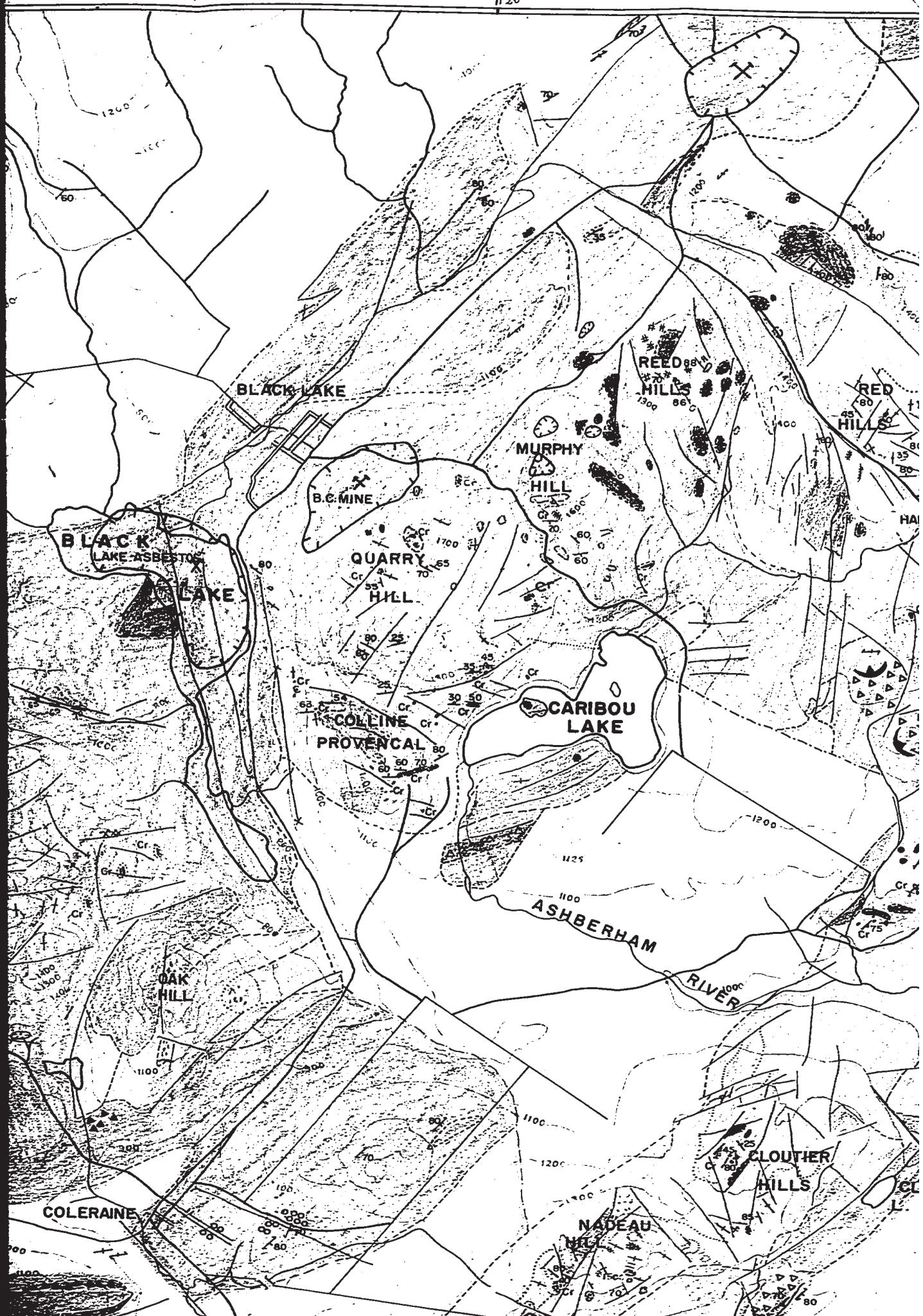
LITTLE
LAKE
ST. FRANCIS

CLOUTIER
HILLS

CLAY

NADEAU
HILL

ULTRA



COLERAINE

NADEAU HILL

CLOUTIER HILLS

ASHBERHAM RIVER

CARIBOU LAKE

COLLINE PROVENCAL

QUARRY HILL

MURPHY HILL

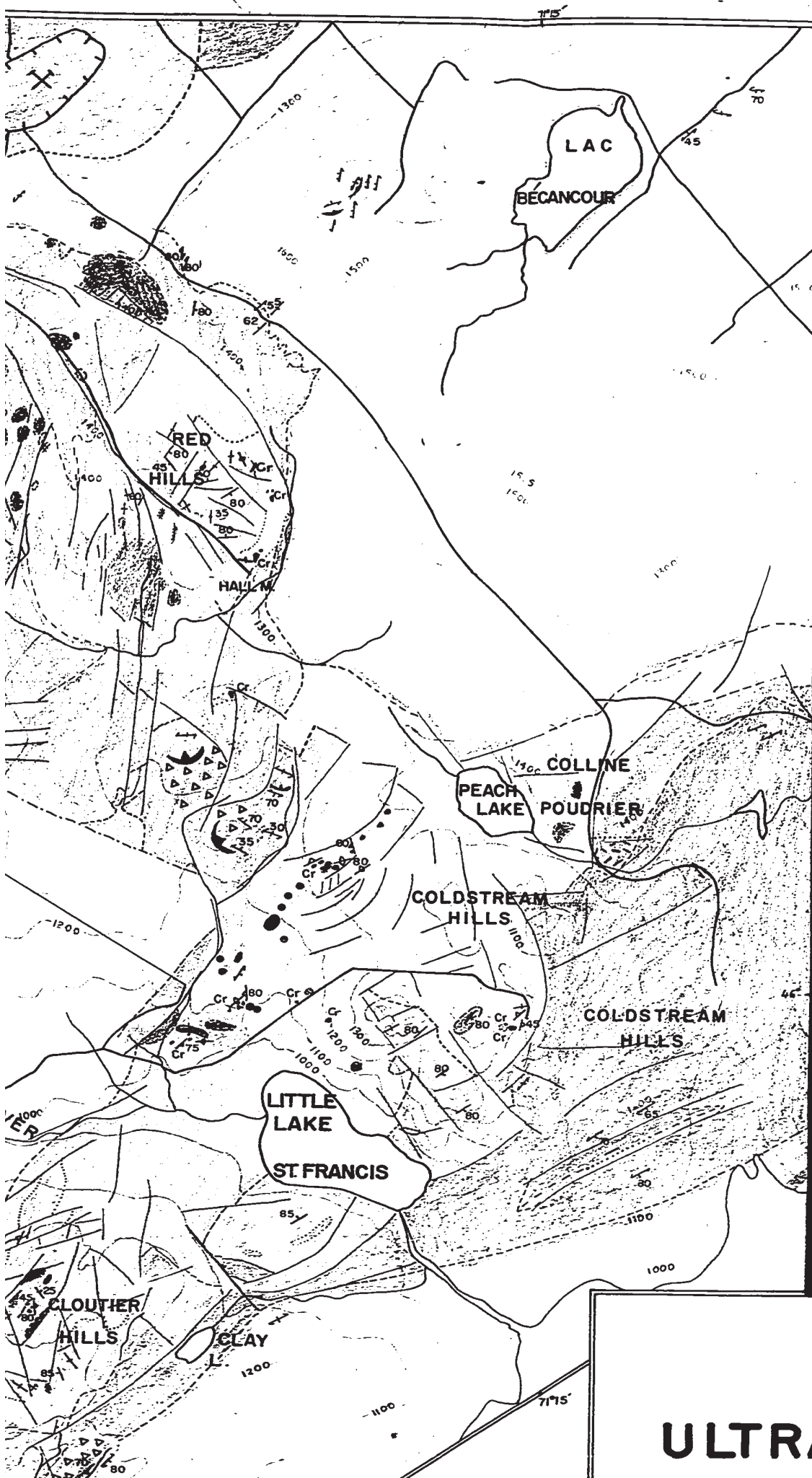
REED HILLS

BLACK LAKE

BLACK LAKE ASBESTOS LAKE

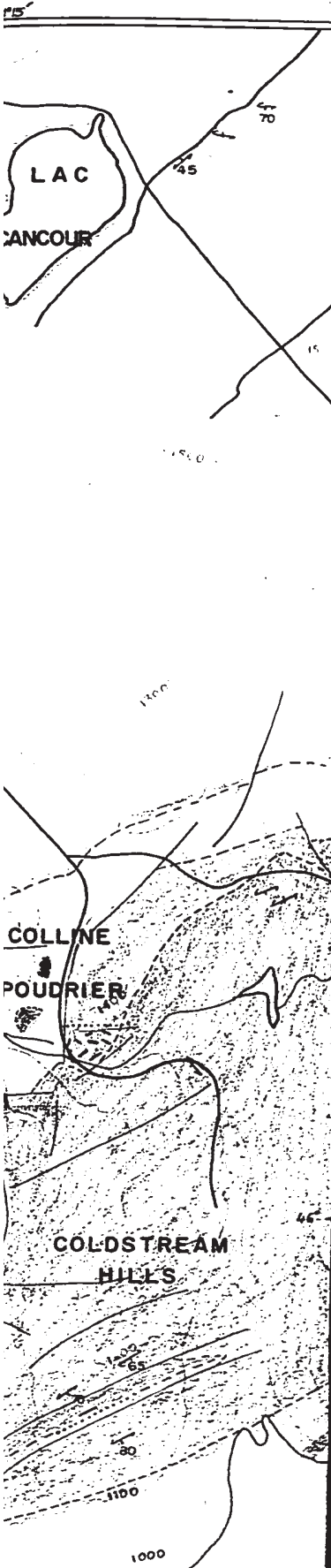
OAK HILL

27





- SEDI**
- Alluvium and glacial drill holes and
 - Amphibolite, Metasedimentary Breccia composed
- VOLC**
- Basalt, pillowed
 - Mainly agglomerate
 - Volcano-sediment Intrusive? Breccia?
- PLUT**
- Granite, syenite
 - Gabbro and diorite
 - Fine-grained gabbro
 - Mainly olivine pyroxenite related
 - Mainly peridotite
 - Peridotite (harz)
 - Serpentine.
- Dunite with rare Dunite breccia w/
 - Dunite breccia w/ Serpentinized, ca
- MINER**
- Chromite pits.
 - Chromite showings
 - Operating asbestos
 - Abandoned asbestos
 - Asbestos prospect
 - Asbestos showings
- CONVE**
- Boundaries
- Observed.
 - Inferred.
 - Transitional.
- DIPS
- Mineral banding at 80°
 - Vertical mineral at 85°
 - Schistosity at 80°
 - Vertical schistosity at 85°
 - Shear plane at 80°
 - Vertical shear plane at 85°
- Faults
- Observed in the field
 - Petrogeological faults, fractures
 - Strike ridge with faults
- Road.
- Road.
- Trail.
- Trail.
- Rivers, streams.
- Rivers, streams.
- Contour line, alt
- Contour line, alt

ULTRABASIC F




27








SEDIMENTARY ROCKS

-  Alluvium and glacial drift (omitted where bedrock inferred from nearby outcrops, drill holes and aero-magnetic map).
-  Amphibolite.
Metasedimentary rocks, mainly quartz-sericite schist, slate and metagreywacke.
Breccia composed of metasedimentary rock fragments.







VOLCANIC ROCKS

-  Basalt, pillowed andesite and some acid volcanic rocks.
Mainly agglomerate.
Volcano-sedimentary breccia: "Coleraine Breccia".
Intrusive? Breccia, diatreme breccia.

















PLUTONIC ROCKS

-  Granite, syenite and leucocratic veins of indeterminate composition.
-  Gabbro and diorite, cut by quartz diorite and diabase dykes.
Fine-grained gabbro with some medium to coarse-grained facies.
-  Mainly 'olivine' pyroxenite, with 'herzolite', pyroxenite and dunite.
Pyroxenite related to gabbro.
-  Mainly peridotite of 'herzolite' variety with 'olivine' pyroxenite and dunite.
-  Peridotite (harzburgite) with some dunite layers, bodies and orthopyroxenite.
-  Serpentinite.
-  Dunite with rare peridotite layers, bodies.
Dunite breccia with pyroxenite matrix.
Dunite breccia with microgabbro matrix.
Serpentinised, carbonatised dunite.

MINERAL OCCURRENCES

-  Chromite pits.
-  Chromite showings and rich disseminations.
-  Operating asbestos mines.
-  Abandoned asbestos pits.
-  Asbestos prospect.
-  Asbestos showings.

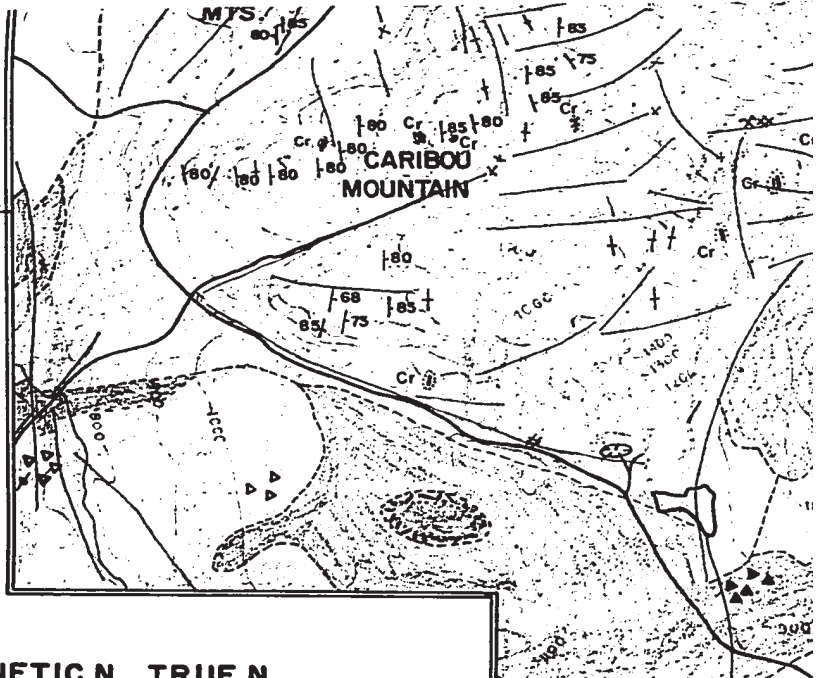
CONVENTIONAL SIGNS

- Boundaries**
-  Observed.
-  Inferred.
-  Transitional.
- Dip**
-  Mineral banding and foliation. Bedding in metasediments.
-  Vertical mineral banding and foliation. Vertical bedding in metasediments.
-  Schistosity.
-  Vertical schistosity.
-  Shear plane.
-  Vertical shear plane.
- Faults**
-  Observed in the field or recorded on mine plans.
- Photogeological symbols**
-  Faults, fractures and shear planes.
-  Strike ridge with direction of dip.
-  Road.
-  Trail.
-  Rivers, streams.
-  Contour line, altitude in feet

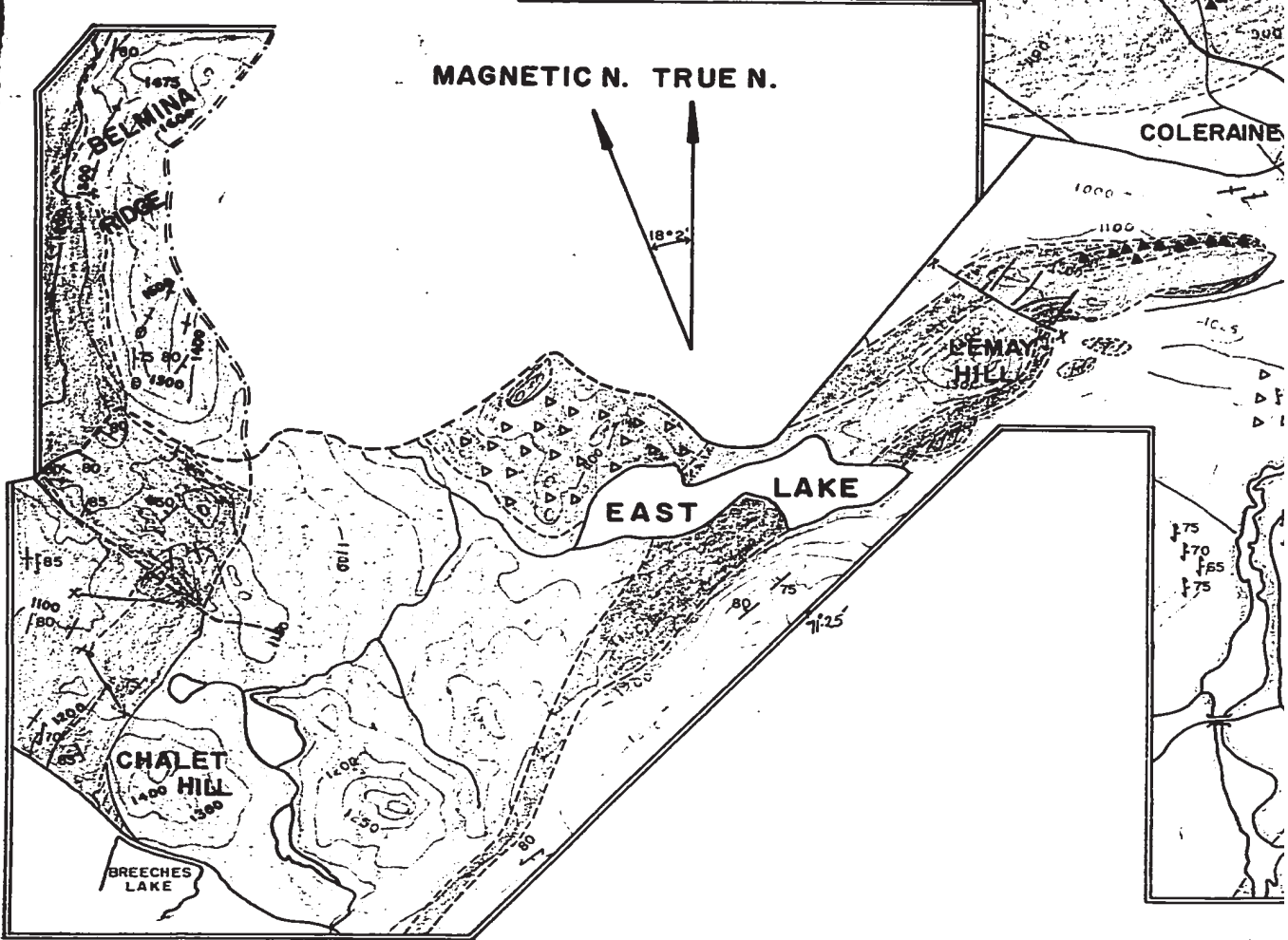
175

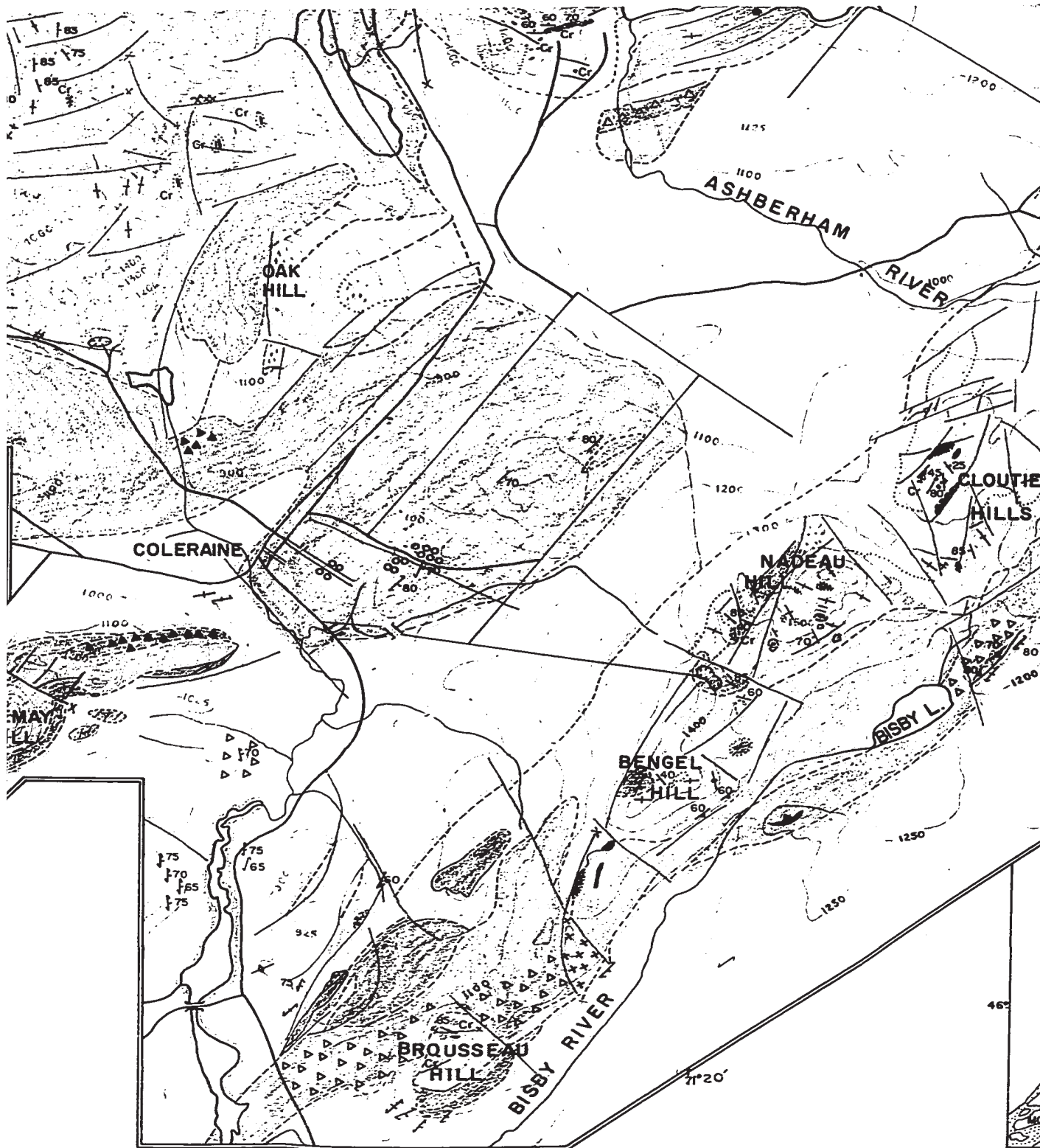
ULTRABASIC ROCKS OF THE

3 of



MAGNETIC N. TRUE N.

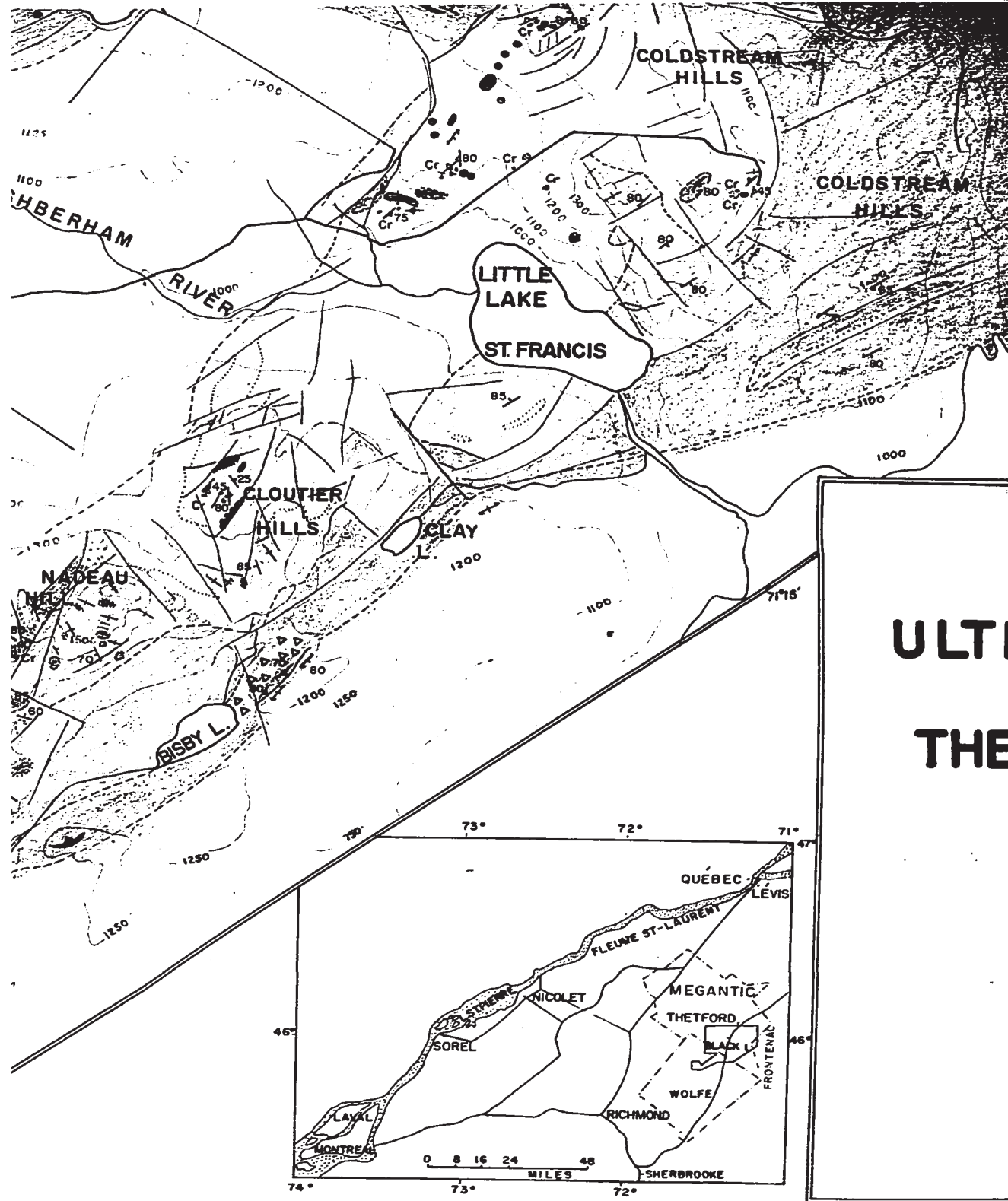




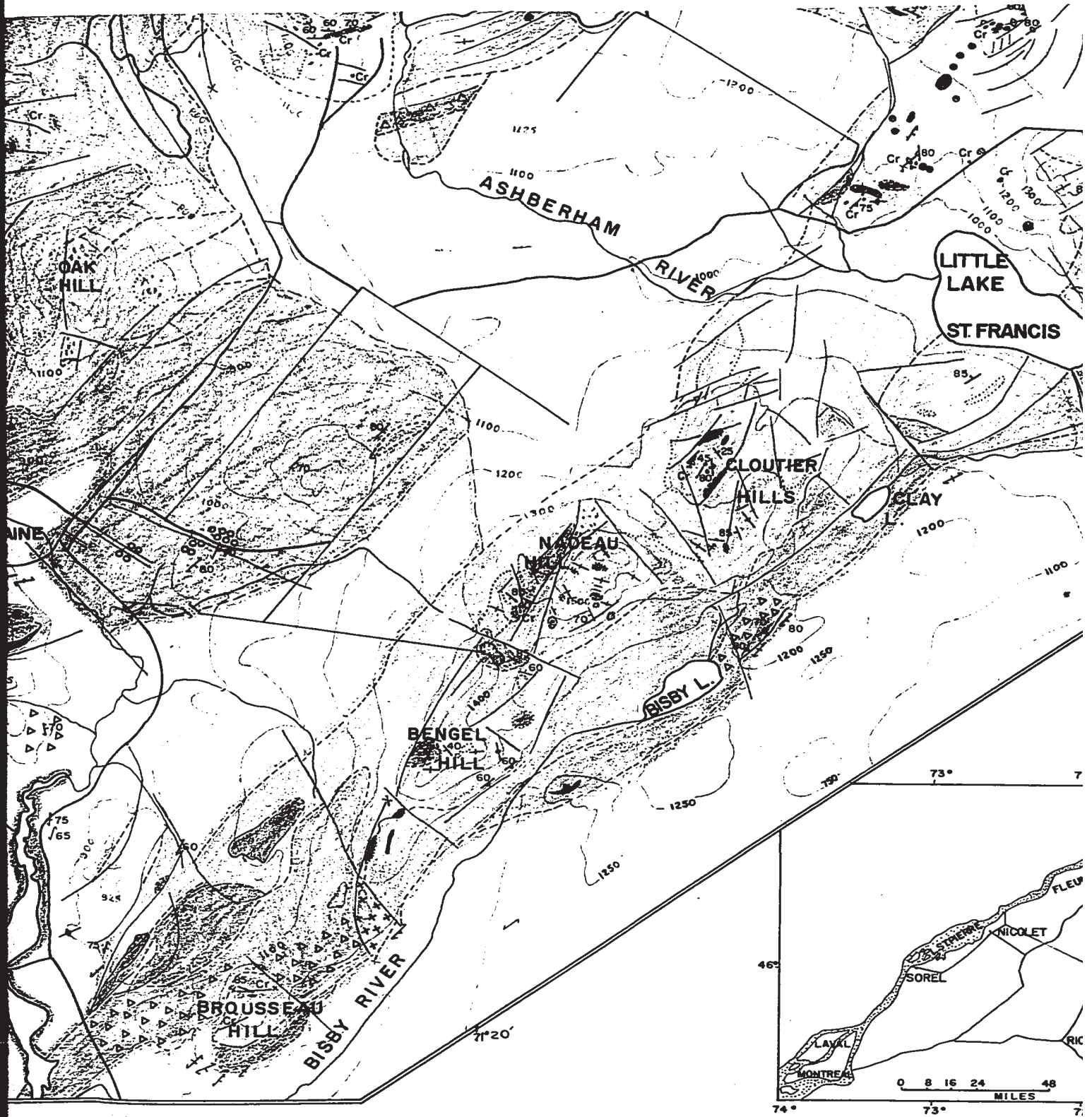
46°

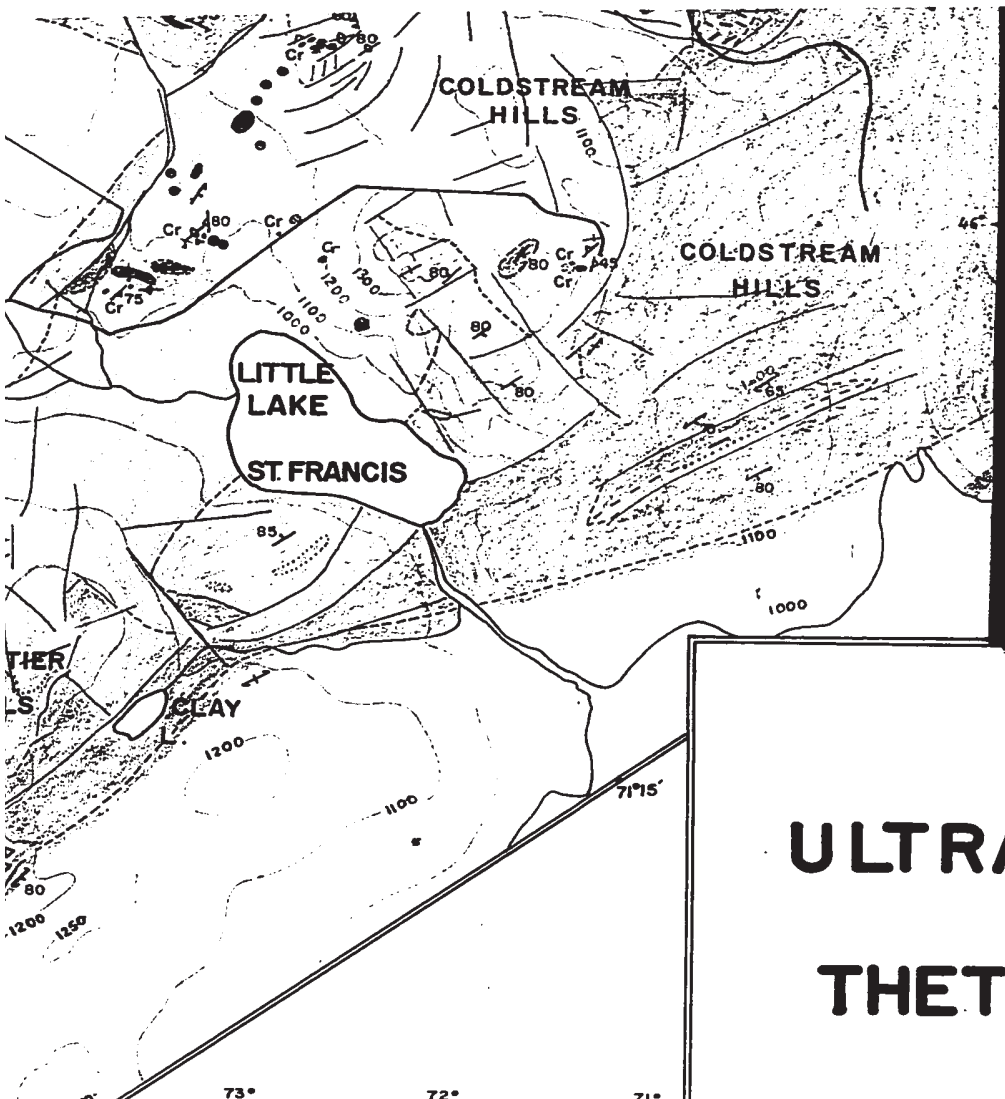
74° 20'

74°

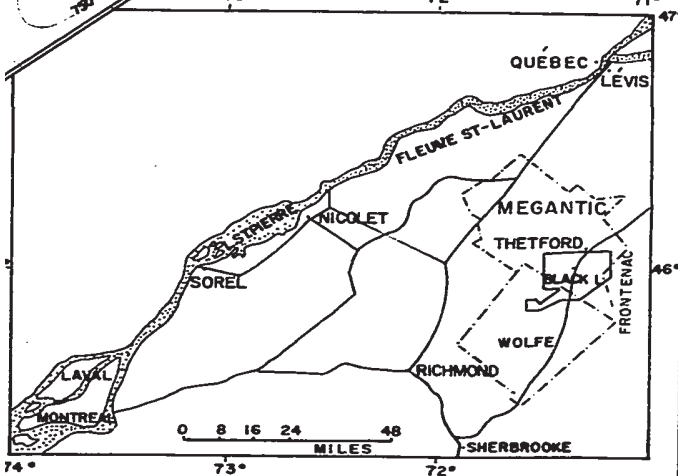


ULT
THE





- Vertical mineral banding and foliation.
- Schistosity.
- Vertical schistosity.
- Shear plane.
- Vertical shear plane.
- Faults**
- Observed in the field or recorded on photogeological symbols.
- Faults, fractures and shear planes.**
- Strike ridge with direction of dip.
- Road.**
- Trail.
- Rivers, streams.
- Contour line, altitude in feet















ULTRABASIC ROCK THETFORD-DISRAE

EASTERN TOWNSHIPS

SCALE: 1 : 25000

1967-1968

-  Vertical mineral banding and foliation. Vertical bedding in metamorphites.
-  Schistosity.
-  Vertical schistosity.
-  Shear plane.
-  Vertical shear plane.
- Faults
-  Observed in the field or recorded on mine plans.
- Photogeological symbols
-  Faults, fractures and shear planes.
-  Strike ridge with direction of dip.
-  Road.
-  Trail.
-  Rivers, streams.
-  Contour line, altitude in feet

40/4

LTRABASIC ROCKS OF THE THETFORD-DISRAELI AREA

EASTERN TOWNSHIPS P.Q.

SCALE: 1 : 25000

1967-1968

N. KAÇIRA

MAP 1

18

LEGEND:



Metasedimentary rocks
Brecciated metasedimentary rocks
Amphibolite

VOLCANIC ROCKS



Basalt, pillowed andesite, acid volcanic rocks, with pyroclastic rocks



Mainly pyroclastic rocks
Volcano-sedimentary breccia "Coleraine breccia"



Intrusive? breccia, diatreme breccia

INTRUSIVE ROCKS



Leucocratic rocks



Gabbro, diorite
Fine grained gabbro with some coarse grained facies



Mainly olivine pyroxenite with lherzolite, pyroxenite and dunite



Mainly pyroxenite; associated to gabbro



Mainly lherzolite with olivine pyroxenite, dunite, pyroxenite



Peridotite with some dunite bodies, layers



Dunite, with rare peridotite layers and bodies



Dunite breccia with pyroxenite matrix



Dunite breccia with microgabbro matrix



Serpentinised, carbonitised dunite



Serpentinite

MINERAL OCCURENCES



Chromite workings



Chromite showings, rich dissemination



Operating asbestos mines



Abandoned asbestos pit and prospect



Asbestos showings

CONVENTIONAL SIGNS



Major geological boundary



Observed exposures



Boreholes and main type of intersected rock



Mineral banding foliation, Bedding in metasediments



Vertical mineral banding, foliation, Bedding in metasediments



Schistosity



Vertical schistosity



Shear plane



Vertical shear plane



Sample location and number

DISTRIBUTION OF OBSERVED EXPOSURE

SCALE:

1:25,000, Approximate



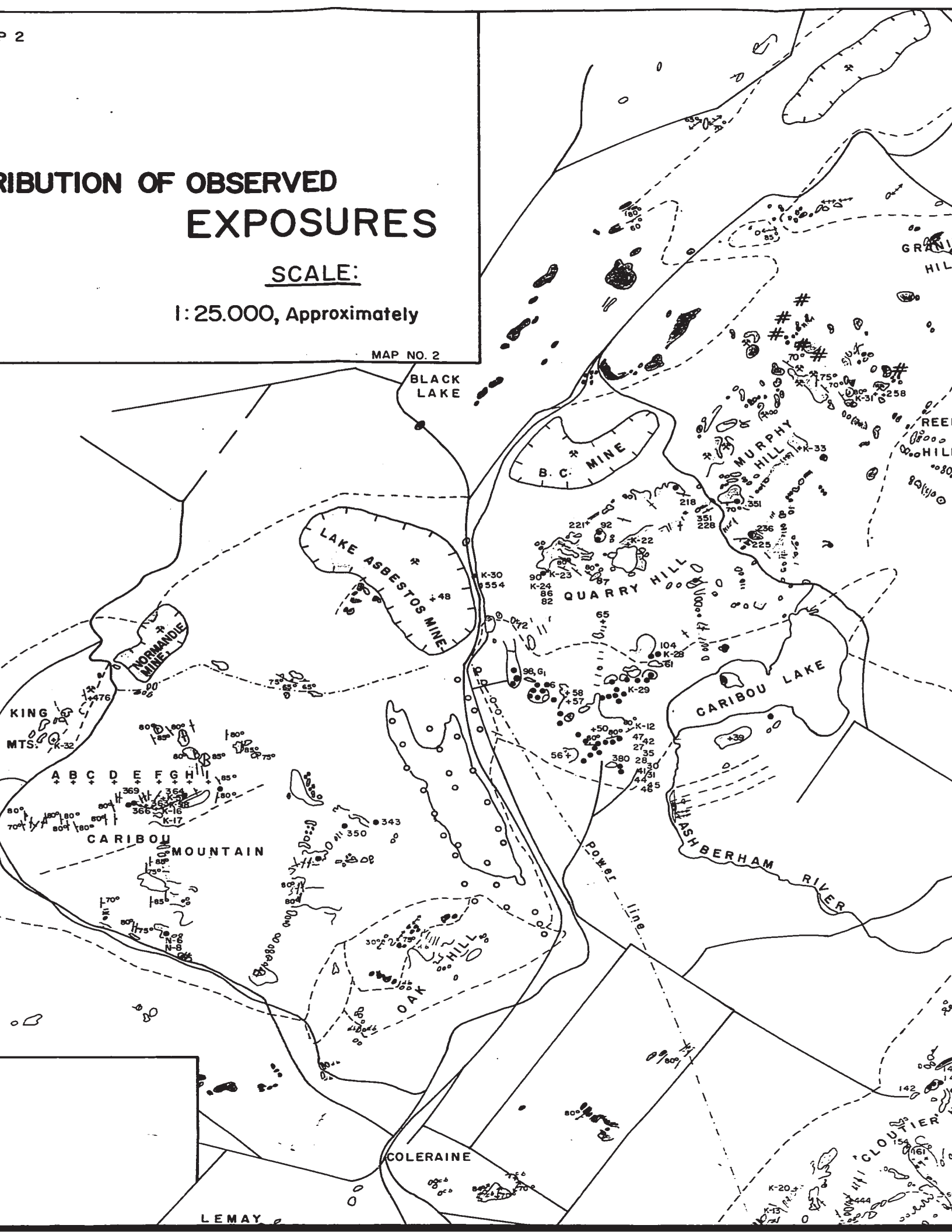
LEMA

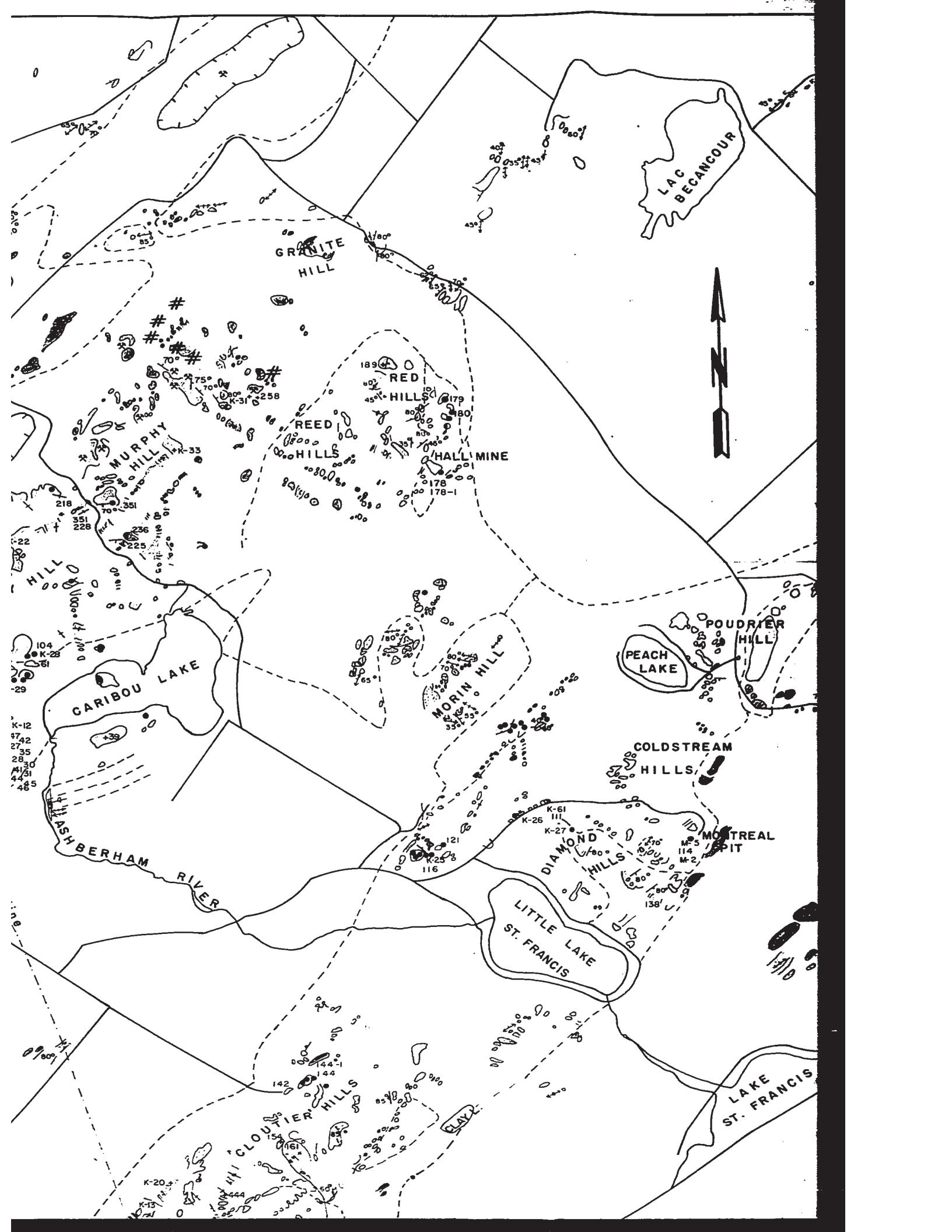
DISTRIBUTION OF OBSERVED EXPOSURES

SCALE:

1:25,000, Approximately

MAP NO. 2





END:

DISTRIBUTION OF OBSERVED EXPOSURES

SCALE:

1: 25.000, Approximately

MAP NO. 2

rocks
 sedimentary rocks

IGNEOUS ROCKS

Basalt, acid volcanic rocks,
 with pyroclastic rocks

rocks
 Breccia "Coleraine breccia"

, diatreme breccia

PLUTONIC ROCKS

ro with some coarse
 grained facies

Pyroxenite with ilmenite,
 pyroxenite and dunite
 associated to gabbro
 with olivine pyroxenite,
 dunite, pyroxenite
 and dunite bodies, layers
 and ilmenite layers and bodies
 in pyroxenite matrix
 and microgabbro matrix
 and magnetized dunite

MINERAL OCCURRENCES

Asbestos, rich dissemination
 in mines
 prospect pits and prospect
 workings

STRUCTURAL SIGNS

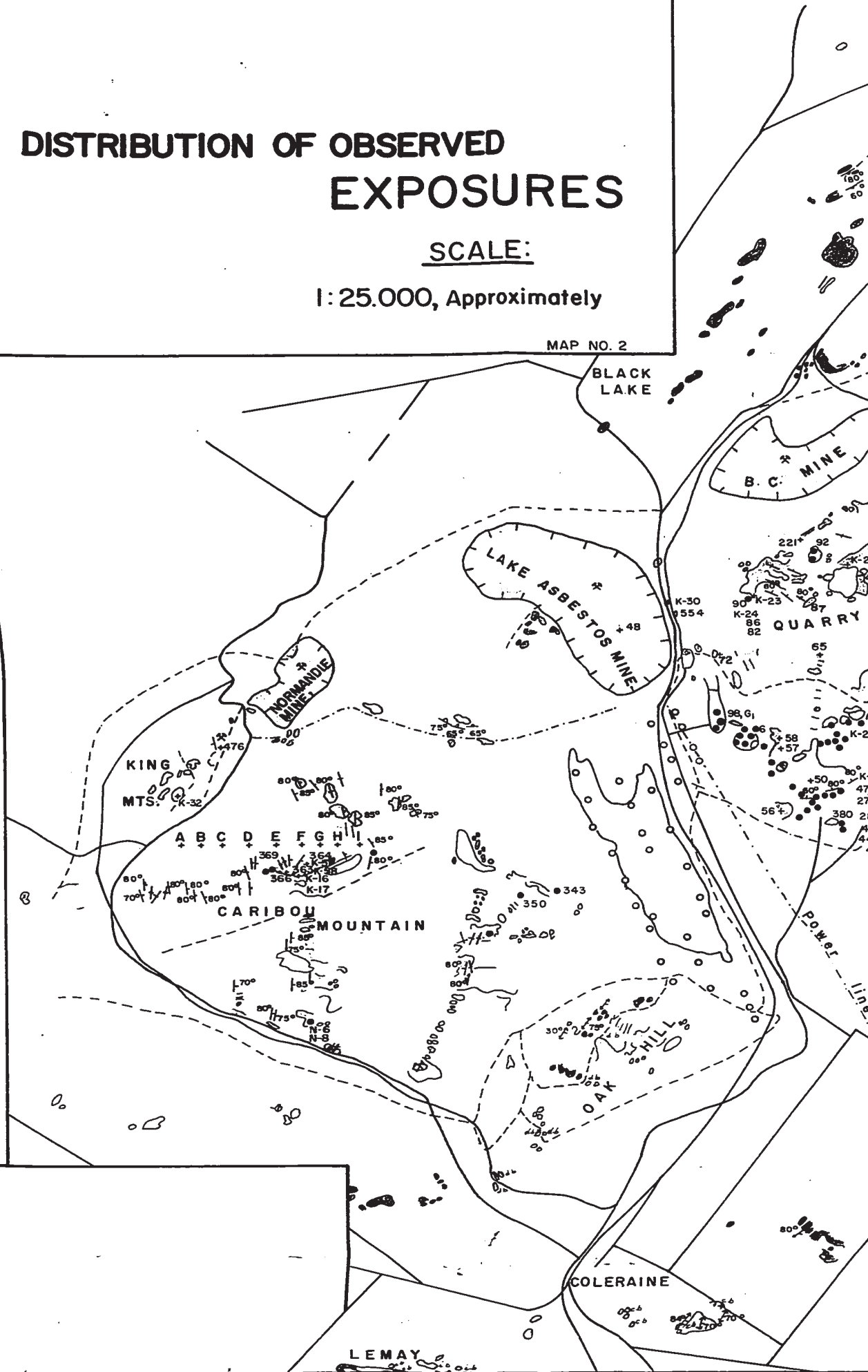
Boundary

in type of intersected rock
 foliation. Bedding in meta-
 sediments

banding, foliation.
 in sediments

Locality

plane
 and number



ES

ely

P NO. 2

BLACK LAKE

ESTOS MINE

COLERAINE

GRANITE HILL

B. C. MINE

MURPHY HILL

REED HILLS

RED HILLS

HALL MINE

QUARRY HILL

CARIBOU LAKE

MORIN HILL

PEA L

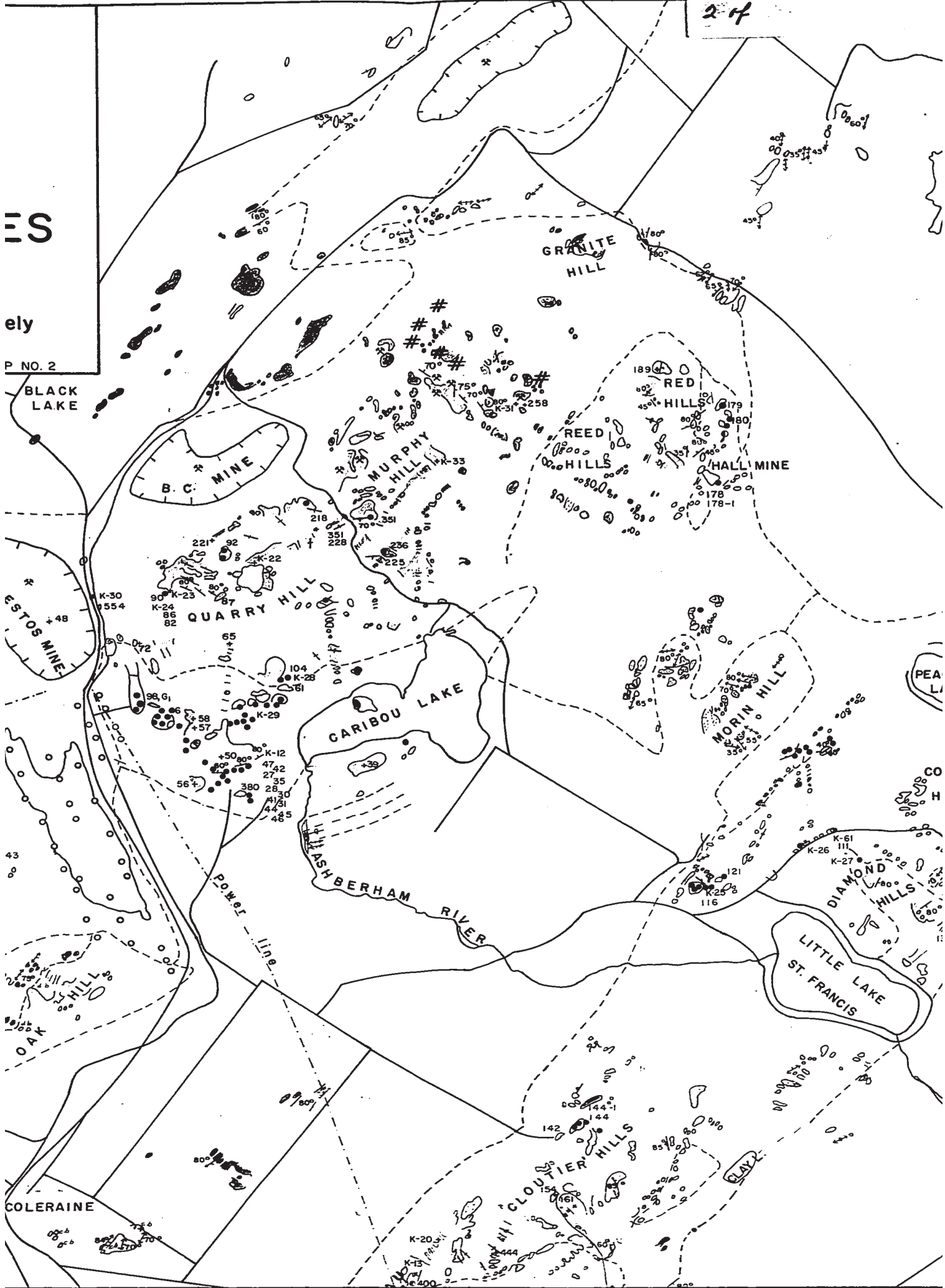
CO H

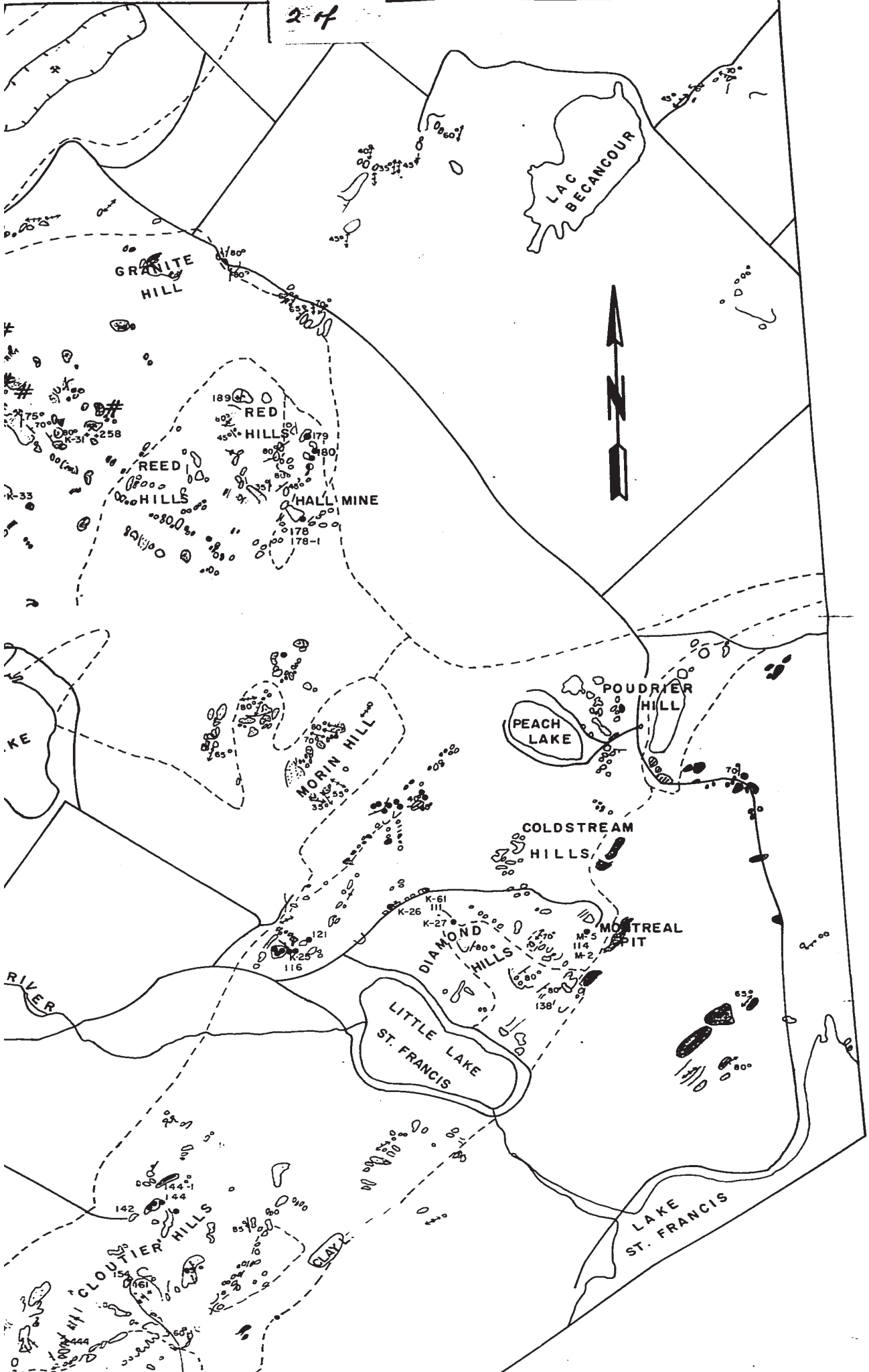
WASHBERHAM RIVER

DIAMOND HILLS

LITTLE LAKE ST. FRANCIS

CLAY



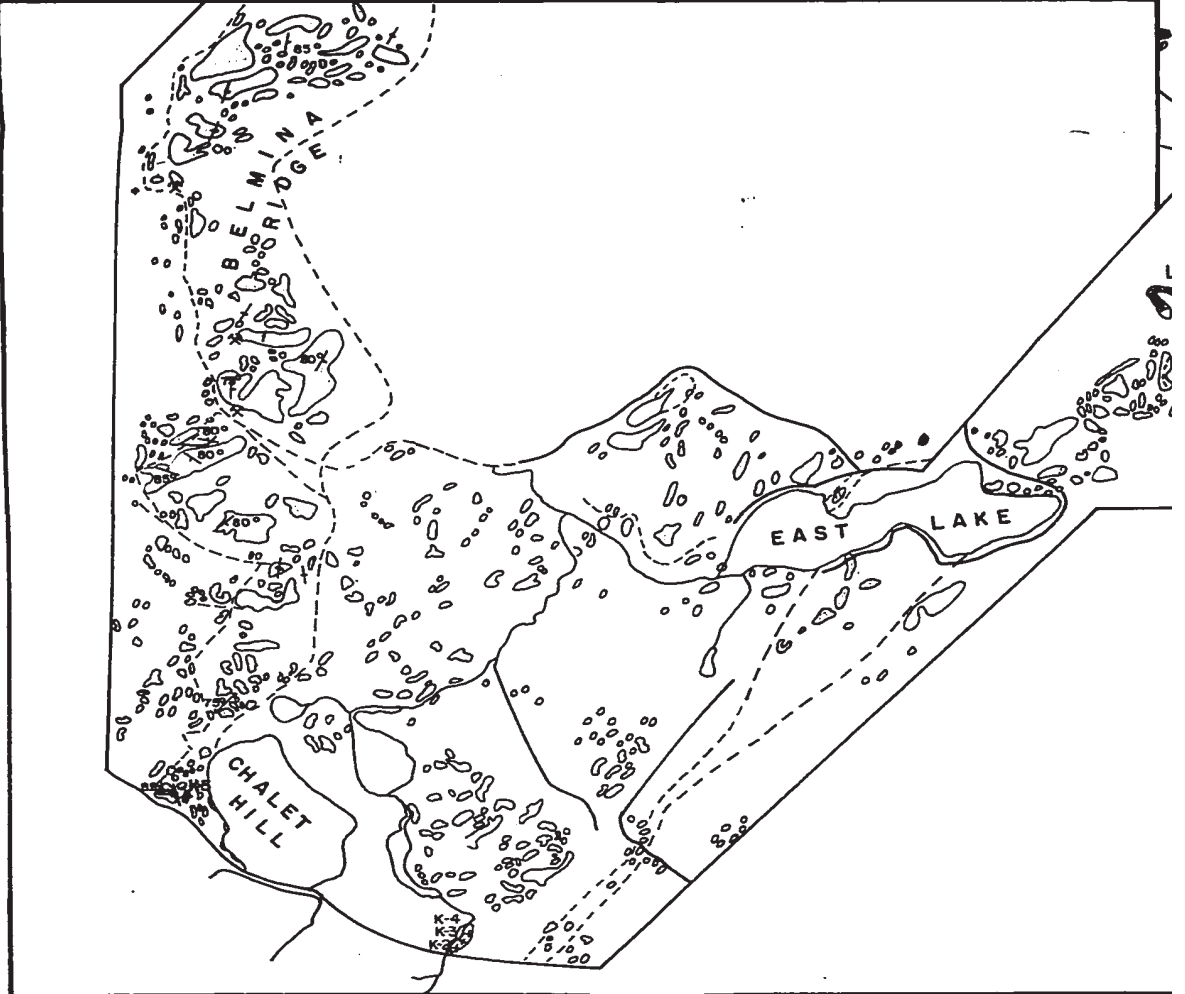
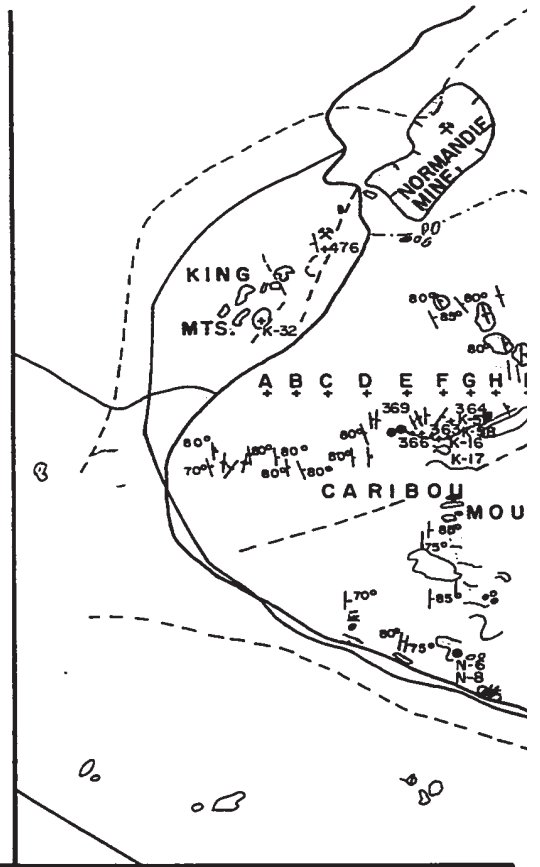


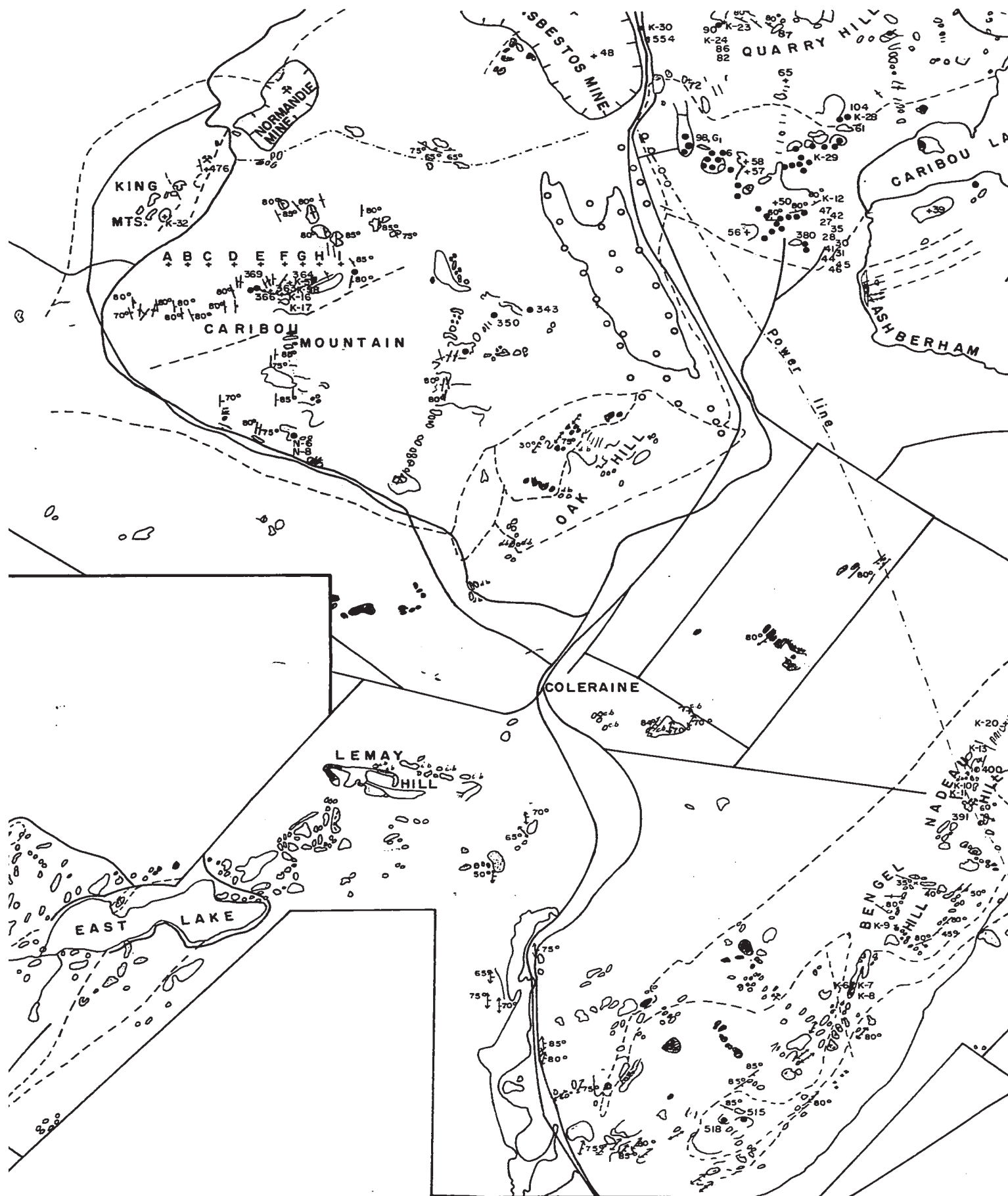
- Chromite workings
- ◉ Chromite showings rich dissemination
- ⊛ Operating asbestos mines
- ⊛ Abandoned asbestos pit and prospect
- # Asbestos showings

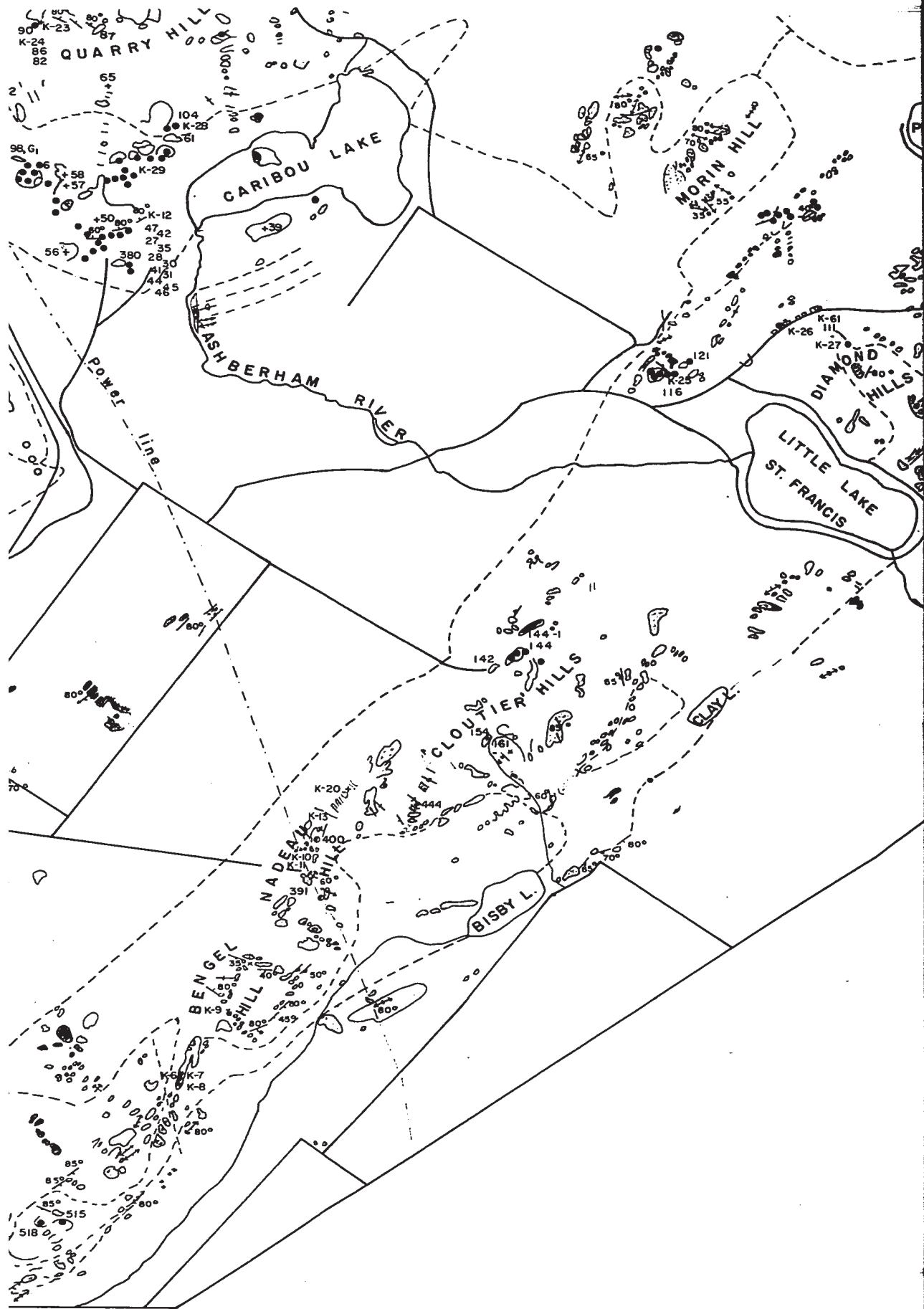
CONVENTIONAL SIGNS

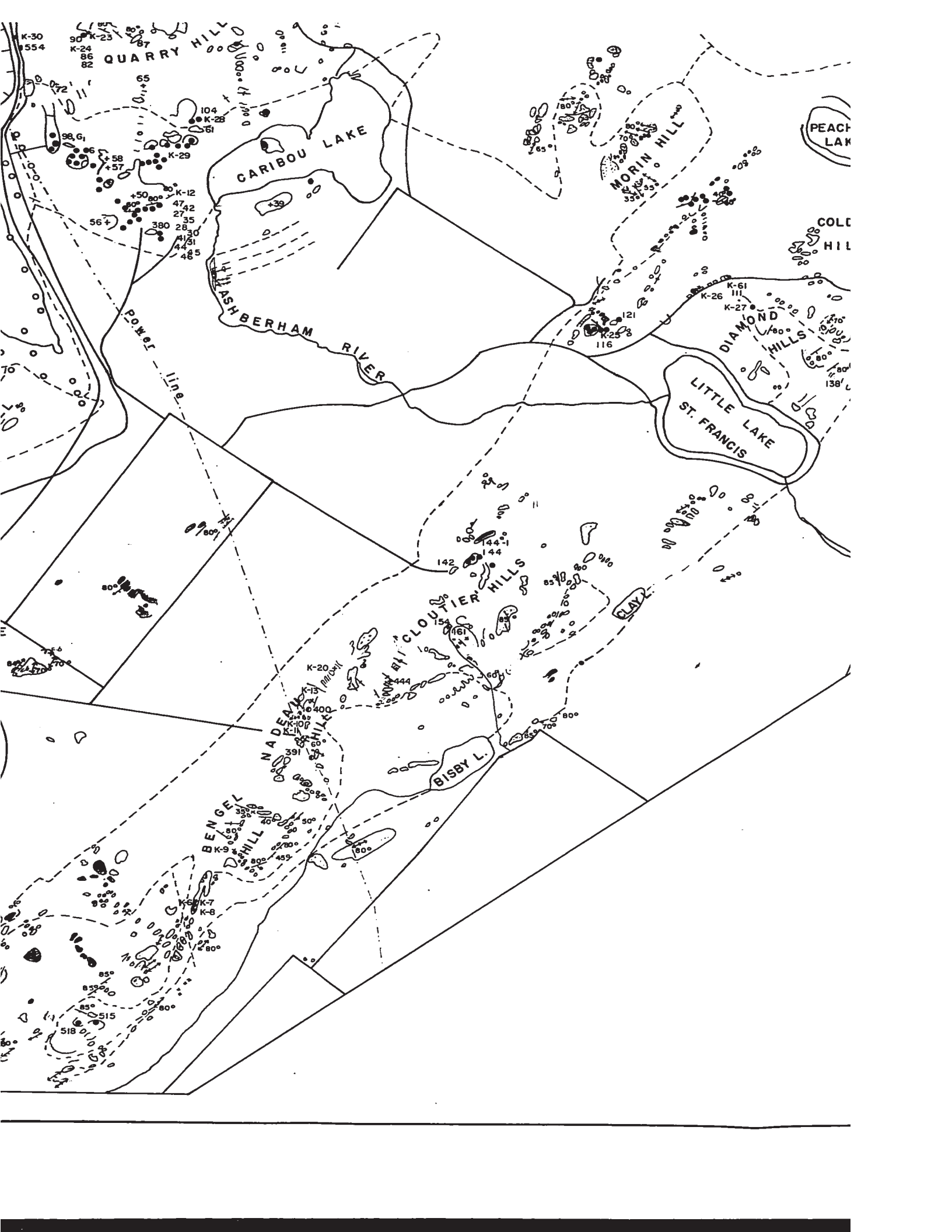
- - - Major geological boundary
- o || Observed exposures
- o | Boreholes and main type of intersected rock
- o | Mineral banding foliation. Bedding in meta-sediments
- + | Vertical mineral banding foliation. Bedding in metasediments
- 70° | Schistosity
- 70° | Vertical schistosity
- ||| Shear plane
- ||| Vertical shear plane
- x 39 Sample location and number

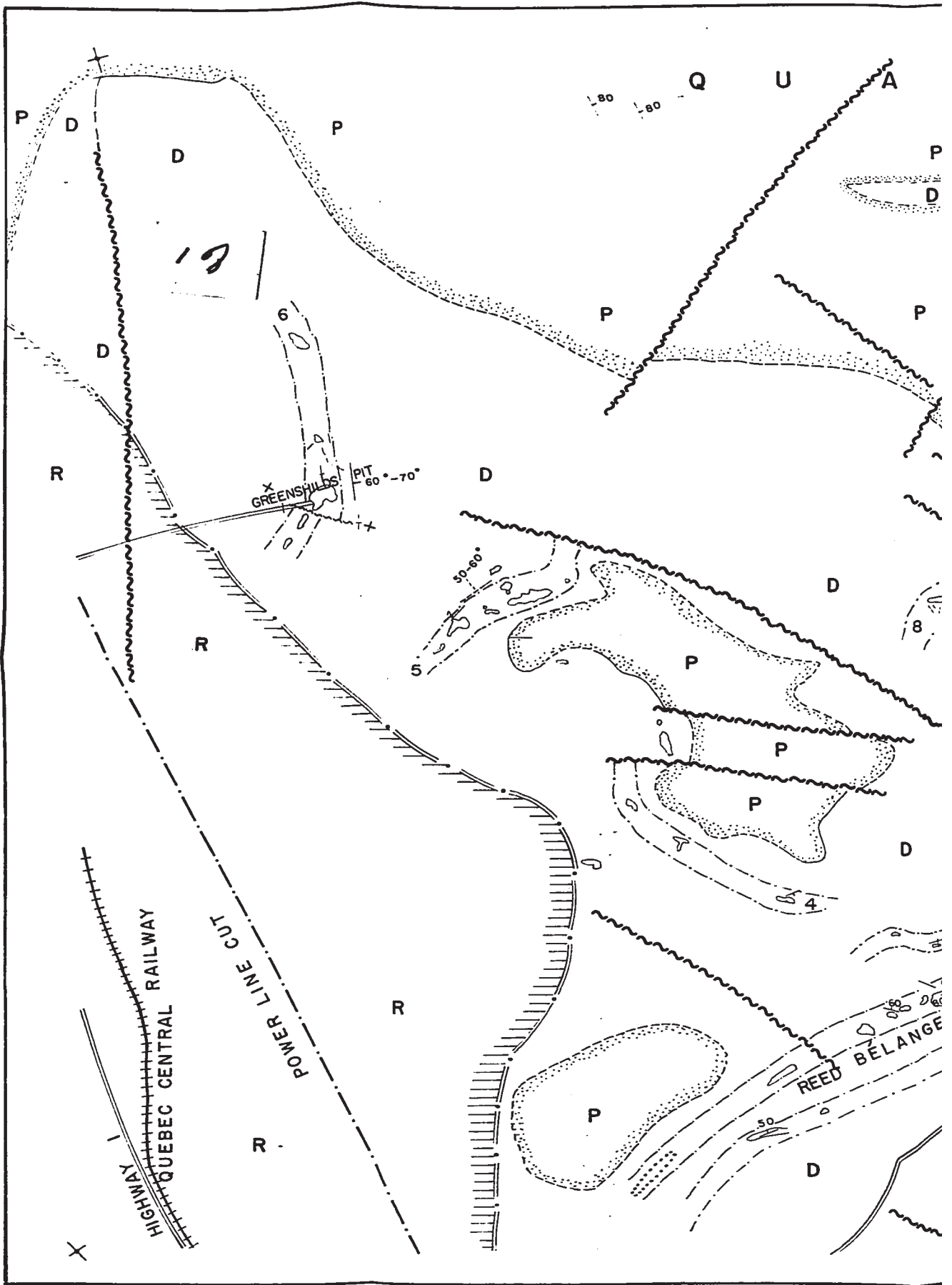
34

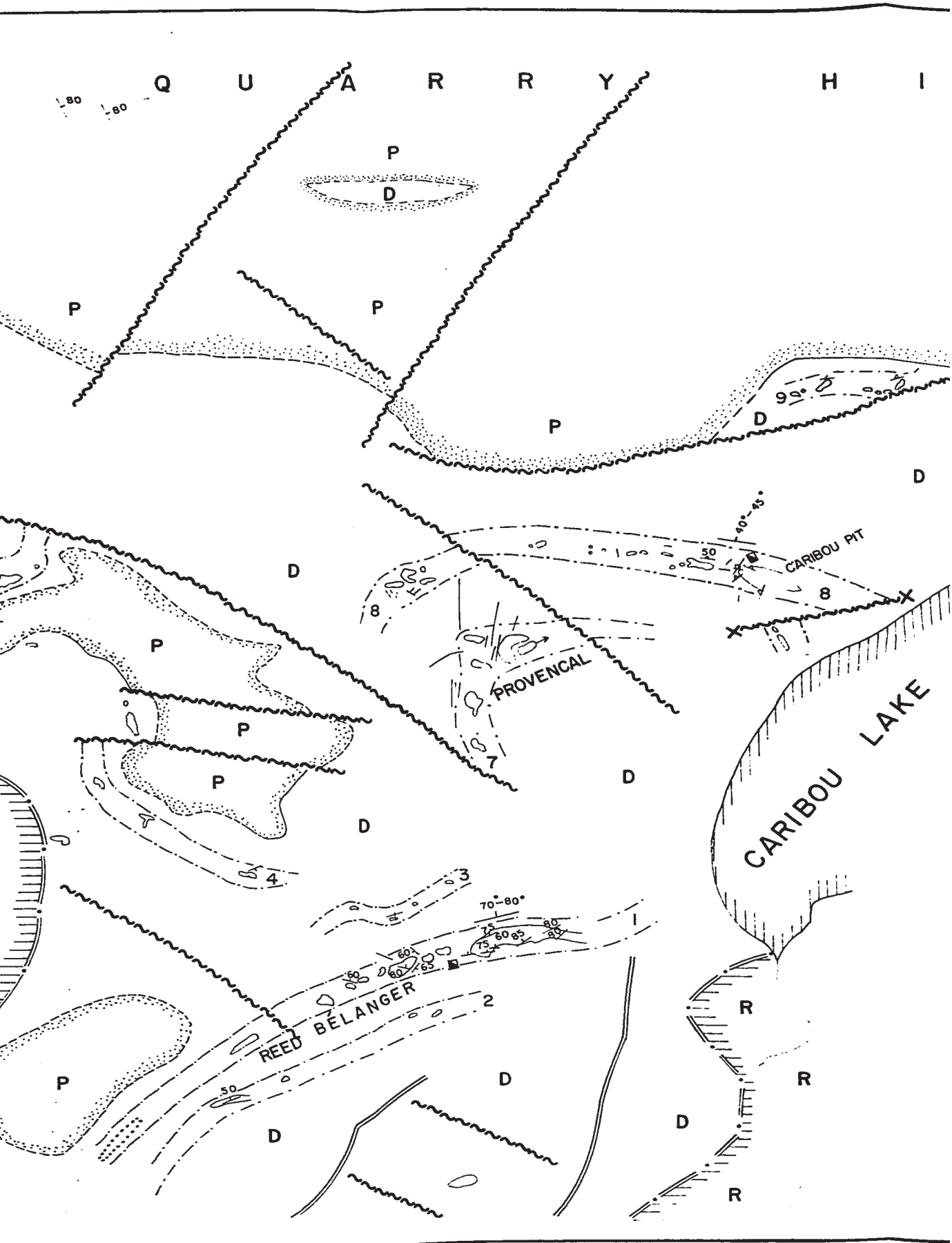




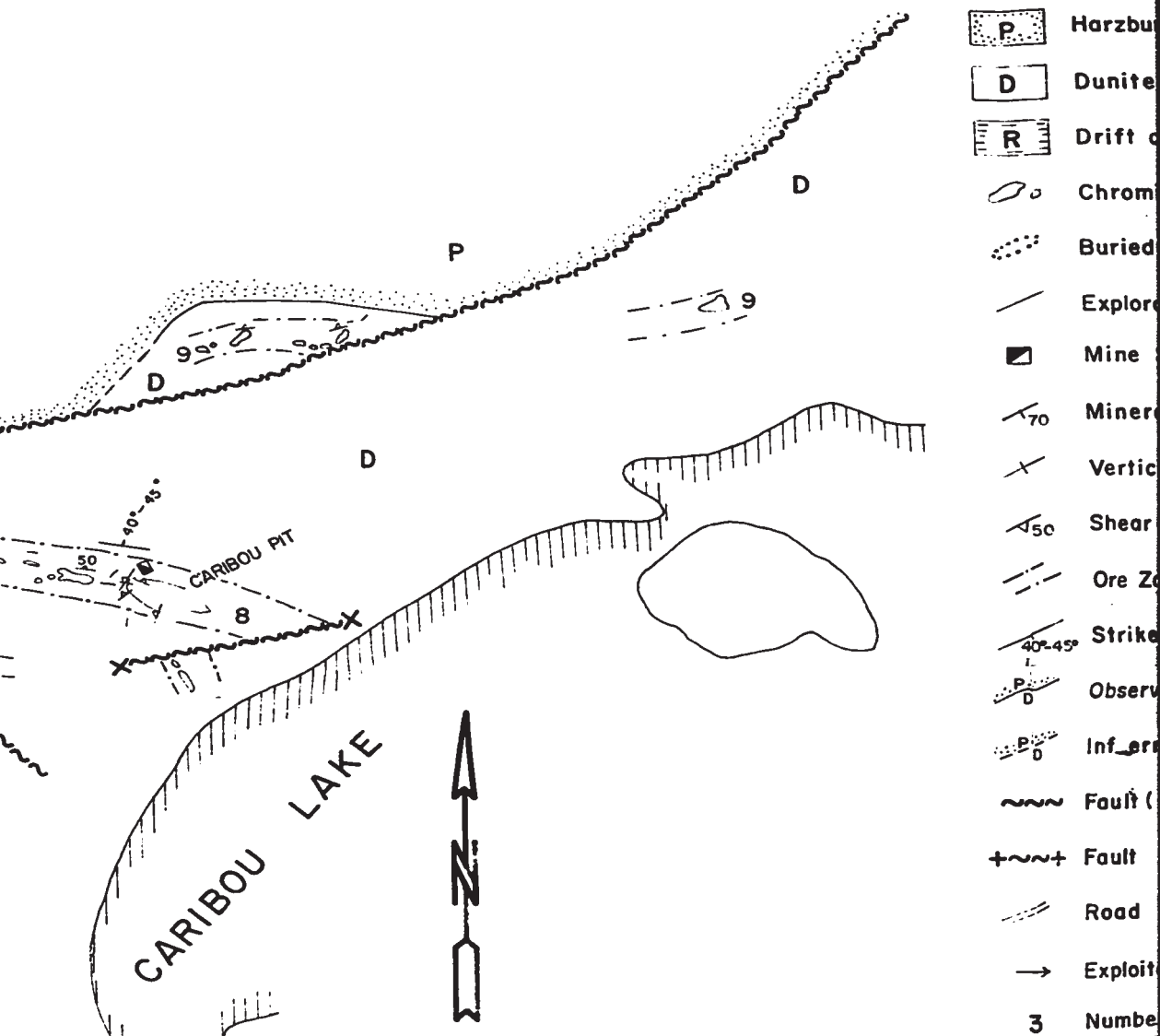








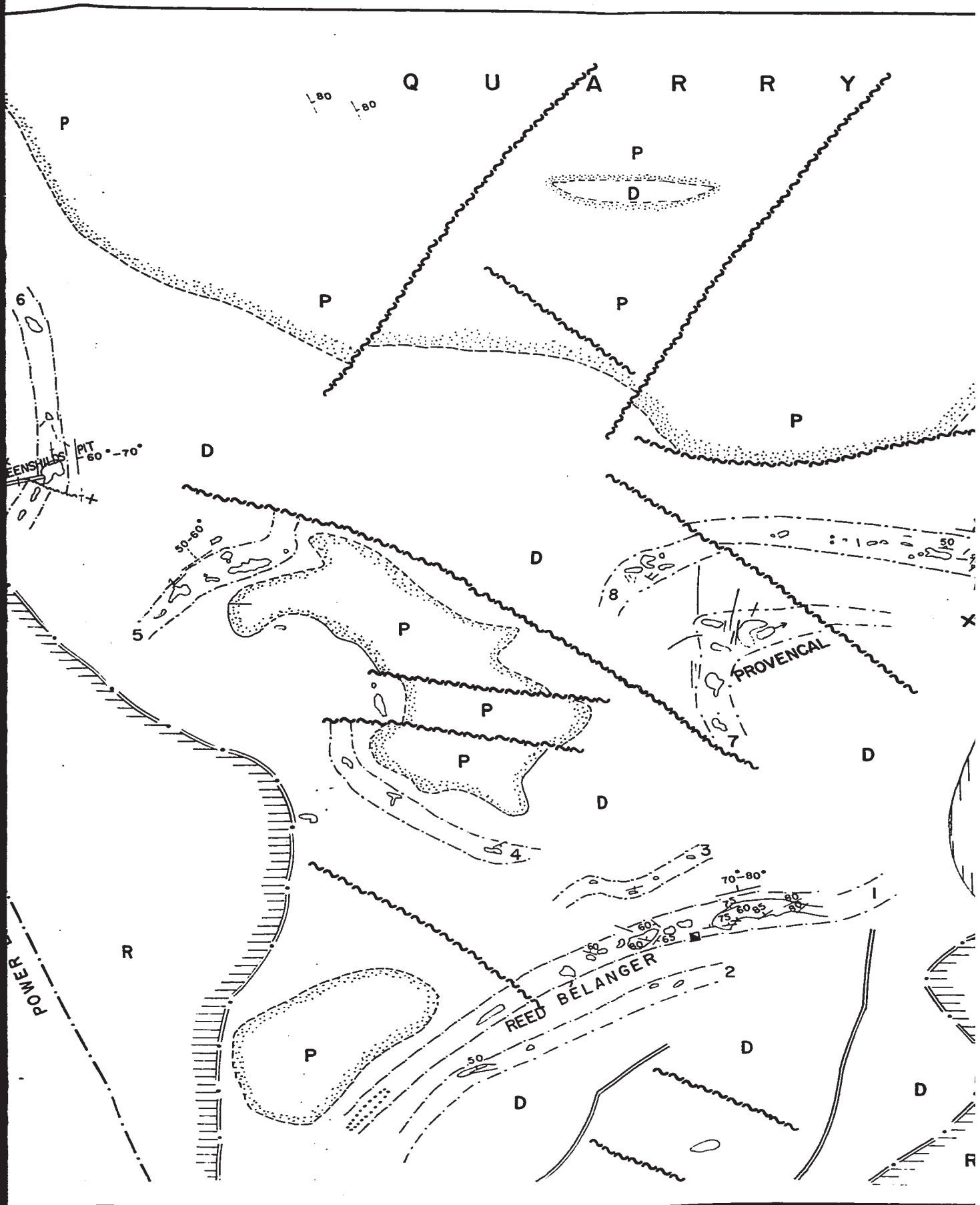
H I L L



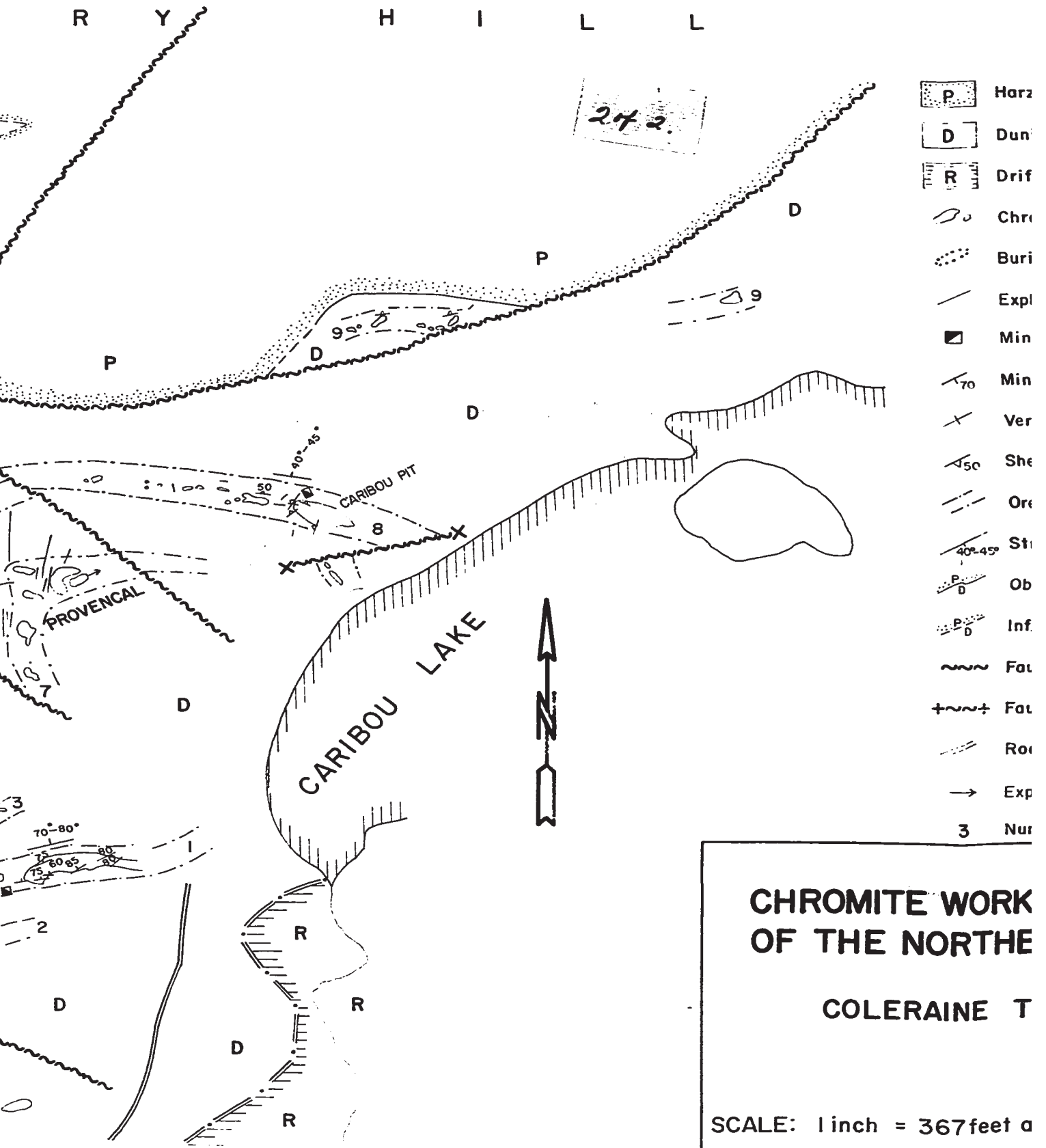
CHROMITE WORKINGS OF THE NORTHERN

COLERAINE TOWN

SCALE: 1 inch = 367 feet approx



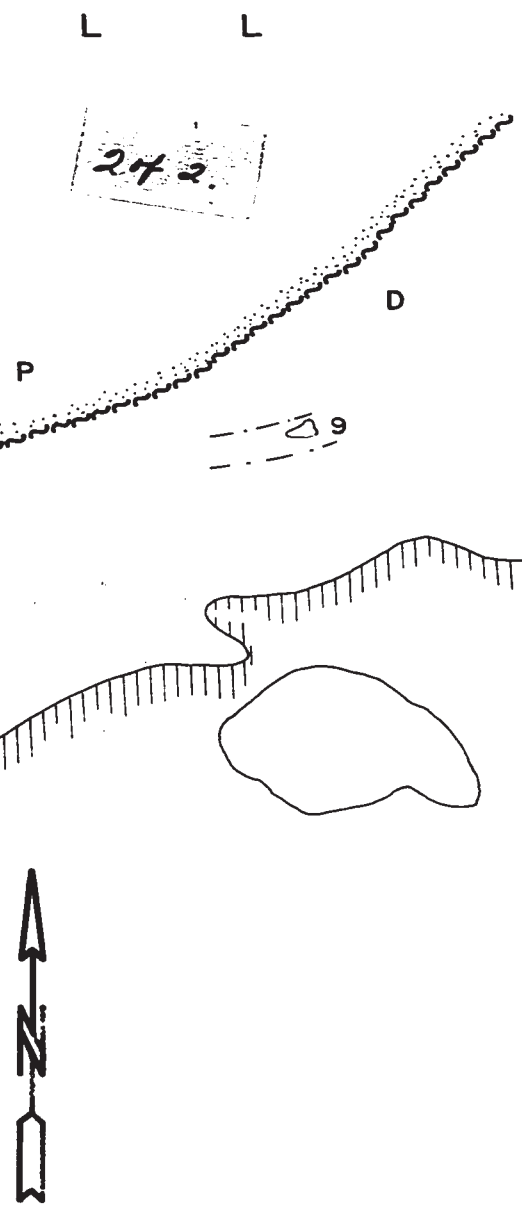
R Y H I L L


















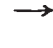


**CHROMITE WORK
OF THE NORTHE
COLERAINE T**

SCALE: 1 inch = 367 feet a

LEGEND



-  Harzburgitic Peridotite
-  Dunite
-  Drift covered Areas
-  Chromite Working
-  Buried Chromite Working
-  Exploration Trenches
-  Mine Shaft
-  Mineral Banding and Foliation
-  Vertical Mineral Banding and Foliation
-  Shear Zone and Dip in Degree where measurable
-  Ore Zone Boundaries
-  Strike and Dip(app.) of the Ore Zone
-  Observed Boundary
-  Inferred Boundary
-  Fault (Photogeological)
-  Fault (Inferred)
-  Road
-  Exploitation Tunnel Direction, Dip
- 3** Number of the Ore Zone

**CHROMITE WORKINGS AND ORE ZONES
OF THE NORTHERN DUNITE ZONE**

COLERAINE TOWNSHIP, QUEBEC

SCALE: 1 inch = 367 feet app.

MAP 3

**N. KAÇIRA
1968**